2023

中華民國核醫學學會年會暨國際學術研討會

2023 Annual Conference of Society of Nuclear Medicine, Taiwan

時間：2023年11月12日（星期日）

地點：臺中榮民總醫院

地址：臺中市西屯區臺灣大道四段1650號

主辦單位

中華民國核醫學學會

臺中榮民總醫院

國家原子能科技研究院

經濟部產業技術司

協辦單位

台灣分子生物影像學會

DOIT 經濟部產業技術司 Department of Industrial Technology, MOEA

中華民國核醫學學會 2023 年會暨國際學術研討會議程

第一會場			
時間	演講題目	講者	座長
08:20~08:45	會員報到		
08:45~09:00	開場致詞 臺中榮總 吳杰亮副院長、 國家原子能科技研究院 高梓木院長、 中華民國核醫學學會 王昱豐理事長		
09:00~09:10	貴賓致詞 健保署 石崇良署長		
09:10~9:50	Opening Remark: Prof. Andreas Buck, University Hospital Würzburg		
	Cutting-Edge Cardio: Imaging the Heart for Precision Medicine	University Hospital Würzburg/Okayama University Prof. Takahiro Higuchi	亞東紀念醫院 吳彥雯 主任
09:50~10:30	Redifferentiation of Radioiodine-Refractory Differentiated Thyroid Cancer: Bench to Bedside	Kyungpook National University Prof. Byeong-Cheol Ahn	高雄榮民總醫院 諶鴻遠 主任
10:30~10:50	BREAK		
10:50~11:30	Planning for TFDA Cleared: Bone Scan AI Platform	中國醫藥大學附設醫院 高嘉鴻 主任	林口長庚紀念醫院 何恭之 主任
11:30~12:10	Artificial Intelligence in PET and SPECT Imaging Physics	Yale University Prof. Chi Liu	林口長庚紀念醫院 林昆儒 教授
12:10~13:30	會員大會		
	LUNCH		
13:30~14:10	失智症診斷與治療最新進展	台灣臨床失智症學會 陳正生 理事長	台北榮民總醫院 彭南靖 主任
14:10~14:50	Tau PET Imaging in Parkinsonism Syndromes	台灣動作障礙學會 林靜嫻 理事長	
14:50~15:30	The Current Status and Perspective of Nuclear Neuroimaging in South Korea.	Severance Hospital, Yonsei University Prof. Mijin Yun	臺大醫院 鄭媚方 主任
15:30~15:40	BREAK		
15:40~16:20	Neuromolecular Imaging: History and New Waves	University of Fukui Prof. Hidehiko Okazawa	三軍總醫院 林立凡 主任
16:20~17:00	Optimizing Molecular Imaging in Dementia and Related Disorders: Insights from Taiwan	長庚大學 蕭穎聰 教授	台灣分子生物影像學會 林康平 理事長
住院醫師考試 13:30-14:30 台中榮總核醫科會議室			

中華民國核醫學學會 2023 年會暨國際學術研討會議程

第二會場			
時間	演講題目	講者	座長
08:20~08:45	會員報到		
08:45~09:10	第一會場：開場致詞		
09:10~9:50	09:20-10:00 AI for the Optimization, Standardization, and Generalization of Brain PET/CT	Severance Hospital, Yonsei University Prof. Mijin Yun	彰濱秀傳紀念醫院 洪光威 副院長
09:50~10:30	10:00-10:40 運用核子醫學技術在動物的神經造影研究 The Studies of Non-human Neuroimaging Using Nuclear Medicine	國防醫學院 馬國興 教授	振興醫院 黃文盛 教授
10:30~10:50	BREAK		
10:50~11:30	醫學資訊標準教育推廣	慈濟大學 蕭嘉宏 副教授	台北馬偕醫院 杜高瑩 放射師
11:30~12:10	照護創新：談 AI 與性別平等	國立臺北護理健康大學 謝佳容 副教授	國家原子能科技研究院 樊修秀 副所長
12:10~13:30	會員大會		
	LUNCH		
13:30~14:10	核醫精準醫療，台灣的發展趨勢 Nuclear Medicine Theranostics in Taiwan	臺大醫院 顏若芳 副教授	中華民國核醫學學會 王昱豐 理事長 國家原子能科技研究院 高梓木 院長
14:10~14:50	伴隨性放射性藥物 YKL40 抗體：開發上皮性卵巢癌之伴同性放射診療抗體藥物 Companion Radiopharmaceutical YKL40 Antibodies: Potential Theranostic Agents for Epithelial Ovarian Cancer Development	國家原子能科技研究院 同位素所 張明誠 副研究員	中華民國核醫學學會 樊裕明 副理事長 國家原子能科技研究院 李振弘 所長
14:50~15:30	小腦萎縮鼠診斷與治療之分子影像評估 Evaluation of Molecular Imaging Probes on Diagnosis and Therapy of Spinocerebellar Ataxia in Mice	國家原子能科技研究院 同位素所 王美惠 研究員	
15:30~15:40	BREAK		
15:40~16:20	PSMA Radioligand Therapy - Lessons Learned from our Inaugural Case and Global Insights	臺大醫院 路景竹 醫師	和信治癌中心醫院 黃玉儀 主任
16:20~17:00			
住院醫師考試 13:30-14:30 台中榮總核醫科會議室			

中華民國核醫學學會 2023 年會暨國際學術研討會議程

<table>
<tr><th colspan="4">第三會場</th></tr>
<tr><th>時間</th><th>演講題目</th><th>講者</th><th>座長</th></tr>
<tr><td>08:20~08:45</td><td colspan="3">會員報到</td></tr>
<tr><td>08:45~09:10</td><td colspan="3">第一會場：開場致詞</td></tr>
<tr><td rowspan="4">09:10~10:30</td><td colspan="3">Advancing Molecular Imaging and Non Imaging Biomarkers in Neurodegenerative Diseases</td></tr>
<tr><td>09:10-09:40
Recent Advancements of Imaging and Fluid-Biomarkers for Alzheimer’s Disease and Disease-Modifying Therapies</td><td>阿拉巴馬大學伯明翰醫學院
方佑華 副教授</td><td rowspan="3">台灣分子生物影像學會
林康平 理事長</td></tr>
<tr><td>09:40-10:10
Automatic Striatal ROI Delineation for Semi-quantitative Analysis of 99mTc-TRODAT-1 Brain SPECT Imaging</td><td>中原大學醫療器材科技轉譯中心
林汶正 助理教授</td></tr>
<tr><td>10:10-10:30
Clinical Experience Sharing on Quantitative Analysis of Dopamine Transport Imaging</td><td>羅東聖母醫院
林明賢 主任</td></tr>
<tr><td>10:30~10:50</td><td colspan="3">BREAK</td></tr>
<tr><td>10:50~11:30</td><td colspan="3" rowspan="2">口頭論文發表
<table>
<tr><th>時間</th><th>組別</th><th colspan="2">評分座長</th></tr>
<tr><td>10:50-11:20</td><td>臨床組</td><td>許沛瑩 主任</td><td>柯冠吟 醫師</td></tr>
<tr><td>11:30-12:00</td><td>臨床組</td><td>林宜瀞 醫師</td><td>蔡雅琴 醫師</td></tr>
</table></td></tr>
<tr><td>11:30~12:10</td></tr>
<tr><td>12:10~13:30</td><td colspan="3">會員大會
12:30~13:30 / LUNCH SYMPOSIUM (西門子)
主題： Driving Clinical Apps to an Intelligent Platform: Semi-Quantitative Dementia Imaging and Tumor Burden Computation
講師： Takeshi Shimizu (Ph.D.), Marketing Professional, Molecular Imaging Global Business Unit, Siemens Medical Solutions USA, Inc.
座長： Prof. Kun-Ju Lin (MD., Ph.D.), Nuclear Medicine Department of Linkou Chang-Gung Memorial Hospital</td></tr>
<tr><td>13:30~14:10</td><td colspan="3" rowspan="3">口頭論文發表
<table>
<tr><th>時間</th><th>組別</th><th colspan="2">評分座長</th></tr>
<tr><td>13:30-14:10</td><td>基礎組</td><td>吳駿一 教授</td><td>張文議 博士</td></tr>
<tr><td>14:20-14:50</td><td>臨床組</td><td>黃玉儀 主任</td><td>陳世欣 主任</td></tr>
</table></td></tr>
<tr><td>14:10~14:50</td></tr>
<tr><td>14:50~15:30</td></tr>
<tr><td>15:30~15:40</td><td colspan="3">BREAK</td></tr>
<tr><td>15:40~16:20</td><td colspan="3" rowspan="2"></td></tr>
<tr><td>16:20~17:00</td></tr>
<tr><td colspan="4">住院醫師考試 13:30-14:30 台中榮總核醫科會議室</td></tr>
</table>

中華民國核醫學學會 2023 年會暨國際學術研討會議程

第四會場			
時間	演講題目	講者	座長
08:20~08:45	會員報到		
08:45~09:10	第一會場：開場致詞		
09:10~10:30	ISO15189(2022) 新版規範重點之簡介	國防醫學院 張錦標 副教授	台北馬偕紀念醫院 王安美 技術主任
10:30~10:50	BREAK		
10:50~11:30	ISO15189(2022) 新版規範重點之簡介	國防醫學院 張錦標 副教授	台北馬偕紀念醫院 王安美 技術主任
11:30~12:10			
12:10~13:30	會員大會		
	12:30~13:30 / LUNCH SYMPOSIUM (台灣諾華) 主題： The Right Timing to Bring New Hope for NET Patients- How to Optimise the Treatment Strategy 講師： 台北榮民總醫院 姚珊汎 醫師 座長： 臺大醫院癌醫分院 柯冠吟 醫師		
13:30~14:10	新型同位素核種治療輻防經驗分享	台大癌醫 張婉柔 放射師	臺大醫院 黃奕琿 技術長
14:10~14:50	EPA 觀念導入及課程設計工作坊	台中榮民總醫院 龔瑞英 放射師	中華民國核醫學學會 陳惠萍 副理事長
14:50~15:30	EPAs 分組：職場觀察評估與回饋演練	大林慈濟醫院 許幼青 放射師 嘉義基督教醫院 陳怡勳 副部主任	
15:30~15:40	BREAK		
15:40~16:20	SPECT/CT 的定量與應用	GE healthcare 施宜伶 Application Specialist	三軍總醫院 王秀珊 放射師
16:20~17:00	Emyway 操作介紹	中華民國核醫學學會 陳惠萍 副理事長	台北榮民總醫院 楊邦宏 放射師
住院醫師考試 13:30-14:30 台中榮總核醫科會議室			

目 次

王心怡

感謝諸位蒞臨在臺中榮民總醫院舉辦的核子醫學年會。在疫情後，我們終於又可以齊聚一堂，共同探討「智慧醫療新時代，精準治療再進化」的主題，這必定是一場富有啟發性和意義深遠的學術盛會。

疫情帶給我們前所未有的挑戰，也讓我們更加深刻地體會到健康的重要性。在這段艱難的時光裡，我們看到了醫護人員的堅韌和奉獻，看到了科研人員的努力和創新。我們一同面對著未知，一同努力尋找解決之道，也因此更加確信核子醫學科的重要性。

在這個迅速發展的時代，核子醫學科技亦不斷進步，為現代醫學提供了更多診斷、治療疾病的方式。過去的努力讓我們取得了長足的進步，然而，面對新的時代，我們不能止步於此。我們必須持續努力，以更高的熱情和開拓精神，迎接智慧醫療新時代的挑戰。

智慧醫療的興起，結合了人工智能、大數據等先進技術，為核子醫學帶來了前所未有的發展機遇。我們擁有了更多數據，更強大的分析能力，可以更加精準地定位疾病和評估治療效果。而「精準治療再進化」正是智慧醫療新時代的核心使命。我們將更加注重個體差異，實現個性化醫療。這將使我們的治療更加靈活、高效，減少不必要的副作用，使我們能夠更好地照顧病患，提高醫療品質，為患者帶來更大的福祉。

本次年會匯聚了來自各地的核子醫學專家，將展示最新的研究成果、分享實踐經驗、交流創新思想。這是一個學習的機會，也是一個合作的平台。我們希望通過這次年會，激發更多的智慧火花，凝聚更多的共識，推動核子醫學的再進化，讓它在精準治療的大潮中展現更強大的魅力。

在最後，感謝王昱豐理事長暨學會理監事委以重任，感謝臺中榮總團隊共同協助，感謝全體工作人員的辛勤付出，沒有你們的辛苦籌備，就沒有這次盛會的順利召開。同時，也感謝各位演講嘉賓和參與者，是你們的參與和支持讓年會更加豐富多彩。

讓我們攜手並進，共同迎接智慧醫療新時代的到來，為精準治療再進化而努力！

王心怡

臺中榮民總醫院核子醫學科

中華民國 112 年 11 月 12 日

Name: **Takahiro Higuchi**
Title: 教授
Institute: Universität Würzburg / Okayama University
第一會場 09:10-09:50

Cutting-edge Cardio: PET Imaging the Heart for Precision Medicine

Precision medicine offers the great promise of individualized diagnosis and tailored treatment, streamlining patient care for increased efficiency. This presentation emphasizes the significance of radionuclide molecular imaging, poised to be a leading technique in the realm of precision cardiology. Radionuclide PET molecular imaging goes beyond traditional structural imaging, illuminating cellular and subcellular processes to provide insights into function and pathology at a molecular dimension. A highlight of this discussion is the newly developed F18 PET tracer, AF78, a state-of-the-art agent for sympathetic nervous imaging. This innovation enables unparalleled visualization of cardiac sympathetic nervous conditions, granting deep insights into diverse cardiac pathologies and their complex relationships with the nervous system. As the horizon of cardiology is continually reshaped by precision medicine, radionuclide PET molecular imaging techniques like these stand at the forefront, paving the path towards tailored therapeutic approaches and heralding a new epoch of patient-focused care.

Name: **Byeong-Cheol Ahn**
Title: 教授
Institute: Kyungpook National University and Hospital
第一會場 09:50-10:30

Redifferentiation of Radioactive Iodine Refractory Differentiated Thyroid Cancers: Bench to Bedside

Although differentiated thyroid cancers (DTCs) show excellent prognosis; however, DTCs with distant metastases reveals relatively poor prognosis.

Metastatic DTCs with iodine avidity can be completely cured by the radioactive iodine (RAI) therapy; however, 2/3 of the metastatic DTCs end up as a RAI refractory (RAI-R) by dedifferentiation, and they do not respond to the RAI therapy. The dedifferentiation downregulates expression of sodium iodide symporter (NIS) in DTCs, and MAPK pathway is one of the most famous signaling pathway which inhibit NIS expression.

Many pre- and clinical reports demonstrated that pharmacologic blocking of the MAPK pathway redifferentiates the RAI-R DTCs and enhance therapeutic effect of the RAI therapy in the cancers. However, the clinical benefit of the pharmacologic interventions was not evident in some of the RAI-R DTCs and the benefit varied considerably depending on characteristics of the cancers. The heterogenous responses to the pharmacologic interventions may be presented by heterogenous dedifferentiation mechanisms of the RAI-R DTCs. So, the redifferentiation strategy for the RAI-R DTCs needs to be individualized to attain the best clinical benefit. Many preclinical studies are on-going to develop new drugs having better redifferentiation effect, and to get better redifferentiation results.

Dedifferentiation mechanisms of the RAI-R DTCs are quite complex and many things are unrevealed still. Comprehensive understanding of the dedifferentiation mechanisms will give us a chance to treat better, even to cure the RAI-R DTCs by applying the RAI therapy again as a salvage therapy for the cancers.

In the presentation, developing redifferentiation strategies for the RAI-R DTCs and their clinical translation will be discussed.

Name: **高嘉鴻**
Title: 主任
Institute: 中國醫藥大學附設醫院
第一會場 10:50-11:30

Planning for TFDA Cleared: Bone Scan AI Platform

骨閃爍顯像 (bone scintigraphy, BS) 是篩檢骨轉移的功能性檢查之一，亦是核子醫學科最大宗的檢查，其流程多年來未見重大改變，因此在臨床運行上顯得緩慢拖沓。為改善此痛點，中國醫藥大學附設醫院核醫科與人工智慧中心組成研發團隊通力合作，提出全球首個用於癌症骨轉移之人工智慧 (artificial intelligence, AI) 解決方案來提升『骨閃爍顯像診斷』作業效率，發展出「骨轉移輔助系統」。其能在限時內協助醫師篩檢有 / 無骨轉移並顯示骨轉移高風險區域，避免遺漏導致誤診，並透過友善且結構化的報告平台，期盼建立一站式的服務平台來輔助臨床核醫科專科醫師，降低在診斷流程與撰寫病歷的負擔，滿足臨床需求，讓醫師能夠更有餘裕在其他的核醫診斷、治療或研究上，有效降低繁瑣的流程以節約時間與醫療成本，大幅提升醫療品質，以嘉惠廣大患者。

Name: **Chi Liu**
Title: 教授
Institute: Yale University
第一會場 11:30-12:10

Artificial Intelligence in PET and SPECT Imaging Physics

This talk will provide an overview of artificial intelligence and deep learning applications in PET and SPECT imaging physics, including image reconstruction, noise reduction, attenuation correction, scatter correction, and motion correction.

Name: **陳正生**
Title: 理事長
Institute: 高雄醫學大學醫學院 / 台灣臨床失智症學會
第一會場 13:30-14:10

失智症診斷與治療最新進展

Update on Diagnosis and Treatment of Alzheimer's Disease

阿茲海默症是失智症最主要的病因。近年對早期發病的個案的治療有新的突破，但是大多阿茲海默症患者並非在疾病早期就醫，治療效果因此受到限制。早期篩檢出潛在的病患是目前的重要議題。除了認知功能減退的 mild cognitive impairment (MCI) 以外，行為障礙也可能是失智症的前驅症狀。最新提出的 mild behavioral impairment (MBI) 診斷是新的研究重點。生物標記的開發也具有重要性，影像或是血液的生物標記研究已有臨床使用的潛力。本次演講將說明阿茲海默症最新的治療以及搭配的提早診斷的方式。

Name: **林靜嫻**
Title: 理事長
Institute: 臺大醫院 / 台灣動作障礙學會
第一會場 14:10-14:50

Tau PET Imaging in Parkinsonism Syndromes

The accumulation of pathological misfolded tau is a feature common to a collective of neurodegenerative disorders known as tauopathies, of which Alzheimer's disease (AD) is the most common. Related tauopathies include progressive supranuclear palsy (PSP), corticobasal syndrome (CBS), Down's syndrome (DS), Parkinson's disease (PD), and dementia with Lewy bodies (DLB). Among these neurodegenerative disorders, atypical parkinsonisms syndromes are a group of diseases linked to 4-repeat tau pathology, including PSP and corticobasal degeneration (CBD). Investigation of the role of tau pathology in the onset and progression of these disorders is now possible due the recent advent of tau-specific ligands for use with positron emission tomography (PET). This talk will review recent findings using both initial and new tau ligands, including their relation to brain MRI findings and plasma biomarkers for tau and neurodegeneration for 4R tauopathy parkinsonism syndromes. Lastly, methodological considerations for the quantification of in vivo ligand binding are addressed, along with potential future applications of tau PET, including therapeutic trials.

Name: **Mijin Yun**
Title: 教授
Institute: Severance Hospital, Yonsei University
第一會場 14:50-15:30

The Current Status and Perspective of Nuclear Neuroimaging in South Korea.

In celebration of six decades of accomplishments in the field of neuroimaging research, the Korean Society of Nuclear Medicine has released a review article that summarizes over 400 remarkable studies carried out by Korean researchers in 2022. To provide a concise overview of the timeline, in the 1990s, multiheaded single-photon emission computed tomography (SPECT) scanners was introduced in South Korea and research mainly focused on brain perfusion imaging. With the introduction of positron emission tomography (PET) in the 2000s, clinical utility of PET utilizing F-18 FDG and other radiotracers was assessed in epilepsy, brain tumors, degenerative brain diseases, and neuropsychiatric disorders. In 2008, F-18 fluorinated-N-3-fluoropropyl-2-b-carboxymethoxy-3-b-(4-iodophenyl)nortropane (FP-CIT) for dopamine transporter imaging was approved for clinical practice by the Korean Ministry of the Food and Drug Safety which has become an imaging modality of choice for research on Parkinson's diseases. During the 2010s, amyloid and tau imaging fueled a rapid expansion in research, demonstrating both the clinical values of PET imaging and underlying pathophysiology in patients with dementia. Recently, there are studies on radiopharmaceuticals targeting mitochondrial translocator protein (TSPO) of microglia and MAO-B in reactive astrocytes for neuroinflammation. In particular, visualization of reactive astrogliosis in vivo showed tremendous impact on diagnosis and treatment of neurodegenerative diseases as well as brain tumors. Not only the development of novel radiopharmaceuticals but also advanced analytical techniques with the integration of artificial intelligence will further contribute to the future of nuclear neuroimaging.

Name: **Hidehiko Okazawa**
Title: 教授
Institute: Biomedical Imaging Research Center, University of Fukui

第一會場 15:40-16:20

Neuromolecular Imaging: History and New Waves

The foundation for today's brain imaging studies was laid by the development of quantitative brain PET in the 1980s and advances in various MR imaging techniques in the 1990s. In the 2000s, with the development of molecular imaging and the widespread use of MRI diffusion-weighted imaging, crossover analysis by various specific parameters is being realized to clarify physiological changes and dysfunction in the brain.

Neuromolecular imaging has been developed since 1980s with inventions of many receptor ligands and analyzing methods. Recently, amyloid and tau PET enables pathophysiology-based diagnosis, which is expected to be applied to staging of Alzheimer's disease. In addition, parameters related to pathologic conditions, such as microglial/glial activation and oxidative stress, have been successfully imaged and expected to elucidate the causes of neurodegenerative disorders. The diagnosis of pathologic conditions will provide useful information for the development of future therapeutic drugs leading to early prevention.

On the other hand, various sequences and analyzing methods have been developed for functional brain imaging using MRI. Their application in the field of dementia and neurodegenerative diseases is also progressing. In addition to resting state fMRI, elucidation of the glymphatic system using diffusion-tensor MR imaging is a promising neuroimaging tool for evaluation of the detergent function in the brain. The development of the PET/MRI system has enabled simultaneous imaging of both modalities, facilitating easy acquisition and analysis of PET and MRI.

This talk will review the history of PET molecular imaging and functional brain imaging, followed by an overview of the multimodality imaging studies conducted for pathophysiologic changes in dementia and neurodegenerative diseases.

Name: **蕭穎聰**
Title: 教授
Institute: 長庚大學
第一會場 16:20-17:00

Optimizing Molecular Imaging in Dementia and Related Disorders: Insights from Taiwan

Molecular imaging techniques, such as MRI, FDG PET, dopamine imaging, and amyloid PET, have revolutionized the diagnosis and management of dementia. This presentation provides an overview of their optimal utilization in dementia and related disorders, with a specific focus on experiences and insights from Taiwan.

MRI, with its excellent spatial resolution, aids in identifying structural abnormalities. FDG PET enables the assessment of regional cerebral glucose metabolism, distinguishing between neurodegenerative and non-neurodegenerative causes of cognitive impairment. Dopamine imaging plays a crucial role in differentiating dementia with Lewy bodies from other types of dementia. Amyloid PET visualizes amyloid-beta deposition, facilitating the differentiation of Alzheimer's disease from other dementias. Furthermore, the challenges associated with interpretation and integration are discussed, emphasizing the optimization of acquisition protocols, standardization of analysis techniques, implementation of AI techniques, and the importance of establishing consensus among imaging and clinical experts for improved correlation with clinical and cognitive assessments.

In conclusion, optimizing the use of MRI, FDG PET, dopamine imaging, and amyloid PET in Taiwan enhances patient care and facilitates early and accurate diagnosis of dementia and related disorders. By sharing experiences and insights, we can contribute to the advancement of molecular imaging in dementia research and clinical practice.

Name: **Mijin Yun**
Title: 教授
Institute: Severance Hospital, Yonsei University
第二會場 09:20-10:00

AI for the Optimization, Standardization, and Generalization of Brain PET/CT

Artificial intelligence (AI) including machine learning and deep learning methods, has become one of the core technologies among the most recent developments in the field of medical imaging. Traditional and quantitative image analysis has been indispensable for investigating clinical significance of nuclear medicine molecular imaging in patients with various neurodegenerative diseases. Of the AI techniques, deep learning consists of the artificial neural networks with multiple convolutional layers and nodes. Unlike machine learning, deep learning performs the feature extraction and learning based on a cascade of multiple layers of nonlinear processing units. High quality data and labels are of utmost importance to improve the performance of deep learning models. In this talk, I will focus on various methods of deep learning that have been applied to positron emission tomography/computed tomography (PET/CT) imaging of neurodegenerative diseases for the optimization, standardization, and generalization. This will include denoising of low-quality imaging, segmentation of volume of interest, automatic image analysis, image to image generation from PET to magnetic resonance imaging (MRI), disease classification, etc.

Name: **馬國興**
Title: 教授
Institute: 國防醫學院
第二會場 09:50-10:30

運用核子醫學技術在動物的神經造影研究

The Studies of Non-human Neuroimaging Using Nuclear Medicine

血清素轉運體 (serotonin transporter) 分佈於整個大腦，血清素轉運體的異常可能與許多神經與精神疾病如：巴金森氏症、重度憂鬱症、精神分裂症、藥物成癮、焦慮症與強迫症有關。然而血清素轉運體在這些疾病所扮演的確切角色，較少被研究探討，其中一個原因可能是缺乏有效的活體研究方法。運用核子醫學藥物配合單光子電腦斷層掃描 (single photon emission computed tomography, SPECT) 或正子電腦斷層掃描 (positron emission tomography, PET) 是在活體研究大腦血清素轉運體狀態的有效方法。本實驗室利用上述核子醫學技術在動物進行各種造影研究，研究結果可在臨床應用提供重要參考。

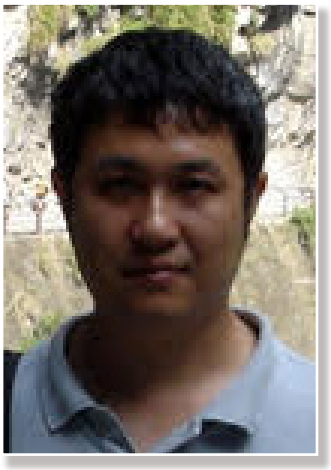

Name: **蕭嘉宏**
Title: 副教授
Institute: 慈濟大學
第二會場 10:50-11:30

醫學資訊標準教育推廣

醫資標準是智慧醫療、精準醫療、整合照護的基礎，但國內熟悉醫資標準的人才甚為稀少。本課程將介紹健康醫療過程資訊處理常用的 FHIR resources。快速了解常用的 FHIR resources 及健康醫療作業流程，學會擴充延伸應用。基於某健康醫療所需專業檢測、診斷、問題狀況，學會如何與專家合作設計對應之 FHIR resources。

Name: **謝佳容**
Title: 副教授
Institute: 國立臺北護理健康大學
第二會場 11:30-12:10

照護創新：談 AI 與性別平等

性別平等是項基本人權，也是世界和平、繁榮和永續發展的必要基礎。於全球永續發展目標 SDG5 為「實現性別平等」的議題，呼籲著我們需重視性平在生活所有場域的落實與行動。在這次的性平講題中，我們將從 AI 與性別平等之間的觀察，來檢視科技如何受人的權力與價值觀影響，當我們研發 AI 的時候，該如何避免複製社會上常見的不平等，不輕易落入「科技決定論」至為關鍵。因此，形成此次演講大綱如下五項內容，期盼透過演講後，我們身為健康產業相關的醫事人員者，能一起推動與營造性別友善之健康照護環境。

主題大綱 :

1. 性別培力的概念與性別敏感度
2. 性別主流化的國際發展趨勢
3. 性別主流化六大工具 vs. 性別交織分析
4. 醫護產業人工智慧 (AI) 的發展與性別平等之間的關係
5. 消弭 AI 偏見之路：性別平等於健康照顧場域的落實與行動

Name: **顏若芳**
Title: 副教授
Institute: 臺大醫院
第二會場 13:30-14:10

核醫精準醫療，台灣的發展趨勢

Nuclear Medicine Theranostics in Taiwan

2022 年學會和核研所合作利用全民健康保險研究資料庫 2014 年至 2020 年間的核醫就醫紀錄，分析核醫診療使用趨勢，並由 2022 年各醫院所回覆人員及設備調查問卷了解台灣目前核醫資源分布情形。根據該研究提供台灣核醫診療的趨勢做為核醫部門未來規劃人力設備與核醫藥物的參考。

Name: **張明誠**
Title: 副研究員
Institute: 國家原子能科技研究院 同位素所
第二會場 14:10-14:50

伴隨性放射性藥物 YKL40 抗體：開發上皮性卵巢癌之伴同性放射診療抗體藥物

Companion Radiopharmaceutical YKL40 Antibodies: Potential Theranostic Agents for Epithelial Ovarian Cancer Development

上皮性卵巢癌因缺乏明顯的症狀，被診斷時通常是晚期且預後較差。幾丁質酶 -3- 類似蛋白 -1 (CHI3L1) 在上皮性卵巢癌會顯著表達。在本研究中我們開發以 CHI3L1 為標的之卵巢癌伴同式放射診療藥物。DTPA 與 CHI3L1 中和抗體 YKL40 接合後構築抗體藥物前驅物 DTPA-YKL40，並進行放射性同位素標誌以建立放射性藥物。藥物安定性試驗數據顯示以放射性同位素標誌的中和抗體在標誌 48 小時其放射化學純度仍可以維持在 90% 以上，進一步以單光子斷層掃描進行活體造影，影像顯示在給藥後 24 小時，本放射性診療抗體藥物會顯著累積在腫瘤部位。腫瘤治療試驗也顯示實驗動物在接受單一劑量的放射抗體藥物治療後會顯著抑制腫瘤生長。研究顯示本放射性同位素標誌的 DTPA-YKL-40 可以做為卵巢癌伴同式放射診療藥物。

Name: 王美惠
Title: 研究員
Institute: 國家原子能科技研究院 同位素所
第二會場 14:50-15:30

小腦萎縮鼠診斷與治療之分子影像評估

Evaluation of Molecular Imaging Probes on Diagnosis and Therapy of Spinocerebellar Ataxia in Mice

Currently, polyglutamine (polyQ) diseases, such as spinocerebellar ataxia (SCA), are fatal and incurable. Diagnosis is primarily reliant on post-mortem examinations, and the existing assessment tools, such as the Scale for the Assessment and Rating of Ataxia (SARA) and coordination tests, lack objectivity. Therefore, there is an urgent need to develop effective diagnostic and therapeutic approaches for SCA.

In this study, we have endeavored to develop imaging agents and related therapeutic techniques for SCA. In the realm of diagnosis, our techniques include genetic tools, behavioral assessments, MRI imaging evaluation, and biomarker imaging. In the therapeutic field, we explore the use of histone deacetylase type 6 inhibitor (HDAC6i) or adipocyte-derived mesenchymal stem cells (ADSC) as therapeutic agents and evaluate their efficacy in treating SCA. Additionally, we conduct a biodistribution study of Ga-67 nano-diamond endocytosed ADSC.

Our study reveals that ^{18}F-florbetaben ([^{18}F]FBB) may be a promising tracer for SCA imaging. Furthermore, our findings suggest that both HDAC6i and ADSC have the therapeutic potential for SCA. However, the imaging study showed the Ga-67 labeled nano-diamond endocytosed ADSC did not penetrate the blood-brain barrier, while exosomes did. Notably, exosomes exhibited greater absorption in the cerebellar region of SCA mice compared to normal mice, indicating that the therapeutic effect of ADSC on SCA may be mediated through the release of exosomes.

Name: 路景竹
Title: 醫師
Institute: 臺大醫院
第二會場 15:40-16:20

PSMA Radioligand Therapy - Lessons Learned from our Inaugural Case and Global Insights

In recent years, Prostate-specific membrane antigen (PSMA)-based theranostics, combining PET imaging and radioligand therapy (RLT), have revolutionized prostate cancer treatment. Lu177-PSMA-617 (Pluvicto) stands as the first FDA-approved PSMA-RLT, showing substantial survival benefits and minimal side effects in large clinical trials, notably the VISION study. In this speech, I will talk about the core principles of PSMA-RLT, clinical evidence, and real-world experiences from Taiwan, emphasizing its precision in diagnosis and therapy.

Name: **方佑華**
Title: 副教授
Institute: 阿拉巴馬大學伯明翰醫學院
第三會場 09:10-09:40

Recent Advancements of Imaging and Fluid-biomarkers for Alzheimer's Disease and Disease-modifying Therapies

With recent breakthrough in disease modifying therapies for Alzheimer's disease (AD), new opportunities have been presented for molecular imaging in various applications for AD and related dementia management. In this presentation, we will examine current research over imaging biomarkers related to AD, especially with molecular imaging methods. We will also examine recent results over the development of fluid biomarkers for AD and how such development may impact the imaging research and applications.

Name: **林汶正**
Title: 助理教授
Institute: 中原大學醫療器材科技轉譯中心
第三會場 09:40-10:10

Automatic Striatal ROI Delineation for Semi-quantitative Analysis of 99mTc-TRODAT-1 Brain SPECT Imaging

課程內容：

1. 介紹目前 SPECT 在腦部紋狀體的造影
2. 臨床在腦部紋狀體的圈選現況
3. 自動化軟體在腦部紋狀體的 ROI 圈選及計算
4. 腦部紋狀體的自動化圈選軟體對於臨床的助益
5. 軟體使用之經驗分享
6. 綜合討論

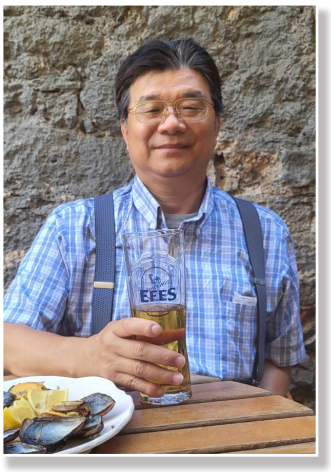

Name: **林明賢**
Title: 主任
Institute: 羅東聖母醫院
第三會場 10:10-10:30

Clinical Experience Sharing on Quantitative Analysis of Dopamine Transport Imaging

Parkinson's disease (PD) patient is the 2nd high incidence of neurodegenerative disease. Dopamine transport image (Tc-99m TRODAT) was first introduced in Taiwan in 1998. Due to its convenience, ease of use, increased sensitivity and quantification, TRODAT became a routine imaging study in NM clinics and as a tool to monitor the progression of PD in the same patient. Sharing on visual interpretation, semi-quantification of specific uptake ratio (SUR) by hand made and Q-striatum of Trodate dopamine image will be present.

Name: **張錦標**
Title: 副教授
Institute: 國防醫學院
第四會場 09:10-11:30

ISO15189 (2022) 新版規範重點之簡介

演講重點如下

一、改版理由：時空環境的不同及專業技術的精進

二、ISO15189 (2012) vs. (2022) 文件改版之差異：

1. 條文新增
2. 條文修改
3. 條文刪除、搬移、合併

三、ISO15189 (2012) vs. (2022) 文件改版後檢驗室的因應措施

1. 實驗室召開相關會議
2. 指派人員參加新版 ISO 15189 (2022) 相關課程
3. 擬定轉換計畫
4. 變更條文的人員教育訓練
5. 監控落實人員說、寫、作的一致性……

四、課程重點說明

- ISO 15189 (2012) 與 (2022) 之轉版說明
- ISO 15189 (2022) 新版文件轉換說明
- ISO 15189 (2022) 4.0 條文重點提示
- ISO 15189 (2022) 5.0 條文重點提示
- ISO 15189 (2022) 6.0 條文重點提示
- ISO 15189 (2022) 7.0 條文重點提示
- ISO 15189 (2022) 8.0 條文重點提示
- Q/A

Name: **張婉柔**
Title: 放射師
Institute: 台大癌醫
第四會場 13:30-14:10

新型同位素核種治療輻防經驗分享

新型同位素核種治療，結合跨領域的緊密合作，因病患的病情複雜性，許多治療相關的細節需要納入考量，因此本團隊建立完善的治療流程，提高病患接受治療的安全性及舒適度，並確保醫療人員的輻射安全。

Name: **龔瑞英**
Title: 放射師
Institute: 台中榮總
第四會場 14:10-14:50

EPA 觀念導入及課程設計工作坊

醫學教育領域開始嘗試以勝任能力為導向的醫學教育模式 (CBME) 代替傳統臨床教育方針；醫事放射職類 2014 年開始建立放射師五大核心能力，2017 年全國師資培育課程導入 EPA，2020 年開始建立 EPA 表單，2022 年導入試辦計畫。本課程介紹 CBME 並導入 EPA 觀念，完整詳述目前完成全國共識之 EPA 表單建置過程，EPA 課程設計與臨床教師訓練程序。

Name: **許幼青**
Title: 放射師
Institute: 大林慈濟

Name: **陳怡勳**
Title: 副部主任
Institute: 嘉義基督教醫院

第四會場 14:50-15:30

EPAs 分組：職場觀察評估與回饋演練

1. 進行方式

(1) 挑選一部 OPA1 影片，共 3 部影片。針對每部影片進行評估與共識討論，共 3 階段。

(2) 學員分組，每組安排一位較具經驗之教師，負責帶領討論、輔導共識討論流程順暢。

2. 進行流程依序討論

(1) 小組選出 1 位負責帶領討論之教師，針對 OPA 之觀察與評估項目進行共識討論

(2) 觀看 OPA 影片

(3) 每位老師將觀察結果填入 ad hoc 評量表，每人填寫 1 份紙本

(4) 小組討論觀察結果，並將小組之評估共識填入 google 表單，每組填寫 1 份

(5) 分享評估與回饋演練

Name: **施宜伶**
Title: Application Specialist
Institute: GE healthcare
第四會場 15:40-16:20

SPECT/CT 的定量與應用

SPECT/CT 的定量已成趨勢，Xeleris 工作站上有多款定量軟體輔助 AI 技術，實現 SPECT/CT 的精準定量，在未來的治療、診斷上提供醫師更多的評估依據。

Name: **陳惠萍**
Title: 副理事長
Institute: 中華民國核醫學學會
第四會場 16:20-17:00

Emyway 操作介紹

醫策會帶領醫事人員 PGY 教學已經歷十多年歷史，對於醫事人員教學近幾年也帶入 CBME 概念，希望評估學員進展是以是否可以獨立作業而非教學時間長短，而本人有幸因擔任全聯會教育委員會委員，在剛開始設計評量方式及取得專家學者共識已在團隊中一起努力，制定四份核醫公版表單。

今年醫策會進一步希望將進行 PGY 教學醫院加入 Emyway 平台，可將教學資料彙整，並開放資源將資料導入核醫學會即將進行的 Elearning 平台，達到互利的目標。因醫事放射師全聯會已與全聯會簽訂合作計畫，在放射師的部分也即將進行，因此藉學會年會的課程，期望可將平台操作介紹給放射師周知。

OB-001

和信核醫診療標靶藥物中心 [^{68}Ga] Ga-PentixaFor 之 TLC 與 Radio HPLC 分析方法確效

楊詩涵、李銘忻、洪綾蔓、林亭君、黃玉儀

和信治癌中心醫院核子醫學科

背景介紹：[^{68}Ga]Ga-PentixaFor 為腫瘤細胞表現 CXCR4 受體之 PET 診斷新藥，具有發展成為新一代 Theranostics 用藥的強大潛力。本中心參考德國原廠 PentixaPharm 公司所提供之分析方法確效文件及 [^{18}F]PSMA-1007 分析方法，制定本中心之 [^{68}Ga]Ga-PentixaFor 分析方法確效，以符合正子調劑作業準則要求。

方法：放射化學特性及放射化學純度此 2 項分析項目是使用色層分析儀 (AMM/TLC-Scan) 與高效能液相層析儀 (Shimadzu LC-40D) 與輻射偵檢器 (EZ PMT SCINT Detector) 組合之放射性高效能液相層析儀 (Radio HPLC) 進行分析。本中心針對此 2 個設備建立 TLC 與 Radio HPLC 分析方法確效。確效過程中對 GMP grade 之 Ga-68 淘洗液（淘洗液）、[^{68}Ga]Ga-PentixaFor 注射劑（注射劑）、[^{69}Ga]Ga-PentixaFor 標準品（標準品）溶液及去離子水進行測定，繼而確認系統適用性 (System suitability)、可重複 (Repeatability)、線性範圍 (Linearity)、量測方法靈敏度 (Sensitivity at the Limit of Quantification)、專一性 (Specificity)、精密度 (Accuracy)、準確度 (Precision)、同一性 (Identity) 及放射化學純度 (Radiochemical Purity) 等系統性分析方法規範之標準。

結果：TLC 分析方法注射劑主峰面積百分比測量的再現性標準偏差 (SD) < 0.2% (N = 3)。淘洗液主峰面積線性回歸係數 (R^2) > 0.99。靈敏度為最低定量濃度 (LOQ) ≤ 0.0135 mCi/mL。淘洗液 Rf (Retardation Factor) < 0.3 和注射劑 Rf > 0.7。放射化學純度測定顯示，離子和膠體雜質 (PICI) ≤ 3%，放射化學純度 (RPTLC) > 97%。

Radio-HPLC 分析方法標準品溶液 RT (Retention Time) 為 4 至 6 分鐘。標準品溶液 RT 測量重複性的變異係數 (% RSD) < 1.0%，主峰面積的變異係數 (% RSD) < 20.0% (N = 5)。淘洗液主峰面積與活度關係的線性回歸係數 (R^2) 均符合標準。靈敏度為最低定量濃度 (LOQ) ≤ 0.00135 mCi/mL。淘洗液 RT 為 1 至 4 分鐘，注射劑 RT 為 4 至 6 分鐘。注射劑 RT 精密度標準偏差 (SD) < 10%。注射劑 RT 準確度在標準品溶液 RT ± 10% 範圍內。通過 0.9 ~ 1.1 範圍內的相對保留時間 (RRT)，證實了注射液和標準品溶液的同一性。放射化學純度測定顯示，各別的非膠體放射性不純物 (NCRI) ≤ 2.5% 且總量 ≤ 6%，放射化學純度 (RPHPLC) ≥ 94%。

結論：本文建立 [^{68}Ga]Ga-PentixaFor 之 TLC 及 Radio-HPLC 分析方法，確效結果均符合德國原廠 PentixaPharm 公司所提供之分析方法確效應達標準，顯示本中心儀器及分析方法適合 [^{68}Ga]Ga-PentixaFor 之 GMP 品管程序。

OB-002

醫療院所正子造影時採用自動注射系統與手動注射程序之醫護人員輻射劑量比較

陳惠萍、吳姿萱、張賴昇平

聯新國際醫院核子醫學科

背景介紹：目前市面上已有數款應用於核醫／正子的自動注射系統，為探討自動注射系統是否可有效降低醫護人員接受劑量，以符合合理抑低之精神，本次利用小型可攜帶式輻射偵檢器監測醫護人員在使用自動注射系統與手動注射 ^{18}F-FDG 過程時劑量率，再乘以注射時間，即可換算注射過程時接受劑量並比較其差異。

方法：醫護人員配戴小型可攜帶式輻射偵檢器於手腕和胸口前，模擬注射時肢端和軀幹劑量率，分別收集自動注射系統與手動注射 ^{18}F-FDG 各 36 名病患所測量之劑量率，測量時紀錄最高值，乘以注射時間，可保守計算得出每支 ^{18}F-FDG 在使用自動注射系統與手動注射接受劑量。數據分析時，將 ^{18}F-FDG 活度全部回推至標準活度 (10 mCi) 以利分析及比較。

結果：在使用自動注射系統情況下，醫護人員肢端平均劑量率為 (1.86 ± 1.16) μSv/h，軀幹平均劑量率為 (1.47 ± 0.82) μSv/h，注射平均時間為 (147 ± 4) sec，計算使用自動注射系統注射每支 ^{18}F-FDG 藥劑醫護人員肢端平均劑量為 (76 ± 46) nSv，軀幹平均劑量為 (60 ± 32) nSv。使用手動注射情況下，醫護人員肢端平均劑量率為 (567.0 ± 230.1) μSv/h，軀幹平均劑量率為 (113.23 ± 70.66) μSv/h，注射平均時間為 (64 ± 9) sec，計算手動注射每支 ^{18}F-FDG 藥劑醫護人員肢端平均劑量為 $(1.02 \pm 0.45) \times 10^4$ nSv，軀幹平均劑量為 $(2.01 \pm 1.27) \times 10^3$ nSv。並由上述結果可得知，在使用自動注射系統時，肢端劑量為手動注射的 1/130 (0.77%)，軀幹劑量為手動注射的 1/34 (3.0%)。

結論：採用自動注射系統注射藥劑，可大幅降低醫護人員所接受劑量。

OB-003

和信核醫診療標靶藥物中心 [^{68}Ga]Ga-PentixaFor 製程確效

洪綾蔓、李銘忻、楊詩涵、林亭君、黃玉儀

和信治癌中心醫院核子醫學科

背景介紹：CXCR4 (The C-X-C motif transmembrane chemokine receptor-4) 為一穿膜趨化因子接受體，其參與胚胎發育、血管新生、造血作用及發炎等生理過程，它的過度表現被發現在促進腫瘤生長和進展、腫瘤侵襲和轉移過程中發揮著關鍵作用。[^{68}Ga]Ga-PentixaFor 是一種對 CXCR4 具有高親和力的 PET 診斷用藥。本院依據「斷層掃描用正子放射同位素優良調劑作業準則」及「西藥藥品優良製造規範」法規，建立 [^{68}Ga]Ga-PentixaFor 標準調劑作業程序並執行製程確效，以建構本院 [^{68}Ga]Ga-PentixaFor 標準製程。

方法：^{68}Ge/^{68}Ga generator (GalliaPharm® 1850 MBq, Eckert & Ziegler) 以高純度無菌 0.1 M HCl (Eckert & Ziegler) 淘洗，利用 Eckert & Ziegler Radiopharma GmbH 正子藥物注射劑合成盒 Modular-Lab PharmTracer system，搭配 C4-GA-PEP 拋棄式合成器卡匣、EZ-102 試劑，以 90 ~ 95℃加熱 200 ~ 300 秒為反應參數，使 Ga-68 和前驅物 PentixaFor 50 μg (GMP, ABX) 進行標誌反應。反應完成之溶液經由 C18 管柱純化後，在 A 級區以 0.22 μm 濾膜過濾除菌，完成 GMP 級 [^{68}Ga]Ga-PentixaFor 注射劑調劑。依據 [^{68}Ga]Ga-PentixaFor 注射劑製程 HACCP 風險分析，並配合放行之最終產品規格，找出影響關鍵參數之測試項目：活度濃度、比活度、產率、無菌度試驗、內毒素試驗、TLC 完整之系統適用性、Radio-HPLC 完整之系統適用性、GC 完整之系統適用性及 pH 值，和傳輸管線清潔時間 (Holding time) 以 60 分鐘為最差狀況 (Worst case) 等，進行三批次製程確效。

結果：反應完成之 [^{68}Ga]Ga-PentixaFor 溶液，以 0.22 μm 濾膜過濾除菌，完成 [^{68}Ga]Ga-PentixaFor 注射劑調劑。[^{68}Ga]Ga-PentixaFor 三批次製程確效結果，Bulk 放射活度於校正時間之活度濃度大於 0.6 mCi/mL，比活度介於 0.1 ~ 1.0 Ci/μmole，產率大於 60%，內毒素試驗結果小於 35 EU/mL，TLC 完整之系統適用性，Blank 不存在放射性波峰或面積小於 [^{68}Ga]Ga-PentixaFor 注射劑主峰面積的 1.0 %，Radio-HPLC 完整之系統適用性結果，[^{68}Ga]Ga-PentixaFor 在 Radio-HPLC 之 UV detector 波峰出現時間與 [^{69}Ga]Ga-PentixaFor 相同，GC 完整之系統適用性，[^{68}Ga]Ga-PentixaFor 波鋒面積不超過 10% 乙醇之波鋒面積，pH 值介於 3.5 ~ 8.0 之間，無菌度試驗在 14 天培養結果為符合規格；最後傳輸管線清潔時間於最差狀況 (Worst case) 60 分鐘做清潔確效結果亦符合標準。

結論：為了提高 [^{68}Ga]Ga-PentixaFor 產率，將 [^{68}Ga]Ga-PentixaFor 製程做了些微調整，並執行連續三批次確效。確效結果皆符合標準，確立本院 [^{68}Ga]Ga-PentixaFor 注射劑之標準調劑作業流程。

OB-004

Pharmacokinetics Study of PSMA-INER-56 by Liquid Chromatography Tandem Mass Spectrometry

Shih-Min Wang, Ming-Wei Chen, Wei-Lin Lo, Wan-Chi Lee, Shih-Wei Lo, Shiou-Shiow Farn

Isotope Application Division, Institute of Nuclear Energy Research, Taoyuan, Taiwan

Introduction: Prostate-specific membrane antigen (PSMA) has become one of the most promising molecular targets in nuclear medicine against prostate cancer. In previous studies, we designed PSMA-specific peptide ligands: PSMA-INER-56. In this study, PSMA-INER-56 will be investigated for in-vitro and in-vivo pharmacokinetics. The in-vitro pharmacokinetics were inclusion plasma stability and liver microsome stability of PSMA-INER-56 and based on this results, suggest appropriate compounds for in vivo pharmacokinetic analysis.

Methods: The in-vivo pharmacokinetics non-GLP study will be conducted in BALB/c mice through single IV (10 mg/kg) dosing route, mice plasma was collected at designed time points (1, 2, 5, 8, 24, 72, 120 and 168 hrs) after dosing. De-protein plasma sample was analyzed by API 4000 liquid chromatography-tandem mass spectrometry system equipped with an Agilent 1200 series high-performance liquid chromatography system. PK parameters will be calculated using WinNonlin 8.1.

Results: The test compound (PSMA-INER-56) were analyzed in the multiple reaction-monitoring mode using the mass transitions m/z 1444.9 → 1272.6. The method was linear in the concentration range of 1–2000 ng/mL with coefficients of determination (R^2) of 0.993 in mice plasma. The maximum plasma concentration (Cmax) was 13.15 ± 6.54 (μg/mL) and occurred at 1.75 ± 0.50 (h) (Tmax). The elimination half-life (T1/2) was 13.33 ± 3.13 (h).

Conclusions: The above results establish the foundation for the stability and pharmacokinetics of the drug, which is great help to subsequent drug development.

OB-005

和信核醫診療標靶藥物中心 [^{68}Ga] Ga-Trivehexin 標準調劑研製

李銘忻、洪綾蔓、楊詩涵、林亭君、黃玉儀

和信治癌中心醫院核子醫學科

背景介紹：近年來，αvβ6- 整合素 (αvβ6 Integrin) 已成為一種極具潛力之診療標靶 (theranostic target)，可用於精確描繪快速生長的惡性細胞。TGF-β 激活細胞粘附受體 αvβ6- 整合素的表達與癌症惡性腫瘤密切相關，因為它驅動侵襲和轉移。αvβ6- 整合素在腫瘤細胞中呈高密度存在，特別是胰腺導管腺癌 (PDAC)；αvβ6- 整合素也存在於鱗狀細胞癌、宮頸癌、肺腺癌和其他癌症以及纖維化疾病（特發性肺纖維化、IPF）中。目前臨床非常需用於表達 αvβ6- 整合素之 PDAC 癌症惡性腫瘤診斷，而 [^{68}Ga]Ga-Trivehexin 是一種對 αvβ6 具有高親和力的極佳 PET 診斷用藥。為使進入臨床應用，須遵循「斷層掃描用正子放射同位素優良調劑作業準則」相關 GMP 法規調劑，建立自動化標誌 [^{68}Ga]Ga-Trivehexin 反應參數與品管分析方法是臨床前最重要之工作。

方法：^{68}Ge/^{68}Ga generator (GalliaPharm® 1850 MBq, Eckert & Ziegler) 經由高純度無菌 0.1 M HCl (Eckert & Ziegler) 淘洗 Ga-68 radionuclide，傳輸進入 Eckert & Ziegler Radiopharma GmbH 正子藥物標誌合成盒 (Modular-Lab PharmTracer system, MLPT)，搭配 C4-GA-PEP 無菌低熱原合成器卡匣與無菌反應試劑組 (EZ-102)，以溫度 90 ~ 130℃ 及加熱時間 200 ~ 900 秒為反應參數測試區間，使 Ga-68 核種與前驅物 Trivehexin 50 μg (non-GMP, TRIMT, Germany) 進行標誌反應。反應完成之溶液經由 C18 管柱純化後，與 [^{nat}Ga]Ga-Trivehexin 標準品進行 HPLC 對比分析，找出關鍵參數之最佳化設定參數及分離純化條件。

結果：[^{68}Ga]Ga-Trivehexin 標誌反應參數實驗，確認前驅物 Trivehexin (50 μg) 添加到 4 ~ 5 mL Ga-68 0.1 M HCl 溶液中，並將反應混合物在 90° C 加熱 12 分鐘進行標誌。在 pH 3.5 ~ 4 下獲得高放射化學純度 (RCP) 和高產率的 [^{68}Ga]Ga-Trivehexin。

OC-001

Performance of ChatGPT Incorporated Chain of Thought Method in Bilingual Nuclear Medicine Physician Board Examinations

Yu-Ting Ting[1], Te-Chun Hsieh[1], Yuh-Feng Wang[2,3,4], Yu-Chieh Kuo[5], Yi-Jin Chen[5], Pak-Ki Chan[5], Chia-Hung Kao[1,5]

[1] *Department of Nuclear Medicine and PET Center, China Medical University Hospital, Taichung, Taiwan*
[2] *Department of Nuclear Medicine, Taipei Veterans General Hospital, Taipei, Taiwan*
[3] *Department of Biomedical Imaging and Radiological Sciences, National Yang Ming Chiao Tung University, Taipei, Taiwan*
[4] *Department of Medical Imaging and Radiological Technology, Yuanpei University of Medical Technology, Hsinchu, Taiwan*
[5] *Artificial Intelligence Center, China Medical University Hospital, Taichung, Taiwan*

Purpose: The study aims to assess ChatGPT ability to accurately answer questions and provide responses in a multilingual environment, while also documenting its performance and analyzing its responses to various problems.

Methods: The study utilized Generative Pre-Trained Transformer (GPT) models, specifically GPT-4, which is based on the Transformer architecture and designed for natural language processing tasks. Additionally, the study incorporated the Chain-of-Thoughts (COT) method, which focuses on providing detailed explanations of the thought process involved in problem-solving. The bilingual format of the nuclear medicine exam, composed in Mandarin Chinese and English, posed a significant challenge for ChatGPT. The experiment analyzed the performance of different variants of GPT-4, including the integration of COT, and compared their scores with those of actual physician candidates.

Results: The results of the experiment demonstrated the potential and capabilities of GPT-4. The average score attained by ChatGPT4-May (COT), the variant enhanced with COT, was the highest among the candidates. GPT-4, particularly the May version, exhibited significant improvements compared to the earlier March version. The analysis of different sections of the exam showed GPT-4 competence in theory-based questions, with correctness rates ranging from 76% to 88%. However, GPT-4 did not perform well in the Medical Regulatory Questions section.

Conclusions: This research contributes to the evaluation and refinement of large language models like ChatGPT in the field of clinical medicine, paving the way for their future applications and advancements.

OC-002

Systolic Function: Correlation of Myocardial Perfusion Imaging with Acoustic Cardiography

Ya-Min Chi[1], Chin-Chuan Chang[1,2]

[1] *Department of Nuclear Medicine, Kaohsiung Medical University Hospital, Kaohsiung, Taiwan*
[2] *School of Medicine, College of Medicine, Kaohsiung Medical University, Kaohsiung, Taiwan*

Introduction: With advancement of nuclear cardiology imaging, myocardial perfusion imaging (MPI) had not only been used solely for evaluation of ischemic heart, but also for evaluation of systolic function. However, problems with expense, scheduling, and radiation exposure limit the potential of MPI application in clinical scenario. Acoustic cardiography, a cheap, non-invasive, and readily available examination, had increasingly been used for evaluation of electronic and mechanical functions of the heart. The purpose of this study was to investigate the correlation of acoustic cardiographic findings to that of myocardial perfusion imaging.

Methods: This study was done retrospectively and patients with both myocardial perfusion imaging and acoustic cardiography performed within three months were screened for inclusion. Patients who had invasive interventions (such as percutaneous intervention) between the two studies or right before either examination were excluded to avoid confounding effects. Correlations between systolic function parameters of MPI (summed motion score [SMS], summed thickening score [STS], and left ventricular ejection fraction [LVEF]) and that of acoustic cardiography (electromechanical activation time [EMAT], third heart sound [S3], fourth heart sound [S4] and systolic dysfunction index [SDI]) were analyzed using Spearman's rank correlation test.

Results: A total of 78 patients with complete data were analyzed. SMS showed correlation with EMAT, LVST, and SDI with correlation coefficient of 0.410, -0.346, 0.5698 and p value of 0.0032, 0.232, and < 0.001, respectively. STS showed correlation with EMAT, LVST, and SDI with correlation coefficient of 0.410, -0.393, 0.602 and p value of 0.0032, 0.0052, < .0001, respectively. LVEF showed correlation with EMAT, LVST, and SDI with correlation coefficient of -0.466, 0.402, -0.647 and p value of 0.0004, 0.004, < .0001 respectively.

Conclusions: Among the parameters of acoustic cardiography, SDI showed the highest linear correlation with that of MPI (SMS, STS, and LVEF), but with only moderate correlation. Hence, both MPI and acoustic cardiography should be done to fully evaluate a patient systolic function.

OC-003

A Comparison of Advanced Primary Oral Cancer (T4) Using PET/CT and MRI

Li-Jen Huang

Chung-Shan Medical University, Taichung, Taiwan

Introduction: Head and neck MRI and FDG PET/CT have long been used to assess the staging of oral cancer in Taiwan.

Methods: This retrospective study included 204 patients (184 men, 20 women; median age, 59 years) with oral cancer who underwent both PET/CT and MRI staging tests within 30 days before pathological proof; two nuclear medicine physicians independently reviewed FDG PET/CT examinations. Eight radiologist physicians independently reviewed MRI examinations. The T, N, and M categories were subsequently assessed using the oral cancer TNM staging guideline.

Results: Accuracy for pT4 oral cancer T staging was lower ($p < .05$) for head and neck MRI (72.59%) than for FDG PET/CT (84.8%). When we add in delayed imaging of PET/CT, the accuracy for T category was also lower ($p < .05$) for head and neck MRI (72.86%) than for FDG PET/CT (84.29%). If we add in additional PET/CT parameters, the most promising of which is total lesion glycolysis, the accuracy for T category still did not show a significant increase ($p > .05$) for PET/CT imaging, but was still significantly more accurate as compared with head and neck MRI (87.14 % vs. 72.86%)

Conclusions: In terms of T staging of oral cancer, MRI was outperformed by FDG PET/CT for T category and assessing extent of local invasion in advanced T (T4) oral cancer.

OC-004

Detection of Medullary Thyroid Carcinoma by Carcinoembryonic Antigen and FDG PET/CT

Po-Sung Huang, Hsiao-Min Chou, I-Lin Su, Yen-Kung Chen

Department of Nuclear Medicine and PET Center, Shin Kong Wu Ho-Su Memorial Hospital, Taipei, Taiwan

Purpose: Medullary thyroid carcinoma (MTC) arises from the parafollicular C cells of the gland. Calcitonin is known as a tumor marker essential for the diagnosis and follow-up of MTC. Carcinoembryonic antigen (CEA) can also be used as a tumor marker because most MTCs often secrete CEA. The full-body scan of fluorodeoxyglucose-positron emission tomography/computed tomography (FDG-PET/CT) may be an assistant for the detection of occult tumors that result in CEA elevation, such as MTC.

Materials and Methods: We collected patients who have the elevation of CEA performed FDG PET/CT and confirmed MTC, retrospectively. All 7 patients whose medical records and results of FDG positron emission tomography (PET)/computed tomography (CT) studies are available after the initial diagnosis are included. Statistical calculations are completed using IBM SPSS Statistics, and $p < 0.05$ is considered statistically significant.

Results: From January 2001 to May 2023, 7 patients (3 female, 4 male; from 25 years to 61 years, median age: 49 years) who have elevated CEA noted and worried about possible colorectal cancer or others. Therefore, they chose to receive FDG-PET/CT for further evaluation. However, the images revealed a thyroid gland with focal FDG uptake. There are 4 patients who accepted the measurement of serum calcitonin and a high calcitonin level was detected. All these 7 patients received histopathology proved medullary thyroid carcinoma. There are 3 patients who were found to have cervical nodal metastasis.

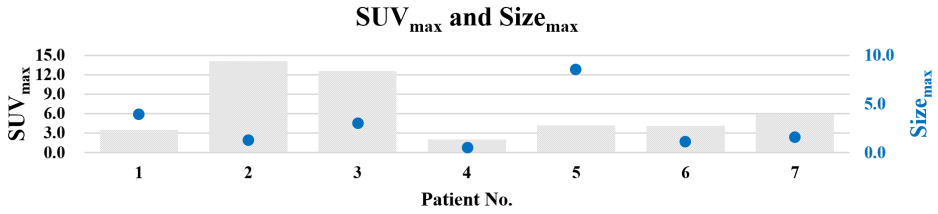

Figure 1. The characteristics of SUVmax and Sizemax among patients.

Conclusion: FDG-PET/CT may detect occult tumors resulting in CEA elevation other than colorectal cancer or lung cancer. Rising CEA levels and coexistence with focal FDG uptake in the thyroid gland can be associated with MTC. Calcitonin correlation should be considered for the possibility of MTC, whether the metabolic activity of thyroid nodules was faint to intense. The occurrence of nodal metastasis seems to be unrelated to the FDG uptake intensity or sizes of the thyroid nodules.

Keywords: Carcinoembryonic antigen, Calcitonin, Fluorodeoxyglucose-positron emission tomography/computed tomography, Medullary thyroid carcinoma

OC-005

Validation of a Real-Time External Dosimetric Detection Method for Biokinetics of Radioiodine in Patients with Thyroid Cancer Undergoing Radioiodine Treatment

Yao-Kuang Tsai[1], Cheng-Yi Cheng[1], Ching-Yee Oliver Wong[2], Daniel Heung-Yuan Shen[3], Sui-Lung Su[4], Chin Lin[4], Li-Fan Lin [1], Sin-Yu Lin[4], I-Feng Chen[1]

[1] *Department of Nuclear Medicine, Tri-Service General Hospital and National Defense Medical Center, Taipei, Taiwan*
[2] *Sutter Health, Sacramento, California, USA.*
[3] *Department of Nuclear Medicine, Kaohsiung Veterans General Hospital, Kaohsiung, Taiwan*
[4] *School of Public Health, National Defense Medical Center, Taipei, Taiwan*

Purpose: The biokinetics of radioiodine in patients with thyroid cancer are complicated and difficult to achieve. This study aimed to validate a simplified, real-time external dosimetric detection method by recording continuously the radiation doses in patients undergoing radioiodine treatment for thyroid cancer.

Methods: The data of patients with differentiated thyroid carcinoma were retrospectively reviewed. After administration of radioiodine, the radiation doses were continuously recorded every five minutes by built-in counters on the ceiling above patients' beds. The data were fitted to a biexponential equation to obtain the estimated ^{131}I uptake fraction of thyroid tissue (K) and effective half-life (T) of non-thyroid tissues. Pearson's correlation analysis was applied to evaluate the correlation of K and T values with different biological characteristics.

Results: In total, 36 patients received radioiodine therapy with mean administered dose of ^{131}I 3.76 ± 1.15 GBq. The mean calculated K and T values were 0.09 ± 0.06 and 7.45 ± 1.43 hours, respectively. Pearson's correlation analysis showed significant correlation between K values and ^{99m}Tc uptake ratios and whole-body radiation retention ratio ($p < 0.05$). No significant associations were noted between T values and BMI, age and renal function.

Conclusion: This simple real-time external dosimetric detection method may be a non-invasive simple approach to the biokinetics of radioiodine. The estimated K value is significantly associated with ^{99m}Tc Pertechnetate uptake ratio and may reflect the metabolic size of residual thyroid tissues post total thyroidectomy. This approach has been validated in this study as a potentially effective method for clinical use.

OC-006

僅執行肺灌流檢查對於肺栓塞與慢性血栓栓塞性肺高壓診斷準確性之影響

李俊德

臺北榮民總醫院核子醫學部

背景介紹：肺臟血流灌注配合肺臟通氣檢查 (V/Q scan)，是臨床時常用來診斷肺栓塞 (PE) 以及慢性血栓栓塞性肺高壓 (CTEPH) 的工具。然而，受限於病人的配合程度、氣化 Tc-99m DTPA 的工具、科部空間等等因素，台灣僅有少數醫院同時執行通氣與灌流檢查。V/Q scan 現行的執行與判讀標準，主要依據 Modified PIOPED-II criteria 以及 EANM guideline for V/Q scan。兩份標準皆建議需同時執行通氣與灌流檢查，以獲得較為準確的結果。本報告嘗試探究僅執行灌流而不執行通氣檢查，是否對病人的報告判讀結果有所影響。

方法：透過本院的報告系統，回溯過去一年中同時執行 V/Q scan 的病人，共 20 位，每位皆重新調閱影像，判讀病人是否有通氣或者灌流缺損，以及 V/Q mismatch 情形。並配合病人執行檢查後一年之醫療病歷紀錄，作為判斷檢查準確性的標準。其中，特別選出 6 位病人做病例系列探討。

結果：被選出的 6 位病人，皆為灌流檢查有缺損的病人。進一步探討 6 位病人的影像可以發現，當中 3 位病人的通氣影像為正常，另 3 位病人的通氣影像雖有缺損，但配合其他解剖性影像，依然可判斷缺損為 segmental/subsegmental、或者是解剖結構變化所導致。

結論：透過 6 個 V/Q scan positive 病人的探究結果，發現灌流出現缺損時，可以配合解剖影像，判斷缺損為 segmental/subsegmental 或者僅是解剖構造異常。通氣試驗進行與否，對於判讀準確率無影響。因此，大部分醫院不執行通氣試驗，或許是可行的替代方案。

OC-007

Comparison of ^{18}F-FLT and ^{18}F-FDG PET/CT for Evaluation of Nasopharyngeal Carcinoma

Xuan-Ping Lu, Pan-Fu Kao

Department of Nuclear Medicine, Chung Shan Medical University Hospital, Taichung, Taiwan

Introduction: [F-18]-FDG PET/CT is currently widely used for staging and detecting recurrences in nasopharyngeal carcinoma. However, [F-18]-FDG is not a tumor-specific tracer and is often taken up by inflamed tissues, leading to false positives. Additionally, in the staging of nasopharyngeal carcinoma, the higher physiological distribution of [F-18]-FDG in the brain makes it more challenging to determine if cancer has invaded the intracranial space (upgrading from T3 to T4 stage). Shields et al. developed FLT, which uses F-18-labeled thymidine to detect cellular proliferation, thereby achieving the detection of malignant tumors.

Methods: This study is a single-center prospective imaging analysis. Participants were recruited between November 2014 and August 2018 and included patients with pathologically confirmed nasopharyngeal carcinoma who were over 18 years old and had undergone two imaging examinations for staging or recurrence detection. The study aimed to compare FDG and FLT uptake regarding brain involvement. Additionally, comparisons were made for the primary tumor, lymph nodes, and distant metastases.

Results: There were a total of 42 patients, including 11 females and 31 males, with 16 being newly diagnosed staging cases and 26 being recurrence detection cases. In the analysis of the primary tumor, FLT showed a detection rate of 100% for intracranial involvement, while FDG had a rate of 37.5%. For detection of primary tumor in initial staging cases, both imaging modalities detected all primary lesions. In recurrence detection, FDG demonstrated a sensitivity of 71% and specificity of 83%, while FLT exhibited a sensitivity of 92% and specificity of 100%.

Conclusions: FLT had a higher detection rate of intracranial involvement due to the absence of physiological uptake in the brain. Additionally, FLT demonstrated superior specificity compared to FDG in the detection of recurrent lesions. This increased specificity is likely attributable to the reduced occurrence of false positives resulting from post-treatment inflammation. However, it's worth noting that FLT showed physiological uptake in bone marrow and the liver, which could potentially hinder the detection of distant metastases in these locations. Therefore, a complementary approach using both FLT and FDG may be beneficial, especially when assessing intracranial involvement and optimizing lesion detection.

OC-008

Transiently Elevated Thyroglobulin Level After COVID-19 Vaccination in Patients with Differentiated Thyroid Cancer Under Complete Biochemical Response Post Treatment

Hao-Wen Cheng, I-Feng Chen, Li-Fan Lin, Yao-Kuang Tsai

Department of Nuclear Medicine, Tri-Service General Hospital, Taipei, Taiwan

Introduction: Serum thyroglobulin (Tg) is a sensitive biochemical marker for detecting disease recurrence in patients with differentiated thyroid cancer (DTC). Elevated Tg level can result from autoimmune or inflammatory response in thyroid tissues. COVID-19 vaccination triggered thyroid autoimmunity and thyroiditis has been reported. However, data on its effect of Tg level in patients with DTC are limited.

Methods: A retrospective review of the medical records of 107 patients with DTC who received at least one dose of COVID-19 vaccination during July 2021 and March 2022 was performed. All patients included had complete biochemical response after treatment and undetectable Tg before COVID-19 vaccination. Thyroglobulin, free thyroxine (fT4), 3,5,3'-triiodothyronine (T3), and antithyroglobulin (anti-Tg) antibody were measured every three months. Data at baseline (before vaccination), within two months and one year post vaccination were analyzed.

Results: A total of 107 patients with 254 vaccinations were included in the analysis. After vaccination, Tg elevation was noted in 23 patients (21%). Recurrent disease was later confirmed in 7 (30%) patients, while 16 patients had undetectable Tg after 3 months and during one year follow-up, with no evidence of disease recurrence based on imaging findings. Elevated Tg in non-relapsing DTC was noted in all types of vaccines, with no difference among groups (7 [6.6%] Moderna, 4 [6.0%] BNT162b2, 5 [6.2%] AstraZeneca, $p > 0.5$).

Conclusions: A transient increase in Tg levels can be observed in patients with non-relapsing DTC after receiving SARS-CoV-2 vaccination. After 3 months, the elevated Tg levels became undetectable. Active surveillance of Tg levels with a one-year follow-up may be sufficient to rule out disease recurrence.

OC-009

Influence of Gender and Body Habitus on Prediction of Obstructive Coronary Artery Disease in a Deep Learning Model for Myocardial Perfusion Imaging Using CZT SPECT

Yu-Cheng Shih[1], Yen-Wen Wu[1,2]

[1] *Department of Nuclear Medicine, Far Eastern Memorial Hospital, New Taipei City, Taiwan*
[2] *Division of Cardiology, Cardiovascular Medical Center, Far Eastern Memorial Hospital, New Taipei City, Taiwan*

Introduction: Myocardial perfusion imaging (MPI) plays an important role in the detection of obstructive coronary artery disease (CAD) and guides treatment strategy. Conflicting evidence exists regarding the varying accuracy of MPI between men and women, as well as among patients with differing body habitus, probably due to soft tissue attenuation. Recently, deep learning (DL) models for single photon emission computed tomography (SPECT) MPI have demonstrated promising potentials in improving diagnostic accuracy as compared with clinical visual reading or current quantitative methods. This study aims to evaluate whether gender and body habitus affect the diagnostic performance of a DL approach for CAD using CZT SPECT.

Methods: Patients who underwent stress thallium-201 MPI and invasive coronary angiography within 90 days at our institute between January 2013 and December 2021 were retrospectively reviewed, and patients with a history of myocardial infarction or prior coronary revascularization were excluded. We compared the diagnostic performance in both genders, as well as in both obese (BMI >27 kg/m^2) and non-obese patients, using receiver operating characteristics curves (ROC) in our self-developed DL model.

Results: A total of 3,324 consecutive patients, including 1,080 women and 2,244 men, were analyzed. In both per-patient and per-vessel analyses, there were no significant differences in the area under the ROC curves (AUCs) for predicting obstructive CAD between genders or among obese/non-obese groups (men/women: per-patient, 0.704 vs. 0.702; P= 0.93; per-vessel, 0.719 vs. 0.728; P = 0.50; obese/non-obese: 0.700 vs. 0.716; P = 0.39; per-vessel, 0.729 vs. 0.722; P = 0.57). Notably, only the AUC for right coronary artery (RCA) disease was significantly higher in women than in men (0.774 vs. 0.721; P = 0.03), might be due to differences in body contour or soft tissue attenuation pattern between genders.

Conclusions: Our DL model showed similar accuracy in predicting obstructive CAD between men and women, as well as among obese and non-obese patient groups. Evaluation of impact of different clinical parameters on DL model MPI can facilitate acceptance of explainable artificial intelligence diagnosis of CAD following MPI.

OC-010

Artificial Intelligence-Assisted Hepatic Arterial Perfusion Imaging in Predication of Survival in Patients with Advanced Hepatocellular Carcinoma after Hepatic Arterial Perfusion Chemotherapy

Dung-Ling Yu[1], I-Cheng Chang[2], Meng-Chieh Yu[2], Hsuen-Fu Lin[3], Chun-Hung Cho[3], Guan-Ting Pan[2]

[1] *Department of Nuclear Medicine, Mennonite Christian Hospital, Hualien, Taiwan*
[2] *Department of Computer Science and Information Engineering, National Dong Hwa University, Hualien, Taiwan*
[3] *Department of Medical Oncology, Mennonite Christian Hospital, Hualien, Taiwan*

Introduction: Hepatic arterial infusion chemotherapy (HAIC) has been used for the treatment of advanced hepatocellular carcinoma (HCC). The purpose of the study is to use artificial intelligence (AI)-assisted analysis of hepatic arterial perfusion imaging (HAPI) to predict survival of patients with advanced HCC after HAIC.

Methods: There were 105 patients (M:F = 76:29, age range = 41–94 y/o, mean age = 62.8 y/o) with advanced HCC included in this study. HAPI was performed immediately after injection of 3 mCi of Tc99m MAA through the intrahepatic catheter on all patients, with 85 patients receiving one HAPI and 20 patients receiving 2 to 4 HAPIs. Totally, 132 HAPIs were collected for analysis. All patients received 5-FU based HAIC, and followed up at least 12 months after HAIC. HAPI images from all patients were adopted as the experimental dataset, with an image size of 128*128, and each patient was associated with 128 image slices. The dataset was clustered into two categories: patients surviving over one year and those surviving less than one year. We developed a survival prediction system to determine if the patient can survive more than one year. The proposed system adopted EfficientNet as the core model since it had better performance when applied to datasets with a small size.

Results: We employed K-FOLD cross-validation to evaluate the prediction accuracy because of the small size of HAPI dataset. This approach helped to mitigate potential bias or imbalance issues with the fixed testing set, ensuring more accurate accuracy evaluations. In our experiments, the HAPI dataset was divided into 10 equal parts, alternating each part as the testing set while using the rest as the training set. Our AI-based prognostication of one-year overall survival achieved an accuracy of approximately 62%, demonstrating there was a correlation between patient survival and HAPI images.

Conclusion: Our preliminary study shows AI-assisted analysis of HAPI has the potential to predict survival in patients with advanced HCC after HAIC.

OC-011

Extracardiac Activity and Low Energy Photon Attenuation Associated with the Diagnostic Performance of Myocardial Perfusion Imaging with CZT Cameras

Chun-Yi Chen, Chi-Lun Ko

Department of Nuclear Medicine, National Taiwan University Hospital, Taipei, Taiwan

Introduction: The accuracy of Tl-201 myocardial perfusion imaging (MPI) can be compromised by artifacts caused by photon attenuation and extracardiac activity (ECA). We developed a method to quantify ECA and low energy photon attenuation, and to evaluate their effects on the diagnostic performance of MPI.

Methods: We retrospectively collected data from 3,986 consecutive patients undergoing Tl-201 MPI using cadmium-zinc-telluride (CZT) cameras and subsequent coronary angiography (CAG) within 90 days. Those who had prior coronary revascularization were excluded. Patients were randomly divided into a training cohort and a validation cohort. We used an in-house automated software to segment the left ventricular (LV) myocardium and to calculate stress total perfusion deficit (sTPD). We used a 7% sTPD cutoff to predict obstructive CAD. In each projection image's LV region, we counted major gamma photons with energy windows centered at 167 keV and 135 keV, and the high energy proportion (HEP) was calculated. We estimated the proportion of extracardiac activity (ECA) with respect to normalized myocardial activity. ECA was further categorized into two groups, depending on whether it was closer (ECA1) or farther (ECA2) from the detector than the center of the LV. Mean values and standard deviations of these parameters were computed. A logistic regression model was developed by stepwise feature selection to predict concordant studies. Receiver operating characteristic (ROC) curves were constructed to validate the findings.

Results: The prevalence of obstructive CAD was 56%. In the training cohort (n = 2,990), the probability of concordance (PC) was successfully modeled as 1/(1+e^-(20.09-6.127×meanECA1-35.65×meanHEP)), $p < 0.0001$. The area under the ROC curve (AUC) in the PC ≥ 0.66 group (n = 2,169, 73%) was significantly higher than the PC < 0.66 group (n = 821, 27%) (0.783 vs. 0.682, $p < 0.0001$). This model's significance was confirmed in the validation cohort (n = 996, AUC: 0.789 vs. 0.683, p = 0.0056).

Conclusions: Extracardiac activity and low energy photon attenuation were significantly and negatively associated with the diagnostic performance of MPI using CZT cameras. By quantification of these parameters, we proposed a predictive model that effectively identified images more susceptible to artifacts.

OC-012

移動校正改善 ^{201}Tl 快速半導體單光子斷層掃描儀心肌血流定量的準確度

徐丞、陳怡潔、黃奕琿、柯冠吟、鄭媚方、柯紀綸

國立臺灣大學醫學院附設醫院核子醫學科

背景介紹：以往對小血管性疾病或瀰漫性冠狀動脈病變導致的平衡性缺氧診斷會使用正子心肌灌注掃描所測出的心肌血流 (MBF) 及血流儲備分率 (MFR) 作為平衡型缺氧的診斷依據。新型心臟專用快速半導體單光子斷層掃描儀 (CZT) 可以克服傳統單光子掃描儀無法做動態影像的限制，因此也可以測量 MBF 及 MFR。近期關於 CZT 動態心肌灌注掃描的血流定量分析發展愈趨成熟，然而患者因呼吸、心跳和移動會影響 MBF 及 MFR 的計算。但尚未有利用位移校正 (motion correction, MC) 於定量心肌血流及儲備分率之估算相關研究，因此本研究要探討 MC 對 MBF 以及 MFR 的影響。

方法：本研究回溯收集 22 位分別執行 ^{13}N-NH$_3$ 正子動態心肌灌注檢查和 ^{201}Tl 動態心肌灌注檢查的病人影像進行分析。以 PMOD 分析 ^{13}N-NH$_3$ 影像測量出的 MBF 與 MFR 作為標準，比較有位移校正 (MC) 或無位移校正 (NMC) 之 ^{201}Tl 影像計算的 MBF 以及 MFR 數值。本研究針對整體心臟 (global) 和心臟內三條主要血管流域（左前降冠狀動脈、左迴旋冠狀動脈和右冠狀動脈）的 MBF 和 MFR 的差異及相關程度進行分析討論。任兩組血流數據使用 Paired Sample t-test 分析其差異性，使用線性迴歸分析計算皮爾森相關係數表示其相關性，對於兩組相關係數的差異使用 Fisher r-to-z 轉換進行統計檢定。

結果：^{201}Tl 影像不管是否進行移動校正，global MBF 及 global MFR 的平均值與 ^{13}N-NH$_3$ 沒有顯著差異 (all $p > 0.1$)。與 NMC 影像相比，MC 影像計算出來整體心肌及三條血管流域的 stress MBF 與 ^{13}N-NH$_3$ 呈現顯著更強的正相關 (all $p < 0.05$)，而 rest MBF 則無顯著差異 (all $p > 0.1$)。MC 影像計算出的 MFR 也同樣有顯著更強的相關性 (all $p < 0.05$)。在三條血管的分析中以右冠狀動脈的 stress MBF 及 MFR 差異最大 (stress MBF $r = 0.830$ vs 0.451, MFR $r = 0.862$ vs 0.403, both $p < 0.01$)。

結論：經由這次的研究我們發現有經過位移校正的 ^{201}Tl 檢查會比沒有經過位移校正的檢查不論在整體或是個別血管的 MBF 以及 MFR 都跟 ^{13}N-NH$_3$ 正子檢查結果具有更強的相關性。

PB-001

地震後 I-131 病房及其管路監測機制之建立及實施成效

陸建華、洪佑昇

奇美醫療財團法人柳營奇美醫院核子醫學科

目的：建立地震後 I-131 病房及其管路監測流程及管制機制並評估其成效。

方法：原能會原規定各醫院在發生四級以上地震後須回報廢水管路狀況，復於 111.01. 公告天然災害通報指引，將通報範圍擴大為土石流、病房及管路，為因應該做為，本院立即修訂地震後 I-131 廢水管路偵測流程，遇公告 4 級以上地震後將原只於工作時段處理方式變更為工作和非工作二時段處理，遇工作時段發生時立即由核醫科輻防人員至現場進行偵測、紀錄及回報，如遇非工作時段則先由工務值班人員至現場巡檢後通報核醫科輻防人員，輻防人員依通報狀況判斷現況，經請示後於規定時間內至現場進行偵測、紀錄及回報，如此方式可以及時掌握病房及管路狀況，以避免發生及擴大輻射汙染及輻射暴露之意外事件。

結果：111.09.17. 晚間台南發生 4 級地震，本院即依修正後監測流程由輻防人員至現場進行巡檢、監測、紀錄及通報，巡檢過程發現第一槽廢水槽溢水位燈閃爍異常，經工務人員檢修後判定為地震後水位搖晃致訊號異常，經調整後即恢復正常。

結論：醫院內 I-131 病房及管路是最可能造成輻射汙染及輻射暴露之處，如無適當之監測及管制機制，於地震發生時很可能因震動破壞而造成輻射汙染或人員暴露事件，而監測及管制方式又須適時及不斷地修正，才能達到良好的預防及避免效果。

PB-002

透過流程改善管控血液透析病人做含鐵蛋白之報告核發時間

王安美

馬偕紀念醫院核子醫學科

前言：血液透析病人鐵劑補充原則以檢測含鐵蛋白 (Ferritin) 值為依據之一，每三個月檢測一次，若小於 100 ng/mL 以下，表示鐵質嚴重不足，100 ng/mL 至 300 ng/mL 表示鐵質不足，300 ng/mL 至 500 ng/mL 表示鐵質濃度為理想，若大於 500 ng/mL 則是不需要施打 EPO。故檢測 Ferritin，對血液透析病人主要是針對是否須施打 EPO 及施打 EPO 濃度之重要檢查，亦是針對病人鐵質流失或過量的一個重要指標。本科放射免疫分析實驗室在檢測血液透析病人三個月一次的體檢時，利用一個快速檢測的流程，縮短檢驗報告值核發時間，讓病人可以快速知道結果，以利病人能立即得到適當的治療。

材料與方法：

- 本科實驗室使用 BECKMAN COULTER RIA 檢驗試劑
- Ferritin 標準曲線濃度：0、4.5、17.0、85.0、455.0、1100 (ng/mL)
- Standard Curve FIT（圖一）
- 為避免 Hook effect，實驗室設定量測值大於 800 ng/mL 須做稀釋才可發報告，且稀釋倍數得到之量測值須介於標準曲線中間段，以確保因落於曲線兩端（圖二），曲線的漂移，造成結果值誤差。

流程改善：

- 因血透病人可能接受 EPO 治療以確保體內鐵質足夠，本科收到檢體時，並不知這批次的檢體是否有打 EPO 治療，造成 Ferritin 實際值是高或低，故本組先將每一病人檢體做 5 倍稀釋，以期得到之結果落於曲線中段，再乘上 5 倍之倍數為實際結果值，以降低因原倍的結果值落於曲線尾端須再重稀釋。
- 病人檢體做 5 倍稀釋，若最終結果小於 25 ng/mL 及大於 800 ng/mL 時，因結果值是落於標準曲線兩端，誤差值較大不穩定（圖二），隔日再重測，小於 25 ng/mL 時以原倍操作，大於 800 ng/mL 時再稀釋 10 倍。

結果：一般常規例行性檢查皆是大於測量最高濃度時，須再做稀釋，由於血透的病人結果值皆落在 300 ng/mL 至 700 ng/mL 左右，有些甚至更高，因此本組將全部檢體先做 5 倍稀釋，絕多數皆能於第一次稀釋 5 倍發出適當的結果，且再次重驗率小於約 10%，多數為檢體稀釋後小於 25 ng/mL 須原倍重驗，只有少數結果是稀釋大於 800 ng/mL 要再稀釋 10 倍數，故顯示此流程是可行的。

結論：此流程不僅縮短病人報告核發時間，節省重驗稀釋的試劑成本、時間及人力，亦是醫病雙贏的流程。

PB-003

運用基於產品品質的風險管理方法於正子製藥之污染管制策略 (CCS) 導入

林欣純、李銘忻、楊詩涵、林亭君、洪綾蔓、黃玉儀

和信治癌中心醫院核子醫學科

背景介紹：國際醫藥品稽查協約組織（PIC/S）於去年 111 年 9 月 9 日宣布修改 Annex 1（Manufacture of Sterile Medicinal Products）to Guide to Good Manufacturing Practice for Medicinal Products。隨即衛福部於 112 年 6 月 14 日公告修正「西藥藥品優良製造規範（第一部、附則）」之「附則 1：無菌藥品之製造」，自 112 年 8 月 25 日施行，以供執行 GMP 之遵循。其中強調品質風險管理（Quality Risk Management, QRM）之運用，使風險管理轉化為積極主動之實務，及導入污染管制策略（CCS）原則。顯示出對於無菌藥品製造的品質更加重視的趨勢，尤其是風險管理與污染管制。國際製藥工程協會（International Society for Pharmaceutical Engineering, ISPE）於 2001 年所提出，供製藥工程相關方用於項目調試和確認的方法：Commissioning and Qualification (C&Q)，其於 2019 年再度提出 C&Q, Baseline Guide Volume 5 的更新版，加入了基於產品品質的風險評估過程。因此本篇應用 ISPE 所提出的 C&Q 方法，作為主動積極之品質風險管理工具，並針對 CCS 導入無菌藥品製造的有效性進行評估。

方法討論：本篇以 ISPE 更新版中的 C&Q 方法替代以往 3Q 的 V 模型，並在影響評估方面，由以往的「影響評估」變更為「系統分類」、「系統風險評估」。V 模型代表設計過程與測試之間的聯繫，但未包含基於產品品質的風險評估過程。而 C&Q 方法則採用了與產品關鍵品質屬性（Critical Quality Attribute, CQA）、關鍵製程參數（Critical Process Parameter, CPP）相關聯的風險評估方法，識別系統 / 設備的關鍵構面（Critical Aspect, CA）/ 關鍵設計要素（Critical Design Elements, CDE）。在影響評估方面，更重視系統對產品品質的風險影響。CCS 為對微生物、內毒素／熱原及微粒之一套計畫性的管制，源自對當前產品及製程的瞭解，以確保製程性能及產品品質。核醫診療標靶藥物中心依據品質源於設計 (QbD) 概念，運用以上方法，於產品設計時即建立產品 CQA，依此在製藥過程中建立 CPP、CA 與 CDE，定義所有關鍵控制點並評估所有控制（設計、程序、技術和組織）和監控措施的有效性，用以管理藥品品質風險和安全，使製程方法持續改進。

結論：本篇運用基於產品品質的系統風險管理，採用與 CQA、CPP 相關聯的系統影響評估，以識別影響系統 / 設備的關鍵設計控制：關鍵構面（CA）／關鍵設計要素（CDE），從而決定驗證的範圍和程度，並定期審核。將之應用於整個藥品生命週期之品質風險管理系統，與評估 CCS 的效能，確保在設施內生產的產品的無菌性，提升民眾用藥的安全。

PB-004

使用 QCC 手法降低正子造影影像不良率

曾柏銘[1]、呂建璋[2]、沈淑禎[2]、門朝陽[1]、林雅婷[2]、蕭聿謙[3]

[1]天主教中華聖母修女會醫療財團法人天主教聖馬爾定醫院正子造影中心
[2]天主教中華聖母修女會醫療財團法人天主教聖馬爾定醫院核子醫學科
[3]亞東紀念醫院核子醫學科

前言：FDG PET 由於具有高解析度、可全身掃描的優點，經常用於癌症病患術前評估及術後追蹤，也可用於健康自費檢查。但功能性影像也產生了許多假影如肌肉及腸道顯影，如能提升正子影像品質，則能更利於病患對於癌症之追蹤，增進醫病關係。

方法：本專案收集了自 2022 年 01 ~ 09 月，排除血糖 < 150 mg/dL，共 304 位受檢者，經統計影像品質不良類別包括：1. 腸道異常顯影、2. 肌肉／軟組織 FDG 異常顯影 (SUVmax < 1)、3. 留置針藥物殘留 (SUVmax < 30)、4. Early/Delay phase 兩次影像不一致 5. 褐色脂肪 (Brown Fat) 顯影。正子造影檢查影像品質不良率係指正子造影影像不良人數占總造影人數之比例，經統計改善前影像品質不良率為 69.6%，依 SMART 原則設定挑戰目標 33.8%；再由醫事放射師依三現原則進行查檢，並以柏拉圖 80/20 法則選出 3 項真因：1. 受檢者高渣飲食導致腸道蠕動較快、2. 受檢者不清楚那些運動不能做致運動過度導致肌肉／軟組織 FDG 異常顯影、3. 護理人員注射技術差異致留置針藥物殘留。並由專案成員進行腦力激盪擬訂以下 3 項對策進行改善：

對策一、打擊腸道顯影

經統計後發現食物的種類與數量會影響腸道的顯影，故與營養師共同設計專屬低渣飲食菜單及 QR code，並於檢查前 48 小時以 LINE 個別提醒，24 小時以電話再次提醒受檢者持續進行低渣飲食。

對策二、建置護理人員注射技術標準

使用錄影比對護理師之技術差異並建立正子造影檢查留置針通順機制，導入注射標準口訣「CPRP」使生理食鹽水沖送至留置針通暢，避免藥物堆積。

對策三、建立檢查前活動過度衛教單

簡化衛教單張內容並增加 QR code，並搭配低渣飲食衛教單放置於網頁供查詢。使受檢者能更了解檢查流程中之細節。

結果：正子造影影像品質不良率，從改善前 69.6%，降低至改善後 24.8%，目標達成率 125.1%，進步率 64.4%。「影像品質不良件數」從改善前每月 21 件減少至改善後 9.5 件、「正子造影檢查重照率」從改善前 40.6% 減少至改善後 21.1%。

結論：本專案透過溝通、統計、觀察、詢問來改善正子造影影像品質不良問題，並建立提醒機制，進而大幅降低影像品質不良率，不僅縮短正子掃描影像後處理時間，提升臨床工作效率，也減少正子造影檢查醫療成本，好的影像品質更能幫助醫師提升診斷之正確性，讓受檢者能及早接受治療。

PB-005

Validation of Automated Production of [^{18}F]AlF-NOTA-octreotide for Patients with Neuroendocrine Tumors

Ching-Hung Chiu, Yu-Ting Chien, Wen-Shing Fu, Hsiang-Ping Wen, Chia-Ju Liu, Mei-Fang Cheng, Steven Shinn-forng Peng

PET Center, Department of Nuclear Medicine, National Taiwan University Hospital, Taipei, Taiwan

Introduction: Currently, somatostatin analogues (SSAs) labeled with gallium-68 is widely used globally for somatostatin receptor (SSTR) PET imaging. However, gallium-68, which is produced from a generator, can only image 2–3 patients per elution. It also has a shorter half-life ($t_{1/2}$ = 68 minutes) compared to fluorine-18 ($t_{1/2}$ = 109 minutes), and the high cost of the generator that needs annual replacement poses challenges for routine clinical use. More recently, a fluorine-18-labelled alternative that also targets SSTR2, [^{18}F]AlF-NOTA-octreotide ([^{18}F]AlF-OC) has been introduced. To implement GMP-compliant production in National Taiwan University Hospital (NTUH), we conducted an in-house validation of [^{18}F]AlF-OC production prior initiating an investigational new drug clinical trial.

Methods: In this study, [^{18}F]AlF-OC was fully automatedly produced using a GE TRACERlab F_{XFDG}. Briefly, an eluent solution of NaCl 0.9%/EtOH was added to the reaction vessel. After [^{18}F]AlF was formed by mixing with 2 mM aluminum chloride ($AlCl_3$), a precursor dissolved in sodium acetate was added for chelation. After [^{18}F]AlF was formed by mixing with 2 mM aluminum chloride ($AlCl_3$), a precursor dissolved in sodium acetate was added for chelation. The final product was then eluted with ethanol into a product vial, passing through a sterile Millex-GV 0.22-μm filter and diluted with sterile formulation solution. Radiochemical purity was assessed via radio-HPLC (column: ACE C18, 4.6 x 100 mm; mobile phase: 0.1% TFA in MeCN/0.1% TFA in H_2O), and the product's identity was confirmed by comparing the relative retention of the principal peak with that of a reference solution.

Conclusions: [^{18}F]AlF-OC is automatically produced at the NTUH PET Center in accordance with GMP guidelines. Each production batch consistently meets the defined acceptance criteria, providing adequate product activity for demand. Additionally, stability tests have been conducted at room temperature, confirming product stability up to four hours post-preparation.

PB-006

腦神經退化造影劑 α-syn-4 前驅物合成研究

施宗佑、張博智、陳威希、樊修秀

原子能委員會核能研究所同位素應用組

背景介紹：巴金森氏症是第二種常見的神經退化疾病，其致病機轉與大量堆積 alpha-synuclein（突觸核蛋白）錯誤摺疊有極大關聯，在核子醫學領域，開發氟 -18 標誌正子造影藥物常應用於腦神經疾病診斷。其中，吲哚酮類化合物是一種被廣泛研究於巴金森病診斷的化學物質，可通過引入不同的官能基與支鏈，調節其化學性質與生物活性，舉例來說，作為合適的正子斷層造影 (PET) 顯像劑，在導入適當核種後，其 LogP 值應在 2 ~ 4 之間，因為適當的親脂性可以確保通過大腦血腦障壁且維持良好的水溶性，因此，我們以吲哚酮衍生物（代號 α-syn-3）為基礎，並透過分子模擬優化，設計了新穎性前驅物代號 α-syn-4，優化結果顯示 CDOCKER interaction energy 由 37.8969 增加至 38.1535。根據合成程序，我們分別合成了步驟一產物 3a，產率 50.3%，步驟二產物 4，產率 4.0%，以及最終產物 5 (α-syn-4 前驅物)，產率有 36.8%，總產率達 0.74%。

方法：藉由現有的市售材料，第一，我們參考羥醛縮合反應於加熱迴流的條件下，合成出步驟一產物 3a；第二，我們參考親核性取代反應於溫和的室溫條件下，合成出步驟二產物 4；最後，我們參考親核性取代反應於加熱迴流的高溫條件下，再經由再結晶方式得到前驅化合物 5。

結果：我們藉由光學儀器，高壓液相層析儀、質譜儀以及核磁共振光譜儀的幫助下，成功鑑定了化合物 3a (98.16%)、化合物 4 (97.71%) 與化合物 5 (96.71%) 的結構和純度。

結論：化合物 3a、化合物 4 與化合物 5，我們利用質譜與核磁共振光譜儀鑑定其結構，利用高壓液相光譜儀確認其純度，前驅化合物 5 的純度達到 95% 以上，總產率為 0.74%；雖然總產率偏低，但純度有符合預期，未來將針對總產率去精進並提升，並利用 LC-Mass 進行安定性測試，以達到供給所外醫院進行標誌與動物造影試驗之目的。

PB-007

Development and Preclinical in vivo Evaluation of ^{18}F-Fluoroacetate: Compared to ^{11}C-acetate

Wen-Sheng Huang[1,2], Chi-Wei Chang[3], Tsung-Hsun Yu[2], Skye Hsin-Hsien Yeh[2,4]

[1] *Department of Nuclear Medicine, Cheng Hsin General Hospital, Taipei, Taiwan*
[2] *School of Medicine, National Defense Medical Center, Taipei, Taiwan*
[3] *Primo Biotechnology, Taipei, Taiwan*
[4] *Brain Research Center, National Yang Ming Chiao Tung University, Taipei, Taiwan*

Introduction: [^{11}C]-acetate positron emission tomography (PET) is used to assess oxidative metabolism in various tissues including the heart, tumor. However, the clinical utilization of [^{11}C]-acetate is limited due to its short physical half-life of ^{11}C (t1/2 = 20.5 min). This prospective study was to develop and validate an cGMP leveled ^{18}F-labeled acetate analog, ^{18}F-fluoroacetate ([^{18}F]FACE) using Eckert-Ziegler module in a rodent model.

Methods: [^{11}C]-acetate and [^{18}F]FACE were synthesized using a custom-built automated synthesis module and Eckert-Ziegler module, respectively. Six ICR mice (three of each compound) were injected intravenously with [^{11}C]-acetate (155±8.5 mCi) and [^{18}F]FACE (150±12.5 mCi), followed by dynamic whole-body PET and MR imaging during 0–30 min post-injection. The time-integrated activity for individual source organs and the whole body after administrations of [^{11}C]-acetate and [^{18}F]FACE were obtained using quantitative analyses of dynamic PET images.

Results: An automated synthesis [^{18}F]FACE using Eckert-Ziegler module which met cGMP level was established that enable us to obtain ethyl and sodium [^{18}F]FACE in a short synthesis time of 32 min, with a reproducible radiochemical yield of 50.2 ± 4.8% (decay corrected). The radiochemical purity of ethyl and sodium [^{18}F]FACE were > 99%. In contrast to [^{11}C]-acetate group, the blood clearance of [^{18}F]FACE exhibited bi-exponential kinetics for the fast and slow phases. A rapid accumulation of [^{18}F]FACE-derived radioactivity was observed in liver, lung, spleen, intestine and kidneys and was excreted into intestine and urinary bladder. The bone uptake of free ^{18}F-fluoride was insignificant during the course of the imaging studies.

Conclusions: The results suggested that [^{18}F]FACE could be a useful alternative to [^{11}C]-acetate for both research and clinical PET imaging.

PB-008

Determination of Metabolic Scheme of APD, a Ligand for Atherosclerotic Molecular Imaging Diagnostic Agents Using HPLC and Tandem-Mass Spectrometry

Weihsi Chen, Shioushiow Farn, Chienchung Hsia

Isotope Application Division, National Atomic Research Institute, Taoyuan, Taiwan

Introduction: A new compound with tetraazacyclododecane and aminomethyl-pyridinyl groups to chelate radioactive $^{67,68}Ga^{3+}$ and binding to CXCR4 receptor (named APD) respectively, were designed by INER based on computer-aided drug design and synthesized to be tested as a PET imaging agent for CXCR4 and diagnosis application for atherosclerosis in early stage. In order to study metabolic pathways of APD in the biosystem, it was incubated with serum for up to 2 h then analyzed the solutions.

Methods: An HPLC method on a C-18 analytical column (25 cm x 4.6 mm, 5 μm, Merck) and programed gradient acetonitrile / DI water spiked with trifluoroacetic acid (0.1%) as the mobile phase to separate matrix and components. Metabolites of APD in serum were identified based on electrospray ionization triple quadrupole tandem mass spectrometry.

Results: There were three metabolites of APD determined in mice serum matrix with molecular weight (MW) of 272, 442, and 456 respectively. One of the bio-transformed products of APD result to degrade and release of tetraazacyclododecane (MW 272). MW 442 is an oxidative deamination reaction and MW 456 is a hydroxylation product on one of the methylene of tertiary amine of APD. After incubated with serum for 30 min, metabolites began to emerge.

Conclusions: APD is a hydrophilic compound with primary, secondary and tertiary amino groups and multiple H-bonds to CXCR4 receptors. APD and thereof metabolites are highly dissolved in aqueous and eliminated through urine. Although APD was metabolized to three products in vitro study after incubated with serum for up to 2 h, it might preserve its original form mostly in vivo and show much of distribution at kidneys and bladder in radio imaging till 1 h after intravenous injection.

PB-009

A Brief Discussion on the Replacement of Lead Aprons

Juang Wei Hsieh

Department of Nuclear Medicine, Ditmanson Medical Foundation Chia-Yi Christian Hospital, Chiayi, Taiwan

Introduction: Lead aprons serve as the first line of defense for all radiation workers, including radiologists and radiologic physicians, when facing situations involving radiation exposure. Currently, there is no standardized criterion for when and under what conditions lead aprons should be replaced in hospitals nationwide, and even globally. In the existing literature, one can mostly find various methods for detecting holes or damage in lead aprons, but there is a lack of relevant replacement standards. This article explores a dose increase formula for damaged lead aprons mentioned in the literature by Kent Lambert and W. Stam and compares it with actual measurements.

Methods: The literature provides a formula for calculating the dose increase due to damaged lead aprons as follows: D(add) = Wt × D(H) × (a/A) × (1-f). In this study, radiation doses were measured behind lead sheets, and X-ray exposure was used to validate the calculated dose rates according to this formula.

Results: After conducting measurements, it was found that in an air environment, the dose rate was 0.2 mGy/s. The measured dose rates for lead aprons with a 1 cm crack were 0.004 mGy/s, a 2 cm crack were 0.01 mGy/s, and a 3 cm crack were 0.02 mGy/s. In contrast, using the formula, the calculated dose rates for the same scenarios were significantly lower, at 0.0005 mGy/s(1cm crack), 0.002 mGy/s(2cm crack), and 0.05 mGy/s(3cm crack), respectively.

Discussion and Conclusion: Based on the measurements, it is evident that the measured values are significantly higher than those calculated using the formula from the literature. The formula underestimates the additional dose caused by damage to a significant extent, raising safety concerns when using damaged lead aprons. Further investigation is needed to explore the detailed reasons for the discrepancies between the formula and actual measurements.

PB-010

Energy Window Optimization for Tc-99m-MIBI/ I-123-MIBG Dual-Isotope Simultaneous Acquisition Using a Semiconductor CZT Scanner

Tsung-Hsiang Hsu[1], Pan-Fu Kao[1], Chih-Chieh Chiang[2], Jui-Hung Weng[1]

[1] *Department of Nuclear Medicine, Chung Shan Medical University Hospital, Taichung, Taiwan*
[2] *Department of Medical Imaging and Radiological Sciences, Chung Shan Medical University, Taichung, Taiwan*

Introduction: Simultaneous dual-isotope I-123-MIBG and Tc-99m-MIBI cardiac imaging can be effectively used to assess myocardial sympathetic innervation and perfusion. However, due to the close energy peaks of the two isotopes, energy crosstalk occurs in the two energy windows, which will affect the analysis results. Our previous research has presented at 2022 Annual Conference of Society of Nuclear Medicine (acceptance number: PC-113) aimed to identify energy window conditions that minimize energy crosstalk in the phantom experiments. To further explore the impact of crosstalk, this study analyzed the differences in heart-to-mediastinum (H/M) ratio and total counts to evaluate restoration accuracy and total counts loss to determine the optimal energy window for the semiconductor cadmium zinc telluride (CZT) detector system.

Methods: To optimize the energy window settings, Radiology Support Device (RSD) heart and thorax phantom experiments were performed in this study. Dual-head GE Discovery NM/CT 670 CZT scanner used to acquire dual-isotope images. Concentrations of 10:5:1 or 6:3:1 were performed in the liver, heart, and mediastinum to simulate patients with different cardiac functions. Acquired list mode data were reframed into new images with 15 asymmetric energy window setup. These SPECT images would be analyzed to assess the effect of crosstalk, total counts and H/M ratio.

Results: The results show that the use of optimized energy windows can effectively reduce the impact of energy crosstalk. The proposed optimized energy windows of Tc-99m are 140-8%~140+3% (129~144) keV, 140-8%~140+4% (129~146) keV and 140-8%~140+5% (129~147) keV. For I-123 are 159-7%~159+8% (148~172) keV, 159-7%~159+9% (148~173) keV, and 159-7%~159+10% (148~175) keV. The H/M ratio ranges are approximately 1.83~2.03, 1.30~1.53 for Tc-99m, and 1.75~1.84, 1.71~1.78 for I-123 in H/M ratio 5 and 3 experiment, respectively.

Conclusions: From this heart and thorax phantom study, CZT scanner with an optimized energy window can provide Tc-99m-MIBI/I-123-MIBG dual-isotope cardiac imaging for future clinical applications.

PB-011

Automatic Adjustment of Range of Contrast in Bone Scintigraphy Based on Convolution Neural Network

Sin-Di Lee[1, 2], Tzer-Jen Wei[2], Chien-Wei Kuo[1,3]

[1] *Department of Nuclear Medicine, Pingtung Veterans General Hospital, Pingtung, Taiwan*
[2] *College of Artificial Intelligence, National Yang Ming Chiao Tung University, Tainan, Taiwan*
[3] *Department of Medical Imaging and Radiological Sciences, Kaohsiung Medical University, Kaohsiung, Taiwan*

Introduction: Bone scintigraphy plays a crucial role in diagnosing and monitoring bone metastasis in cancer patients. Typically, gamma cameras and workstations offer the capability to manually adjust image contrast. In this study, we have developed a convolutional neural network (CNN) model designed to automatically adjust the contrast of bone scintigraphy images.

Methods: We compiled a dataset comprising 262 bone scintigraphy images, each of which with range of contrast (ROC) adjusted by radiographers. The dataset was divided into a training set (n = 209) and a testing set (n = 53). To predict the ROC for each image in the training set, we employed a pretrained ResNest50 model and conducted training for 200 epochs. In the testing set, a difference of less than 10 between the predicted value and the manually adjusted value is considered correct.

The image quality of 53 images of the testing set was assessed by two physicians with over 10 years of expertise. They rated the image quality based on the ROC manual adjusted by radiographers and the ROC predicted by the CNN model.

Results: During the training process, the loss reduction trend in both the training set and testing set was generally similar. After 200 epoch, in the testing set, our model predicted the ROC of images with an accuracy of 79.3%. The average image quality score for images with manual adjusted ROC is 4.60, while the average score for images with CNN-adjusted ROC is 4.36.

Conclusions: In conclusion, our CNN-based approach shows feasibility in the task of contrast adjustment for bone scintigraphy images with non-inferior performance than manual adjustment. Moreover, it serves as a valuable data preprocessing step for other models. Further refinements and extensive validation are warranted to establish its robustness in clinical practice.

PB-012

手機之電磁波對電子式個人劑量計之影響探討

謝政道、蔡昭瑋、蔡世傳

臺中榮民總醫院核醫科

目的：了解並確認電子式個人劑量計與具有發送電磁波的電子產品過度接近，對其輻射偵測數據有無高估之影響。

材料方法：採用兩種不同作業系統的手機（iOS 與 Android），分別對兩種電子式個人劑量計進行測試。兩種劑量計分別為半導體式 ALOKA PDM-122-SH 與 Canberra Dosicard/E。測試手機分成 3 種使用狀態：1. 距離手機 0 公分，持續連網及播放影片；2. 距離手機 0 公分，以飛航模式待機且關閉螢幕；3. 距離手機 5 公分，持續連網及播放影片。以上述條件之不同組合，將劑量計、手機依不同距離置放於鉛屏蔽中，以確認手機對劑量計偵測數據之影響程度。

結果：兩種手機採持續連網及播放影片，且與偵測器貼合（距離 0 公分）時，劑量計偵測到數據皆有顯著增加趨勢。兩者距離超過 5 公分時，手機不管是否處於持續連網狀態，對劑量計偵測數據則無明顯影響。另外，當處於持續連網狀態的手機貼近劑量計 ALOKA PDM-122-SH 時，會產生較嚴重的偵測數據影響。

結論：當使用半導體式電子個人劑量計時，注意手機不要貼近該偵測器，不要放置於衣服同口袋中，偵測數據將會有嚴重高估的表現，距離大於 5 公分為偵測數據將幾無影響力。可提醒日後使用輻射偵測器時須留意不要過度接近具有發送電磁波的電子產品。

PB-013

Comparison of Attenuation Correction Methods in Cerebral Perfusion SPECT/CT

Yu-Tzu Chang, Chun-Che Lo

Department of Nuclear Medicine, Chung-Shan Medical University Hospital, Taichung, Taiwan

Introduction: Cerebral perfusion imaging is a widely used technique in nuclear neurology, but its accuracy is affected by factors such as attenuation, scatter, and resolution degradation. Attenuation correction (AC) methods, such as Chang's method and CT attenuation correction (CTAC), have a historical track record of utility in addressing these challenges. However, there is a lack of direct research comparing the performance of different AC methods in cerebral perfusion imaging. This study aims to evaluate the influence of AC methods on cerebral perfusion imaging.

Methods: Data from 28 patients who underwent cerebral perfusion imaging with a hybrid CT system were collected. Three sets of images were reconstructed using the ordered-subset expectation maximization (OSEM) algorithm: OSEM (non-attenuation-corrected, NAC), OSEM (Chang's method), and OSEM (CT attenuation correction, CTAC). The average counts in these images were analyzed using count profile curves, and count ratios within predefined regions of interest (ROI) were calculated.

Results: The counts within the ROI in the OSEM (NAC) and OSEM (CTAC) images were approximately 10% higher than in the other methods. Conversely, the counts in the OSEM (Chang method) and OSEM (CTAC) images exhibited similar values. Additionally, counts near superficial bone structures were notably higher in the OSEM (NAC) images compared to both OSEM (Chang method) and OSEM (CTAC) images.

Conclusions: This study demonstrates significant differences in the performance of various attenuation correction (AC) methods, particularly in the counts within the region of interest (ROI). The use of the OSEM (NAC) method resulted in significantly higher counts compared to the other methods. In contrast, images obtained using OSEM (Chang's method) and OSEM (CTAC) showed similar results. These findings emphasize the importance of selecting an appropriate AC method for accurate cerebral perfusion imaging.

PB-014

Power BI 於核醫科作業量管理之應用

李怡旻[1,2]、莊紫翎[2,3]

[1]佛教慈濟醫療財團法人大林慈濟醫院研究部
[2]佛教慈濟醫療財團法人大林慈濟醫院核子醫學科
[3]慈濟學校財團法人慈濟大學醫學系

目的：為使醫療機構永續經營，持續守護民眾的生命安全，定期審視業務量有其必要性。過往每個月本科書記會下載及統計排程系統的檢查量並統計本科上個月檢查量後，再呈核給科室主管審視。然若要比較不同時間的檢查量，則須找出先前資料自行比對或是委請相關單位提供資料，此作法不但勞師動眾且曠日廢時。爰此，本研究擬透過 Power BI 軟體定期審視本科檢查量，作為檢討改善之用，以期達到永續經營的目標。

材料方法：1. 委請資訊部協助建置「核醫作業資料庫」，資料庫內資料，資訊部會定期於每月月初更新上個月資料，故確保每次開啟 Power BI 時數據最為完整。2. 透過內建函數功能，將原為文字格式之檢查日期，轉換為日期格式，方便往後資料撈取與分析。3. 因自資料庫內資料為醫師所開立檢查項目，因此隸屬同一種檢查可能會有不同的檢查名稱，舉例如：骨頭密度檢查，可能包含「Bone mineralodensity (HealthExam)」、「hip (left)」、「hip (right)」、「HIP(R`T)」、「lumbar spine」，因此建置「檢查名稱資料庫」以便同一屬性之檢查項目予以歸類，並將該資料庫與「核子醫學科檢查資料庫」建立連結，以利後續統計使用。4. 透過儀表板功能建立長條圖、樹狀圖、趨勢圖視覺化圖表，以便單位主管隨時審視。

結果：資料庫自 2019 年 1 月起至 2023 年 7 月底累積共計 44,071 筆資料。每月書記擷取上個月作業檢查量數據時間約為 30 ~ 40 分鐘，然藉由 Power BI 軟體僅需 1 秒即可檢視，而且還能透過比較不同時間、不同檢驗量的改變趨勢，以便單位主管進行管理。

結論：雖然剛開始透過 Power BI 建立「核醫作業資料庫」及學習操作資料庫耗費許多人力物力與時間，然而如今能透過 Power BI 軟體讓單位主管隨時檢視單位的作業量及趨勢分析，大幅提升管理效率。

PB-015

探究農曆七月是否會影響民眾的就醫行為——以某區域醫院核醫科檢查量為例

李怡旻[1,2]、莊紫翎[2,3]

[1]佛教慈濟醫療財團法人大林慈濟醫院研究部
[2]佛教慈濟醫療財團法人大林慈濟醫院核子醫學科
[3]慈濟學校財團法人慈濟大學醫學系

目的：華人對於鬼神十分敬畏，而農曆七月又稱為鬼月，更有許多禁忌如不宜結婚、買房、買車、戲水等，甚至是避免進行一些醫療行為。雖然已有研究結果顯示，頭頸癌病人於農曆七月進行手術，其術後預後優於非在農曆七月患者。然而對於非緊急的檢驗檢查醫療行為，民眾是否仍抱持避免農曆七月去醫院的觀點呢？故本研究目的為探究農曆七月是否會影響民眾的就醫行為。

材料方法：本研究為回溯性研究，資料來源為台灣南部某區域醫院核子醫學科，2019 年 1 月 1 日起至 2022 年 12 月 31 日止之排程資料。統計方法採用平均值、標準差、個數、百分比等描述平均每日核醫檢查數，並以獨立樣本 T 檢定，探究農曆七月（鬼月）對於民眾就醫行為的影響。統計軟體採用 SAS 9.4 進行資料處理與分析。

結果：本研究 2019 ~ 2022 年間共計 37,721 筆排程資料，共計 984 天，其中有 84 天為農曆七月 (8.5%)。並依檢查日期統整每日就診量，其結果發現，農曆七月平均每日檢查量為 40.1 ± 11.8 筆，而非農曆七月之平均每日檢查量為 38.2 ± 13.2 筆，未達統計上的顯著差異 ($P = 0.205$)。並進一步探究 2019 年 ~ 2022 年的鬼門開（農曆 7 月 1 日）、中元節（農曆 7 月 15 日）及鬼門關（農曆 7 月最後一天）共 10 天的檢查量，結果發現平均每日檢查量為 39.9 ± 8.0 筆，但仍未與其他農曆七月之檢查量達統計上的顯著差異 ($P = 0.912$)。由本研究結果可知，農曆七月病人的檢查量不僅沒有顯著較少，反而高於非農曆七月檢查量平均值。而若單就農曆七月重要的鬼門開、中元節、鬼門關等重要節日，其平均檢查量僅略低於其餘鬼月平均檢查量，但仍高於非農曆七月的平均檢查量。

結論：本研究結果顯示，病人農曆七月與否與排定檢查的日期無關，雖然本院地理位置為南部且中老年人口較多，但農曆七月的檢查量仍與平時相似，甚至是更勝非農曆七月。推估原因可能為本單位有較多須定期回診檢查是否有轉移的癌症病人，而且本單位僅進行檢查，而非侵入性治療，因此較無農曆七月不宜動刀的顧慮。此外，本研究結果與原推論病人可能會因中元節需準備祭拜而造成檢查量較低不符合，其原因可能為民眾選擇前往廟宇（較方便）或是選擇非中元節當日祭拜的比例變多，也因此較不會有當日因忙碌而無法前往就醫的情形發生。

PB-016

Covid-19 疫情對就醫行為的改變——以骨頭掃描檢查為例

李怡旻[1,2]、莊紫翎[2,3]

[1]佛教慈濟醫療財團法人大林慈濟醫院研究部
[2]佛教慈濟醫療財團法人大林慈濟醫院核子醫學科
[3]慈濟學校財團法人慈濟大學醫學系

目的： Covid-19 疫情全球肆虐，不僅深深的改變我們的生活，而疫情期間民眾對於醫院可說是避之惟恐而不及。研究顯示疫情期間，內視鏡門診量減少 63%，但是住院量仍與疫情前相似。雖然核醫科與內視鏡檢查同屬於二線檢查單位，然而癌症病人需透過定期骨頭掃描、正子攝影、淋巴結等核醫科檢查追蹤病情發展，因此，本研究目的為探討不同疫情期間骨頭掃描檢查量是否有差異。

材料方法：本研究為回溯性研究，資料來源為南部某區域醫院核子醫學科檢查資料庫，資料期間為 2019 年 1 月 1 日起至 2023 年 2 月 28 日，並選取檢查項目為骨頭檢查。依我國疫情發展，將 2019 年全年度定義為非疫情期間、2020 年 1 月 ~ 2021 年 5 月 18 日止為疫情前期，2021 年 5 月 19 日政府宣布全國三級警戒起至 2022 年 2 月 28 日解除二級警戒止，為疫情嚴峻期；2022 年 3 月 1 日起至 2023 年 2 月 28 日，則為疫情後期。採用 SAS 9.4 進行資料處理與統計分析，以描述性統計顯示不同期間檢查量的平均值、標準差，再以單因子變異數分析探究不同疫情期間對平均每日骨頭掃描檢查量的差異。

結果：資料期間共計 10,608 筆骨頭掃瞄檢查量，共計 1,023 天，不同疫情期間的天數及骨頭掃瞄平均每日檢查量依序為非疫情期間（249 天，44.3 ± 13.9 筆）、疫情前期（347 天，39.6 ± 13.6 筆）、疫情嚴峻期（173 天，30.6 ± 9.3 筆）、疫情後期（254 天，35.7 ± 10.4 筆）。而 ANOVA 分析結果顯示，不同疫情期間其骨頭掃瞄檢查量達統計上的顯著差異 ($F = 48.0$；$P < .001$)，進一步以 Scheffé 進行事後檢定，發現非疫情期間檢查量顯著高於其他三種期間，疫情前期顯著高於疫情後期與嚴峻期，而疫情後期則僅高於嚴峻期。

結論：骨頭掃描為核醫科最常見的檢查項目之一，也為癌症病人須定期進行檢查腫瘤是否有轉移的方法之一，而本研究結果顯示，骨頭掃描檢查量會因疫情而顯著減少，尤其是疫情嚴峻期，然而這些因疫情而延緩進行檢查，是否會造成病人預後或是存活率的差異，值得未來研究進一步分析。

PB-017

Optimization of the Semi-Automated Production of I-123 MIBG Injection for Clinical Trial in Taiwan

Chun-Tang Chen[1], Ying-Hsia Shih[1], Te-Sheng Liang[1], I-Chung Tang[1], Yu-Min Kuo[1], Cheng-Liang Peng[1], Tsai-Yueh Luo[2]

[1] *National Atomic Research Institute, Taoyuan, Taiwan*
[2] *Taipei Economic and Cultural Representative Office in the U.S.*

Introduction: Iodine-123 metaiodobenzylguanidine (I-123 MIBG) has been widely used for the imaging of neuroendocrine tumors and cardiac sympathetic diseases for many years. We had successfully developed the semi-automated production of I-123 MIBG and provided I-123 MIBG injection to collaborate with domestic hospitals for clinical trials in Taiwan since 2022. In this study, we report a semi-automated method for the radiosynthesis of I-123 MIBG and evaluate radioactivity distribution on the module parts after using different amounts radioactive iodine-123 (450–700 mCi) in order to optimize production yield.

Results: A total of I-123 MIBG injection batch productions were performed from September 2021 to August 2023 and carried out to optimize the conditions for obtaining maximum product yield. The batch results obtained in terms of radiochemical yield (RCY), residual radioactivity of module parts and reproducibility. I-123 MIBG radiosynthesis was carried out with RCY of 37.3 ± 5.0% (n = 16). The radiochemical purity was greater than 90% for I-123 MIBG. Increasing the radioactive iodine-123 load to 601–700 mCi leads to a significant increase in radioactivity measured in the vial A (reaction vial) and RP-18 column; however, production yield is not expected increased. Therefore, the use of radioactive iodine-123 in the range of 501–600 mCi for the radiosynthesis of I-123 MIBG on the semi-automated production has a better product yield. The stability of I-123 MIBG injection at room temperature was tested up to 10 hours by radio-HPLC.

Conclusions: It was observed that optimum amount of radioactive iodine-123 required for the production of I-123 MIBG was in the range of 501–600 mCi. Semi-automated production of I-123 MIBG had a consistent and reliable I-123 MIBG injection for clinical application. In the future, we will establish PIC/S GMP automated production facility to increase production yield and expect that stable supply of I-123 MIBG injection for domestic hospitals in clinical usage to benefit patients in Taiwan.

PB-018

智慧型檢查流程紀錄暨叫號系統於核醫科之應用

張志維、陳耀文、蔡世傳

臺中榮民總醫院核子醫學科

背景介紹：隨著時代的進步與病人檢查量成長，中榮核醫科內使用傳統人工給號及叫號方式，需花費較多人力及時間處理受檢者之順序，且需於檢查室及等候區來回往返叫號，工作效率也因此降低；對於受檢者來說，等候造影時間與檢查順序之資訊相對不透明，容易引起疑慮甚至產生糾紛。除此之外，檢查相關記錄都是使用紙本方式，保存不易，在這個數位資訊化的時代來說不環保。另外，醫師打報告時若需了解檢查時所記錄的狀況，也必須在大量的檢查單中翻找，相當費時。基於上述環境背景，欲改善目前之困境，提升工作效率及受檢者滿意度，因此著手規劃智慧型檢查流程叫號暨紀錄系統。

方法：本系統使用開發工具 ASP .Net Core，所有資料交換採用 WebAPI 方式，配合現有檢查流程設計叫號模式與規則設定方便跨系統資料介接整合。系統流程設計上，臨床醫師 HIS 開單即進入系統執行檢查排程，以櫃檯、注射室、造影室、影像後處理、醫師確認等站點，依原有各項檢查流程串起，再依不同檢查加入所需格式範本執行紀錄。硬體規劃上，分別設置櫃檯旁自動取票機與櫃檯內取票機一臺，受檢者可於自動取票機插健保卡取號或櫃檯人工報到領取號碼牌。在每間造影室及注射室外各設置一臺叫號機，受檢者依其檢查流程插入健保卡或掃描檢查單之條碼作報到，並於造影室之控制室內設置專用叫號電腦，等候區設置公播系統螢幕兩臺，可用於顯示目前等待受檢之號碼，以及檢查相關衛教內容之宣導。

結果：100 位門診病人，對於系統及流程，滿意度平均為 92%。等候造影時間透明滿意度 95%。放射師可節省分配病患造影與前往等候區呼叫號碼的往返時間，平均往返時間為 20 秒，平均檢查執行 15 人次／日，可節省 30 分鐘。在檢查紀錄方面，醫師、護理師、放射師檢查記錄（含醫囑審核）直接使用電腦從系統上填寫紀錄，無任何檢查單之紙張傳遞，省下可平均 50 人次紙張 / 日。

結論：相較於過往人工給號叫號的方式，受檢者對於受檢順序資訊感覺更透明化且容易理解，櫃檯人員不需花時間心力編排號碼，直接由系統依檢查分類及報到順序給號。系統叫號時只呼叫號碼，而非以患者姓名唱名方式，可保護病人隱私。醫師打報告時，可直接於系統查詢檢查相關記錄，大幅降低查找受檢者檢查時之相關記錄。整體而言，明顯減輕臨床工作人員之負擔，且提升病患滿意度。

PB-019

行政院原子能委員會年度輻射安全查核注意事項經驗分享——以南部某醫院為例

卓世傑、張南雄、陳興隆、林凡珍、顏玉安、李將瑄

奇美醫院永康總院核子醫學科

背景介紹：行政院原子能委員會（以下簡稱原能會）基於主管機關管制作為，以往每年皆會對各大醫院進行年度輻射安全查核。但自 2020 年 1 月迄至 2023 年 4 月止，因 COVID-19 疫情之影響，原能會之年度輻射安全查核也配合中央疫情指揮中心之管制作為而暫停。不過隨著疫情解封，相關管制措施陸續放寬、解除，原能會也開始恢復年度輻射安全查核之作為。因此經過數年的查核空窗，原能會之查核要點以及查核方法有無改變，是頗值得討論與注意的。本文即為以南部某醫院之查核經驗為例，討論原能會之年度輻射安全查核注意事項之重點。

方法：1. 收集原能會年度輻射安全查核時之查核要點。2. 收集原能會年度輻射安全查核時之查核方法。3. 收集臨床輻射安全之實際作為。4. 彙整提出原能會年度輻射安全查核注意事項因應之可行方法。

結果：1. 原能會年度輻射安全查核時之查核要點分為 A. 輻射暴露品保人員暨訓練相關部分，B. 可發生游離輻射設備，C. 密封射源，D. 非密封射源以及 F. 輻射安全委員會作為。2. 查核方法則依據相關法規之規定，主要有兩種，A. 實地查核，B. 文件查核。3. 臨床輻射安全之實際作為則可分為，A. 輻射作業方式，B. 輻射防護法規規範文件之紀錄內容與方式，C. 其他輻射防護法規規範之相關作為。

結論：依據結果顯示，行政院原子能委員會之年度安全查核，與以往相同的是，仍然依據相關法規之規定以實地及文件查核兩種方式針對 A. 輻射暴露品保人員暨訓練相關部分，B. 可發生游離輻射設備，C. 密封射源，D. 非密封射源以及 F. 輻射安全委員會作為等 5 個部分進行查核。因此臨床單位因應原能會年度輻射安全查核的可行方法，即為依據相關法規之規定落實於實際之輻射作業、文件紀錄與其他輻射防護法規規範應作為之相關規定。

PB-020

機器學習方法於國人專屬之核醫腦功能影像資料庫的分析：針對阿茲海默症嚴重程度之探討

林家榆[1]、曾繁斌[1]、楊惠絜[1]、洪光威[2]、林昆儒[3]、曾聖彬[1]、倪于晴[1]、廖美秀[1]

[1]國家原子能科技研究院輻射防護所
[2]彰濱秀傳醫院核子醫學部
[3]林口長庚紀念醫院核子醫學部

背景介紹：本研究使用「國人專屬之核醫腦功能影像資料庫」之認知與實驗室檢查表格及 ECD SPECT 影像數據。運用隨機森林進行阿茲海默症嚴重程度 3 分類，分別為認知功能正常之健康人、輕微阿茲海默症及阿茲海默症案例。

方法：「國人專屬之核醫腦功能影像資料庫」內的案例皆由臨床醫師診斷，且 ECD SPECT 影像由核醫科醫師判斷進行嚴重程度分類。本研究隨機挑選該資料庫中 59 例認知功能正常之健康人、50 例輕微阿茲海默症案例與 47 例阿茲海默症案例，認知與實驗室檢查表格數據為臨床收集數據，需要進行資料清理與缺值補植，在實驗室檢查數據確認單位一致性，在類別欄位進行獨熱編碼，在缺值補植運用欄位眾數進行補植。ECD SPECT 影像數據運用 SPM 對位，再使用模板腦區計算各個腦區平均值與標準差，每個腦區以此 2 個特徵值作為分類模型輸入。本研究主要比較單純使用認知與實驗室檢查表格數據和使用認知與實驗室檢查表格數據及 ECD SPECT 影像特徵值結構化數據之結果準確度差異。在隨機森林特徵重要性測試中，得到使用前 5 個重要性高之特徵有最佳之準確度，因此 2 種分析方式使用前 5 個重要性高之特徵進行隨機森林方法預測。

結果：單純使用認知與實驗室檢查表格數據分析結果準確度為 75%，使用認知與實驗室檢查表格數據及 ECD SPECT 影像特徵值結構化數據分析結果準確度為 83%，較單純使用表格數據分析準確度高 8%。

結論：在「國人專屬之核醫腦功能影像資料庫」的阿茲海默症嚴重程度分類預測，結果顯示兩種方法都有一定的分辨能力，然而結合 ECD SPECT 影像特徵值之結構化數據能更提升準確度。顯示 ECD SPECT 影像數據所提供更多有助於疾病分辨的資訊。後續可以針對資料清理與影像特徵萃取相關工作精進，以提升資料品質進而提升分析結果。

PB-021

放射性從業人員與醫護人員導入眼球劑量評估

鍾沛霖、楊融華、王美惠

國家原子能科技研究院同位素應用研究所

背景介紹：核醫作業人員執行放射性作業或處理放射性物質時，身體會接收輻射劑量，而超量輻射對眼球組織具有損害性，因此必須測量和監測眼球的輻射劑量，以確保工作者的視力和眼睛健康不受損害。許多國家和地區的法規要求核醫設施追蹤人員作業動態和控制職業暴露於輻射的程度，其中也包括眼球的輻射劑量，通過使用眼球劑量評估程式，核醫相關單位可以評估醫護人員的職業風險，確保其在工作場所中暴露於輻射的風險保持在可接受之水平下。

方法：VARSKIN 是一種皮膚劑量計算軟體工具，其中包含了眼球劑量模式（EyeDose），用於評估核醫作業人員在處理輻射材料和進行核醫程序時眼球所受到的輻射劑量，這是為確保人員的視力和眼睛健康而設計，因為長期暴露於輻射可能會對眼睛造成損害。EyeDose 會考慮粒子類型（電子和光子）、粒子能量、射源與眼睛的相對距離、射源發射率以及是否佩戴防護眼鏡等因子。

結果：EyeDose 中使用的計算方程是通過對距離程式化眼睛模型不同距離的單能放射源進行蒙特卡羅（MCNP）模擬而開發的，模式考慮了粒子類型、能量、射源發射率和防護眼鏡。EyeDose 計算方程適用於 100 keV 至 11 MeV 範圍內的電子能量、7 keV 至 11 MeV 範圍內的光子能量以及 0 至 20 米的距離。並透過與文獻數據驗證，證明計算結果函數整體趨勢與數據非常匹配，計算結果具有相當程度之可靠度。

結論：眼球劑量計算對於從事核醫作業人員至關重要，因為其有助於確保人員眼睛不受到輻射劑量之危害，因此通過遵守規定要求、評估職業風險並實施必要的防護措施，此評估模式有助於保護核醫工作者的視力和眼睛健康，同時確保核醫程序的安全執行。

PB-022

迴旋加速器產製鎵 -67 之研發與應用

楊融華、杜定賢、陳遠寧、王美惠

國家原子能科技研究院 同位素應用研究所

背景介紹：中型迴旋加速器產製 [鎵 -67] 於醫療與製藥領域具優異應用潛力，其中核研檸檬酸鎵 [鎵 -67] 合併單光子斷層掃描影像診斷於霍金氏病、淋巴瘤、支氣管性腫瘤等惡性腫瘤之助診具有優異的核醫學應用潛力，此外亦可以應用於新藥開發與除了應用於治療用細胞活體動力學追蹤，是現代科學和精準醫療領域中重要的放射性核種。有鑑於國內對核醫藥物鎵 -67 需求逐漸提升，為彌補我國基礎科學研發與產業應用的缺口，除現有 30MeV 中型迴旋加速器，目前也正在研擬以 70 MeV 迴旋加速器產製核醫藥物鎵 -67 之技術，以開發新產線以及作為核醫藥物生產備援，達到核醫藥物鎵 -67 穩定供藥之目的。

方法：本文以核研檸檬酸鎵 [鎵 -67] 進行卵巢癌偵測，並以 2M [鎵 -67] 氯化鎵進行奈米鑽石標誌，經脂肪間質幹細胞胞吞後，可以作為細胞追蹤使用。此外本文評估以迴旋加速器高能量質子射束照射 Zn-68 靶材，依照不同核反應會產生 Zn-68(p,n)Ga-68、Zn-68(p,2n)Ga-67、以及 Zn-68(p,3n)Ga-66，由於 Ga-68、Ga-67、以及 Ga-66 半衰期分別為 68 分鐘、78 小時、以及 9.5 小時，如何藉由以上不同放射性同位素之特性，以達到鎵 -67 製程最佳化與產率最大化之目的。

結果：核研檸檬酸鎵 [鎵 -67] 進行卵巢癌偵測有很好的靈敏度，並可觀察到脂肪間質幹細胞的生物體分布。由於以 28MeV 高能量質子射束照射 Z-68 靶材，相較於現 30MeV 迴旋加速器以 25 MeV 能量質子射束照射 Z-68 靶材可以預期照射後的靶材 Ga-66 放射性同位素含量（雜質）會較高，因此勢必需要精進化學分離與純化製程，以求生產高純度之核研檸檬酸鎵 [鎵 -67]。另外，以 28 MeV 能量質子照射 Zn-68 靶材所產生之同位素 Ga-66, Ga-67, Ga-68 產率和比例則不同，且同位素 Ga-66, Ga-67, Ga-68 的活度也會隨時間而變化。

結論：核研檸檬酸鎵 [鎵 -67] 可能具有偵測卵巢癌之潛力， [鎵 -67] 核種經化學標誌可用以觀察超過 1 周的生物體分布；至於高能產製核醫藥物鎵 -67 之研發與技術精進，能強化核研檸檬酸鎵 [鎵 -67] 之生產穩定性，並藉由 70 MeV 迴旋加速器作為核醫藥物生產備援，未來勢必能穩定供給核醫藥物，並滿足國內醫療需求，以避免供藥中斷之危機。

PB-023

Lifespan Improvement Study for the ion Source Filament of Cyclotron for Nuclear Medicine Applications

Kuo-Yuan Chu, Jung-Hua Yang, Mei-Hui Wang

National Atomic Research Institute, Taiwan

Introduction: The cyclotron is a type of particle accelerator used in the production of radioisotope for nuclear medicine applications. It operates on the principles of electromagnetic fields and circular motion to accelerate charged particles, typically protons or deuterons, to high energies. The radioactive isotopes produced in these reactions are then collected and processed to create radiopharmaceuticals. These radiopharmaceuticals are compounds that incorporate the radioactive isotopes and are designed to selectively accumulate in specific organs or tissues in the human body when administered to a patient. The radiopharmaceuticals can be used for various nuclear medicine applications, including diagnostic imaging (such as positron emission tomography or single-photon emission computed tomography) and therapeutic treatments (such as targeted radiation therapy).

Methods: To investigate the impact of hydrogen gas flow rate on the efficiency and lifespan of the ion source filament, two experiments were planned. The first experiment involved maintaining a fixed arc current while varying the hydrogen gas flow rate to determine the optimum flow rate that yields the highest current output to the Ion Beam Source (IBS). In the second experiment, the effect of filament height on filament lifespan was studied. When the filament height was lowered, and the ion source back plate's magnetic field was utilized to protect the filament, thereby reducing particle collisions and extending filament lifespan. By conducting these experiments, it aims to gain insights into the factors influencing ion source efficiency and filament lifespan, enabling us to optimize the ion source performance for enhanced operation and longevity.

Results: Based on the results of the first experiment concerning hydrogen gas flow rate, it is evident that as the arc current increases, the hydrogen gas flow rate should also be moderately increased to optimize overall efficiency. In the experiment of the filament life, the consumption index for the experimental group is $N = 3.92\times10^{-3}$, and for the control group, it is $N = 5.62\times10^{-3}$. This means that the filament lifespan in the experimental group is approximately 43.3% longer than that in the control group.

Conclusions: According to the experimental results, there is a positive correlation between the hydrogen flow rate and the peak value of the output current. However, it should be noted that the TR-30 ion source system exhibits a slower gain response when adjusting the hydrogen gas flow rate. Therefore, operators should wait for a longer period to ensure the effectiveness of the modified settings when changing the flow

PB-024

In vivo Pharmacokinetics Study of Novel Peptidic Molecules for Triple Negative Breast Cancer Treatment

Mao-Chi Weng[1], Yu-Wei Liu[2], Lun Kelvin Tsou[2], Kai-Hung Cheng[1], Chung-Li Ho[1], Ya-Jane Chang[1], Yu-Min Kuo[1], Wei-Chuan Hsu[1], Shih-Min Wang[1], Shiou-Shiow Farn[1]

[1] *National Atomic Research Institute, Taoyuan, Taiwan*
[2] *Institute of Biotechnology and Pharmaceutical Research, National Health Research Institutes, Miaoli, Taiwan*

Introduction: Triple negative breast cancer (TNBC) is considered the most serious subtype of human breast cancer. However, effective tracers and drugs specific for TNBC are still under investigation. Receptors of luteinizing hormone-releasing hormone (LHRH-R) are regarded as potential targets for TNBC and widely investigated as yet. In 2022, the peptidic molecule, BPRSY22, was developed by Institute of Biotechnology and Pharmaceutical Research (IBPR) and bio-distribution of ^{131}I-BPRSY22 in tumor-bearing mice was investigated by National Atomic Research Institute (NARI) after radio-iodination. In this research, we further evaluated the *in vivo* pharmacokinetics of BPRSY22 for preclinical reference.

Materials and Methods: As previous study, BPRSY22 was first synthesized and evaluated by a mass spectrometer and high performance liquid chromatography (HPLC) at IBPR. After radiolabeled with I-125, ^{125}I-BPRSY22 was purified by a C18 cartridge at INER. The radiochemical purity (R.C.P.) was analyzed by both radio-thin-layer-chromatography (radio-TLC) and radio-HPLC systems. After intravenous (i.v.) injection of ^{125}I-BPRSY22 into ASID mice, the *in vivo* pharmacokinetics was performed at 5 min, 1, 4, 24, and 48 h. The activity of samples was then counted and the parameters were calculated by a WinNonlin software.

Results: The R.C.P. of ^{125}I-BPRSY22 was determined > 90% by both radio-TLC and radio-HPLC after purification. In results of pharmacokinetics, it showed fast distribution and there found low signals in blood at 1 h after i.v. injection of ^{125}I-BPRSY22. The elimination of ^{125}I-BPRSY22 takes longer time; the terminal elimination half-life (HL_Lambda_z) is calculated as 10.5 h and area under the plasma concentration-time curve to the last measurable plasma concentration (AUClast) is about 74.0.

Conclusions: This preclinical research has further demonstrated the characteristics of BPRSY22 for LHRH-R over-expressive tumors *in vivo*. The fast distribution and longer elimination in blood of ^{125}I-BPRSY22 in pharmacokinetics study might elevate the distribution in TNBC tumors; we suggested that BPRSY22 will be an appropriate candidate for IBPR's next research and it would also bring innovative information for development of TNBC patient's treatment strategies in the future in Taiwan.

PB-025

Study on the Use of Reference Regions for Tau PET in Alzheimer's Disease (AD)

Shao-Yi Huang[1], Kun-Ju Lin[1,2,3], Ing-Tsung Hsiao[1,2,3]

[1] *Department of Medical Imaging and Radiological Sciences, Chang Gung University, Taoyuan City, Taiwan*
[2] *Molecular Imaging Center and Nuclear Medicine, Chang Gung Memorial Hospital, Taoyuan, Taiwan*
[3] *Medical Imaging & Radiological Sciences and Healthy Aging Research Center, Chang Gung University, Taoyuan, Taiwan*

Introduction: The cerebellar crus is the most commonly used reference region in Tau-PET semi-quantification for AD. However, various factors affect the reference value in crus, and that results in uncertainty of the quantification. The goal of this study is to explore two reference regions for the [^{18}F] Florzolotau PET tracer including both the anatomy-based crus and the data-driven PERSI method by investigating the influence of semi-quantification in different reference regions in the cross-sectional and longitudinal analysis in AD.

Methods: Two cohorts with retrospective data were included in this study. Cohort 1 (20 HC, 20 MCI, 20 AD) and cohort 2 (50 MCI/AD with two PET scans) were used for cross-sectional analysis and longitudinal analysis, respectively. Image processing including spatial and intensity normalizations was performed using PMOD 3.7 software. SUVr images were generated using cerebellar crus and PERSI as reference regions. Differential diagnosis power in cross-sectional analysis, and annual change rates in SUVr based on the two reference regions were evaluated.

Results: For the cross-sectional analysis, as compared with cerebellar crus, PERSI illustrates better performance in the diagnostic power measured by AUC (area under the ROC curve) in NC vs. AD (cerebellar crus: 0.52; PERSI: 0.75) and NC vs. MCI (cerebellar crus: 0.79; PERSI: 0.83). For the longitudinal analysis, the average annual change (ACR) rate in meta-group VOI based on PERSI (ACR: 0.04 ± 0.10) was higher than those based on cerebellar crus (ACR: 0.02 ± 0.15).

Conclusions: The study shows that, compared with cerebellar crus, PERSI exhibits better diagnostic power and the ability of detecting longitudinal change for [^{18}F]Florzolotau PET imaging in AD.

PB-026

Evaluating Glymphatic Function in AD Using Amyloid PET Imaging

Jyh-Ruey Lin[1], Kun-Ju Lin[1,2], Ing-Tsung Hsiao[1,2]

[1] *Department of Medical Imaging & Radiological Sciences, College of Medicine, Chang Gung University, Taoyuan, Taiwan*
[2] *Department of Nuclear Medicine, Chang Gung Memorial Hospital, Taoyuan, Taiwan*

Introduction: Recent studies have discovered that glymphatic system plays an important role in clearing brain metabolites (including amyloid beta and tau proteins). Methods to assess the function of the glymphatic system include the use of amyloid PET imaging. This study attempts to use 18F-Florbetapir amyloid PET imaging to evaluate and compare the glymphatic functions among patients with Alzheimer's disease (AD), mild cognitive impairment (MCI) subjects and normal controls (NC).

Methods: Totally 115 subjects (NC = 55, MCI = 60, and AD = 65) with 18F-Florbetapir imaging were included in this study including clinical assessments. Through image processing including both spatial normalization and intensity normalization, the standard uptake value ratio (SUVR) of cortical regions (frontal [FL], temporal [TL], parietal [PL] and occipital [OL]) and the lateral ventricle (LV) frontal horn were calculated. The SUVR in LV was used as an indication of brain glymphatic function. The LV and cortical SUVR among the three groups were compared, and the correlation between SUVR and the MMSE scores were also assessed.

Results: As expected, the cortical SUVR indicating amyloid deposition for AD is significantly higher than both MCI and NC while no significant difference between MCI and NC. The LV SUVR for glymphatic function in NC showed significantly higher than those in MCI and AD, but no significant difference between MCI and AD. A mild but significant correlation between LV SUVR and MMSE (R squared = 0.08895, P value < 0.0001) was observed in a linear regression analysis.

Conclusions: The study explored the use of LV SUVR from amyloid 18F-Florbetapir PET image as an indicator of the glymphatic function, and the result illustrates higher LV SUVR in NC than those in AD and MCI patients. Nevertheless, the glymphatic function is affected by various factors, and LV SUVR is an indirect measurement for glymphatic function. Therefore, more studies are needed including more rigorous criteria using different measures for glymphatic functions to verify the accuracy of lateral ventricular quantification in PET imaging as a biomarker for measuring glymphatic function.

PB-027

以鎵 -67 標誌的碳酸酐酶 IX 標的探針進行大腸腫瘤缺氧造影及分布研究

官孝勳、蔡宜樺、于鴻文、樊修秀

國家原子能科技研究院同位素應用研究所

背景介紹：腫瘤缺氧會降低放射療法或化學療法的效果。而臨床上使用放射療法與化學療法的患者仍占很高的比例，若醫師沒有正確的診斷或評估腫瘤缺氧狀態，就可能錯失正確治療黃金時期，造成患者病情惡化，增加後續治療的社會成本。

因此，準確診斷腫瘤缺氧位置及程度，是影響治療效果和生存率的重要關鍵。

其中，核醫分子影像可作為理想的腫瘤缺氧診斷工具。我們以腫瘤缺氧生物標誌物 - 碳酸酐酶 IX (CA9) 為標的物，設計其抑制劑和對應胜肽序列作為雙靶向探針並標記鎵 -67 用於體內大腸癌腫瘤缺氧成像偵測。我們期盼以精準醫學之概念去提供個別化的診斷而達到正確醫療決策之目的。

方法：將 CA9 標的胜肽 (NARI-GSS-01) 和乙醯唑胺 (AAZ) 鍵結 1,4,7,10- 四氮雜環十二烷 -1,4,7,10- 四乙酸 (DOTA) 和 Gallium-67 (G-67)，作為腫瘤缺氧造影劑 (^{67}Ga-DOTA-AAZ-CA9) 進行標誌效率和穩定性測試。以人類大腸癌細胞株 (HCT15) 進行藥物細胞表面結合 / 膜穿透試驗。然後，以 HCT15 誘導的腫瘤缺氧動物，每隻動物以靜脈注射方式給予 0.5 mCi ^{67}Ga-DOTA（對照組）和 ^{67}Ga-DOTA-AAZ-CA9（實驗組)。給藥後 1、4、24 小時分別進行 nanoSPECT/CT 分析，比較腫瘤缺氧的藥物成像及生物分布差異。

結果：^{67}Ga-DOTA-AAZ-CA9 的標誌效率大於 95%，且在人和小鼠血清中的穩定性持續 72 小時超過 90%。^{67}Ga-DAA-AAZ-CA9 腫瘤缺氧細胞表面結合與細胞膜穿透比率為 40:1。此外，與對照組 (^{67}Ga-DOTA) 相比，^{67}Ga-DAA-AAZ-CA9 處理組別，其動物腫瘤缺氧位置有明顯藥物聚集。對於 ^{67}Ga-DOTA-AZ-CA9 在 HCT15 誘導的異種移植小鼠中的分布，腫瘤組織部位藥物聚集隨時間增加，第 4 小時為 4.3%ID/g，第 24 小時可提升至 6.5%ID/g。

結論：上述結果證實，^{67}Ga-DOTA-AAZ-CA9 主要結合在腫瘤細胞表面，能準確聚集在腫瘤缺氧位置。我們認為 ^{67}Ga-DOTA-AAZ-CA9 具有潛力可應用在大腸癌患者的缺氧腫瘤成像，以實現精準醫學之目標。

PB-028

New Y/Zr Radionuclide Chemical Separation Method Development for Zr-89 Radioisotope Purification

Jenn-Tzong Chen, Yean-Hung Tu, Fang-Hsiu Kuo, Shiou-Shiow Farn

Department of Isotope Application, Taoyuan, Taiwan
Institute of Nuclear Energy Research, Taoyuan, Taiwan

Introduction: This study develops a new radionuclide separation method to reduce unknown energy peaks in producing of high purity Zr-89 (half-life: 78.4 hrs) radioisotope.

Methods: A new resin of producing Zr-89 has been applied in Y and Zr radionuclides separation. Th/Pa element resin ion exchange separation method of applying Dowex 1X10 resin might provide potential Y/Zr element separation from the periodic table for chromatographers. We apply the new PCX resin with similar property in this study in order to obtain higher Zr radionuclide purity product by absorption with 2N HCl and then desorption with 1N oxalic acid.

Results: The separation product contains Zr-88 (393keV) and Y-88 (898keV, 1836keV) related peaks only. Compared with the proton irradiated target material, all the unknown peaks such as 37, 122, 814, and 1324 keV have been removed. According to their net area counts and intensity ratio, Yttrium element can be reduced from more than fifty percent to less than ten percent; Zirconium element can be increased from less than forty percent up to more than ninety percent.

Conclusions: This new radioisotope separation method is potential to obtain higher radionuclide purity of Zr-89 radioisotope because the Y radionuclide removing ratio is larger than traditional method.

PC-001

全身骨骼掃描 (Tc-99m MDP) 肝臟異常攝取——案例報告

李佩璇[1]、楊朝瑋[1]、張文釧[2]

[1]澄清綜合醫院中港院區核子醫學科
[2]澄清綜合醫院中港院區放射診斷科

背景介紹：全身骨骼掃描是核醫科應用非常廣泛的檢查項目之一。透過靜脈注射 Tc-99m MDP 來進行造影。Tc-99m MDP 為磷酸鹽類似物，與骨骼中的結晶羥基磷灰石結合。常應用於檢測各種惡性腫瘤的骨骼轉移，有時也會偶然發現軟組織病變，良性或惡性病變皆有可能。

病例報告：一名 56 歲女性，有乳癌病史。於 2022 年 8 月進行全身骨骼掃描 (Tc-99m MDP)，在肝臟發現不均勻的放射性攝取增加，電腦斷層掃描也顯示在肝右葉有融合性轉移病兆。同年 9 月做腹腔鏡切除，病理報告的腫瘤細胞學為 GATA-3(+)，證實是乳腺轉移癌。該患者於 2023 年 7 月再次進行全身骨骼掃描，肝臟並無特別攝取增加。

討論：全身骨骼掃描常見的非骨性 Tc-99m MDP 攝取部位，有腎臟和膀胱（正常放射性藥物排泄）、甲狀腺、胃（未標記的 Free Tc）、原發性和轉移性腫瘤、良性腫瘤與注射部位等。本案例患者腹部右上象限意外出現軟組織吸收，這代表放射性藥物在肝臟中被吸收。研究指出，因轉移性腫瘤局部血管分佈增強、通透性增加與組織鈣含量升高，與在全身骨骼掃描中看到肝臟攝取增加有關。

結論：乳癌患者中，有肝轉移的 Tc-99m MDP 攝取是鑑定進展性疾病的重要線索。因此，當全身骨骼掃描影像有軟組織攝取時，需對此發現識別所涉及的器官或來源並認識攝取的重要性。

PC-002

正子造影中心人員與空間暴露劑量研究

趙俐琪[1]、黃馨儀[1]、李全孝[1]、張晉銓[1,2]

[1]高雄醫學大學附設中和紀念醫院核子醫學部
[2]高雄醫學大學醫學院醫學系核子醫學科

背景介紹：本研究測量南部某醫學中心核子醫學部正子斷層造影檢查，對於醫事人員及周圍環境的輻射暴露數值，作為空間改建前後的比較，以及檢查動線設計上的參考。

方法：針對來本院接受正子造影檢查病患，不同時間點（注射室、第一次檢查及第二次檢查前後），分別以輻射偵檢器測量不同距離（距離體表 10 公分、1 公尺及 3 公尺處）的輻射劑量率。

結果：實測受檢人數為 30 位，其中男性 20 位、女性 10 位，平均注射 11.64 mCi 的 F-18 FDG。本研究測到最大劑量率 281.23 mSv/h（10 公分、注射後），最小劑量率 1.75 mSv/h（3 公尺、第二次檢查後）。隨著等待時間，測得劑量率持續下降；隨著距離拉大，測得劑量率明顯降低。

結論：經由這樣的研究，我們更清楚執行正子造影的技術師，在這樣的條件下，可能會累積多少輻射曝露。有助於我們調整檢查流程，確保輻射劑量不超標。

PC-003

以準直儀優化前哨淋巴結定位檢查品質

黃美瑩、李佳鴻、莊凱文、吳雅嵐

佛教慈濟醫療財團法人臺北慈濟醫院核子醫學科

背景介紹：腋下淋巴結是否受侵犯，是臨床上預測乳癌存活期及制定輔助治療方針的重要因素。前哨淋巴結定位檢查是透過皮下注射放射性藥物後，藉由伽瑪閃爍攝影機定位出距離腫瘤最近的前哨淋巴結位置，提供手術參考。本研究主要探討選擇合適的準直儀以提升前哨淋巴結定位檢查的影像品質。

方法：本研究使用 ^{99m}Tc-Phytate 0.5 mCi 進行前哨淋巴結定位檢查。經由皮下注射後，每 5 分鐘收集一張平面影像，直到核醫科醫師判定前哨淋巴結已顯影，在病人身上標記前哨淋巴結的位置。鍶 -99m 的能量為 140 keV，通常搭配低能量準直儀進行攝影。本科室因儀器更新，新購入 LEHRS、HEGP 準直儀，並加上已有使用的 MEGP，收集 2022 年 7 至 8 月間進行的前哨淋巴結定位檢查，分別使用 LEHRS、MEGP、HEGP 三種不同的準直儀之定位檢查影像並比對影像的差異。

結果：在 2022 年 7 至 8 月間進行的前哨淋巴結檢查影像中，明顯可以看出在使用 LEHRS 準直儀的時候，由於高濃度藥物在注射位置積聚，伽瑪射線穿透準直儀的鉛隔造成假影；若假影與前哨淋巴結顯影的位置重疊，有可能會被誤認為沒有顯像而無法完成定位。然而，在使用 MEGP 或 HEGP 準直儀進行檢查時，由於鉛隔較厚，影像上沒有出現因伽瑪射線穿透造成的假影，故可以更明確快速地觀察到前哨淋巴結顯影位置，這兩種準直儀對於阻擋伽瑪射線穿透的效果同樣良好。

結論：一般來說，核醫檢查多是依照檢查所使用核種的能量高低來選擇適合的準直儀。然而，本研究顯示，根據檢查特性及影像結果來選擇準直儀可以獲得更佳的品質。放射師應該要了解儀器的特性，活用所學，從而提高檢查結果的準確性。

PC-004

Incidental Finding of Reverse Rotated Kidney in a Bone Scintigraphy

Chao-Wei Tsai, Shih-Chuan Tsai, Shin-Yi Wang, Yi-Jing Lin, Jing-Uei Hou

Department of Nuclear Medicine, Taichung Veteran's General Hospital, Taichung, Taiwan

Kidney malrotation refers to a congenital abnormality in which the kidneys are located in an abnormal position in relation to the hilum, and it can occur unilaterally or bilaterally. A large portion of the patients are asymptomatic, and are often diagnosed incidentally by examinations including CT or MRI. There are several subtypes of kidney malrotation, and reverse rotation is one of them. Here, we present Tc-99m MDP bone SPECT/CT findings of a case of reverse rotated kidney in a 80-year-old woman with colon adenocarcinoma.

PC-005

Assessment of Discharge Time of Patients with Thyroid Cancer Treated With I-131

Chien- Hua Lu, Yu-Sheng Hung

Division of Nuclear Medicine, Chi Mei Medical Center, Liouying,Tainan,Taiwan

Purpose: Patients with well-differentiated thyroid cancer who receive I-131 drug treatment after surgery need to be isolated in an isolation ward. They can be discharged from the hospital only when the body radiation exposure rate drops below a certain standard. This research is to detect the radiation dose rate at 1 m of the patient's body after taking the medicine for 24 hrs, and to evaluate the discharge time of the patient, so as to make the most effective use of the ward.

Method: Count the patients with thyroid papillary or follicular carcinoma between 109.01–112.05. After the operation, they received the dose of I-131 drug 80–200 mCi in our hospital, and detected the radiation exposure rate at a distance of 1 m from the body after 24 hrs, the SrCr of all patients is normal, and appropriate health education is given before hospitalization, and they are told to drink plenty of water to increase urine excretion to reduce the residual radiation in the body 2 hrs after taking the medicine, and detect it with ATOMTEX AT1121 scintillation detector body radiation dose rate.

Results: In this study, a total of 374 person-times were retrospectively analyzed between 109.01–112.05.The average dose rate was 30.37μSv/hr after taking the medicine for 24 hrs.

Conclusion: According to the new draft of the Atomic Energy Commission of Taiwan, the radiation exposure rate at 1m from the patient's body surface is lower than 70 μSv/hr, and can be released from the hospital under appropriate guidance and control. According to the statistical results of this study, the patient can be released from the hospital after 24 hrs of hospitalization.

PC-006

F-18 FDG PET/CT 橫膈膜肌肉異常攝取——案例報告

李佩璇、楊朝瑋

澄清綜合醫院中港院區核子醫學科

背景介紹：F-18 FDG PET/CT 可用於評估原發性、轉移性腫瘤以及肌肉組織的感染或炎症。肌肉構成了身體很大一部分，也是葡萄糖的主要使用者之一。在 PET/CT 上的肌肉 FDG 攝取可能是生理性的，也可能是各種不同的病理狀況造成。

病例報告：一名 54 歲男性，有蝶竇癌病史，懷疑有肝臟轉移。於 2023 年 6 月進行 F-18 FDG PET/CT，在影像中發現肋間肌與橫膈膜肌肉異常攝取增加。查詢其血液報告，PCO_2 為 26.4 mmHg (正常：35.0–45.0 mmHg)、PO_2 為 125.0 mmHg (正常：83.0–108.0 mmHg)，以及胸部 X 光顯示有心臟肥大與雙側肺部浸潤。且該患者檢查當日有使用鼻導管供給氧氣，且呈現很喘的狀態。因此，橫膈膜肌肉異常攝取 FDG 極大可能是因呼吸太用力導致。

討論：肌肉攝取 FDG 除了惡性腫瘤和炎症外，還有運動負荷或肌肉緊張導致。在大多數情況下，肌肉攝取 FDG 通常為生理性不具有病理意義。有研究指出，在呼吸困難時，需考慮呼吸肌（橫膈膜及肋間肌）、胸鎖乳突肌、斜角肌及腹部肌肉會有 FDG 攝取增加情況發生。本案例所觀察到的，橫膈膜肌肉高度攝取 FDG 亦屬於呼吸原因造成。

結論：了解肌肉中攝取 FDG 的正常生理變異，對於區分病理性攝取和生理性攝取是很重要的，以避免對實際病理病變的誤診。

PC-007

Early Prediction of Distant Metastasis in Patients with Uterine Cervical Cancer Treated with Definitive Chemoradiotherapy by Deep Learning Using Pretreatment [18F] Fluorodeoxyglucose PET/CT

Kuo-Chen Wu[1,2], Shang-Wen Chen[2,3,4,5], Te-Chun Hsieh[6,7], Kuo-Yang Yen[6,7], Chao-Jen Chang[2], Yu-Chieh Kuo[2], Ruey-Feng Chang[1,2,8], Chia-Hung Kao[2,6,9,10]

[1] *Graduate Institute of Biomedical Electronics and Bioinformatics, National Taiwan University, Taipei, Taiwan*
[2] *Center of Augmented Intelligence in Healthcare, China Medical University Hospital, Taichung, Taiwan*
[3] *School of Medicine, College of Medicine, China Medical University, Taichung, Taiwan*
[4] *School of Medicine, College of Medicine, Taipei Medical University, Taipei, Taiwan*
[5] *Department of Radiation Oncology, China Medical University Hospital, Taichung, Taiwan*
[6] *Department of Nuclear Medicine and PET Center, China Medical University Hospital, Taichung, Taiwan*
[7] *Department of Biomedical Imaging and Radiological Science, China Medical University, Taichung, Taiwan*
[8] *Department of Computer Science and Information Engineering, National Taiwan University, Taipei, Taiwan*
[9] *Graduate Institute of Biomedical Sciences, School of Medicine, College of Medicine, China Medical University, Taichung, Taiwan*
[10] *Department of Bioinformatics and Medical Engineering, Asia University, Taichung, Taiwan.*

Introduction: A deep learning (DL) model using image data from pretreatment [18F] fluorodeoxyglucose ([18F]FDG)-positron emission tomography (PET) or computed tomography (CT) augmented with a novel imaging augmentation approach was developed for the early prediction of distant metastases in patients with locally advanced cervical cancer.

Methods: This study used baseline [18F]FDG-PET/CT images of newly diagnosed uterine or cervical cancer patients. Data from 186 and 25 patients were analyzed for training and validation cohort, respectively. All patients received chemoradiotherapy (CRT) and follow-up. PET and CT images were augmented by using three-dimensional techniques. The proposed model employed DL to predict distant metastases. Receiver operating characteristic (ROC) curve analysis was performed to measure the model's predictive performance.

Results: The area under the ROC curves of the training and validation cohorts were 0.818 and 0.830 for predicting distant metastasis, respectively. In the training cohort, the sensitivity, specificity, and accuracy were 80.0%, 78.0%, and 78.5%, whereas, the sensitivity, specificity, and accuracy for distant failure were 73.3%, 75.5%, and 75.2% in the validation cohort, respectively.

Conclusions: Through the use of baseline [18F]FDG-PET/CT images, the proposed DL model can predict the development of distant metastases for patients with locally advanced cervical cancer treatment by CRT. External validation must be conducted to determine the model's predictive performance.

PC-008

Imaging Prediction of KRAS Mutation in Patients With Rectal Cancer Through Deep Metric Learning by Using Pretreatment [18F]Fluorodeoxyglucose Positron Emission Tomography/Computed Tomography

Kuo-Chen Wu[1,2], Shang-Wen Chen[2,3,4,5], Te-Chun Hsieh[6,7], Kuo-Yang Yen[6,7], Chao-Jen Chang[2], Yu-Chieh Kuo[2], Yu-Ju Hsu[2], Ruey-Feng Chang[1,2,8], Chia-Hung Kao[2,6,9,10]

[1] *Graduate Institute of Biomedical Electronics and Bioinformatics, National Taiwan University, Taipei, Taiwan*
[2] *Center of Augmented Intelligence in Healthcare, China Medical University Hospital, Taichung, Taiwan*
[3] *School of Medicine, College of Medicine, China Medical University, Taichung, Taiwan*
[4] *School of Medicine, College of Medicine, Taipei Medical University, Taipei, Taiwan*
[5] *Department of Radiation Oncology, China Medical University Hospital, Taichung, Taiwan*
[6] *Department of Nuclear Medicine and PET Center, China Medical University Hospital, Taichung, Taiwan*
[7] *Department of Biomedical Imaging and Radiological Science, China Medical University, Taichung, Taiwan*
[8] *Department of Computer Science and Information Engineering, National Taiwan University, Taipei, Taiwan*
[9] *Graduate Institute of Biomedical Sciences, School of Medicine, College of Medicine, China Medical University, Taichung, Taiwan*
[10] *Department of Bioinformatics and Medical Engineering, Asia University, Taichung, Taiwan*

Introduction: To predict KRAS mutation in rectal cancer (RC) through computer vision of [18F] fluorodeoxyglucose (18F-FDG) positron emission tomography (PET)/computed tomography (CT) by using metric learning (ML).

Methods: This study included 160 patients with RC who had undergone preoperative PET/CT. KRAS mutation was identified through polymerase chain reaction analysis. This model combined ML with the deep learning framework to analyze PET data with or without CT images. The Batch Balance Wrapper framework and K-fold cross-validation were employed during the learning process. A receiver operating characteristic (ROC) curve analysis was performed to assess the model's predictive performance.

Results: Genetic alterations in KRAS were identified in 82 (51%) tumors. Both PET and CT images were used, and the proposed model had an area under the ROC curve of 0.836 for its ability to predict a mutation status. The sensitivity, specificity, and accuracy were 75.3%, 79.3%, and 77.5%, respectively. When PET images alone were used, the area under the curve was 0.817, whereas the sensitivity, specificity, and accuracy were 73.2%, 79.6%, and 76.2%, respectively.

Conclusions: The ML model presented herein revealed that baseline 18F-FDG PET/CT images could provide supplemental information to determine KRAS mutation in RC. Additional studies are required to maximize the predictive accuracy.

PC-009

Using Deep Learning Model to Categorize Tumor Mutation Burden in Non-Small Cell Lung Cancer

Yu-Hung Chen[1,2,3], Kun-Han Lue[3], Sung-Chao Chu[1,4], Kuang-Chi Chen[5], Shu-Hsin Liu[2]

[1] *School of Medicine, Tzu-Chi University, Hualien, Taiwan*
[2] *Department of Nuclear Medicine, Hualien Tzu-Chi Hospital, Buddhist Tzu Chi Medical Foundation, Hualien, Taiwan*
[3] *Department of Medical Imaging and Radiological Sciences, Tzu Chi University of Science and Technology, Hualien, Taiwan*
[4] *Department of Hematology and Oncology, Hualien Tzu Chi Hospital, Buddhist Tzu Chi Medical Foundation, Hualien, Taiwan*
[5] *Department of Medical Informatics, Tzu-Chi University, Hualien, Taiwan*

Background: Tumor mutation burden (TMB) is regarded as a biomarker for predicting treatment response of immune checkpoint inhibitors. We evaluate the value of ^{18}F-FDG PET-based deep learning model in predicting the TMB in non-small cell lung cancer (NSCLC).

Methods: We prospectively recruited patients with NSCLC who received pre-treatment ^{18}F-FDG PET. Our study has been approved by a local Institutional Review Board and Ethics Committee. TMB was calculated from whole-exome sequencing (WES) derived from tissue samples of the primary tumor. A TMB > 10/MB was defined as high TMB. To construct the deep learning model, we used the ResNet-18 architecture with primary tumor ^{18}F-FDG PET imaging as input. Tumor images were augmented and randomly divided into training (70%), validation (15%), and testing (15%) datasets.

Results: We analyzed the ^{18}F-FDG PET and WES data from 52 NSCLC patients. The sensitivity, specificity, positive predictive value, negative predictive value, and accuracy of deep learning model were 97.1%, 98.1%, 98.1%, 97.1%, and 97.6%, respectively for predicting high TMB.

Conclusions: Our preliminary results demonstrate that deep learning model may be used to categorize TMB in patients with NSCLC. Deep learning model may serve as a surrogate biomarker for predicting the response of immune checkpoint inhibitors.

PC-010

Cross-Scanner Validation of the Prognostic Value of Glycolytic Entropy in Lung Cancer

Ho-Yan Rong[1], Yu-Hung Chen[1,2,3], Kun-Han Lue[3], Shu-Hsin Liu[2]

[1] *School of Medicine, Tzu-Chi University, Hualien, Taiwan.*
[2] *Department of Nuclear Medicine, Hualien Tzu-Chi Hospital, Buddhist Tzu Chi Medical Foundation, Hualien, Taiwan*
[3] *Department of Medical Imaging and Radiological Sciences, Tzu Chi University of Science and Technology, Hualien, Taiwan*

Background: In lung cancer, survival outcomes varies significantly, highlighting the need for better stratification tools. ^{18}F-FDG PET-derived entropy is associated with survival outcomes in lung cancer patients. However, most of the studies on ^{18}F-FDG PET-derived entropy were based on analog PET, the potential benefits of entropy-based model in the era of digital PET remain largely unexplored.

Methods: We retrospectively reviewed medical records from 177 patients with lung cancer (131 and 46 patients underwent analog and digital PET, respectively). The study has been approved by the local Institutional Review Board and Ethics Committee, and the need for consent was waived. Pre-treatment ^{18}F-FDG PET-derived features and patients' demographics were included for analysis. We analyzed the overall survival (OS) using the Cox regression model and evaluate the model performance using Harrell's c-index. We construct the OS prediction model in the analog PET cohort and cross-scanner validate the model in the digital PET cohort.

Results: In the analog PET cohort, we found that the T status (HR = 1.4680, p = 0.0476) and entropy (HR = 2.0261, p <0.0001) independently predicted unfavorable OS. The OS prediction model, including the T status and entropy, outperformed the AJCC staging status (c-indices of 0.768 versus 0.651, p = 0.013). The model also significantly predicted OS in the digital PET cohort (HR = 1.016, p = 0.001).

Conclusion: Model based on glycolytic entropy outperformed traditional staging system in predicting OS in lung cancer. The entropy-based model also show predictive value in digital PET cohort, suggesting that applying entropy-based model across different generations of PET scanners may be feasible.

PC-011

Primary Hyperparathyroidism Caused by a Parathyroid Carcinoma Mimicking a Parathyroid Adenoma in the Tc99m-sestamibi Parathyroid Scan: A Case Report

Yi-Chen Wu[1,2,3], Huei-Yong Chen[1], Jyum-Ying Huang[1]

[1] *Department of Nuclear Medicine, E-Da Hospital, I-Shou University, Kaohsiung, Taiwan*
[2] *Department of Medical Imaging and Radiological Sciences, I-Shou University, Kaohsiung, Taiwan*
[3] *School of Medicine for International Students, College of Medicine, I-Shou University, Kaohsiung, Taiwan*

Introduction: Parathyroid carcinoma is a rare endocrine neoplasm and cause of primary hyperparathyroidism. The diagnosis of parathyroid carcinoma is difficult and usually confirmed on histopathological examination after parathyroidectomy. Dual-phase 99mTc-sestamibi imaging plays an important role in the localization of hyperfunctioning parathyroid tissue in primary and secondary hyperparathyroidism. We report findings of 99mTc-sestamibi parathyroid scan in a case with primary hyperparathyroidism caused by a parathyroid carcinoma.

Case report: This 37-year-old male patient suffered from left lower leg intermittent numbness and pain for 3 months. Associated symptoms included bilateral buttock, left thigh to left knee pain at the same time. He became unable to sit stably and could not walk on his own due to weakness. In orthopedic out-patient clinic, x-ray revealed a mild compression fracture with anterior wedge deformity of the thoracolumbar vertebras. Magnetic resonance imaging showed Left L5-S1 paracentral disc herniation and mild multilevel lateral recess and foraminal narrowing. After discussion, he was admitted for lumbar discectomy. Renal echo showed bilateral nephrocalcinosis. Blood test shows hypercalcemia and hyperparathyroidism. Primary hyperparathyroidism is considered. Technetium99m-Sestamibi parathyroid scan shows a hyperfunctioning parathyroid nodule in the right lower moiety, suggesting a parathyroid adenoma. After right lower parathyroidectomy performed, the pathology shows a parathyroid carcinoma, pT1Nx.

Conclusions: Parathyroid carcinoma is a rare endocrine malignancy. Preoperative diagnosis is challenging. The 99mTc-sestamibi parathyroid scan cannot differentiate between benign and malignant parathyroid lesions. It is utilized in localizing the primary and metastatic parathyroid carcinoma.

PC-012

利用 SPECT/CT 鑑別 ^{99m}Tc-PYP 閃爍掃描法對 Amyloidosis Transthyretin Cardiomyopathy 成像檢查之經驗分享

朱麗蓉、鄭如金、王淑芳、王毓婷、陳世欣

基隆長庚紀念醫院核子醫學科

背景介紹：罕見的轉甲狀腺素蛋白類澱粉沉積心肌症 (Amyloidosis Transthyretin Cardiomyopathy, ATTR-CM) 主要因變異的類澱粉蛋白沉積在心肌中，造成心臟壁厚度增加，形成充血性心臟衰竭。其相關症狀有呼吸急促、疲勞、下肢水腫等。ATTR-CM 誘發之心臟衰竭確診後，若無治療是一個致命的疾病，平均存活期只有 2 至 3.5 年。近年，隨著醫學的發達，可使用非侵入性核子醫學焦磷酸鹽 (^{99m}Tc-pyrophosphate, ^{99m}Tc-PYP) 造影檢查心肌是否積聚有害的類澱粉蛋白。希望藉由 ^{99m}Tc-PYP 心肌檢查早期診斷 ATTR-CM，使病人及早得到治療。

方法：本研究回顧性數據分析從 2019 年 12 月至 2023 年 7 月接受 ^{99m}Tc-PYP 靜脈注射 20 mCi 後 3 小時進行胸部平面成像及 SPECT/CT (Siemens/Symbia Intevo Excel sn.2146) 掃描診斷 ATTR-CM 的 141 名患者（78 名男性，年齡 63.95 ± 12.56 歲 ; 63 名女性，年齡 71.06 ± 11.02 歲）的數據。通過視覺等級（相對於肋骨的視覺分級量表) 和半定量方法評估心肌放射示蹤劑的攝取，繪製兩個 ROI ：一個在心臟 (H) 上，另一個在對側半胸 (CL) 上，以計算 H/CL 計數比。將其分成三組：低攝取率（H/CL < 1.2 ＋視覺等級 0/1）、中攝取率（H/CL 1.2 ~ 1.49 ＋視覺等級 2/3）、高攝取率（H/CL ≥ 1.5 ＋視覺等級 3），將半定量數據和 SPECT/CT Fusion 定位以確認是否為類澱粉蛋白沉積在心肌。

結果：本研究結果將 81 位病患歸類為低攝取率，將 58 位病患歸類為中攝取率，將 2 位病患歸類為高攝取率，若僅透過視覺等級和半定量方法將平面影像分別病患攝取率，無法判定平面心肌影像是 ^{99m}Tc-PYP 沉積在心臟腔室還是在心肌，易誤判成假陽性 ATTR-CM，因此需借由 SPECT/CT 的低劑量 CT 精準定位心肌，才能更確認半定量及視覺評估數據高的病患，類澱粉蛋白沉積是否確實在心肌上。

結論：使用非侵入性 ^{99m}Tc-PYP SPECT/CT 的方法診斷 ATTR-CM，使 ATTR-CM 病人能及早診斷並治療，以增加 ATTR-CM 患者的存活率。

PC-013

以可信賴專業活動 (EPAs) 為導向提升醫事放射實習學生之教學成效

郭家怡、楊士頤、李世昌

國立成功大學附設醫院影像醫學部核子醫學科

背景介紹：對於實習學生們來說，實習是入職場前熟知未來工作環境及累積經驗的必經之路。但我們面臨的困題為：如何讓學生在有效時間內磨練至獨立上手完成單項檢查並且能有機制的評估信賴等級。為達到此目的我們利用信賴專業活動 Entrustable Professional Activities (EPAs) 的教學模式，以整體性與統合性的角度去評估學員及其信賴等級。

方法：信賴專業活動 Entrustable Professional Activities (EPAs)，依等級 Level 1 ~ Level 4 來分級其被信賴程度及其可進行之臨床工作。以此原則設計符合放射實習學生的教學活動，並應用在核醫單光子造影檢查 - 全身骨骼造影。從 Level 1 起始通過考核後才能邁向下一層級，使實習學生在學習最終可達到一致的標準。本次參與的放射實習學生有共有 25 人。進行核醫知識筆試前測後依序，Level 1 進行衛教影片示範並測驗，Level 2 由臨床教師實際帶領操作講解，Level 3 放射實習學生操作由教師評分。Level 4 DOPS 測驗技術考核，Level 5 核醫知識筆試後測。並利用 kirkpatrick 四層次評估模式來呈現此教學方案的成果表現。

結果：醫事放射實習生對 EPAs 活動整體的滿意度，非常滿意的比率達到 62.5% 其餘滿意的比率為 37.5%。核醫檢查的相關知識測驗平均分數從 78 分提升到 91 分。

結論：利用信賴專業活動 Entrustable Professional Activities (EPAs)，使實習學生在學習最終可達到一致的標準。條列式的步驟，循序漸進的考核讓學習更加容易。未來期望能拓展到其他核醫的檢查，用來訓練醫放實習生或是核醫新進同仁。。

PC-014

Ga-68 PSMA 正子造影發現攝護腺癌患者的純粹淋巴結轉移：一病例報告

陳琬淇[1]、翁瑞鴻[1,2]

[1]中山醫學大學附設醫院核子醫學科
[2]中山醫學大學醫學系

背景介紹：攝護腺癌經治療後有復發和（或）轉移時常伴隨 PSA 上升。此時核醫骨掃描常用來偵測是否發生骨骼轉移。一懷疑復發患者的 PSA 達 15 ng/mL，但骨掃描未發現骨轉移，故建議其接受 Ga-68 PSMA-11 正子造影。

方法：Ga-68 PSMA-11 由本院放射藥局自行合成。靜脈注射 5 mCi 的 [Ga-68]-PSMA-11。60 分鐘後，在 GE Discovery MI PET/CT 掃描儀上進行全身掃描。隨後進行無對比劑增強低劑量衰減校正 CT 掃描。掃描區域涵蓋頭頂到大腿中段。透過衰減校正反覆運算重建影像。

結果：Ga-68 PSMA 正子造影發現局部復發，以及多處淋巴結轉移，包括雙側的骨盆淋巴結、雙側腹腔後的淋巴結與左側鎖骨下淋巴結。但未發現其他遠端轉移。

結論：Ga-68 PSMA 正子造影的高敏感度與高特異性，彌補了骨掃描診斷能力的不足；其正確有效的診斷，為臨床醫師的適當處置決策，提供了關鍵的訊息。

PC-015

Disseminated NTM Infection Mimicking Malignancy with Metastases: A Case Report

Chien-Cheng Wang, Jui-Hung Weng, Pan-Fu Kao

Department of Nuclear Medicine, Chung Shan Medical University Hospital, Taichung, Taiwan

Introduction: Nontuberculous mycobacteria (NTM) are mycobacteria other than *M. tuberculosis* and *M. leprae* and they can be found in soil, dust, animals, food, and water pipelines. NTM can infect humans and cause lung disease, lymphadenitis, disseminated disease, skin, and soft tissue infection. As a non-specific radiotracer, infectious and inflammatory disease or responses may mimic and be misinterpreted as malignant disease at times in oncologic FDG PET scan, and so does NTM infection.

Methods: We reported a patient with urothelial carcinoma of urinary bladder and the ^{18}F-FDG PET/CT was requested for clusters of enlarged lymph nodes noted by CT scan during follow-up. The FDG PET scan was performed after fasting for 6 hours with a GE Discovery MI PET/CT scanner at 60 minutes after intravenous injection of ^{18}F-FDG. The scan area covers vertex to above knees. Images are reconstructed iteratively with attenuation correction. One ^{18}F-FDG-avid lymph node in neck was sampled for pathological analysis. The sputum and catheter cultures with molecular analysis for micro-organisms were also done.

Results: The ^{18}F-FDG PET/CT scan showed multiple increased glucose metabolic lymph nodes in neck, mediastinal, abdominal paraaortic, and pelvis, as well as multiple bones. No lesion likely suggestive of lung infection was identified in attenuation CT scan. Multiple metastases from prior urothelial carcinoma were impressed and reported. The biopsy of the neck lymph node was reported to be caseating granulomatous inflammation pathologically. Serial acid-fast stains and cultures were negative. The molecular analysis showed Mycobacterium fortuitum. The patient was referred to department of infectious disease and prescribed anti-mycobacterial treatment.

Conclusions: For cancer or immunocompromised patients, they have a much higher risk to get opportunistic infections. When presenting in disseminated disease, such infections may mimic multiple lymph nodes involvement and distant metastases, especially when no coexistent lung infection is present. Whenever encountering multiple lymphadenopathies and even bone lesions on ^{18}F-FDG PET scan during oncologic survey, the possibility of granulomatous/mycobacterial infection should be taken into account.

PC-016

使用 PET/CT 檢側到乳癌病患有大量皮下轉移病灶——案例分析

曾柏銘 [1], 呂建璋 [2], 沈淑禎 [2], 門朝陽 [1], 林雅婷 [2], 蕭聿謙 [3]

[1]天主教中華聖母修女會醫療財團法人天主教聖馬爾定醫院正子造影中心
[2]天主教中華聖母修女會醫療財團法人天主教聖馬爾定醫院核子醫學科
[3]亞東紀念醫院核子醫學科

前言：癌症是造成人類死亡最多的病別，但人們對轉移的生物學知識甚少。轉移指的是腫瘤細胞從原發腫瘤擴散到繼發部位的多步驟過程，通常被描述成一系列簡單的連續事件；轉移性症狀通常是在手術或全身治療後長期無法檢測到疾病後表現出來的。乳癌的皮膚轉移可能是惡性腫瘤的最初跡象，但更多的是廣泛轉移的晚期表現。

案例分析：一名 54 歲女性乳癌病患，自友院轉自本院後被安排進行正子造影掃描，使用正子造影 (PET/CT) 進行追蹤，使用 Siemens biograph 16　PET/CT，FDG 劑量 10 mCi，Early Phase 2min/bed 進行掃描，該病患在進行正子掃描前已知胸部皮膚潰爛且散發異味，已無法完全平躺進行掃描。在正子造影後發現腋下淋巴節及肝臟轉移、胸腔肋膜積水，胸部皮膚及皮下組織、胸壁處有強烈的 FDG 攝取並延伸至腹部皮膚，該病患至正子中心掃描時已全身不適，右手無法舉起，表現十分痛苦。

討論：目前癌症仍然是全世界的一個主要健康問題。轉移性癌症可以從一開始就發生，即在最初發病時就有轉移，但更多的是作為廣泛傳播疾病的一部分，晚期的腫瘤會造成相關死亡，通常是由於重要器官功能遭到損害。乳癌腫瘤的皮膚轉移相對罕見。雖此前也曾遇過乳癌轉移至皮下案例，但此病例為多年罕見的廣泛皮下組織轉移，故將之寫成報告。

結論：乳癌的皮膚轉移約占內臟原發腫瘤的 0.7 ~ 10%。它們可能是內部惡性腫瘤的第一個表現，但更多的时候是廣泛擴散的後期事件。乳癌的皮膚轉移在臨床中雖相對罕見，但它們是非常重要的。乳癌的轉移可能會在手術後數月至數年表現出來，但皮膚轉移可能暗示著癌症的惡化。早期的辨識則可進行準確和迅速的及時治療，因識別皮膚轉移對於治療計劃往往會有極大的改變，特別是原本被認為已經治愈的癌症。有些腫瘤的轉移會偏向特定區域。識別這樣的模式可有助於尋找潛在的腫瘤。

PC-017

使用 FDG PET/CT 發現膀胱的腹股溝疝氣——案例報告

曾柏銘[1]、呂建璋[2]、沈淑禎[2]、門朝陽[1]、林雅婷[2]、蕭聿謙[3]

[1]天主教中華聖母修女會醫療財團法人天主教聖馬爾定醫院正子造影中心
[2]天主教中華聖母修女會醫療財團法人天主教聖馬爾定醫院核子醫學科
[3]亞東紀念醫院核子醫學科

前言：腹股溝膀胱疝氣並不常見，但 10 歲以上肥胖男性的發病率可能高達 50%。危險因素包括男性、高齡、慢性尿路梗阻、盆腔肌肉無力和肥胖，約有 1 ~ 5% 的病例發生，大部分是靠著影像學的診斷而意外偶然發現。雖然這些病患大多無任何症狀，但在急性腎衰竭的風險則會增加、另外外傷性的破裂、廔管形成、膀胱結石、以及膀胱排空不完全導致感染、及其它罕見腫瘤的風險也會增加；而腹股溝疝氣在傳統的平面影像 (骨骼掃描除外) 中，想要發現也可能是有難度的。

案例報告：一名 72 歲男性因直腸癌至本院進行治療並使用正子造影 (PET/CT) 進行追蹤，使用 Siemens biograph 16　PET/CT，劑量 10 mCi，2min/bed 進行掃描，在影像結束後顯示出膀胱區下側右陰囊發現有一強烈 FDG 吸收現象，與膀胱濃度相近 (SUVmax)，CT 顯示膀胱的下側通過右腹股溝管疝出。兩處 FDG 顯影區域是完全獨立的，尿液在膀胱處偏少，SUVmax 在腹股溝處略高於膀胱，沒有證據表明有右陰囊局部發炎症狀，醫師懷疑可能為陰囊水腫或腹股溝疝氣。

討論：膀胱疝氣是一種相對不常見但並非罕見的疾病，通常發現在右側部。當膀胱或輸尿管疝入腹股溝管、陰囊或股骨管時就會發生這種狀況。本病例在右側腹股溝發現一局部 FDG 強烈吸收區域，易誤判為惡性腫瘤，仔細對照 CT 發現為一膀胱疝氣，故將之寫成病例報告。

結論：任何 50 歲以上的男性都必需注意腹股溝疝氣，因為病患可能在不知情的情況下，在疝氣切除術中造成膀胱損傷，導致感染、敗血症或死亡。膀胱疝氣雖然患者並不知情，但患者可能會出現排尿困難、頻尿、尿急、夜尿或血尿等症狀。為腹股溝疝氣患者看病的醫師可能要注意患者可能也同時患有腹股溝膀胱疝氣，特別是針對膀胱出現症狀的患者。

PC-018

Aspergillosis Infection of Skull Base in FDG PET/CT and Bone SPECT/CT

Tzyy-Ling Chuang

Department of Nuclear Medicine, Dalin Tzu Chi Hospital, Buddhist Tzu Chi Medical Foundation, Chiayi, Taiwan
School of Medicine, Tzu Chi University, Hualien, Taiwan

Introduction: We present a case of nasopharyngeal carcinoma (NPC) with an Aspergillus infection of the skull base which was difficult to differentiate from tumor invasion by bone scan and FDG PET/CT.

Case Report: A 63-year-old male had non-keratinizing squamous cell carcinoma of nasopharynx, cT2N1M0, stage II, s/p concurrent chemoradiotherapy in 2019, recurrent in 2021/04, rpT1 (AJCC 8), s/p nasopharyngectomy. However, three months later, he complained of headache on and off during this period. MRI showed abnormal signals of the clivus with enhancement; tumor invasion is suspected. Bone scan and FDG PET/CT were arranged to differentiate tumor invasion or osteomyelitis of the clivus. FDG PET/CT showed intense FDG-avid (SUVmax 9.4), probably malignant or infectious lesion of nasopharynx and clivus with left neck an intense FDG-avid (SUVmax 5.3) lymphadenopathy. Bone scan showed intensely increased radioactivity to bilateral skull base areas. Nasopharyngeal lesion biopsy and sequestretomy of clivus bone showed fungal infection, compatible with Aspergillosis.

Discussion: In skull base osteomyelitis, the common organism in typical cases is Pseudomonas aeruginosa, but Gram-positive bacteria, fungi, especially Aspergillus and Mucormycosis, and even Salmonella have also been reported in atypical cases. Skull base aspergillosis is an unusual clinical disorder that usually occurs in cases with known associated factors such as immunosuppression and maxillary sinusitis. Skull base osteomyelitis can be life-threatening if not recognized and treated promptly. In NPC, a SPECT/CT bone scan can be used to assess skull base and adjacent bone involvement and may influence treatment planning for NPC. Although there are many causes of infection, tuberculosis and fungal infections (cryptococcus, histoplasmosis, coccidioidomycosis, blastomycosis, and aspergillosis) are most commonly described as sources of false-positive FDG PET/CT results. FDG PET/CT has been found to be a valuable tool for treatment monitoring in patients with aspergillosis. The diagnosis of aspergillosis depends on clinical and radiological evidence of infection, isolation, and identification of Aspergillus species at the site. Our NPC case demonstrated Aspergillus infection of the skull base both at bone SPECT/CT and FDG PET/CT after CCRT and surgery.

PC-019

Osteitis Condensans Ilii on Bone Scan

Tzyy-Ling Chuang

Department of Nuclear Medicine, Dalin Tzu Chi Hospital, Buddhist Tzu Chi Medical Foundation, Chiayi, Taiwan
School of Medicine, Tzu Chi University, Hualien, Taiwan

Introduction: We present a case with breast cancer whose bone scan showed bony destruction to right SI joint, which finally demonstrated osteitis condensans ilii by CT and clinical history.

Case Report: A 36-year-old female had right nipple discharge sometimes with blood for about 4 months. Mammography showed right breast microcalcification. Breast echo showed no lesion found in the breast. Breast examination showed no mass palpable, but right nipple erosion with discharge. Core biopsy of right upper lateral breast showed microinvasive carcinoma, arising in grade 3 ductal carcinoma in situ (DCIS). Right total mastectomy with skin sparing, sentinel lymph node biopsy, left prophylatic mastctomy, and reconstruction were performed and pathology showed microinvasive carcinoma, grade 2, arising in extensive grade 3 ductal carcinoma in situ, pT1mi(m)N0(sn, i-) (AJCC 8) and Paget disease of nipple and skin. Bone scan showed bony destruction at right SI joint. CT showed bony sclerosis over bilateral sacroiliac joints likely sacroiliitis. Tracing her history, she gave birth to children in 2005 and 2010. Osteitis condensans ilii was diagnosed during follow up.

Discussion: Osteitis condensans ilii is a rare benign pelvic bone disorder that primarily affects the auricular portion of the ilium near the sacroiliac joint and causes intermittent low back pain that may radiate to the buttocks and posterior thighs. Typically, this is a relatively symmetrical process bilaterally in women, including pregnancy, while men are rarely affected. Although a definitive etiology has not been identified, the leading theory may be mechanical stress across the sacroiliac joint (specifically the auricular portion of the ilium). This constant mechanical strain on the sacroiliac joint can lead to premature degeneration and arthritis of the joint. The radiographic and CT findings of osteitis condensans ilii are well-circumscribed sclerosis, usually affecting the iliac side of the sacroiliac joint, mainly the lower part, but without evidence of sacroiliitis, such as joint space narrowing of less than 2 mm, obvious erosion, or bony ankylosis. Bone scan findings vary among patients. Although some reported focal bone uptake, others have not confirmed this finding. Treatment is mainly conservative, with physical therapy and analgesia as needed, and surgical resection is reserved for refractory cases.

PC-020

Sialoscintigraphy as a Diagnostic Clue for Subclavian Vein Stenosis

Tzyy-Ling Chuang

Department of Nuclear Medicine, Dalin Tzu Chi Hospital, Buddhist Tzu Chi Medical Foundation, Chiayi, Taiwan
School of Medicine, Tzu Chi University, Hualien, Taiwan

Introduction: We present a case whose sialoscintigraphy showed a high peak to the bilateral submandibular glands at the first minute in time-activity-curve and as a clue for high degree stenosis in the left subclavian vein.

Case Report: A 70-year-old female had lung adenocarcinoma post operation and chemotherapy. During pre-chemoimmunotherapy evaluation based on liquid biopsy with next generation sequencing, an immunologist was consulted to prevent an immune-related adverse event. Sialoscintigraphy showed a high peak to the bilateral submandibular glands at the first minute in time-activity-curve. Dynamic flow showed reflux from the left subclavian vein to the left jugular vein then draining to the bilateral neck vessels, which caused high uptake at the bilateral submandibular glands at 0–80 seconds. Chest computed tomography showed high degree stenosis in the left subclavian vein with collateral circulation in the left neck and chest wall.

Discussion: Central venous stenosis is primarily related to the placement of intravascular devices (eg, dialysis catheters, pacemakers, or defibrillators) or central catheters, but can sometimes be idiopathic. Subclavian stenosis is a major complication of subclavian dialysis catheters. The most plausible mechanism is damage to the endothelial cells of the vessel wall adjacent to the catheter. Clinically, subclavian stenosis is not important unless further vascular access is attempted. Impaired venous return may lead to swollen arm with dilated veins. To restore blood flow, symptomatic patients require balloon dilatation and percutaneous angioplasty. However, in our case, the Port-A catheter was inserted through the right subclavian approach. Venous stenosis can be diagnosed with CT venography, venography, duplex ultrasound, or intravascular ultrasound and confirmed by the pressure gradient across the stenosis. The patient's paravertebral venous collaterals had elevated flow, exacerbated by venous stenosis. This case showed an interesting clue of subclavian vein stenosis by sialoscintigraphy.

PC-021

Demonstration of Small Urinary Bladder Diverticulum on ^{99m}Tc-MDP Bone Scintigraphy: A Case Report

Yu-Sheng Liu, Yi-Jing Lin, Jing-Uei Hou, Shin-Yi Wang, Shih-Chuan Tsai

Department of Nuclear Medicine, Taichung Veteran's General Hospital, Taichung, Taiwan

Introduction: Urinary bladder diverticula rarely produce clinical symptoms and are usually found incidentally on image studies. In this case report, we demonstrated a small urinary bladder diverticulum on ^{99m}Tc-MDP bone scintigraphy.

Case Presentation: A 86-year-old man with right tongue base cancer received wide resection and face and neck reconstruction surgery. He underwent Technetium-99m methylene diphosphonate (^{99m}Tc-MDP) bone scintigraphy after the surgery in order to detect bone metastasis. The anterior and posterior whole body plain images revealed a small area of increased radiotracer uptake adjacent to the urinary bladder in the right hemipelvis. Enhanced abdominal computed tomography (CT) demonstrated a small diverticulum arising from the right side of the bladder. The finding on the bone scintigraphy was resulted from the retention of the radiotracer within the urinary bladder diverticulum.

Discussion: Urinary bladder diverticula are either congenital or acquired. The etiology is herniated bladder mucosa penetrated through detrusor muscle. The congenital bladder diverticula account for 10% of the disease, while most of the cases are secondary to elevated intravesical pressure. The majority of the patients have no symptoms, and no treatment or surgical intervention is required. Multiple case reports revealed incidental visualization of urinary bladder diverticula on ^{99m}Tc-MDP bone scintigraphy. However, anatomical images such as computed tomography or magnetic resonance imaging (MRI) are usually needed to confirm the final diagnosis. In some cases, the accumulated radiotracer may be misinterpreted as metastasis, and SPECT/CT can be used to differentiate urinary bladder diverticula from bone metastases.

PC-022

Atypical Bone Metastasis Mimicking Metabolic Bone Disease in Squamous Cell Carcinoma of Lung: A Case Report

Ching-Yi Wang, Jui-Hung Weng

Department of Nuclear Medicine, Chung Shan Medical University Hospital, Taichung, Taiwan

Introduction: Squamous cell carcinoma (SCC) of the lung is a type of non-small cell lung cancer, ranking second only to adenocarcinoma in terms of incidence and representing the second most common subtype of lung cancer. This type of lung cancer is highly correlated with smoking and typically forms in the central regions of the lungs and larger trachea. We present the case of a young patient with SCC who exhibited diffuse bone metastasis, along with atypical chest CT findings and a false-negative bone scan report.

Method: A 38-year-old male presented with symptoms of palpitations and dyspnea on exertion. He received chest X-ray, chest CT scan, bone scan, and eventually, echo-guide biopsy of left lung lesion. All the above-mentioned studies were performed in usual fashion.

Result: Either on CXR or chest CT scan, the radiopacity lesions in left lung seemed atypical of lung cancer although diffuse sclerotic change of vertebrae. Antibiotic treatment was prescribed initially. Bone scan showed diffuse inhomogeneous uptake in the skeleton, suspected metastatic bone disease or myeloma irrespective of malignancy. Biopsy revealed poorly-differentiated carcinoma with squamous differentiation, suspicious of NUT midline carcinoma. Although NUT midline carcinoma was excluded by subsequent genetic analysis, the initial impression of bone scan was turned into false negative for bone metastasis.

Conclusions: Given that young age of the patient despite a history of prior smoking, the likelihood of being malignancy for the lung opacity was relatively low. Along with the atypical presentation of bone scan before pathological result, no wonder false negative interpretation was impressed. From the experience in this case, extensive bone metastasis may at times present diffuse inhomogeneous pattern mimicking metabolic bone disease.

PC-023

核醫腦室腹膜腔引流管通暢掃描：小兒案例報告

王靖誼、翁瑞鴻

中山醫學大學附設醫院核子醫學科

背景介紹：兒童腦瘤五成以上伴隨有腦瘤性水腦 (tumoral hydrocephalus)，為了要引流腦脊髓液降低腦壓，經常採取腦室腹膜腔分流 (ventriculo-peritoneal shunt, V-P shunt) 手術。當腦脊髓液無法順利引流至腹腔，持續有水腦症狀時，臨床上會開立核醫腦室腹膜腔引流管通暢掃描檢查，查看管路是否發生阻塞 (obstruction)，以及幫助決定阻塞的確切位置。本案例為 3 歲男孩，因腦瘤術後建立 V-P shunt。臨床表徵哭鬧、意識變差，經腦部磁振造影檢查確認水腦復發，臨床醫師懷疑管路阻塞，遂至本科執行檢查。

方法：V-P shunt 壓力閥 (reservoir) 處上方頭皮剃髮。在壓力閥處局部注射 Tc-99m phytate 2 mCi。採集局部平面影像。

結果：檢查影像可看到放射性藥物大多聚集於注射處與較遠端頸部高度，未如預期順利流至腹膜腔，因此影像報告判定為管路阻塞，並建議臨床端與 X 光比對。胸部 X 光影像，意外發現胸部管路佚失，經加照腹部 X 光確認該引流管實已斷落，並蜷曲於腹腔內。

結論：臨床上 V-P shunt 管路不通原因，經常為管路日久黏液阻塞或彎折，而使得腦脊髓液無法順利引流。本案例除呈現另一種 V-P shunt failure 的原因外，亦揭示普通 X 光可能提供幫助診斷之訊息，值得臨床上參考。

PC-24

Exercise Habits Brain Networks Explored with Simultaneous PET/MR Imaging of Metabolism and Connectivity

Yuh-Feng Wang[1,2], Bang-Hung Yang[1,2], Yi-Ru Li[2], Jyh-Cheng Chen[2], Tsung-Min Hung[3]

[1] *Department of Nuclear Medicine, Taipei Veterans General Hospital, Taipei, Taiwan*
[2] *Department of Biomedical Imaging and Radiological Sciences, National Yang-Ming Chiao-Tung University, Taipei, Taiwan*
[3] *Department of Physical Education and Sport Sciences, National Taiwan Normal University, Taipei, Taiwan*

Introduction: With the advancement of medical technology, Taiwan is experiencing a projected trend of rapid population aging, resulting in a larger elderly population susceptible to cognitive decline. This study aims to examine the relationship between different types of physical activities (PA) and brain function, with a focus on exploring strategies to prevent or delay the progression of cognitive decline.

Methods: Healthy participants aged 50–60, all with college degrees and without cognitive impairments, will be recruited. They will be divided into three groups: an open-ended (racket sports) exercise group, a closed-ended (aerobic) exercise group, and an irregular exercise group. Before undergoing PET/MRI scanning, participants will be required to complete a personal information form, the Beck Depression Inventory (BDI), and the Taiwanese version of the International Physical Activity Questionnaire (IPAQ). Participants will first perform an executive function task, taking approximately 15–30 minutes, followed by a dynamic PET/MRI scan lasting approximately 90 minutes, which will acquire FDG PET dynamic images, structural MRI images, resting-state MRI (rsMRI) images, and magnetic resonance spectroscopy (MRS) data.

For image analysis, PET images will undergo quantitative analysis using PMOD 3.7 software, including the establishment of kinetic models for radiotracer analysis. Structural and functional MRI images will be analyzed using SPM12 software. In the statistical analysis, correlations will be conducted between the scores obtained from the executive function tasks, IPAQ scores, and the quantitative data obtained from the image analysis. This analysis aims to explore the relationship between brain function and different exercise modes.

Preliminary Study Result and Expected Outcome: In our preliminary experiment, one participant was recruited for each of the three groups, with the irregular exercise and open-ended exercise participants being male, and the closed-ended exercise participant being female. The experimental results revealed that the closed-ended (aerobic) exercise participant exhibited the highest level of brain activity. The open-ended exercise participant showed the shortest executive function response time, and the FDG uptake in the medial frontal cortex (MFC) was higher compared to both the closed-ended exercise participant and the irregular exercise participant, indicating superior executive decision-making capabilities in the brain.

PC-025

Cervical Osteomyelitis and Epidural Abscess Identified by ^{18}F-FDG PET/CT in a Previously Treated Hypopharyngeal Cancer Patient

Yu-Erh Huang[1], Chih-Lin Chuang[2], Shang-Heng Wu[3], Yu-Ming Chang[4], Pan-Fu Kao[5]

[1] *Department of Nuclear Medicine, Jen-Ai Hospital, Taichung, Taiwan*
[2] *Department of Radiology, Jen-Ai Hospital, Taichung, Taiwan*
[3] *Department of Otolaryngology, Jen-Ai Hospital, Taichung, Taiwan*
[4] *Department of Neurosurgery, Jen-Ai Hospital, Taichung, Taiwan*
[5] *Department of Nuclear Medicine, Chung Shan Medical University Hospital, Taichung, Taiwan*

Introduction: Chemoradiation-induced cervical spondylitis and epidural abscess, although is rare, can rapidly worsen and potentially result in fatal outcomes. Early detection and treatment are crucial to prevent severe neurological deficits, including quadriplegia and respiratory failure.

Case: A 57-year-old man, previously diagnosed with hypopharyngeal cancer and treated with surgery and adjuvant chemoradiation therapy, presented with odynophagia for one week. A CT scan revealed a mucosal defect in the right pyriform sinus, extending into the adjacent retropharyngeal and prevertebral spaces. Further ^{18}F-FDG PET/CT showed hypermetabolic lesions in these areas and the nearby cervical vertebrae. Notably, gas bubbles were observed within the cervical spinal canal on attenuation CT images, concerning for an infection which could be life-threatening. Further investigation revealed that the patient had experienced right limb weakness since the day before the PET/CT exam. An emergency MRI was arranged 8 hours after the PET/CT exam, prompted by symptoms of urine retention and loss of muscle power. This MRI subsequently confirmed the diagnosis of cervical spondylodiscitis with an associated epidural abscess. The patient rapidly developed quadriplegia on the same day as the PET/CT exam and underwent urgent decompression surgery. This was followed by administration of appropriate intravenous antibiotics. After 4 months of dedicated treatment, the patient was discharged with persistent lower limb weakness without evidence of tumor recurrence.

Conclusion: Incorporating intraspinal gas findings from attenuation CT images of ^{18}F-FDG PET/CT, along with medical history and clinical symptoms, aids in identifying critical cervical spinal infections in patients previously treated for hypopharyngeal cancer.

PC-026

鎦 - 前列腺特異性膜抗原 (Lu-177-PSMA) 靶向治療之輻射安全監控及實測劑量

林亭君[1]、洪綾蔓[1]、張筱琪[1]、楊詩涵[1]、李銘忻[1]、黃玉儀[1,2]

[1]和信治癌中心醫院核子醫學科
[2]國立陽明交通大學醫學院醫學系

背景介紹：Lu-177-PSMA，前列腺特異性膜抗原 (PSMA) 靶向治療。本院於 2022 年 8 月至今有 12 位病人共執行 27 次治療，在此提供治療作業中工作人員接收之輻射劑量及環境輻射監測之結果。

方法：

（一）Lu-177-PSMA-617 治療：採重力法靜脈輸注，給藥過程約 30 分鐘，治療後 30 分鐘及六小時離院前量測病人體表及距離 30 公分、100 公分之輻射劑量率。最後病人離院後環境監測及廢棄物量測。

（二）輻射偵測項目及使用設備：監控給藥過程之人員劑量、病人離開病房環境監測、住院期間廢棄物的量測、病人給藥後 30 分鐘及 6 小時離院前之體內輻射劑量率。人員劑量監控使用個人輻射警報器 (Thermo, Electronic Personal Dosimeter)，病人體內輻射劑量率及病房環境、廢棄物的監測使用 Atomtex AT1121 偵檢儀。

結果：

(一) 工作人員：

1. 給藥過程：放射師、核醫醫師、藥師、核醫護理人員監控結果平均分別 13.7、3.7、2.61、2.52 μSv。
2. 同位素治療病房護理師於藥物注射後 30 分鐘至 6 小時期間進入病房照護：由 14 位護理人員輪值，進入病房次數共 44 次，平均一位護理師進入 2 至 3 次，每一次照護約接受 2.02 μSv。

(二) 病人給藥後 30 分鐘距離病人腹部體表、30 公分、100 公分量測之輻射劑量率平均為 312.8、69.6、15.4 μSv/hr。

(三) 病人給藥後 6 小時距離病人腹部體表、30 公分、100 公分量測之輻射劑量率平均為 210.4、52.4、11.9 μSv/hr。

(四) 病人離院後病房環境及廢棄物監測：量測過程中病房環境設備都低於 0.3 μSv/h。僅量測到尿布廢棄物為 0.35 ~ 1.2 μSv/h，病人所穿著病人服量測數值為 0.3 ~ 6.8 μSv/h。

結論：本次給藥過程主要輻射工作人員輻射暴露都可控制在 15 μSv 以內，同位素治療病房護理師於每次照護平均都於 3 μSv 以內，若依據上述結果推算，一般醫護人員年劑量限度小於 1 mSv，可容許每年執行 495 次此治療。輻射工作人員以一年不超過 20 mSv，可容許醫師每年執行 5,405 次；放射師每年執行 1,459 次此治療。

PC-027

Successful Localization of Sentinel Lymph Node by SPECT/CT in an Oral Cancer Patient: A Case Report

Pei-Jung Li[1], Wei-Chun Wang[2], Guang-Uei Hung[1]

[1] *Department of Oral and Maxillofacial Surgery, Show Chwan Memorial Hospital, Changhua, Taiwan*
[2] *Department of Nuclear Medicine, Show Chwan Memorial Hospital, Changhua, Taiwan*

Background: For clinically N0 patients with oral cancer, there were about 50% eventually found to have micrometastasis of lymph node. Sentinel lymph node biopsy had been suggested as a reliable method for predicting regional lymph node metastasis in such group of patients. In the presented case, lymphoscintigraphy was performed in a patient with recurrent oral cancer for sentinel lymph node mapping as pre-operative assessment.

Methods: Immediately after subcutaneous injection of 1 mCi of Tc-99m phytate in per-tumoral regions, 15-minute dynamic and static planar imaging were performed using a dual-head SPECT/CT system (NM860, GE Healthcare). Then SPECT/CT imaging was performed for obtaining cross-sectional images and used as anatomy correlation.

Results: On planar images, it is not easy to confidently discriminate the tracer uptakes in lymph nodes and the interfering uptakes shining from injection sites. On SPECT/CT images, three radioactively nodular foci were demonstrated in right submandibular area and level II/III areas of right neck, consistent with sentinel and regional lymph nodes. For facilitating localization of these lymph nodes, color markers were further placed on skin. In following surgery, sentinel lymph node was successfully dissected with pathology confirmation.

Conclusions: Our case suggested that combination of SPECT/CT and planar imaging may be useful for localizing sentinel lymph nodes in patients with oral cancer.

Keywords: lymphoscintigraphy, head and neck cancer, sentinel lymph node

PC-028

Outcomes of Supraclavicular Lymph Node Metastasis in Esophageal Squamous Cell Carcinoma Patients Undergoing Chemoradiotherapy

Yung-Cheng Huang, Chien-Chin Hsu, Kun-Tsung Li

Department of Nuclear Medicine, Kaohsiung Chang Gung Memorial Hospital, Chang Gung University College of Medicine, Kaohsiung, Taiwan

Introduction: In the 8th edition of AJCC esophageal cancer TNM staging, the supraclavicular lymph nodes (SCLN)s is categorized as distant metastasis (M1) rather than regional lymph nodes, regardless of the primary tumor's location. However, some studies suggest that SCLN metastases may have a more favorable prognosis compared to metastases in other organs. Our study aims to analyze the prognostic impact of SCLN metastasis in esophageal squamous cancer and provide insights to guide treatment decisions.

Methods: We analyzed the retrospectively collected data of 114 patients with esophageal squamous cell carcinoma (ESCC) and their FDG PET/CT scans. All patients were treated by chemoradiotherapy and followed-up until September 2016 or until death. The Kaplan-Meier method was used for survival analysis, and the difference between survival curves was analyzed using a log-rank test.

Results: According to AJCC 7th edition, the 114 patients (3 women and 111 men, median age 54.8 years) were in stage II (n = 6), III (n = 93), and IV (n = 15). A total of 18 patients (15.8%) had SCLN metastasis; 5 had additional distant metastases, while 13 had SCLN metastasis alone (defined as stage IV in AJCC 8th edition). Median follow-up for surviving patients was 33.2 months (range: 20.3–69.2 months). Stage IV patients had worse prognoses compared to stage II–III (p = 0.04). No significant difference in overall survival (OS) was found between SCLN (+) and SCLN (−) groups (p = 0.47), nor between combined stage II–III SCLN (+) plus stage IV (AJCC 8th stage IV) and stage II–III SCLN (−) groups (p = 0.16). Additionally, no notable distinction in OS was observed between stage II–III SCLN (+) and stage II–III SCLN (−) groups (p = 0.94).

Conclusions: For patients with ESCC received chemoradiotherapy, SCLN metastasis or not had no significant difference in prognosis. Considering SCLNs as regional rather than distant metastasis and pursuing curative strategies might be appropriate for these patients.

PC-029

Transient PSA Flare in Patients With Metastatic Castration-Resistant Prostate Cancer Undergoing Lu-177-PSMA Treatment: a Single Institutional Experience

Yu-Yi Huang[1], Pei-Ing Lee[1], Bor-Tau Huang[1], Kuo-Cheng Huang[2]

[1] *Department of Nuclear Medicine, Koo-Foundation Sun Yat-Sen Cancer Center, Taipei, Taiwan*
[2] *Department of Hematology and Medical Oncology, Koo-Foundation Sun Yat-Sen Cancer Center, Taipei, Taiwan*

Background: Prostate-specific membrane antigen (PSMA)-radioligand therapy (PRLT) with Lu-177-PSMA-617 is a therapeutic option for patients with metastatic castration-resistant prostate cancer (mCRPC). Our institution commenced PRLT in August 2022, and during this initial phase, we observed instances of transient PSA elevation among patients undergoing treatment. The aim of this study was to assess the incidence of transient PSA flares in this patient cohort.

Method: This study examined the clinical characteristics of patients and tracked changes in their PSA levels throughout the treatment courses. PSA measurements were conducted at the onset of treatment and subsequently at two-week intervals. Transient PSA flare was defined as a temporary increase in PSA levels during the 2-week and/or 4-week follow-up periods, followed by a subsequent decline to a level lower than the initial PSA measurement at the time of treatment, typically observed at the 6-week or 8-week follow-up (which may coincide with the timing of the next treatment).

Result: Between August 2022 and August 2023, our institution administered Lu-177-PSMA-617 therapy to 12 patients. The average age of these patients was 78 years, ranging from 54 to 90 years. Their mean pre-treatment PSA level was 589.24 ng/mL, ranging from 20.1 to 3,760 ng/mL. Of the 12 patients, 8 received two or more treatment cycles, amounting to a total of 23 cycles. Notably, 4 out of these 8 patients (50%) and 11 out of the 23 cycles (48%) exhibited a transient PSA flare response. PSA levels during these flare responses ranged from 20.1 to 3,760 ng/mL, while the PSA levels at the commencement of treatment for these flare-response cycles ranged from 12.56 to 3,760 ng/mL.

Conclusion: Transient PSA flare response at 2 to 4 weeks after drug administration is frequently seen in this study cohort, and a follow-up during 6 to 8-week time frame would be more representative of treatment response of that single treatment. The underlying cause, mechanism, and clinical significance of this flare response warrant further comprehensive research for confirmation and deeper understanding.

PC-030

Incidentally Detected Hyperparathyroidism During a Bone Scan in a Patient Presenting with Left Shoulder Pain: A Case Report

Xuan-Ping Lu, Jui-Hung Weng, Pan-Fu Kao

Department of Nuclear Medicine, Chung Shan Medical University Hospital, Taichung, Taiwan

Introduction: In early hyperparathyroidism, patients may experience no symptoms or some nonspecific symptoms such as joint pain, muscle weakness, fatigue, and loss of appetite. In severe hyperparathyroidism, patients can develop symptoms including bone pain, nausea and vomiting, reduced kidney function, renal stones, and osteoporosis.

Case Report: We present the case of a 30-year-old male patient who was referred for a whole-body bone scan due to an X-ray that showed a non-specific but abnormal image of the left clavicle. The patient had a history of a motor vehicle accident and left shoulder sprain approximately four months prior to the bone scan. During the examination at that time, bilateral renal stones and chronic kidney disease were also diagnosed.

The whole-body bone scan was conducted 2.5 hours after the intravenous injection of 16.3 mCi Tc-99m MDP. The scan revealed symmetrically increased uptake in the skull, mandible, sternum, costochondral junctions, as well as the cortex and metaphyses of long bones, with decreased uptake in soft tissues. These findings are characteristic of hyperparathyroidism on a bone scan. Given the patient's history of bilateral renal stones, hyperparathyroidism was strongly suspected.

Subsequently, the patient was referred to the endocrinology department, where blood tests confirmed hypercalcemia and elevated levels of intact parathyroid hormone (iPTH). A parathyroid scan was performed, revealing an adenoma in the right inferior parathyroid gland. Subsequently, the patient underwent parathyroidectomy, confirming the presence of a parathyroid adenoma in the right inferior parathyroid gland.

Discussion: Severe hyperparathyroidism can result in heightened bone turnover, leading to a significantly elevated skeleton-to-soft tissue ratio, poor renal visualization, and high levels of uptake in the axial skeleton and proximal long bones, presenting as a superscan pattern on a bone scan. It is crucial to consider metabolic bone diseases in addition to bone metastases when interpreting bone scan results.

PC-031

Diffuse Large B-cell Lymphoma Relapsing as Neurolymphomatosis: Detection with F-18 FDG PET/CT

Bor-Tau Hung, Pei-Ing Lee, Yu-Yi Huang

Department of Nuclear Medicine, Koo Foundation Sun Yat-Sen Cancer Center, Taipei, Taiwan

Introduction: Neurolymphomatosis (NL) is a relatively rare but serious manifestation defined as peripheral or cranial nerve, nerve root, or plexus infiltration by malignant lymphocytes, usually of B-cell non-Hodgkin's lymphoma origin; the most common subtype is diffuse large B-cell lymphoma. Considering its severity, early detection and treatment are crucial. F-18 FDG PET/CT, a noninvasive molecular imaging modality, has been extensively applied in clinical practice and has resulted in increasing number of NL cases being recognized. We herein present a rare case of NL detected with F-18 FDG PET/CT.

Case Presentation: A 73-year-old woman with a history of diffuse large B-cell lymphoma (DLBCL) had been in remission for 2 years. She presented with rapidly progressive bilateral lower limbs weakness and facial numbness two weeks before having a biopsy to rule out recurrence. MRI of brain revealed a 27 × 43 mm enhanced mass in right infratemporal fossa, enhanced lesions in bilateral thalami, right internal and left external capsule, right temporal lobe, and bilateral trigeminal ganglia, suggesting recurrent disease. Restaging F-18 FDG PET/CT was performed for systemic survey and demonstrated a big hypermetabolic mass in right infratemporal fossa, linear uptake along bilateral cranial nerve roots and nerves, bilateral lumbosacral plexus nerve roots, and along sciatic nerves, highly suggestive of neurolymphomatosis. Histopathologic examination of right infratemporal fossa mass confirmed the diagnosis of DLBCL. The patient died of lymphoma within 4 months of diagnosis despite directed-therapy.

Conclusion: This case highlights the importance of multimodality imaging when there is strong clinical suspicion of neurolymphomatosis (NL).There was relative concordance between PET/CT and MRI in detection of affected cranial nerves. While both two modalities successively identified affected cranial nerves, F-18 FDG PET/CT revealed the full extent of this patient's disease and helped plan for a representative biopsy site, which finally established a diagnosis of recurrent diffuse large B-cell lymphoma involving brain, cranial nerves, peripheral nerves, nerve roots and plexus. Further studies and a larger case series will be required to fully clarify NL imaging features by CT, MRI, as well as F-18 FDG PET/CT.

PC-032

Medical Staff Radiation Exposure from Patients Receiving Nuclear Medicine Procedures—Revisited and Prospected

Wen-Sheng Huang[1,2,3], Chien-Ying Li[2+], Ching Yee Oliver Wong[4], Skye Hsin-Hsien Yeh[3#], Bang-Hung Yang[2*]

[1] *Department of Nuclear Medicine, Cheng-Hsin General Hospital, Taipei, Taiwan*
[2] *Department of Nuclear Medicine, Taipei Veterans General Hospital, Taipei, Taiwan*
[3] *School of Medicine, National Defense Medical Center, Taipei, Taiwan*
[4] *Department of Radiology, University of Southern California, Los Angeles, U.S.A.*

[+] *contribute equally as the first author.*
[#] *contribute equally as the corresponding author.*

Objective: Nuclear medicine (NM) has played an important role in clinical practice. The justification, optimization and "as low as reasonably achievable" are principle to get the best benefit patients, caregivers, and the public. Radiation concerns or undue panic thinkings remain since the Fukushima nuclear disaster in 2011. To clarify this issue, we observed the personal and environmental radiation exposure in hospital wards where most inpatients received NM procedures. Sampling for this study yielded a proof of concept regarding radiation issues of the current NM procedures.

Methods: Fifty-two thermoluminescent dosimeters (TLDs), except one for the environmental background control, were distributed to the wards. The TLDs were worn autonomously by medical staff or mounted on areas that were determined to be the most likely exposed areas of radioactivity from NM procedures to persons by the ward leaders, without giving any hint or constraint. There was also no limitation in the wards' daily activities. The TLDs were retrieved and read by a third-party qualified Institute for radiation exposure analyses.

Results: All 51 TLDs were reported as background in dosage (μSv) of both personal and environmental allocations after one month of exposure.

Conclusions: Radiation exposure from NM procedures appeared insignificantly affect the hospital medical staff and environment when the NM procedure guidelines were followed and the patients were instructed well regarding radiation safety.

Keywords: nuclear medicine procedures; radiation exposure; medical staff; environment

PC-033

GE DISCOVERY NM530 應用於右位心 (Dextrocardia) 患者之核醫心臟灌注造影儀器設定及影像分析

陳泓尹、陳恩賜、鄭皓文、陳義丰、鄭澄意

三軍總醫院核子醫學部

背景介紹：右位心 (Dextrocardia) 是心尖偏向於身體右側時的總稱。先天性右位心是一種罕見的先天結構異常，發生率約為萬分之一，通常發生於完全性臟器轉位 (Situs Inversus Totalis)，即胸腔及腹腔器官的位置與一般人左右相反，因此稱為鏡像右位心 (Mirror-image Dextrocardia)。本院使用奇異公司 GE DISCOVERY NM530 執行心肌灌注影像掃描，儀器機架構造為 L 型多針孔式半導體偵測系統，機架設定是針對正常人左位心造影設計，因此右位心病人執行造影時會發生心肌影像偏離影像中心或無法收取情形。本文內容是針對右位心患者心肌灌注造影，將儀器設定及影像分析進行變更，以符合臨床上放射師執行儀器造影及醫師心肌影像判讀之應用。

方法：

一、NM530 儀器設定及病患造影方式 : 更改病人影像姿勢 (Patient Location) 選項改為臥姿 (Prone) 及機架角度變更為 135 度。待患者注射完核醫藥物後請病人向右側躺 (Decubitus Lateral Right)，身體盡量靠近偵測器採右側臥位姿勢且抬舉右手執行心肌灌注造影，即可將右位心影像收集在照野中心。

二、右位心患者心肌灌注影像分析：心肌影像分析工作站 (Xeleris 4DR) 是針對正常人左位心影像分析設計，若將右位心資料直接套用，影像分析結果會發生心肌灌注影像左右相反情形，因此要針對右位心心肌灌注影像進行前處理。將原始 Stress 和 Rest 影像 Recon gated Tomo 有 1 筆、Recon gated 有 8 筆、全部改成 Y-mirror，將影像進行 180 度左右翻轉後，再進行影像 3D 立體定位分析。

結果：經由變更 NM530 儀器設定及右位心病患側躺方式照影，確認右位心影像收集在照野中心且影像清晰。心肌灌注影像分析上，若將影像直接套用分析，可以觀察到影像表現與一般左位心病人類似，但心肌灌注影像左右相反情形，即心室側壁 (Lateral) 及中隔 (Septa) 位置相反。經由 Y-mirror 處理過後再分析灌注影像，可得到與一般左位心病人一致的心室相對位置及影像表現。

結論：先天性右位心之患者在造影時使用特殊的擺位及角度輔以影像後處理， 可以獲得無異於左位心者之影像，但對於後續與資料庫比對之各式功能評估，僅可參考無法提供正確冠狀動脈分布資訊。

PC-034

利用院內制式處方系統建立核醫放射性藥品處方開立與治療流程

洪綾蔓[1]、許派洲[2]、楊詩涵[1]、林亭君[1]、黃玉儀[1]

[1]和信治癌中心醫院核子醫學科
[2]和信治癌中心醫院藥劑科

背景介紹：以往核醫放射性藥品治療主流為甲狀腺癌之碘 131 治療，其治療給藥流程相對單純，僅單一投藥之動作。然而近年來核醫診療合一 (theranostic) 世代來臨，核醫治療藥物也開始蓬勃發展，並且給藥之流程開始複雜化，例如 Lu-177-Dotatate 治療需搭配前置準備之止吐藥，跨越給藥前後之保護腎臟用之高濃度胺基酸，以及完成治療後之長效體抑素投藥。為確保核醫放射性藥品治療過程所有給藥流程之正確性，將治療流程標準化，使治療能正確地執行並完整地紀錄於病歷中是核醫診療進入臨床操作的重要任務。此報告提供本癌症專科醫院之因應模式，可做為準備採用核醫診療之醫療機構快速參考。

方法：本院為癌症專科醫院，原已有完善的化療制式處方系統，系統包含藥品為健保或自費，各藥品給藥的時間、順序、天數，藥品或點滴的流速設定，給藥方式，劑量的計算和調整，注意事項的提醒等設置項目，其模式與核醫診療所需之條件相符，因此我們利用相同模式，建立核醫放射性藥品治療制式處方。首先參照化學治療制式處方格式，規劃好核醫放射性藥品治療時所需使用的點滴和藥品，治療流程和給藥順序，一一將其設定進對應的欄位：Daily-IV-Fluid、Pre-hydration、Pre-medication、Therapy、Post-hydration、Post- medication 及 Notation，並可先預設好執行時間，即完成核醫診療藥品之制式處方範例。在醫師開立處方後，臨床單位便能依照其設定之時間及處方依序開始執行醫囑、給藥和紀錄。

結果：本院已制定好核醫放射性藥品治療制式處方範本 NM001 和 NM002，分別為 Lu-177 PSMA-617 (Pluvicto) 和 Lu-177 dotatate (Lutathera) 治療處方，核醫科醫師及臨床醫師能預先選擇所需的 protocol 開出治療處方，藥師確認處方後，處方收單即匯入醫院所有醫療系統，護理人員及核醫科可以清楚知道什麼時候給什麼藥物，並記錄執行狀況，所有的資訊及執行紀錄都會清楚且完整的呈現於病歷中。除保障治療流程執行之正確性，同時藉由此系統正確匯入和計價本次治療中投與之所有藥品（包含核醫放射性藥品）、耗材，避免帳務之異常。

結論：核醫放射性藥品治療越來越蓬勃發展並趨向複雜化的時代，利用既存之化療制式處方邏輯建置核醫放射性藥品專用的制式處方範本是一個快速的捷徑，建置同時須注意使系統貼近核醫放射性藥品使用狀況。採取此制式處方和給藥流程，可確保使核醫放射性藥品治療執行之標準化與正確性，並使治療資訊正確有效率的融合入醫院中央系統，兼具輔助病歷紀錄與正確計費的功能。

PC-035

癌症患者進行『真正』全身氟化葡萄糖正子／電腦斷層造影於下肢的額外發現

陳迺傑

嘉義長庚醫院

摘要：慣例上，進行氟化葡萄糖正子造影時，其造影範圍通常為顱頂至大腿近端。因此，慣例上氟化葡萄糖正子造影可能無法檢測到在造影範圍之外的病灶，特別是在雙下肢的部份。本回顧性研究目標是評估在『真正』全身氟化葡萄糖正子造影中，與傳統的掃描模式相比的額外發現。

方法：本研究的研究人員回顧自 2010 年 1 月至 2016 年 12 月間進行的 3,310 例進行『真正』全身氟化葡萄糖正子造影的案例。若在下肢發現疑似惡性病灶，則藉由病理結果或臨床追蹤來驗證其結果。

結果：85 例研究（2.6%）在常規全身掃描覆蓋範圍之外的下肢發現了額外病變。其中，61 例中觀察到額外的骨病變，11 例中有軟組織病變，13 例中有淋巴結病變。在這當中，只有一名患者因為下肢的額外發現，其臨床分期發生變化。與此同時，有三名患者因造影範圍之外的病變接受了治療。

結論：『真正』全身掃描在研究案例中，有額外發現的比例為 2.6%。在淋巴癌、原發自下肢的黑色素瘤、肺癌和乳癌患者中有相對較高的發生率。於這些特定癌症上，進行『真正』全身氟化葡萄糖正子造影有其臨床價值在。

PC-036

Lymphoscintigraphy with SPECT/CT Aids in Diagnosing Lymphoma in a Lymphedema Patient

Shin-Yuan Chang, Chieh Lin

Department of Nuclear Medicine and Molecular Imaging Center, Chang Gung Memorial Hospital at Linkou, Taoyuan, Taiwan

Introduction: Lymphoscintigraphy combined with SPECT/CT can aid in the diagnosis of lymphedema in patients where the underlying cause cannot be identified. In this case report, we introduce a patient whose lymphoma was diagnosed through lymphoscintigraphy combined with SPECT/CT. This highlights both the uncommon initial symptoms of lymphoma and serves as a reminder to remain vigilant when the cause of lymphedema is unclear, ensuring timely diagnosis and treatment for patients.

Case Report: A 69-year-old male came to our plastic surgery outpatient clinic due to bilateral leg swelling that persisted for two years. He had no history of surgery, major trauma, or underlying medical conditions, indicating the absence of apparent risk factors for secondary lymphedema. The plastic surgeon arranged lymphoscintigraphy combined with single photon emission computed tomography/computed tomography (SPECT/CT) to assess the extent and underlying cause of the lymphedema.

Lymphoscintigraphy showed bilateral lymphatic obstruction. SPECT/CT identified enlarged lymph nodes and infiltrates in the retroperitoneal region. We therefore suspected a slow-growing lymphoma based on the imaging findings.

Consequently, the patient was referred to the hematology department for further evaluation. The pathological examination confirmed the diagnosis as grade 1-2 (low grade) lymphoma.

Conclusion: Cancer-associated lymphedema can occur in various ways, including tumor compression of lymphatic channels or nodes and infiltration of lymphatic vessels (also known as lymphangitic carcinomatosis). Similar case report had been published in 2013, describing a 33-year-old male with progressive unilateral lower limb lymphedema over three years, ultimately diagnosed with Non-Hodgkin lymphoma.

We hope that this case story serves as a reminder not to overlook the exploration for the causes of lymphedema, since lymphoma can be a rare but significant differential diagnosis. Furthermore, timely utilization of lymphoscintigraphy combined with SPECT/CT can provide valuable insights.

PC-037

以正子輸液系統注射藥物評估護理師輻射劑量變化——以臺大醫院為例

陳庭儀、李婷嫣、呂惠敏、黃奕琿、鄭媚方、彭信逢

國立臺灣大學醫學院附設醫院核子醫學部

背景介紹：核子醫學檢查是利用放射性同位素以及其製劑，注射到病人體內或以口服方式來吸收，然後再利用造影機，得到影像以協助臨床醫師診斷或疾病分級，是高靈敏度與專一性的檢查。正子掃描 (PET SCAN) 是目前應用最廣泛的癌症檢查，給予病患注入正子追蹤劑，追蹤劑會集中跑到代謝功能異常的特定細胞，再由正子掃描儀造影得到影像。

因為核醫檢查的追蹤劑是有輻射劑量，故在核醫工作的同仁因必須執行檢查與照顧病患，會接受到輻射劑量，依輻射防護相關法規規定須監測輻射工作人員劑量，每月透過劑量佩章 (TLD) 進行監測。護理師為正子中心主要施打正子藥物之執行者，本篇旨要藉由引進正子輸液系統與傳統鉛屏蔽下手動施打藥物兩者方式，比較護理師所接受輻射劑量。

方法：正子輸液系統於 2020 年 3 月啟用，為排除因操作不熟練增加接觸時間而影響數據準確性，選定鉛屏蔽下手動施打藥物期間 (2019 整年度) 及正子輸液系統施打藥物期間 (2022 整年度) 之護理師每月劑量佩章 (TLD) 輻射劑量紀錄，進行比較及分析。

結果：經由統計與分析發現，使用正子輸液系統施打藥物的平均吸收劑量 (mSv) 顯著低於鉛屏蔽下手動施打藥物 (0.12 mSv ± 0.097 vs. 0.357 mSv ± 0.057, p = .000, 95% CI [0.164, 0.309])。

結論：正子輸液系統注射藥物時間短暫且輸液時護理師會退至注射室外，降低了施打藥物及接觸施打輻射藥物後的病患時間。但仍有可能因為病患檢查項目不同無法使用正子輸液系統或者因病患病況不穩定需時常協助病患護理或搬運病患間接造成吸收劑量增加等諸多因素而不適用。此分析顯示使用正子輸液系統相較於鉛屏蔽下手動施打藥物在平均吸收劑量有顯著性的降低，顯示使用正子輸液系統能有效降低人員輻射暴露。

PC-038

骨頭掃瞄影像中肺、肝及軟組織之 ^{99m}Tc-MDP 攝取——Case Report

許文齡、張淑敏、莊雅雯、張晉銓、王榛婷

高雄醫學大學附設中和紀念醫院核子醫學部

背景介紹：骨頭掃描是常見用於偵測骨頭病變的檢查，其原理是利用放射性示蹤劑 Tc-99m methylene diphosphonate 經由靜脈注射後，進入骨頭與骨質成份中的礦物部份結合，而在骨頭有放射性聚集或呈現放射性冷區的現象。轉移性鈣化 (Metastatic calcification) 是一種全身性不正常的鈣化，其原因是由於血液中鈣或磷酸的濃度過高，或副甲狀腺亢進而導致。而血鈣過高可能來自於：副甲狀腺素過度分泌、骨的破壞（骨腫瘤、轉移性腫瘤）、或維他命 A 或維他命 D 中毒。在骨頭掃瞄影像中呈現骨頭以外器官（肺、肝等）或軟組織攝取。

Case report 1:

一位 62 歲男性，腎臟癌病史，全身骨頭掃描影像呈現：右側第六肋骨前部、右側第八肋後部放射聚積、胸腔內骨外放射性示蹤劑聚積，搭配 SPECT/CT 斷層影像顯示活性主要聚積於雙側肺野上部、右側橫膈、左胸壁後部。

Case report 2:

一位 58 歲男性，脊椎疾病，全身骨頭掃描影像呈現：T11-12 扁平，右側第 6 肋骨前外側，右第 8 肋軟骨交界處有熱點，全身瀰漫性骨骼，特別是顱骨，顏面骨和四肢長股。胸腔內瀰漫性骨外放射性示踪劑積聚。

結論：核醫骨頭掃描在偵測早期骨頭病變有很好的靈敏度，因此被廣泛應用。然而許多疾病都有可能造成軟組織或骨頭外放射性藥物聚積而在掃描過程中被發現。轉移性鈣化的鈣沉積，會因高血鈣或高磷酸的原因去除時而消退，進而影響影像的表現。臨床影像判讀時，應配合相關病史詢問、檢驗數據 (parathyroid hormone, PTH)、適當的搭配 SPECT/CT 檢查，可以大幅提升骨頭掃描的特異性。

PC-039

A Rare Case of Pancreatic Tail Tumor Detected by Positron Emission Tomography/Computed Tomography Combined with Ultrasonography

Shu-mei Lu, Yu-Ling Hsu

Department of Nuclear Medicine, Ditmanson Medical Foundation Chia-Yi Christian Hospital, Chia-Yi, Taiwan

Case: Here we demonstrate a 80 year-old male who has abnormal CA-199 level for tumor survey. (CA-199:4490.0 IU/Ml, that is way high above normal range 0–37 IU/mL) PET/CT scan is indicated for decision making and treatment planning. FDG-PET/CT (low dose CT scan) revealed: A 5.5 × 6.4 cm pancreatic tail tumor with regional lymph nodes (Figure 1), combined with ultrasonography (Figure 2,3) suggest a pancreatic tail malignancy with regional lymph nodes and liver metastasis. According to later distal pancreatectomy microscopically, the pancreatic tumor reveals a moderately-differentiated adenocarcinoma as irregular shaped and with glandular structures infiltrating through pancreas into the adventitial fat.

Discussion: Pancreatic cancer has a poor prognosis, and the best chance for survival is to diagnose the tumour at an early stage. Abdominal ultrasound, computed tomography, magnetic resonance imaging and endoscopic retrograde cholangiopancreatography are the most commonly used radiological techniques for imaging the pancreas. The diagnostic accuracies, applications and limitations of the various modalities are discussed. Functional imaging is helpful, especially if the images are fused with those of computed tomography or magnetic resonance imaging. Pancreatic cancer is a common gastrointestinal tumor with increasing morbidity and mortality, and it is difficult to differentiate it from chronic mass pancreatitis. F-18- FDG PET/CT can be used for diagnosis of pancreatic cancer, staging, radiotherapy planning, evaluation of efficacy and recurrence, and differentiation from post-treatment fibrosis but the sensitivity and specificity of diagnosis of chronic pancreatitis are poor. There are reports in the literature that sensitivity and NPV of EUS and PET/CT were equal (100%) and higher than MDCT and MRI. Specificity, PPV and NPV of PET/CT were significantly higher than MDCT. PET/CT contributed to the management of pancreatic cancer in 30% of patients. FDG PET/CT is a valuable imaging method for the diagnosis and management of pancreatic cancer, especially when applied along with EUS as first line diagnostic tools. This case also demonstrates that clinical ultrasound combined with PET/CT imaging are helpful diagnostic tools.

PC-040

評估心肌灌流檢查語音衛教執行效果

許天睿、陳在揚、張毓真、陳義丰、鄭澄意

三軍總醫院核子醫學部

研究動機與目的：因新冠疫情影響，為了減少與病人近距離接觸交談時間，本組試行語音衛教方式，以期減少放射師染疫風險，由於心肌灌流檢查衛教內容較多，且檢查量又為傳統機型的 2.5 倍，因此我們使用現有衛教單內容，錄製心肌灌流的衛教語音，試行後確能減少接觸時間、且減輕工作負擔，然而具體的使用方式、適合之年齡族群，尚須研究清楚，避免病人忘記下午檢查時間及漏拔針之風險。

研究方法：本研究使用 Google 的語音功能，於對話框輸入心臟灌流衛教日常用語，轉錄成語音檔案，提供有需求的放射師使用個人準備的舊手機或筆電播放，造影設備是 GE Discovery NM 530c 半導體閃爍攝影機，過程中不改變原本鉈 -201 心肌灌流造影之流程，僅在資料採集（5 分鐘）中撥放錄音，並排除住院、認知障礙及重聽病人，以避免影響病人權益，步驟如下 : 在掃描時播放預錄之語音衛教 (重複 3 次) 約需 3.5 分鐘，播畢後詢問病人對於 (1) 拔針程序 (2) 心電圖貼片 (3) 飲水及食物 (4) 下午檢查時間等，衛教內容的熟悉程度，將結果區分為「不了解」、「需補充說明」、「了解」由放射師詢問及主觀判斷結果，紀錄於語音衛教統計表單上，檢查結束後原訂之口述衛教及發給衛教卡流程不變。

資料統計年齡與語音衛教了解程度之關聯性，以觀察各年齡層對播放語音衛教的理解能力，作為調查適合以語音方式衛教之族群，此外，統計病人對上述 4 項各別衛教內容的了解程度，觀察語音陳述所用詞語是否合適於病人理解，做為調整改進之依據。

結果：資料蒐整 2023 年 3 月 8 日至同年 4 月 17 日間，總計 153 位病人的語音衛教統計數值，依年齡區分為「59 歲以下」、「60 到 69 歲」及「70 歲以上」三個群組，可以了解語音衛教的占比分別為 96%、94% 及 69%，此外，以衛教內容區分，其中拔針程序為 76%，其餘則分別為 93%、為 89% 及 88%，統計結果可見 70 歲以上病人，對語音衛教的理解能力大幅下降，而拔針程序可能因為語音播放時，無斷句及語氣起伏容易使病人誤解。

結論：使用語音衛教於造影時播放，可以相對減少放射師口述衛教，近距離面對病人的時間，降低輻射劑量及染疫風險，並且提升檢查效率，然而在使用上仍需注意年長受檢者是否能確實的理解，於 70 歲以上的病人，建議維持透過家屬或口述衛教時觀察並確認病人反應的方式進行，以確保病人安全及診斷影像的品質，最後語音衛教不能取代原本的檢查程序，但在病人量多及衛教複雜的情況下，可以成為很好的輔助工具。

PC-041

增加注射放射性同位素吸收時間能否提高核醫前哨淋巴結定位檢查之偵測率？

尤毓甯、林虔睦

衛生福利部雙和醫院核子醫學科

背景介紹：自 1991 年有學者提出前哨淋巴結切除手術後，在臨床上取代了傳統腋下淋巴結廓清手術。前哨淋巴結 (Sentinel Lymph Node) 為乳癌細胞在腋下淋巴轉移時的第一個淋巴結，前哨淋巴結切除手術的理論基礎正是基於乳癌細胞擴散是由原來病灶處，有順序地沿淋巴管轉移至局部淋巴結，因此其感染與否能十分準確地預測其他淋巴結受疾病侵犯之程度。

手術前核醫前哨淋巴結定位檢查是透過注射放射性同位素後，藥物經淋巴系統擴散後積聚，藉此定位前哨淋巴結。若能提高此項檢查之偵測率，就能避免患者進行不必要之淋巴廓清手術，減少患者因術後併發症，如腋下疼痛、肩關節活動限制、神經損傷後遺症及患側上肢淋巴水腫等，提升手術患者的術後生活品質。

方法：本研究收集 2022 年五月至 2023 年三月共 184 位進行前哨淋巴定位檢查之病人資料。因病人淋巴引流的生理成分、引流系統的狀態及腫瘤本身的特徵等個體因素無法改變，故本研究在臨床上增加注射放射性藥物後到定位前的藥物吸收時間，觀察能否提高前哨淋巴結定位檢查之偵測率。

由核醫科醫師以皮下方式注射方式注射藥物於乳暈周圍，使用藥物為放射性同位素鎝製劑 (^{99m}Tc- Phytate)。原檢查方式為注射後經過 15 至 20 分鐘進行第一次造影，若無淋巴結顯影則於 100 至 120 分鐘後進行第二次造影。2022 年 8 月開始將檢查方式調整為注射藥物後 30 分鐘進行第一次造影，若無顯影則於超過 120 分鐘後進行第二次造影。

結果：2022 年五月至 2022 年七月 52 位患者使用原檢查方式，偵測率為 71.2%。2022 年八月至 2023 年三月共 132 位患者使用增加藥物吸收時間後之檢查方式，偵測率為 74.2%。

結論：根據上述結果得知，偵測率並未顯著增加。且若依單個月份分別計算會發現偵測率與藥物注射後的吸收時間並無正相關。

PC-042

降低核醫排檢作業流程干擾件數

王士甫、許友齡、杜東峻、林宛靛

戴德森財團法人嘉義基督教醫院核子醫學科品質管理中心

研究目的：隨著受檢量的增加以及疫情的影響，櫃檯的技術人員處理事務的複雜度也相對變高，為了在精簡的人力下提升效率，在排檢系統的整合跟前置作業流程的改善就有其必要性，當前排檢系統的整合已於精實專案進行中，但前置作業流程尚有太多干擾因素致使櫃檯作業變的繁雜，故希望藉此收集櫃檯人員意見並與主管討論決定朝此方向做改善。

研究方法：

我們請櫃檯技術員統整工作流程中最大的干擾因素在哪，以 80/20 法則找出主要干擾原因，並與團員腦力激盪討論出對策，主要問題點如下：

1. 病人詢問：詢問衛教相關問題及檢查籃子放哪？
2. 電話干擾：來電找科內人員等非排檢相關電話。
3. 病房檢查單刪單未告知：醫令系統刪單在週邊檢查排檢系統不會呈現。導致當日檢查藥物支數與患者數量比對不正確。

對策

1. 病人詢問：對策 1-1 提供衛教小貼示給病人，設置檢查報到按鈴投單區。對策 1-2 設置籃子置放區。
2. 電話干擾：對策 2-1 更改查詢區部分科室人員分機，增加部分科室分機。
3. 病房檢查單刪單未告知：對策 3-1 自動寄發信件通知櫃台排檢技術員醫令系統取消檢查單。

研究結果：干擾件數由 126 件降到 17 件，進步率 86%。附加效益：工作人員無效工時由每月 851.5 分降至 32 分鐘。工作人員壓力評估表從中度情緒困擾降至輕度。平均注射報到等候時間由 159 秒降至 75 秒；平均注射報到等候時間由 128 秒降至 19 秒。病人滿意度由 91.4 分提升到 95.5 分。

研究結論：櫃檯技術人員一直以來都是科室很重要的門面，但面對諸多的干擾多少對櫃檯人員情緒會有所影響，進而影響到工作的效率。鼓勵櫃檯人員說出他們日常工作中的難言之處，並集思廣益解決其難處，對於櫃檯人員身心靈都能有所提升，對於此次活動櫃檯人員給予的評價回饋中更可以感受到櫃檯人員在干擾件數降低後，更能顧及病患受檢時的感受與需求。

PC-043

改變乳房姿勢位置可協助偵測前哨淋巴結

張秀瑛[1]、莊紫翎[1,2]

[1]佛教慈濟醫療財團法人大林慈濟醫院核子醫學科
[2]慈濟學校財團法人慈濟大學醫學系

簡介：乳房前哨淋巴結檢查是在乳暈周圍以皮下注射的方式打入放射性同位素 Tc-99m Phytate，經一段時間加以按摩之後再取得多角度影像及皮膚定位。然而前哨淋巴結可能會因其所在位置、注射處的活性過高、乳腺組織過於豐滿導致衰減等因素而使得前哨淋巴結不易在部分角度的影像中被看見，在此報告中我們介紹一名因乳腺組織過於豐滿的病患，藉由改變乳房組織位置（利用醫療膠帶將患側乳房往中心處固定）來協助辨別前哨淋巴結。

病例報告：一名 45 歲左側有一 1.47 公分的非特殊類型浸潤乳癌患者，在今年 7 月到本科執行術前的前哨淋巴結定位檢查。在患側乳暈四周以皮下注射方式注入 Tc-99m Phytate，經 30 分鐘按摩後造影，除常規的前位、前斜位及側位像外另加照 SPECT/CT 以精確定位。在進行前位像時並無發現前哨淋巴結，但在前斜位及側位像時發現有 2 處活性攝取，因該病患的乳腺組織過於豐滿，因此在經由病患同意之後我們利用醫療膠帶將患側乳房往中心方向固定，並重新收取前位像，結果發現相較於原始姿勢的影像，在改變乳房姿勢位置的影像中明顯呈現了淋巴結的活性攝取。

結論：前哨淋巴結檢查對於乳癌的前哨淋巴結的辨別及定位可以提供非常好的幫助，尤其病灶的定位可使外科醫師提高執行手術的效率，對此名乳腺組織過於豐滿的病患而言，因仰臥時乳房組織自然向旁下垂導致在前位像時，注射處活性完全遮蔽住前哨淋巴結的活性攝取，雖然加照 SPECT/CT 也可發現未在前位像中出現的活性攝取，但卻無法執行皮膚定位，因此藉由改變患側乳房的姿勢、位置是有利於發現被遮蔽的淋巴結活性攝取，以此與大家分享。

PC-044

利用人工智慧模型偵測癌症病患 [18F]FDG-PET 影像病灶與評估預後

詹勝傑[1]、劉民翔[2]、王志傑[2]、吳彬安[2]、劉淑馨[1]

[1]花蓮慈濟醫院 核子醫學科
[2]花蓮慈濟醫院 人工智慧醫療創新發展中心

背景介紹：近年來越來越多人工智慧 (artificial intelligence) 的應用進入醫學影像領域，雖然目前已有一些商業上人工智慧的產品協助醫師判讀影像，但多集中於非核子醫學領域。這個研究旨在探討人工智慧深度學習技術，在 (1) 偵測癌症病患 [18F]FDG-PET 影像中病灶準確度與 (2) 評估癌症病人預後上的應用。

方法：我們選取 190 位頭頸癌病患的 [18F]FDG-PET 影像來做分析。病灶自動檢測上，我們團隊使用 U-net 模型，這模型整合 5 層網路，每層都以 2 的倍數進行下／上採樣。在預測病人是否復發和整體存活率上，則是使用 DenseNet 模型，此模型整合 116 層卷積密集塊 (Dense Block) 與 3 過度層 (Transition Layer) 。最後人工智慧模型自動檢測病灶效力會與核醫科醫師手動圈選的結果相比，以 Dice coefficience 呈現差異。

成果：在偵測 [18F]FDG-PET 影像中病灶上，我們開發之病灶自動檢測模型與核醫科醫師手動圈選結果相比後，呈現高度正相關，Dice coefficience 為 74 ~ 76%。在預測癌症病人是否復發 (recurrence)，DenseNet 模型準確度為 73.6%。預測病患整體存活率 (overall survival) 上，模型的預測力 c-index 為 0.738。

結論：我們開發出的人工智慧模型，在自動檢測病患 [18F]FDG-PET 影像病灶和預後評估上，呈現中高程度之準確性與效力。不過將來仍需要引入更大數量病患來研究，以提高模型的精確度。

關鍵字：人工智慧、機器學習、深度學習、正子斷層掃描

PC-045

評估蟹足腫復發並確認放射治療劑量：發展活化纖維母細胞抑制蛋白之核子醫學診斷藥物

劉惠菁

臺北醫學大學附設醫院

由異常疤痕組織增生所致的蟹足腫，在台灣是一種常見疾病。此症因會嚴重影響患者的日常生活與外觀，故令患者特別困擾。現今已有許多治療蟹足腫的方法，例如類固醇藥膏、類固醇注射藥物以及手術合併進行放射線治療等。其中以手術切除後合併放療是目前去除蟹足腫最有利的治療方式之一，因蟹足腫不易進行臨床病理分類，且常因個體產生差異，致使術後合併放療尚有極高的復發率，因此治療方式仍有進步空間。然而開發與評估可能的抗蟹足腫標靶技術，將有效助於減低術後合併放療的復發率和併發症。所以必須要鑑別有關促使蟹足腫形成和復發的生化學、組織學、遺傳機制等因素。

在傷口癒合的機制中，纖維母細胞活化蛋白 -alpha（FAP-α）的表現僅限於活化的纖維母細胞，而在蟹足腫疤痕中亦有相同的 FAP-α 增加趨勢。這顯示 FAP-α 可能參與蟹足腫疤痕的形成，由於這些原因，我們的假說是 FAP-α 可能是預測蟹足腫疤痕復發的指標分子；且某些以 FAP-α 為標靶的特異性抑製劑（FAPI）可抑制或阻礙高表現 FAP-α 的蟹足腫纖維母細胞。總合而言，我們經由合成和純化的 Lu177-labeled FAPI 偵測其在蟹足腫上的表現，並於 F18-FDG、F18-FEPPA 相比較，使它可以成為分析、精確檢測與治療蟹足腫疤痕癒後療效評估的分子醫學影像工具。

關鍵詞：蟹足腫復發、纖維母細胞活化蛋白 -alpha、Lu-177- 纖維母細胞活化蛋白抑制劑

PC-046

因漂白水殘留自動試管清洗儀水桶導致 CA125 實驗失效之分析

陳芃嘉[1]、方雅潔[1]、余景陽[1]、韓璞[1]、林慶齡[1,2]

[1]國泰綜合醫院 放射免疫實驗室
[2]國泰綜合醫院 內分泌新陳代謝科

背景介紹：實驗室同仁發現在自動試管清洗儀季保養後，當日接著清洗的 CA125 實驗報告數據異常。緊急詢問代班工程師得知，因交接疏漏而不知實驗室另有準備專門裝稀釋漂白水的水桶，而誤用了平常清洗實驗的水桶直接倒入了漂白水。實驗室同仁們推測清洗實驗的水桶內儘管經沖洗，仍有漂白水殘留，以致影響了 CA125 的實驗結果。

方法：在了解原因後，實驗室同仁迅速更換了備用的全新水桶，且使用了大量清水清洗自動試管清洗儀的管路，並重做了整批實驗。

結果：比對一開始受漂白水的實驗數據（圖一）與重做的實驗數據（圖二），可發現標準品及品管液的 CPM 落差極大，重做的實驗其標準曲線亦恢復正常（圖三）。

結論：實驗室驗證出的每一筆實驗結果都緊繫著病人的健康安全，所幸實驗室同仁及時發現實驗失效並迅速找出失效原因，得以發出正確報告，應小心防範此類事件，避免再次發生。

PC-047

Effects of First Radioiodine Treatment on Salivary Gland Function in Patients with Differentiated Thyroid Cancer

Pei Ing Lee, Yu-Yi Huang, Bor-Tau Hung

Department of Nuclear Medicine, Koo Foundation Sun Yat-Sen Cancer Center, Taipei, Taiwan

Introduction: Salivary gland dysfunction is one of the common complications after radioiodine (RAI) treatment for differentiated thyroid carcinoma (DTC). This study aims to assess the impact of first RAI treatment on salivary gland functions in DTC patients.

Methods: Eighty-five DTC patients (mean age 43.9 years, 55 women and 30 men) who underwent total thyroidectomy followed by first RAI treatment were enrolled in this study. Salivary gland scintigraphy was performed to evaluate salivary gland functions at two time points: (1) prior to RAI treatment (2) 12–24 months after RAI treatment. Quantitative parameters of salivary gland functions, including maximum uptake value (UV) and excretion fraction (EF in %, as defined as [maximum uptake value-minimum uptake value]/maximum uptake value) were measured and compared. Salivary gland uptake or excretion dysfunction was defined as a reduction of > 30% in maximum uptake value or excretion function in any salivary gland after RAI treatment. Associations between gender, renal function, radioiodine dosage, and salivary gland dysfunction were also assessed. Paired-t test and Fisher's exact test were used for statistical analysis.

Results: After first RAI treatment, both parotid glands showed a significant reduction in UV and EF ($p < 0.05$), whereas UV and EF of both submandibular glands remained relatively unchanged. In per-patient analysis, 43 of 85 patients (50.6%) experienced salivary gland uptake dysfunction, while 35 patients (41.2%) had salivary gland excretion dysfunction. Parotid glands were more affected than submandibular glands. Salivary gland damage was significantly correlated with radioiodine dosage, with fewer instances in patients treated with 100 mCi compared to those treated with 150 mCi ($p = 0.038$). But no association was found between gender, renal function, and salivary gland dysfunction.

Conclusions: First RAI treatment can affect salivary gland function, particularly in patients receiving higher RAI doses. Parotid glands demonstrated a higher susceptibility to radiation-related damage. This study emphasizes the importance of precise radioiodine dosing to mitigate salivary gland dysfunction in DTC patients undergoing high dose RAI.

PC-048

Investigating the Relation between Volumetric Semi-quantitation Metrics and Conventional Planar Metrics in Suspected ATTR-CM Cases

Ting-Yen Lee, Yi-Chieh Chen, I-hwuen Hwang, Mei-Fang Cheng

Department of Nuclear Medicine, National Taiwan University Hospital, Taipei, Taiwan

Introduction: Amyloid transthyretin cardiac amyloidosis (ATTR-CM) is a subtype of systemic amyloidosis where misfolded transthyretin (TTR) protein deposit in the heart. The ATTR-CM patients may present different symptoms such as cardiomegaly, left ventricular dilation, and diastolic dysfunction, and with the progression of the disease, which could lead to poor prognosis. Therefore, it is critical to detect the cardiac involvement for timely intervention.

To date, the heart-to-contralateral lung ratio (H/CL ratio) computed from planar images of 99mTc-PYP scintigraphy poses the key role to aid the diagnosis. However, there are instances where diagnosis is still difficult based on planar scintigraphy alone, especially at an early stage of disease with few TTR deposits. Limited to 2-dimension images, it is difficult to differentiate the myocardial region and blood pool, or the heart and the bone uptake. Recently, several studies reported the potential utility of volumetric quantitation using 3-dimension images (single-photon emission tomography, SPECT) in the diagnosis of ATTR-CM using 99mTc-PYP scan. Thus, the aim of the article is to find out the value of the metrics from 99mTc-PYP SPECT images on diagnosing ATTR-CM.

Methods: Patients who underwent 99mTc-PYP scan were collected from February, 2022 to December, 2022. The images were analyzed by the built-in software and the semi-quantitative indices, including the cardiac standardized uptake value (SUV), the volumetric heart-to-lung (H/L) ratio, and the planar heart-to-contralateral lung (H/CL) ratio were calculated. SUV was calculated from activity distribution of Tc-PYP with unit of kBq/mL standardized to the time of injection with the body weight and injected does correction. A volume of interest (VOI) of heart encompassed the left ventricle contour on the SPECT images depending on CT scan. The VOI included the blood pool due to the disability to exclude the blood pool without CT contrast. For a VOI of whole lung was automatically segmented by Auto lung 3D toolbox (Syngovia., Siemens). These parameters were established the correlation with each other through statistic software, SPSS.

Results: We retrospectively analyzed 99mTc-PYP images from 121 patients (average age, 63.24 ± 15.28; male: female, 70: 51). Preliminary results showed a mild to moderate correlation between the SUV and volumetric H/L ratio and the planar H/CL ratio ($r = 0.396$ and 0.288, respectively; both $p < 0.05$).

Conclusions: Based on the result, despite of the mild to moderate correlation in these metrics, SUV-based metrics still shows the potential in diagnosis of ATTR-CM. However, the further investigation of its diagnostic value may be carried out.

PC-049

Use Artificial Intelligence in Interpretation of Myocardial Perfusion Imaging

Wei-Hsuan Chen[1], Fang-Shin Liu[1], Yi-Da Li[2,3], Tzyy-Ling Chuang[1,3]

[1] *Department of Nuclear Medicine, Dalin Tzu Chi Hospital, Buddhist Tzu Chi Medical Foundation, Chiayi, Taiwan*
[2] *Division of Cardiology, Dalin Tzu Chi Hospital, Buddhist Tzu Chi Medical Foundation, Chiayi, Taiwan*
[3] *School of Medicine, Tzu Chi University, Hualien, Taiwan*

Introduction: Myocardial perfusion imaging (MPI) is a functional study that can evaluate the location and degree of myocardial ischemia. Cardiac catheterization is an invasive examination that can see the location and degree of coronary arteries stenosis. Therefore, we hope to use the AI MPI image interpretation training module to establish the correlation between the two.

Methods: This study collected patients who underwent both myocardial perfusion scan and cardiac catheterization within six months. MPI results and polar map images based on the 17 myocardial segments defined by the American Heart Association, and AI are used for training of the labeling. The degree of stenosis of different sections of the three coronary arteries in cardiac catheterization is used as the gold standard. Through AI module training, we establish the correlation between functional imaging and the degree of vascular stenosis in catheterization and ultimately predict the location and degree of coronary artery stenosis based on the results of MPI for providing a reference for clinicians.

Results: 126 patients were collected. Among them, 113 were trained with AI module. The rest 13 were put into AI mode, and their results were compared with their gold standard. After interpreting the images of 13 subjects with the AI module, a paired sample T test was performed with the results of their cardiac catheterization. It found that there were 3 vessel groups with statistical significance (Table 1), namely left anterior descending artery - second diagonal branch (LAD-D2), left circumflex artery- second obtuse marginal branch (LCX-OM2) and right coronary artery-posterolateral branch (RCA-PL).

Conclusions: Through AI module training, AI learning for nuclear medicine imaging can improve the correlation between MPI and cardiac catheterization. It can predict the location and degree of coronary arteries stenosis based on the results of MPI, providing reference for clinicians, and enable patients to reduce invasive examinations, thereby providing better medical quality and medical services, and maximizing the value of cardiac examinations.

PC-050

Atypical Thymic Carcinoid with PRRT: A Case Report

Kuan-Chen Chen[1], Kuan-Yin Ko[2]

[1] *Department of Nuclear Medicine, National Taiwan University Cancer Centre, Taipei, Taiwan*
[2] *Department of Nuclear Medicine, National Taiwan University Cancer Centre, Taipei, Taiwan*

Introduction: Thymic carcinoid is an exceedingly rare tumour with a dismal prognosis. In the realm of neuroendocrine tumours (NETs), Lutetium-177 DOTATATE (Lu-177 DOTATATE) or Lutathera® has obtained approval for treating unresectable or metastatic, progressive, well-differentiated, somatostatin receptor (SSTR)-positive gastroenteropancreatic NETs in adults. Numerous studies have demonstrated the efficacy of peptide receptor radionuclide therapy (PRRT) in lung carcinoids as well, warranting urgent prospective trials. Consequently, PRRT is under consideration as a potential alternative third-line or fourth-line therapy for patients whose tumour deposits exhibit positive uptake on somatostatin receptor Imaging. In this report, we present a clinical case of a 39-year-old male who experienced postoperative recurrence and metastatic atypical thymic carcinoid and who was subsequently treated with Lu-177 DOTATATE.

Case Report: The patient had a history of atypical carcinoid of the thymus and underwent anterior mediastinal tumour resection in 2018. However, after two years, the disease recurred and was managed with several lines of systemic anti-tumour therapy. Due to progressive disease, PRRT was considered, and both Gallium-68 DOTATOC (Ga-68 DOTATOC) and Fluorine-18 FDG (F-18 FDG) scans were arranged. These scans revealed lesions with both DOTATOC uptake (Krenning Score 2-3) and FDG avidity. Subsequently, the patient underwent PRRT using Lu-177 DOTATATE for three cycles. However, after the third PRRT cycle, a post-treatment single photon emission computed tomography/computed tomography (SPECT/CT) scan indicated increased tracer accumulation at previous lesions and the enlargement of pulmonary nodules with low uptake. Therefore, PRRT was discontinued due to the suspicion of disease progression, and the patient needed to be transitioned to alternative medical modalities.

Conclusions: It is crucial to emphasize that a multidisciplinary team, comprising nursing, radiological technologists, radiologists, and oncologists, is essential for establishing effective patient communication and fostering subsequent collaboration strategies.

PC-051

Positron Emission Tomography in Langerhan Cell Histiocytosis: A Case Report

Hsuan Hsu, Kuo-Wei Ho

Department of Nuclear Medicine, Chiayi Chang Gung Memorial Hospital, Chiayi, Taiwan

Introduction: Langerhan cell histiocytosis (LCH) is a rare disease. A case of LCH who underwent fluorodeoxyglucose positron emission tomography/computed tomography (FDG PET/CT) was presented.

Case Report: An 81-year-old woman suffered from right chin swelling for days. Computed tomography (CT) of head & neck with and without contrast disclosed bilateral cervical lymphadenopathies and bilateral oropharyngeal walls thickening. Additionally, due to elevated serum hepatobiliary enzyme levels and abdominal pain, magnetic resonance cholangiopancreatography (MRCP) was done and showed multiple enlarged abdominal lymph nodes. Further CT of chest & abdomen with and without contrast showed enlargements of multiple lymph nodes on both sides (above and below) of the diaphragm, which was suggestive of lymphoma. The patient then received right inguinal lymph node excisional biopsy. Before the pathology reports were released, FDG-PET/CT was arranged for lymphoma staging, giving the impression of disseminated lymphoma involving lymph nodes on both sides of the diaphragm, spleen, and bone marrow. Later, the pathology report revealed Langerhan cell histiocytosis. Based on the clinical presentation, pathology, and FDG-PET/CT reports, the final diagnosis was high risk multisystem Langerhan cell histiocytosis.

Discussion: Langerhan cell histiocytosis (LCH) is a rare malignant histiocytic disorder of myeloid origin. Patients can present with single or multiple organ involvement including bone, pulmonary, central nervous system, spleen, bone marrow, and lymph nodes. Identification of multiple or risk organ involvement is crucial because it determines treatment decisions. According to NCCN Guidelines Version 1.2023, FDG-PET/CT is an essential examination for LCH staging, since it is useful for determining the extent of the disease and for guiding biopsies. In follow-up and evaluation of treatment response, FDG-PET/CT is also superior to other conventional imaging such as CT or magnetic resonance imaging (MRI) owing to the advantages in whole-body monitoring and precise anatomic localization of metabolically active lesions. Studies have shown that FDG-PET/CT can demonstrate more active LCH lesions and allow the detection of therapeutic response earlier compared with conventional imaging. The case report presents the essential roles of FDG-PET/CT in LCH.

PC-052

Survival of Patients Undergoing Radium-223 Therapy for Metastatic Castration-Resistant Prostate Cancer Following National Health Insurance Reimbursement in Taiwan

Nan-Jing Peng[1,2], Shan-Fan Yao[1], Willam J Huang[3], Tzu-Chun Wei[3], Yuh-Feng Wang[1], Ko-Han Lin[1], Lien-Hsin Hu[1,2], Chien Hsin Ting[1], Tse-Hao Lee[1], Skye Hsin-Hsien Yeh[2]

[1] *Department of Nuclear Medicine, Taipei Veterans General Hospital, Taipei, Taiwan*
[2] *School of Medicine, National Yang-Ming Chiao Tung University, Taipei, Taiwan*
[3] *Department of Urology, Taipei Veterans General Hospital, Taipei, Taiwan*

Introduction: Radium-223 dichloride (Ra-223) has exhibited substantial efficacy in prolonging overall survival (OS) in patients suffering from metastatic castration-resistant prostate cancer (mCRPC) with symptomatic bone metastases. However, there can be considerable variation in outcomes among individuals. This study aims to evaluate the prognostic determinants associated with patient survival following National Health Insurance (NHI) reimbursement in Taiwan.

Methods: Enrolled in this study were patients diagnosed with mCRPC who underwent Ra-223 treatment at Taipei Veterans General Hospital. Each intravenous dose of Ra-223 was administered at a fixed rate of 55 kBq/kg with a four-week interval. Clinical outcomes were obtained from medical records, and potential prognostic factors for survival were assessed. Kaplan-Meier analysis was used to generate a cumulative survival curve, and between-group differences were evaluated using the Chi-squared test. Statistical significance was set at $p < 0.05$.

Results: A total of 76 patients underwent Ra-223 therapy, with 62 patients receiving NHI reimbursement and the remaining patients self-paying. Among them, 50 patients (65.8%) successfully completed six cycles of treatment, while 26 (34.2%) received 1–5 cycles. Mortality was observed in 47 patients. Factors significantly associated with survival included the presence of ≤ 5 bone metastases ($p = 0.0018$), a baseline prostate-specific antigen level ≤ 36 ng/mL ($p = 0.0004$), a baseline alkaline phosphate level < 115 U/L ($p = 0.0007$), a baseline hemoglobin level > 12 g/dL ($p = 0.0029$). Patients who completed six cycles of treatment exhibited significantly higher OS rates compared to those who did not ($p < 0.0001$). There has been a 4.4-fold increase in the number of patients, without a significant difference in OS, between patients who received NHI reimbursement and those who self-paid.

Conclusions: The administration of Ra-223 has demonstrated considerable potential in extending the survival of patients with mCRPC. The outcomes may be influenced by various prognostic factors. However, no significant difference in OS was observed subsequent to the reimbursement of Ra-223 therapy for mCRPC through the NHI system in Taiwan.

PC-053

Prognostic Assessment of F-18 BPA-PET in Salvage Boron Neutron Capture Therapy for Malignant Brain Tumors

Nan-Jing Peng[1,2], Ko-Han Lin[1], Yi-Wei Chen[3], Ling-Wei Wang[3], Yuh-Feng Wang[1], Lien-Hsin Hu[1,2], Chien Hsin Ting[1], Tse-Hao Lee[1], Jia-Cheng Lee[3]

[1] *Department of Nuclear Medicine, Taipei Veterans General Hospital, Taipei, Taiwan*
[2] *School of Medicine, National Yang-Ming Chiao Tung University, Taipei, Taiwan*
[3] *Department of Radiation Oncology, Taipei Veterans General Hospital, Taipei, Taiwan*

Introduction: Boron neutron capture therapy (BNCT) stands out as a propitious anti-cancer modality. F-18 boronophenylalanine positron emission tomography (F-18 BPA-PET) holds the potential to ascertain the concentration of BPA within the tumor, enabling meticulous treatment planning and outcome evaluation. This study endeavors to analyze the correlation between F-18 BPA-PET and BNCT in the context of malignant brain tumors and assess the survival outcomes following BNCT.

Methods: Patients were stratified into two groups: those subjected to BNCT (Group 1) and those not (Group 2). The tumor to normal tissue (T/N) ratio derived from F-18 BPA-PET was set at 2.5. The findings were scrutinized based on clinical follow-up. Student's t test and Chi-squared test were employed to discern differences between the groups. A cumulative survival curve was constructed employing the Kaplan–Meier method. Differences were considered statistically significant at $p < 0.05$.

Results: In total, 116 patients with T/N ratios obtained from F-18 BPA-PET were enrolled. BNCT was administered to 58 patients, while mortality was observed in 100 patients. The median overall survival (OS) for the two groups was 8.5 and 6.0 months, respectively. The cumulative OS exhibited no significant discrepancy between the two groups, nor in their T/N ratios. Within Group 1, 44 out of 58 (75.9%) patients exhibited T/N ratios exceeding 2.5. Excluding 3 patients who expired within 3 months, 55 out of 58 patients were evaluated for response after BNCT. The objective response rate (ORR) was 30.9%. Patients achieving ORR displayed substantially higher survival rates compared to those without (median OS 13.5 vs. 8.3 months, $p = 0.0021$), particularly when T/N ratio exceeded 2.5 (median OS 14.8 vs. 9.0 months, $p = 0.0199$).

Conclusions: BNCT does not appear indispensable for prolonging the survival of patients afflicted with malignant brain tumors. Nevertheless, it proves advantageous when ORR is attained, a condition closely linked to the values of T/N ratio derived from F-18 BPA-PET.

PC-054

淋巴癌患者做正子檢查意外發現副甲狀腺有活性吸收

朱秀蘭[1]、顏維徵[1]、游慧貞[2]

[1]高雄醫學大學附設中和紀念醫院核子醫學部
[2]高雄醫學大學附設中和紀念醫院影像醫學部

背景介紹：癌症病況有許多不同症狀，根據位置、癌症分期、是否轉移等，適用不同治療方針，且許多癌症初期，其細胞組織代謝活動變化會早於發生在解剖之變化，這時可顯示細胞組織代謝變化的正子斷層造影就具有相當優勢。正子斷層造影能早期診斷癌症，對於已轉移的癌細胞可偵測原發性病灶、評估癌症分期及作出手術前之正確評估，追蹤後續治療效果和評估癌症復發情形。因此如果缺少正子斷層造影檢查，就無法精確分期進而幫助病患之後續治療方針。

正子斷層造影能夠有效檢查淋巴相關的病變，受檢人必須在靜脈中注射放射性同位素去氧葡萄糖後，其癌症細胞與發炎部位都會有所反應，原理為利用正常組織和惡性腫瘤組織對於去氧葡萄糖吸收及留存有不同程度之差異，造成癌症病變位置，將會顯示非常清晰，因而可協助臨床醫師有效率及正確之診斷癌症。

國內目前健保給付之正子斷層造影適應症，在腫瘤方面為包括淋巴癌、黑色素癌、頭頸部癌（不含腦瘤）、食道癌、甲狀腺癌、原發性肺癌、乳癌、大腸癌、直腸癌及子宮頸癌。

病例報告：男性患者因淋巴癌來做正子斷層造影，惡性腫瘤細胞因為繁衍速度很快、能量需求大，在人體內代謝葡萄糖速度較正常細胞旺盛，正子斷層造影就是利用此特性，觀察人體組織或器官生理變化。此放射藥劑進入體內後（如 18F-FDG 葡萄糖），會聚集於葡萄糖代謝旺盛區域，影像顯示會異常明亮，一般即為惡性腫瘤細胞所在位置。

此病患除在淋巴細胞有發現異常吸收之外，在副甲狀腺處亦有活性吸收。（圖一）查核病人病史後，發現此病人有洗腎病史，故懷疑在副甲狀腺吸收部分可能是副甲狀腺機能亢進造成，而非癌症轉移。故建議安排病患接受核醫科 Tc-99m MIBI 副甲狀腺功能檢查，以確認是否因副甲狀腺機能亢進而造成正子影像有異常吸收。（圖二）

結論：對於洗腎的病患而言，因長期洗腎而造成體內鈣、磷離子長期偏高，容易形成副甲狀腺機能亢進。本次病例之患者便是因正子斷層造影檢查發現副甲狀腺區域有異常活性吸收，透過進一步的 Tc-99m MIBI 副甲狀腺功能檢查，協助確認患者實際狀況為洗腎導致之副甲狀腺機能亢進，也避免因正子斷層造影檢查而誤判其癌症分期，影響治療方式。

PC-055

改善核醫廢水監控

方雅潔[1]、余景陽[1]、韓璞[1]、陳芃嘉[1]、林慶齡[1,2]

[1]國泰綜合醫院放射免疫實驗室
[2]國泰綜合醫院內分泌新陳代謝科

背景介紹：本院配置六桶廢水槽，一桶為預備槽，其餘五桶為儲存槽。功能在於讓廢水活度（貝克）衰退之後排入大槽，大槽廢水抽樣合格後始可排入衛生下水道。因桶身的容量及檢體量差異每桶儲存時間不同，歷年紀錄皆於 1 至 1.5 個月換槽，然而輻防人員觀察已有 3 個月未換槽，因此請廠商檢測，廠商回覆無異狀。然而可能檢體量減少，後續抽驗廢水報告結果偏高，因此再次請廠商檢修。檢修後發現預備槽計電器受損，廢水由預備槽溢流管直接流入大槽。輻防人員於輻防會議提出本次狀況，建議進行改善。

方法：實驗室監控廢水槽之監控儀表板遷移至易觀察區域，並增加遠端監控功能、裝置訊號傳遞軟體。如此一來，當廢水槽排放至大槽或發生高液位皆會傳簡訊至負責人員手機。年度檢測廢水槽運轉功能、廢水槽液面高度偵測、廢水排放監測系統及警示功能測試。

結果：為能及時處理異常狀況，訊息傳送給輻防人員及工務組值班人員。當下班時間發生異常，值班人員可立即至現場查看並進行通報。年度檢測廢水槽運轉功能及監測系統不僅能確保功能正常，亦可提早更換老舊耗材達到預防效果。

結論：近年推動實驗室自動化，使用機器手臂及自動清洗儀之後廢水量上升，改善監控廢水槽設備及檢測廢水槽運作功能實為重要，也是原委會輻射防護稽查的要項之一，重視輻射防護安全亦是大家的責任。

PC-056

增加 Alpha-Fetoprotein 最高校正液濃度以提高精確度

韓璞[1]、方雅潔[1]、余景陽[1]、陳芃嘉[1]、林慶齡[1,2]

[1]國泰綜合醫院放射免疫實驗室
[2]國泰綜合醫院內分泌新陳代謝科

背景介紹：本實驗室在去年將 Alpha-Fetoprotein (AFP) 試劑廠牌由 CISBIO 更換為 BECKMAN，使用一段時間後，發現原 CISBIO 試劑之校正液最高濃度為 850.0 ng/mL，而 BECKMAN 試劑之校正液最高濃度為 482.0 ng/mL，兩廠牌試劑之校正液最高濃度相差接近 1.8 倍，因此在更換 BECKMAN 試劑後，實驗室需稀釋之檢體增加，稀釋過後結果精確度較為下降，同時使實驗室人力、耗材之成本增加。故實驗室與 BECKMAN 原廠進行溝通，並建議可將 AFP 試劑之校正液最高濃度提高。

方法：實驗室同仁搜尋 AFP 表現、癌症與區域性的相關性論文，以佐證台灣地區對於檢驗 AFP 高濃度的需求，以利向原廠 BECKMAN 建議將 AFP 試劑之校正液最高濃度提高。

結果：在 2020 年衛生福利部統計，Hepatocellular Carcinoma (HCC) 在台灣常見癌症為第四名，且癌症死亡數佔居第二名。在台灣地區有 73% 的原發性 HCC 之病患，血清中的 AFP 濃度會顯著上升，並超過判斷值 400.0 ng/mL。在癌症的判定、預測病情變化、監控治療的結果與癒後的追蹤，AFP 為重要指標。故實驗室以此為依據，向 BECKMAN 原廠表達提高 AFP 校正液最高濃度之需求。

結論：BECKMAN 原廠接收實驗室提供之需求與佐證，並回覆將進行相關研究與評估開發的可行性。BECKMAN 原廠於 2023 年起，額外提供第六點校正液，濃度為 895.4 ng/mL。經歷此過程，實驗室減少需稀釋之檢體，因此達到提升結果精確度，以及降低實驗室人力、耗材之成本的目標，以上顯示適時與廠商提出需求與良性溝通的重要性。

PC-057

以不同廠牌軟體分析 ERPF 其結果一致性之評估

楊士頤、吳佩珊、邱南津

國立成功大學醫學院附設醫院影像醫學部核子醫學科

背景介紹：有效腎血漿流量 effective renal plasma flow (ERPF) 是核醫檢查了解個別腎臟功能以及總腎臟功能的判斷。放射性藥物經靜脈注射，由腎絲球過濾或腎小管上皮細胞分泌，由伽瑪造影機 (γ-camera) 連續收集兩側腎臟之影像，迅速聚集在腎實質，逐漸由腎實質流向集尿系統的過程。主要探討在不同軟體分析下，提供臨床醫師一致性的半定量結果。

方法：收集 2022 年 8 月至 2022 年 12 月共 26 位受檢者，使用西門子 Siemens EVO excel (Itoh ERPF) 和飛利浦 Philips BrightView 兩家影像分析軟體圈選 ROI (region of interest)，並採用 SPSS 統計軟體對其 26 例左右腎臟 Split Function (%) 相互線性 (Linearity) 評估。

結果：統計 26 例受檢者 Split Function (%) 資料，年齡層位在 8 ~ 83 歲之間，男性 13 例，女性 13 例。以西門子和飛利浦兩家軟體分析加以測定結果，將兩側腎臟數據結果評估 (T-test) 其線性，左側腎臟 $R^2 \geq 0.95$ (correlation = 0.997，N = 26，$p < 0.05$），右側腎臟 $R^2 \geq 0.95$（correlation = 0.997，N = 26，$p < 0.05$），結果顯示兩者呈現有高度正相關，表示受檢者在這兩台不同軟體分析，不影響臨床診斷的準確性。

結論：核醫檢查以報告準確度之前提下，思考面臨不同機台與廠牌更換時，能不影響病人數據追蹤判讀的情況下，有效的使用軟體分析達到一致性，是值得去探討研究的課題。

PC-058

功能性甲狀腺轉移性濾泡癌導致外釋延遲之特殊個案

張秀瑛[1]、莊紫翎[1,2]

[1]佛教慈濟醫療財團法人大林慈濟醫院核子醫學科
[2]慈濟學校財團法人慈濟大學醫學系

簡介：接受放射性碘 131 大劑量（從 31 mCi ~ 200 mCi 視病況而定）治療病患需住院隔離（3 ~ 4 天），由於碘 -131 在體內 24 小時期間約有 76% 的放射性活度會隨尿液、唾液、汗等排出體外，雖碘 -131 代謝情況依病患而定，但大部分皆可於治療後 72 小時內順利外釋（本院外釋標準 < 70μSv/hr），因此多以 3 天來規畫病患住院排程。在此我們介紹一名罕見的功能性甲狀腺轉移性濾泡癌患者，其轉移性病灶可分泌甲狀腺荷爾蒙以至於在進行碘 131 治療時其轉移性病灶持續吸收碘 131 使得劑量值緩慢下降至治療第 6 天才順利外釋出院。

病例報告：一名 78 歲女性患者自述於 2023 年 4 月底感到身體不適，經胸部 X 光檢查顯示肺炎，左肋骨有腫瘤，在進一步的 CT-guide 切片檢查後，病理報告證實為轉移性甲狀腺濾泡癌，pT2N0M1（左側肋骨轉移）。因此，她於 2023 年 5 月接受了甲狀腺全切除術，病理為微侵襲性濾泡癌結節性增生，伴有明顯的 Hurthle 細胞改變。後轉介至本院進行碘 131 大劑量治療，劑量為 150 mCi (T4 withdrawal)。治療當天的抽血結果分別為 T3 型甲狀腺毒症；T3：2.62 ng/mL (正常值 0.78 ~ 1.82)、TSH：0.04 μIU/mL (0.17 ~ 4.05)、Free T4：0.99 ng/dL (0.89 ~ 1.79)、Thyroglobulin：6654.40 ng/mL (0 ~ 50)，進行治療後前三天所分別測得劑量值為 258 μSv/hr、186 μSv/hr、145 μSv/hr，該病患的腎功能正常，且每天至少攝取超過 2000 毫升的水幫助代謝，但我們發現相較於其他病患，此名病患的輻射劑量值下降速度異常緩慢，且在治療期間所進行的全身掃描影像中明顯可看出多處活性強烈的攝取，該病患直到第六天才勉強通過外釋標準順利出院。

結論：分化良好的甲狀腺癌分泌甲狀腺荷爾蒙導致甲狀腺功能亢進、甲狀腺毒症或維持甲狀腺功能正常狀態的病例是罕見的，因為分化良好的癌症很少具有侵襲性，並且侵襲性癌症很少會分泌甲狀腺荷爾蒙。由此名病患可得知功能性甲狀腺轉移性濾泡癌會因保有分泌甲狀腺荷爾蒙能力而持續吸收碘 -131 進而導致碘 -131 代謝減緩，因此在安排治療時，針對功能性甲狀腺轉移性濾泡癌的病患應以 3 天以上的治療時間來規畫住院排程較為安心。

PC-059

輻射物質意外事件之處理

張春梅

高雄榮民總醫院核子醫學科

背景介紹：未預期發生的意外事件，可能引發輻射曝露，而直接或間接地危害到人員者，均稱之為輻射意外事件。依據游離輻射防護法之規定設置輻射防護委員會，下設輻射防護安全室為負責本院輻射防護之業務單位，審核院內可發生游離輻射設備及放射性物質各使用單位之輻射防護安全措施，預防人為因素、地震、火災、水災、天然災害等所引起的輻射外洩，以確保輻射安全，並將輻射外洩事件所可能造成的傷害減至最低。

方法：非密封放射性物質意外事故處理程序，工作人員於意外事故發生時，應立即停止工作並通報主管及輻防人員，儘速採取適當應變措施。放射性物質濺溢污染事故發生時，工作人員、場所疑似污染時，應立即予以管制。實施人員及衣物、場所之輻射偵測。若遭受放射污染時，人員、場所應立即予以除污，衣物則收存放置至放射線衰減後再洗滌。工作人員懷疑可能受到意外曝露時，將該員所配戴之人員劑量計，立刻送回計讀單位緊急計讀。給予該員充分照顧，增加營養及休息時間，並適當調整其工作。根據劑量評估結果，採取必要之醫務檢查或醫務監護。

結果：輻射意外事件發生的主要原因「天然災害延、人為因素造成、機械材料變異」。統計本院 2018 年 ~2023 年發生「非密封放射性物質意外事故」件數共有 4 例，皆為人為因素導致。為避免造成核醫科病患、家屬及工作人員恐慌，應加強核醫科工作人員輻射外洩處理演練，並於注射核醫藥物時，增加對病患、家屬衛教宣導頻次。

結論：善用輻射之特性，可增進醫療技術之進步，然而一旦操作不當、管理不良，則可能造成輻射外洩之危機。防患未然，依據醫院作業特性，擬定符合游離輻射防護安全標準之輻射物質意外事件應變計畫，除可降低輻射外洩發生之機率，並可於輻射外洩情況發生時，有依循之準則，使傷害降到最低。

PC-060

自製針頭回套筆座於輻射暴露之應用

蘇詩琪、林雯君、邱宇莉、胡瑁

高雄榮民總醫院核子醫學科

背景介紹：台灣於 2011 年 12 月修正醫療法規定「醫療機構對於所屬醫事人員執行直接接觸病人體液或血液之醫療處置時，應自中華民國 101 年起，五年內按比例逐步完成全面提供安全針具」，迄今已逾十年，但核醫科藥物注射因安全針具使用，易有藥物滲漏而有輻射外洩之虞，故無法完全適用「安全針具」注射，為確保核醫科藥物注射同仁無潛在的針扎危險，本科自製多款針頭回套用具應用於臨床核醫藥物注射。

方法：本科自製針頭回套用具，從第一代的木頭回套座、第二代 3D 列印回套立方，至第三代 3M 膠台加螺母的 Insulin 針回套座，各款式皆有其優缺點，缺點不乏便利性、穩固性及屏蔽效果。第四代回套筆座研發想法來自於第二代回套立方及第三代螺母的概念，考量材料容易取得，使用了「螺母和墊片」做成第四代回套筆座，成品不僅增加了回套用具的穩固性，另因為筆座的螺母金屬材質，還兼具輻射屏蔽效果，為核醫科注射上添加許多優點。

結果：第四代回套筆座的材質及尺寸，底座墊片材質讓回套筆座更多了穩固性，回套針頭時不至於因傾倒而回套失敗，造成感控汙染之虞；第四代回套筆座的螺母金屬材質也有達到屏蔽效果，使輻射暴露劑量相較第二代 3D 列印回套立方減少 61.7%；回套筆座總體的尺寸大小也好攜帶、收納。

結論：「針頭回套筆座」製作所需之「螺母和墊片」於坊間都可購買加工製作，應用於無法完全適用「安全針具」注射的核醫科，除了可避免針扎危險還可降低輻射暴露劑量。

PC-061

調整唾液腺檢查分析技巧之特殊病例報告

陳薇璇[1]、許幼青[1]、廖建國[1]、莊紫翎[1,2]

[1]佛教慈濟醫療財團法人大林慈濟醫院 核子醫學科
[2]慈濟學校財團法人慈濟大學 醫學系

簡介：唾液腺檢查可提供修格連氏症候群 (Sjögren's syndrome) 之適應症，本科唾液腺檢查過程需要完整收集第 1 秒到 50 分鐘的影像，以利分析計算出時間 - 活性曲線圖與半定量分析結果，檢查過程由手部靜脈注射藥物，以利收到藥物進入血管第 1 秒鐘之影像，若從腳部靜脈施打則很難抓取第 1 秒鐘的影像，而放射性同位素在動態攝影的情況下，能完整地顯示藥物由手部周邊靜脈流至上腔靜脈，進入體循環，而後分散至唾液腺。

病例報告：一名 70 歲女性，懷疑有修格連氏症候群 (Sjögren's syndrome)，醫師安排進行唾液腺檢查，影像分析結果在時間 - 活性曲線圖顯示，發現於第 1 分鐘時其兩側頷下線 ROI 與喉部背景 ROI 的峰值都有明顯飆高，導致其數值會影響到最大積累量的結果；進一步尋找原因，在原始影像發現病人的左側頸靜脈逆流造成兩側頷下線區域附近，一開始有高度的活性攝取。與醫師討論後，選擇用後處理的方式將前面的 1 ~ 6 張影像移除，並且複製第 7 張影像將前面的補上，讓系統依然能讀取影像並進行分析，修改後的分析結果則可見曲線圖於前面曲線持平，喉部 ROI 呈現背景值的曲線，兩側頷下線的平均最大積累量也從數值 0% 提高到 42.7%（正常值 62.4 ± 7.0），雖然呈現結果稍低，但也比一開始數值趨近於真實。

結論：唾液腺檢查分析的時間 - 活性曲線，正常會依據時間的增加而活性持續累積，在第 40 分鐘給予檸檬酸刺激後會因為唾液排出而降低活性攝取，所以正常的第 1 分鐘不會有最高峰，在分析時察覺到異常故進一步探討，而病人本身的血管狹窄逆流造成檢查結果呈現頷下線一開始的偽活性攝取之數據偏差，透過後處理可有效的解決偽活性攝取造成的困擾，同時可提高醫師判讀的準確度。

PC-062

探討心臟冠狀動脈左支配優勢與心肌血流灌注陽性之關係

張添信、陳慶元

佛教慈濟醫療財團法人台中慈濟醫院 核子醫學科

背景介紹：心臟支配優勢是指冠狀動脈分支發出後降支並供應下壁，其特徵為左、右或共主導據估計，70 ~ 80% 的人口以右支配為主，後降支動脈 (PDA) 起源於右冠狀動脈，大約 5 ~ 10% 的人以左支配為主，PDA 源自左旋支動脈，約 10 ~ 20% 的人以左旋動脈和右冠狀動脈共同支配供應的 PDA 為主。

心肌血流灌注掃描 (MPI) 主要用於評估心臟的血流狀況和心臟肌肉的血流供應情況，通常用於 1. 檢測心臟缺血 2. 評估心臟功能 3. 評估冠狀動脈疾病 4. 心臟血管重建後監測治療效果等等……。

本篇主要在評估左冠狀動脈優勢與其對下壁 / 下壁側壁可逆性缺血在灌注影像中準確識別之間可能存在的關係。

方法：利用回溯分析單一機構資料探討冠狀動脈主導方式與心肌血流灌注影像中下壁 / 下側壁缺血之間的可能關聯性，自 2021 年 1 月至 2022 年 12 月，有施行 MPI 與 180 天內有施行心導管檢查 (CATH)，期間共收入 13 位左冠狀動脈支配優勢病人進行相關探討。

結果：分析 13 位 (12 男：1 女) 病人 MPI 與 CATH 資料，年齡平均數為 57.7 歲 ± 11.6，MPI 結果為陽性有 10 人，MPI 偽陽性率為 77%，CATH 為陽性有 1 人，MPI 判斷為陽性中出現下壁 / 下壁側壁可逆性缺血的影像有 11 人，下壁 / 下壁側壁灌注缺損出現率為 85%。

結論：非右冠狀動脈支配優勢解剖結構可能會在下壁和下側壁區域出現高度的假陽性 MPI 結果。因此，在對這些患者進行臨床評估時，判讀醫生可能需要更多臨床佐證資料與其他檢查訊息及病人過去相關病史，不然檢查結果容易出現偽陽性判讀，資訊量不對等對臨床科醫師有失判讀公平性。

PC-063

初探智能化放射性廢水管理之歷程

張春梅

高雄榮民總醫院 核子醫學科 輻射安全室 輻射防護師
高雄師範大學 教育學博士
台南應用科技大學 助理教授

背景介紹：設置同位素治療病房，規建放射性廢水槽，免疫分析實驗放射性廢水槽（地下室3槽），同位素治療病房（6＋2槽）。

方法：依據核醫科檢查、治療、檢驗業務需求，設計興建放射性廢水槽，放射性廢水採樣及排放，改以智能化操作模式，降低操作人員職業曝露量。修定放射性廢水管理程序書，更新廢水槽巡邏表（周次）、巡查表（月次）、廢水取樣地面污染擦拭計測表等紀錄單，以符合核能安全委員會、iso45oo1 及輻射防護委員會管理規範。

結果：依據核能安全委員會自主檢查表項目，參考國內他院作法，彙整同位素治療方面專家、臨床輻防師意見，修訂放射性廢水管理程序書。

結論：智能化放射性廢水管理措施，藉由固定式與手持式環境偵檢器、監視器、示警系統、智能控制盤，確實可提升輻安管理效能。

PC-064

探析人員劑量計紀錄行動基準限值超標原因與異常事件之發生率

張春梅

高雄榮民總醫院 核子醫學科 輻射安全室 輻射防護師
高雄師範大學 教育學博士
台南應用科技大學 助理教授

背景介紹：以人員劑量計紀錄超過行動基準限值者，進行原因分析，調整劑量計管理策略。安裝新佩章架、增設監視器，加強輻防衛教宣導，降低異常事件之發生率。

方法：依據本院輻防計畫書訂定行動基準限值，調查異常事件發生之經過。劑量異常案件係指人員接受職業曝露，超過游離輻射防護安全標準規定之職業曝露劑量限度。人員接受職業曝露，任何單一年內，超過游離輻射防護安全標準規定之職業曝露劑量限度十分之四，劑量計遺失、損毀或污染，導致無劑量紀錄。其他造成無劑量紀錄或人員劑量異常情形。分析異常事件原因，進而改善輻射防護管理措施。

結果：統計 2021 年 1 月 ~ 2023 年 8 月，超過行動基準限值者，紀錄與調查件數有 11 例。人員劑量計遺損案件有 5 例，究因歸類主要是人為因素、設備不良導致。

結論：加強輻射工作人員教育訓練，增設佩章架監視器，將注意事項設計成可視化圖解海報，張貼於佩章架周遭明顯處，有效降低異常事件之發生率。

PC-065

輻射工作人員危害控制及相關管理措施

張春梅

高雄榮民總醫院核子醫學科輻射安全室輻射防護師
高雄師範大學教育學博士
台南應用科技大學助理教授

背景介紹：統計輻工游離輻射健檢分級結果，追踪人員劑量計紀錄，超過行動基準限值者，進行分析。

方法：健康管理級數定義如下，第一級管理：特殊健康檢查或健康追蹤檢查結果，全部項目正常或部分項目異常，經醫師綜合判定為無異常者。第二級管理：特殊健康檢查或健康追蹤檢查結果，部分或全部項目異常，經醫師綜合判定為異常，而與工作無關者。第三級管理：特殊健康檢查或健康追蹤檢查結果，部分或全部項目異常，經醫師綜合判定為異常，而無法確定此異常與工作之相關性，應進一步請職業醫學科專科醫師評估者。第四級管理：特殊健康檢查或健康追蹤檢查結果，部分或全部項目異常，經醫師綜合判定為異常，且與工作有關者。依據本院之輻射工作人員認定標準，從事游離輻射作業者 (包含新增、內轉單位)，輻工每年須完成勞工特殊體格，職安室保存健康檢查紀錄，輻安室統計健檢分級資料。

結果：全院輻工健檢分級，統計 2021 年 1 月至 2022 年資料，皆為一、二級，並無三、四級。劑量計紀錄超過行動基準限值者 (月報表)，已調整其工作內容或改善相關設備，皆符合限值 (年報表) 規定。

結論：游離輻射作業勞工特殊體格及健康檢查紀錄需保存三十年，全院輻工無第三級管理以上者，若有第三級管理以上者，應由職業醫學科專科醫師實施健康追蹤檢查，必要時應實施疑似工作相關疾病之現場評估，且應依評估結果重新分級。屬於第四級管理者，經醫師評估現場仍有工作危害因子之暴露者，應採取危害控制及相關管理措施。本院 E 化危害控制宣導之教材，提供員工多元學習管道，優化輻防智能管理平台，輻工健康管理效益佳，值得他院參酌。

PC-066

不明原因疼痛病人全身骨骼掃描之有趣影像——病例報告

許幼青[1]、廖建國[1]、林昱璁[1]、陳薇璇[1]、莊紫翎[1,2]

[1]佛教慈濟醫療財團法人大林慈濟醫院核子醫學科
[2]慈濟學校財團法人慈濟大學醫學系

簡介：全身骨骼掃描是一種非侵入性，敏感度高的檢查項目，同時可以快速獲得骨骼上是否有其他變化，若額外搭配單光子電腦斷層造影檢查 (SPECT/CT) 時，便可更清楚獲得更多資訊，當患者若有莫名其妙的骨骼疼痛，且沒有任何癌症病史，其他檢驗檢查都正常時，全身骨骼掃描則是一項非常適合的項目。

病例報告：一名 42 歲男性，無不良嗜好，病人全身骨骼疼痛尤其是髖關節處最為嚴重，其疼痛感已維持一年半多，這期間看了風濕免疫、關節中心、中醫…等科，檢驗檢查報告皆為正常，最後看了骨科門診，醫師安排磁振造影，結果報告為輕微椎間盤退化性疾病，但醫師建議進一步執行全身骨骼掃描檢查及單光子電腦斷層掃描，發現雙側肋軟骨連接處（念珠樣 rosary beads）、雙側股骨頸、近端脛骨和足部有對稱的放射性示踪劑積聚，除此之外，腎臟的部位沒有放射性示踪劑攝取。

結論：全身骨骼掃描本身敏感度高，前面提到影像發現結果，則有可能為提示骨軟化症、佝僂病、代謝性骨病（如腎性骨營養不良、甲狀腺機能亢進症）或骨骺閉合延遲（如腦下垂體功能低下或腦下垂體瘤），這些都有可能是此病人病症。當病人骨疼痛時，若醫師沒有執行全身骨骼掃描，則病人就無法快速地得知自己身體狀況的可能性，由此可知，全身骨骼掃描有可能不能馬上讓醫師及病人得知確定的答案，但是可提供醫師及病人該如何執行下一步，所以全身骨骼掃描在不明原因的疼痛來說，是非常重要的檢查項目。

PC-067

多囊性腎臟病之全身骨骼掃描影像——病例報告

許幼青[1]、廖建國[1]、林昱璁[1]、陳薇璇[1]、莊紫翎[1,2]

[1]佛教慈濟醫療財團法人大林慈濟醫院 核子醫學科
[2]慈濟學校財團法人慈濟大學 醫學系

簡介：多囊性腎臟病是指腎臟出現囊腫，是一種基因變異遺傳性腎臟疾病。成人發病型好發於 40 歲左右，在臨床上常合併有高血壓、血尿、泌尿道感染，平均在 50 歲左右會面臨洗腎。骨頭是肺癌最常轉移的器官之一，而全身骨骼掃描可以針對全身的骨骼進行掃描，以偵測是否有骨骼轉移。全身骨骼掃描主要排泄路徑從泌尿道排泄，所以腎臟及膀胱內尿液放射性示蹤劑活性會有增加現象，當腎臟及膀胱內尿液放射性示蹤劑活性減少表示可能是泌尿道系統有問題，需進一步了解。

病例報告：一名 68 歲男性，有抽菸、喝酒病史，且血液透析 17 年之久，之前有執行經皮冠狀動脈介入治療，但最近由於心跳過速看心臟科門診，突然胸部 X 光顯示右肺門或前縱膈腫瘤，電腦斷層檢查證實為肺腫瘤，同時有肺轉移、縱膈淋巴結腫大、腦轉移伴隨水腫等情形，故安排住院進行治療，同時安排全身骨骼掃描結果顯示左側第 8、9、10 肋骨後外側有放射性示蹤劑聚積，除此之外，由於腎臟和膀胱沒有放射性示蹤劑活性，但因病人本身有長年血液透析，故查看電腦斷層影像結果顯示為多囊性腎臟病。

結論：骨骼是肺癌最常轉移的器官，全身骨骼掃描可以偵測其骨骼是否有轉移，故敏感度很高，檢查後的結果往往需要搭配其他的檢查項目去判斷如電腦斷層等，才能更準確知道病人實際病情及診斷，像此個案有進一步搭配電腦斷層影像得知病人有多囊性腎臟病，故全身骨骼掃描顯示腎臟放射性示蹤劑活性減少的現象為正常情形而非轉移性超級影像 (metastatic superscan)，尚未達到代謝性超級影像 (metabolic superscan) 之腎性骨營養不良 (renal osteodystrophy)，可幫助病人後續治療更為準確。

PC-068

以自製下肢淋巴固定器運用於下肢淋巴檢查之成效

王苡安[1]、廖建國[1]、陳薇璇[1]、莊紫翎[1,2]

[1]佛教慈濟醫療財團法人大林慈濟醫院核子醫學科
[2]慈濟學校財團法人慈濟大學醫學系

目的：淋巴閃爍攝影是使用核醫藥物 ^{99m}Tc-phytate，藥物經皮下注射後會經由淋巴系統進入淋巴循環，因此可用來做淋巴閃爍攝影。由於大多數檢查台的床墊偏硬且患者躺下去腳部自然呈現外翻的姿勢，偶而會有患者除了下肢腫脹之外同時合併傷口存在，因檢查方式採用皮下注射，注射時由於患者疼痛加劇及腳部晃動厲害，所以在執行這項檢查時，需要一人固定患者腳部並扳開腳趾，另一位人員進行藥物注射，所以執行過程費時費力。本研究目的即為探討患者使用本科製作而成的下肢淋巴固定器後，患者的舒適度及施打者的便利度是否得到改善。

材料方法：使用一塊長 42 公分、寬 42 公分、高 10 公分的泡棉，描繪出成人腳部大約的長度與寬度，再將泡棉挖空描出腳的大小，最後將泡棉用床單包覆起來，即成為下肢淋巴固定器。從 2023 年 4 月至 2023 年 8 月收集下肢淋巴閃爍攝影之個案，患者躺至檢查台後，施打人員將患者腳部固定於下肢淋巴固定器，施打方式為一位護理人員負責施打，另一位人員協助將腳趾扳開，使用 1 c.c. 空針，施打 4 支，每支 1 mCi，以皮下注射方式打在左右下肢第二及三趾縫，皆不反抽，固定由患肢先施打。

結果：總共收集 30 位下肢淋巴檢查患者，這些患者表示使用下肢淋巴固定器後，躺在檢查台其後腰部不會那麼痠痛，比較舒適，也有患者表示，打針時不會特別感覺疼痛，在護理端方面，有下肢淋巴固定器後，患者的腳就不會呈現外翻且不會移動，另一位人員協助時不需要很費力去壓制病人患肢，不僅操作省力，同時經統計可節省約 5 分鐘的時間，所以操作者整體執行的便利度及效率都有所提升。

結論：下肢淋巴檢查由於採皮下注射對患者來說本來就很痛很不舒服，使用由核醫科同仁一起討論製作而成的下肢淋巴固定器，且沒有花費到任何的費用，經過這段期間的測試，患者反應相當良好，可有效提升整體醫療品質。

PC-069

以簡訊提醒隔日檢查之意願調查

王苡安[1]、廖建國[1]、林昱璁[1]、許幼青[1]、莊紫翎[1,2]

[1]佛教慈濟醫療財團法人大林慈濟醫院核子醫學科
[2]慈濟學校財團法人慈濟大學醫學系

目的：開院至今本院核醫科一直以來都以電話方式提醒隔天至本科作檢查的患者，隨著科技的進步及民眾使用手機普及化，同仁每日花費電訪給受檢者的時間平均約為 30 分鐘，除了要處理線上作業之外還要執行電訪，對工作作業上影響甚大。本研究目的為探討患者是否希望由原本電訪方式改為簡訊通知方式，以作為持續改進之參考。

材料方法：使用 Google 表單的方式進行問卷調查，其表單內容包含三大項，首先，第一項將當日患者檢查項目分四組，分別為心肌灌注檢查、全身骨頭檢查、正子檢查及其他檢查。第二項為患者年齡，我們分為 19 歲以下、20 ~ 40 歲、40 ~ 60 歲、60 ~ 80 歲及 80 歲以上。第三項為詢問患者之後是否同意改為簡訊通知隔日檢查，再將表單設置好後轉換成 QR-Code 方式，將 QR-Code 張貼於注射室、正子休息室以及櫃檯，方便患者或家屬進行填寫。

結果：從 2023 年 8 月 21 日至 9 月 1 日止共收集 103 位患者，有效問卷為 102 份。填寫問卷時，許多患者表示改為簡訊較為方便，原因是不明來電不會接、打電話的時間剛好在上班無法接聽電話、老人家重聽、醫院撥出去的電話民眾要回撥找不到哪個單位打的、小孩接的只會說好，無法明確表達給大人等。分析調查結果，各項目中，全身骨頭的患者占了 53.9%、心肌灌注掃描占了 14.7%、正子檢查占了 9.8%、其他檢查占了 21.6% (圖 1)；受檢年齡 20 ~ 40 歲占了 14.7%、40 ~ 60 歲占了 42.2%、60 ~ 80 歲占了 34.3%、80 歲以上占了 8.8%（圖 2）；往後是否願意以簡訊通知隔天核醫檢查，回答是的人占了 89.3%，否的人占 10.7%（圖 3）。

結論：利用簡訊通知，除了節省人員打電話的時間外，對於電訪患者所遇到的問題也都可以得到改善，換句話說，以簡訊提醒病人之方式，有助於提升品質及效率，因此我們進一步規劃以簡訊通知之執行細節，以持續提升作業品質。

PC-070

^{99m}Tc-Labeled Red Blood Cell Scan with SPECT/CT for Detecting Intrathoracic Bleeding

Dallas Shun-Yu Yew[1], Tzyy-Ling Chuang[1,2]

[1] Department of Nuclear Medicine, Dalin Tzu Chi Hospital, Buddhist Tzu Chi Medical Foundation, Chiayi, Taiwan;
[2] School of Medicine, Tzu Chi University, Hualien, Taiwan

Introduction: A case of right hemohydrothorax where ^{99m}Tc-labeled red blood cell (RBC) scan with SPECT/CT was used to determine the bleeding location.

Case Report: A 67-year-old man presenting with hepatocellular carcinoma and right hemohydrothorax. Computed tomography angiography (CTA) was unable to localize the bleeding site; therefore, Tc-99m labeled RBC scan was performed. The scan revealed a small amount of extravascular blood in the right upper lung field. Finally, trans-arterial embolization was arranged to resolve the bleeding.

Discussion: Although RBC scan is widely utilized for detecting gastrointestinal bleeding, it is rarely used for intrathoracic bleeding where conventional imaging is the norm. However, sometimes the bleeding site is difficult to ascertain even when CTA is implemented, especially if the hemorrhage is small or when concurrent with other complications such as hydrothorax. In these cases, RBC scan with SPECT/CT is advantageous for precise bleeding localization.

PC-071

骨骼掃描合併 SPECT/CT 對於創傷性眼睛鈣化的探討

林昱璁[1]、廖建國[1]、許幼青[1]、莊紫翎[1,2]

[1]佛教慈濟醫療財團法人大林慈濟醫院 核子醫學科
[2]慈濟學校財團法人慈濟大學 醫學系

簡介：眼球鈣化有多種原因，從良性到惡性不等。當在眼球後半部看到鈣化時，它可能與眼球的任何一層（鞏膜、脈絡膜或視網膜）病變有關，一般在電腦斷層影像上很難明確將鈣化點位置區分開。而鈣化引發原因有眼球萎縮症，亦稱眼球癆 (phthisis bulbi)、鞏膜脈絡膜鈣磷代謝異常之轉移性鈣化（包含副甲狀腺功能亢進症、偽副甲狀腺功能低下症、腎小管酸血症）與營養不良性鈣化等，最常見的是眼球萎縮症，原因包括眼睛嚴重外傷、感染或身體健康因素造成，但眼睛嚴重受傷是最主要的原因，會留下縮小的鈣化腫塊，進而影響眼睛功能造成永久視力喪失。

影像報告：一名 46 歲男性，經臨床診斷為下咽部右側梨狀窩之下咽癌，目前正在化療療程中，近期經由醫師安排全身骨骼掃描檢查，影像發現在右邊眼球有異常的活性攝取，與一般正常影像不同，醫師懷疑癌細胞可能有轉移到眼球，之後為進一步了解病情，針對頭頸部執行 SPECT/CT 的檢查，結果發現其右側眼部鈣化有活性攝取，且病人表示之前有創傷過，所以此病人所造成眼球鈣化，亦即眼球癆，且具 MDP 活性，在核醫臨床上較為特殊。

結論：眼睛如果有受傷或病變其內部組織可能會鈣化而慢慢形成像石頭一樣硬的組織，此鈣化組織在一般 X 光下無法清楚診斷，雖然軟組織超音波可鑑別並量測鈣化的大小與定位，但是病人在臨床上並沒有安排超音波檢查，因此沒有診斷出眼球鈣化，但是在全身骨骼掃描時可藉由 Tc-99m MDP 標誌化合物可沉積在鈣磷化物的特性以及高靈敏度的偵測效率，可清楚辨別組織鈣化的變異，再加上 SPECT/CT 掃描，對於眼球癆（創傷性眼球鈣化）的診斷能有一個實質的依據，提供臨床醫師及病人做後續的治療與處置。

PC-072

MUGA 檢查的 R-R Interval 設定對於心律不整病人的影響

林昱璁[1]、廖建國[1]、許幼青[1]、莊紫翎[1,2]

[1]佛教慈濟醫療財團法人大林慈濟醫院 核子醫學科
[2]慈濟學校財團法人慈濟大學 醫學系

簡介：多頻道心室功能攝影 (multigated blood pool analysis, MUGA) 為核子醫學心室功能檢查，主要測量左心室射出率 (left ventricular ejection fraction, LVEF)，大部分臨床試驗的收案條件也是以 LVEF 來做為心臟衰竭的分類，MUGA 檢查能提供具非特異性症狀患者之心臟功能、偵測冠狀動脈疾病影響左心室功能之程度、評估急性心肌梗塞之預後、心肌病變患者之心室功能性、肺部疾病及胸、肋骨畸形患者之心臟功能及精確了解病人各種心臟功能參數以掌握病人的心室功能與化療的成效。

病例報告：一名 51 歲女性乳癌病人，在化學治療之前，經由醫師安排治療前 MUGA 檢查，分析影像時發現 LVEF 偏低只有 32%，醫師懷疑病人有心衰竭的可能，後續安排心肌灌注掃描及心臟超音波檢查，結果發現心肌灌注與超音波檢查其 LVEF 皆為 70% 以上，醫師懷疑為何 MUGA 檢查 LVEF 只有 32%，進一步發現其左心室 phase 的影像與 histogram 有收縮不同步的情形，為了確定病人是否有心衰竭與心律不整，故重新再做一次 MUGA 檢查。在執行 MUGA 檢查時發現病人有心律不整的狀況，並將此次的 gated 的 R-R interval 週期的 PVC threshold 設定加寬為 ± 90%（預設為 ± 15%），檢查結果其 LVEF 為 72%，與其他心肌灌注掃描與心臟超音波兩項檢查結果一致。

結 論：心律不整可能與心臟問題包括冠心病 (Coronary heart disease)、心肌病變 (Cardiomyopathy)、心肌缺氧等等問題相關，透過心電圖檢查可以評估心臟的功能及心律週期，MUGA 檢查所使用的 gated 會設定剛好可以監控病人在檢查時的心臟狀況，藉由適當的延長 R-R interval 週期設定，將動態影像收集範圍加寬，可以減少因心律不整所導致的結果錯誤，造成影像分析時電腦對於影像的誤判，對於後續病人手術及化學治療後的 LVEF 變化也比較能夠掌握。

PC-073

COVID-19 疫情對病人數量影響之研究——以南部某醫院核醫科 BONE SCAN 之開單量為例

吳麗君、卓世傑、張南雄、江佳諭、陳懿貞、李將瑄

奇美醫院永康總院 核子醫學科

背景介紹：自 2020 年 1 月開始顯著加劇，並延續至 2023 年 4 月底，始告一段落之 COVID-19 疫情，無疑是迄今人類所面臨最受關注與影響最廣泛的疫情之一。由於 COVID-19 疫情幾乎對全世界各方面都造成了改變，所以可以想像的到，首當其衝的醫療端，所受到的衝擊，應該也是最大的。但是究竟衝擊了什麼？又改變了多少？是頗值得多方面探討與量化的。本文即是以南部某醫院核醫科 BONE SCAN 之開單量為例，藉由門診病人與住院病人開單數量之變化，探討 COVID-19 疫情對核醫科 BONE SCAN 開單數量之影響。

方法：1. 收集南部某醫院核醫科自 2018 年 1 月至 2023 年 8 月，每月 BONE SCAN 門診與住院病人之開單數量，各 68 筆。2. 以 2018 年門診與住院病人，每月開單量之平均數各為 1，依比例計算其他各月之數值。

結果：1. 門診開單數量部分，2018 至 2020 年之比例並無顯著之變化，每年平均大致都為 1.0，但 2021 至 2023 年 8 月止，平均值則逐年上升約 10%，分別是 1.1，1.2 及 1.3。2. 住院開單數量部分，比例變化則較不顯著，2018 至 2023 年，每年平均分別為 1.0，1.0，1.1，1.1，1.0，1.2。

結論：COVID-19 疫情對南部某醫院核醫科門診 BONE SCAN 之開單量之影響，除了疫情初起的 2020 年，該年似乎壓抑了成長趨勢，導致開單量持平外，往後年度之開單數量，即已恢復成長之態勢。BONE SCAN 之住院開單數量部分，比例變化則較無趨勢，惟 2023 年之開單數量，相較 2018 及 2019 年有顯著之提升。因此依據本文之研究結果，COVID-19 疫情期間對南部某醫院核醫科 BONE SCAN 之開單量，並無顯著之影響。

PC-074

放射免疫分析實驗室生物安全緊急應變演練——經驗分享

沈宜瑾[1]、張素雲[1]、黃筱崴[1]、廖建國[1]、莊紫翎[1,2]

[1]佛教慈濟醫療財團法人大林慈濟醫院 核子醫學科
[2]慈濟學校財團法人慈濟大學 醫學系

目的：臨床實驗室之生物安全要求相當嚴謹，緊急應變的演練頻率每年必須一次，緊急應變演練可測試實驗室生物安全災害緊急應變的能力，加強同仁的防災意識和處理能力。本文目的為整理本科放射免疫分析實驗室於 2023 年 4 月進行生物安全緊急應變演練之流程及演練狀況，進行經驗分享。

材料方法：1. 準備演練相關用品：包含 (1) 實驗衣、口罩、鞋套。(2) 漂白水溶液、(3) 拋棄式手套、(4) 夾子或鑷子、(5) 抹布或毛巾之可擦拭的物品、(6) 生物醫療廢棄紅色垃圾袋、(7) 有蓋的堅硬容器或垃圾桶、(8) 橡膠手套等其他用品。2. 演練模擬情境：離心機內盛裝 B 型肝炎陽性檢體之試管發生破裂，應變處理步驟包括：(1) 關閉離心機電源，讓儀器密閉 30 分鐘使氣膠沉積，立即通知主管。(2) 戴上厚實之手套 (如厚橡膠手套) 或穿戴適當之拋棄式手套。(3) 使用鑷子清理玻璃碎片，破碎之離心管等放在一個裝有 10%(稀釋 10 倍) 漂白水之有蓋容器中，然後丟至感染性垃圾桶中。(4) 使用鑷子夾沾有 10% 漂白水的棉花或紗布清潔離心機內部。(5) 未破損之有蓋離心管應在離心機內腔使用 10% 漂白水擦拭，然後用水沖洗並乾燥。清理時所使用之全部物品，都應依感染性廢棄物處理。

結果：此次實驗室生物安全緊急應變演練，模擬情境為離心機內盛裝 B 型肝炎感染性檢體試管發生破裂，演練狀況大致都很順暢，不過還有一些演練細節仍有改善的空間，例如離心杯拿出來清理的步驟及其注意事項，還可以做得更好，像是注意使用鑷子將破碎的離心管放在含稀釋 10 倍的漂白水有蓋容器中，並記得清理時使用的全部物品都應依感染性廢棄物處理。生物安全危險等級分為低、中、高度危害三個等級，第一級為發生在設備內；第二級為設備外、實驗室內；第三級則為實驗室外。此次演練之情境為發生在離心機內的意外事件，屬於第一級的意外事件，因風險較低且實驗室可自行處理，依規定不需通報生物安全會但應通報實驗室主管。另外，如果此次潑灑的檢體同時含有放射性同位素時，考量本實驗室碘 -125 之輻射劑量較低且無立即的輻射危害，因此處理原則仍應以處理生安污染為優先，輻射污染次之。

結論：透過實地操作實驗室生物安全緊急應變演練，可強化實驗室生物安全災害緊急應變能力，真正有狀況時才不會慌亂，也能更熟悉實驗室應變處理步驟。臨床工作都一定會遇到不同的緊急事件，藉由平常的訓練才能妥善的應變處理，提升實驗室作業安全。

PC-075

CA199 放射免疫分析誤加抗血清時之結果查證

黃筱崴[1]、張素雲[1]、廖建國[1]、莊紫翎[1,2]

[1]佛教慈濟醫療財團法人大林慈濟醫院 核子醫學科
[2]慈濟學校財團法人慈濟大學 醫學系

目的：實驗室可能因試劑、設備或人為操作的因素，而導致實驗結果的偏差。其中人為因素的操作誤差可發生在檢驗流程中的每個步驟，例如發生在加抗血清的操作步驟。本研究目的即為查證當誤加抗血清時，其檢驗結果是否影響最終報告結果。

材料方法：收集曾經誤加抗血清 (200 μL) 之病人檢體，使用 IZOTOP 廠牌試劑 (IRMA CA19-9 antigen) 重新進行檢測，重檢使用標準方法，依原廠試劑說明書操作流程進行操作（抗血清加 100 μL），並使用同一加馬計數器進行計數。重新檢測後，再使用 Excel 軟體計算誤加抗血清之檢測值與原標準方法結果之差異 (%)，並依此項目內部品管之 ± 2 倍 CV 值判定差異是否可接受。

結果：總計收集 17 支誤加抗血清之病人檢體，CA199 檢驗值介於 1.55 ~ 93.04 U/mL 間，其中檢驗值大於正常參考值 (< 37 U/μL) 者有 4 件，其餘 13 支檢體之檢驗值皆落在正常範圍內。再比較誤加抗血清之檢測值與原標準方法結果之差異，發現檢驗值大於正常參考值之檢體，誤加之檢測值與原標準方法結果的差異皆在可接受的範圍，而檢驗值小於正常參考值之檢體，有 3 支檢體（編號 8、9、14）的差異較大（超過允收值）。整體來看，大部份誤加之檢測的結果與原標準方法的差異是可以接受的（占 82%），也就是都在正常檢測可接受的變異之內。由於此項目使用 IRMA 方法之試劑，IRMA 方法中標記抗體和固相抗體在反應中都是過量的，理論上誤加抗血清時對於檢驗結果的影響應非常小，只有檢體的加樣誤差才會影響分析結果，因此推測這 3 支檢體的差異較大的原因，可能與加樣誤差有關。

結論：本實驗室因發生誤加抗血清的情況，因此進行檢驗結果的比對與查證，結果顯示雖大部分誤加之檢測的結果與原標準方法的差異是可以接受的，但仍有少部分誤加之檢測的結果不可接受，表示未經重覆檢測前報告不宜發出。雖然實驗室可查證人為操作疏失是否影響檢驗結果，但實際作業上仍應依原廠操作說明書執行，以符合實驗室的品質要求。

PC-076

T-cell Lymphoma Involving Posterior Mediastinum and Spine Evaluated by F-18 FDG PEC/CT: A Case Report

Yu-Chien Shiau, Ya-Huang Chen, Chia-Wen Lai, Che-Wei Chang, Po-Wei Li, Chao-Chun Huang, Yen-Wen Wu, Shan-Ying Wang

Division of Nuclear Medicine, Far Eastern Memorial Hospital, New Taipei, Taiwan

Introduction: In literature review, T-cell lymphoma involving posterior mediastinum and spine is a relatively rare disease condition. We report a case of T-cell malignant lymphoma involving posterior mediastinum and spine. F-18 FDG PET/CT was arranged for staging and clinical evaluation.

Case Report: The 69-year-old woman was well but her health examination by PET/CT in other hospital showed posterior mediastinal tumor. CT-guide biopsy was further arranged and showed lymphoid tissue, T-cell predominant. She denied fever, night sweats, and weight loss. CT showed homogeneous confluent mass > 2.8 × 8 × 6 cm in posterior mediastinum at T8-T11 level, R/I lymphoma or other neoplasm. Suggest further survey. And osteoblastic lesions in T6-8, T10, Lt 2nd rib, also R/I lymphoma or bone metastasis from unknown origin. Tissue proof was needed for ruling out lymphoma. After a thorough discussion with the patient in our hospital, VATS mediastinal tumor biopsy with left side approach was arranged. Pathology report showed posterior mediastinum malignant lymphoma, favoring T-cell type. F-18 FDG PET/CT was arranged again in our hospital for more accurate staging and showed lymphoma involvement in bilateral paravertebral masses at about T10 level of posterior mediastinum, T6 and T7 vertebrae, osteoblastic T6-8 and T10 vertebrae, and suspicious spinal cord around T6-7 level. The clinical staging according to AJCC 8th edition was stage IV. She was admitted and received chemotherapy with intrathecal therapy with dexa, MTX, Ara-C, and C1D1 CHOP-E. Then her condition was stable and was arranged for OPD follow-up.

Conclusions: T-cell lymphoma involving mediastinum and spine is a relatively rare disease condition. Using F-18 FDG PET/CT for evaluation and more accurate staging was considered to be beneficial in clinical situation. In the future, we hope to gather more cases for more detailed statistical analysis.

PC-077

鐳 223 治療病人注射前身體狀況之研究——以南部某醫院核醫科為例

卓世傑、梁育雅、張虹麗、陳懿貞、江佳諭、李將瑄

奇美醫院永康總院 核子醫學科

背景介紹：去勢抗性攝護腺癌 (castration-resistant prostate cancer, CRPC) 病人，可能發生包括骨頭不舒服及其他不適症狀的情形。而鐳 223 (Radium-223) 放射性同位素藥物，即用於治療或舒緩去勢抗性攝護腺癌病人的症狀與不適。但是接受鐳 223 治療病人當下的身體狀況，卻是病人能否接受鐳 223 藥物注射治療，非常重要的依據。因此，病人注射前之身體狀況，是頗值得探討之問題。本文即為以南部某醫院核醫科為例，探討鐳 223 治療病人注射前身體狀況之研究。

方法：1. 收集南部某醫院核醫科，自 2022 年 12 月 5 日至 2023 年 9 月 1 日止，每次鐳 223 注射前病人身體狀況之資料。2. 以口頭詢問之身體狀況資料包括，第幾次注射，不適情形，不適程度等 3 項資料，共獲得 71 人次，共 213 筆之資料。3. 整理、統計前項數據，以提出結果。

結果：1. 注射前身體有不適狀況的有 12 人次，占全體病人 71 人次的 16.9%。2. 身體狀況不適病人中，第一次注射的病人有 4 人次，占不適病人 12 人次的 33.3%。3. 身體狀況不適病人中，可能是骨骼相關之不適情形共有 5 人次，占不適病人 12 人次的 41.6%。

結論：依據南部某醫院核醫科收集之鐳 223 治療病人，注射前身體狀況之資料，本研究發現：

1. 注射前身體有不適狀況的有 12 人次，占全體 71 人次的 16.9%。
2. 身體狀況不適病人中，第一次注射的病人有 4 人次，占不適病人 12 人次的 33.3%。
3. 身體狀況不適病人中，可能是骨骼相關之不適情形共有 5 人次，占不適病人 12 人次的 41.6%。

PC-078

鐳 223 治療病人注射前後輻射劑量率變化之研究——以南部某醫院核醫科為例

卓世傑、陳興隆、林凡珍、張南雄、張虹麗、李將瑄

奇美醫院永康總院 核子醫學科

背景介紹：核子醫學科近來用於去勢抗性攝護腺癌 (castration-resistant prostate cancer, CRPC) 病人治療的 α 射源，鐳 223 (Radium-223) 放射性同位素藥物，使用量有逐漸增加的趨勢。由於鐳 223 治療的標準療程是每月注射一劑，分 6 個月完成共 6 劑藥物之注射。而病人注射鐳 223 藥物後，身體即成為射源，病人至下次注射前，身體所含鐳 223 藥物產生之輻射，未必即會代謝至背景值。因此，病人注射前後之輻射劑量變化，是頗值得探討之問題。本文即為以南部某醫院核醫科為例，探討鐳 223 治療病人注射前後輻射劑量率之變化研究。

方法：1. 收集南部某醫院核醫科，自 2022 年 7 月 4 日至 2023 年 9 月 11 日止，每次鐳 223 治療病人注射前、後之輻射劑量率資料。2. 以 Inspector 型蓋格式偵檢器，於每位病人注射鐳 223 前、後，測偵距背部 5 cm 之輻射劑量率並記錄。3. 剔除偵測背部時有障礙物之病人劑量率資料，共獲得第一次注射病人 21 人次，非第一次注射病人 69 人次，共 90 人次，180 筆之劑量率資料。4. 整理、統計前項數據，以提出結果。

結果：1. 第一次注射病人，注射前之劑量率平均、最高、最低以及中位數分別為 0.1、0.15、0.06 與 0.12 uSv/h，注射後之劑量率平均、最高、最低與中位數則為 4.1、6.39、2.94、4.03 uSv/h。2. 非第一次注射病人，其注射前之劑量率平均、最高、最低、中位數則為 0.2、0.9、0.08、0.16 uSv/h，而注射後之劑量率平均、最高、最低與中位數則為 4.1、6.6、1.32、3.92 uSv/h。3. 第一次注射病人，注射前、後劑量率之相關性為 0.159，非第一次注射病人，注射前、後劑量率之相關性則為 -0.014。

結論：依據南部某醫院核醫科收集之鐳 223 治療病人，距背部 5 cm 輻射劑量率之資料，本研究發現：

1. 鐳 223 治療第一次注射病人與非第一次注射病人注射前之劑量率確實有差異平均為 0.1 及 0.2 uSv/h，最高劑量率則分別為 0.15 與 0.9 uSv/h，但注射後之平均劑量率則均為 4.1 uSv/h。
2. 鐳 223 治療第一次注射病人與非第一次注射病人，注射前、後之劑量率相關係數皆不高，分別為 0.159 與 -0.014，顯示注射前、後之劑量率並無顯著相關。

PC-079

Thyroglobulin 試劑更換與甲狀腺全切除病人參考值調整之討論研究——以南部某醫院核醫科放射免疫分析室為例

張朝鈞、卓世傑、段淑薰、顏吉龍、曾宜玲、李將瑄

奇美醫院永康總院 核子醫學科

背景介紹：甲狀腺全切除病人之 Thyroglobulin 檢驗值，為判斷術後病人狀況之重要參考值之一。而不同試劑之檢驗值，其分布情形當然並不相同。因此放射免疫分析室如果更改試劑，如何調整新試劑之檢驗參考值，以符合臨床之需求，當然為實際且必要之研究。本文即為，Thyroglobulin 試劑更換與甲狀腺全切除病人參考值調整之討論研究。

方法：1. 隨機收集南部某醫院核醫科放射免疫分析室 Thyroglobulin 試劑更改前、後，均有接受該項檢驗之 263 位病人，如該病人有多筆檢驗資料，則以最接近更改試劑日期前、後各一筆檢驗數值為限。2. 將收集之 263 位病人檢驗數值分為更換前與更換後兩組，各 263 筆數據資料。3. 整理，統計前項兩組數據以提出結果。

結果：1. 試劑更改前、後之最高值、最低值與中位數值，分別為 1,000、1,530 ，0.2、0.27 以及 0.59、1.47，更改後之數值均較高。2. 更改前之參考值設為小於 1，更改前小於 1 之數值，有 135 筆，比例 51.33%，更改後小於 1 之筆數則為 126 筆，比例 47.91%。3. 更改前小於 2 之數值，共有 144 筆，比例 54.75%，更改後小於 2 之筆數為 143 筆，比例 54.37%。

結論：依據南部某醫院核醫科放射免疫分析室，試劑更改前、後隨機之 263 位病人 Thyroglobulin 檢驗值資料，本研究發現：

1. 試劑更改後之最高值、最低值與中位數值，皆有上升，尤其是中位數值由 0.59 上升至 1.47 影響最為重要。
2. 試劑更改後，參考值大於 1 之病人數增加了 9 位，比例為 3.42%，需要進行 Recheck 之工作。
3. 試劑更改後，參考值小於 2 之病人數僅減少了 1 位，比例下降了 0.38%。。

因此 Thyroglobulin 試劑更改後，甲狀腺全切除病人檢驗值參考值由原設為小於 1，變更為小於 2，較可符合臨床之需求，亦可減少該放射免疫分析室 Recheck 之工作負荷。

PC-080

甲狀腺攝取計數儀 QC 數據與碘 131 藥劑計數值關係之研究

張淑芬、卓世傑、顏吉龍、段淑薰、林凡珍、李將瑄

奇美醫院永康總院 核子醫學科

背景介紹：甲狀腺攝取計數儀，係核子醫學科執行病人甲狀腺攝取率檢查所使用的儀器。甲狀腺攝取計數儀於使用前，必需使用標準射源及內部程式進行必要之 QC 作業。但 QC 作業所產生之相關數據，與實際測量藥劑之計數值有無相應之關係，則是頗為有趣又值得探討的問題。本研究即為以甲狀腺攝取計數儀 QC 所產生之相關數據，再與碘 131 藥劑實際計數值比較之研究。

方法：1. 以 Capintec,Inc. 公司生產之 CAPTUS 4000 型甲狀腺攝取計數儀，及 Eckert & Ziegler 公司生產之 GF-0008 型，Cs-137 射源以及 GF-0009 型，Eu-152 射源 執行檢查前 QC 作業。2. 收集 2020 年 2 月 11 日至 2023 年 7 月 19 日止，共 18 位病人，每人兩次之碘 131 藥劑計數值資料，並將第一次數值減掉第二次數值，得到 18 筆計數值差距資料。3. 收集該 18 位病人檢查前之 QC 作業數據，包括 Gain，Zero Offset (%)，FWHM，Constancy Deviation (%) 等 4 項，各 18 筆共 72 筆資料。4. 整理、統計前項數據，以提出結果。

結果：1. 兩次之碘 131 藥劑計數值差距平均為 98，最高為 458，最低為 -443，中位數為 111.5。2. 計數值差距數與 Gain，Zero Offset，FWHM，Constancy Deviation 等 4 項資料之相關性，分別為 -0.503，0.109，-0.460，0.029。

結論：依據本研究收集之資料，本研究發現：

1. 碘 131 藥劑兩次之計數值差距平均為 98，最高為 458，最低為 -443，中位數為 111.5，顯示符合 QC 作業要求儀器之計數效率相當穩定。
2. 計數值差距數與 QC 作業相關數據之 Gain 及 FWHM，有較高之負相關性，分別為 -0.503 與 -0.460，至於 Zero Offset 與 Constancy Deviation 則與計數值差距數無顯著相關。

PC-081

放射免疫分析室試劑活度更改與放射性廢棄物產出輻射劑量率關係之研究——以南部某醫院核醫科放射免疫分析室為例

曾宜玲、卓世傑、顏吉龍、段淑薰、張朝鈞、李將瑄

奇美醫院永康總院 核子醫學科

背景介紹：南部某醫院核醫科放射免疫分析室於 111 年 4 至 5 月更換 6 個檢驗項目試劑，包括 TSH、T3、TG、AFP、CEA、ALDO 等，且新試劑活度均較以往為高。由於試劑活度變高，可能造成放射性廢棄物輻射劑量率之改變。而放射性廢棄物輻射劑量率之改變，又可能直接影響儲存時間與空間之變動，進而影響放射免疫分析室之作業。所以試劑活度更改對放射性廢棄物產出輻射劑量率之影響究竟有多少？是非常值得討論的問題。本文即為探討，試劑活度更改與放射性廢棄物產出輻射劑量率關係之研究。

方法：1. 收集南部某醫院核醫科放射免疫分析室試劑活度更改前、後各 13 個月每月之檢體總量，並以某一基準值換算為比例。2. 收集試劑活度更改前、後各 13 個月，不定期產生之更改前 153 筆及更改後 148 筆廢棄物之重量與輻射劑量率，並以月為單位相加統計。3. 將不定期產生之廢棄物重量與輻射劑量率相乘，得到個別之總輻射劑量率，再以月為單位相加統計。4. 比較前、後之檢體量、廢棄物重量、輻射劑量率以及總輻射劑量率之變動比率。

結果：1. 試劑活度更改前、後，各單筆廢棄物輻射劑量率之最高、最低值與中位數，分別為 0.76、0.8 uSv/h，0.27、0.24 uSv/h 以及 0.53、0.57 uSv/h。2. 試劑活度更改前、後之檢體量、廢棄物重量、輻射劑量率以及總輻射劑量率平均各為，1.60、1.74，60.46、59.58 kg，6.13、6.50 uSv/h 及 31.82、34.37 uSv/h。3. 試劑活度更改後，相較更改前之檢體量、廢棄物重量、輻射劑量率和總輻射劑量率之增加比率各為，8.62、-1.46、6.03、8.02。

結論：依據南部某醫院核醫科放射免疫分析室，試劑更改前、後之檢體數量與廢棄物輻射劑量率資料，本研究發現：

1. 試劑活度更改後，各單筆廢棄物輻射劑量率之最高值與中位數，均較更改前之數值略高，分別由 0.76 上升至 0.8 uSv/h 以及 0.53 增長至 0.57 uSv/h。
2. 試劑活度更改後，每月之輻射劑量率平均由 6.13 增加至 6.50 uSv/h，總輻射劑量率平均，亦從 31.82 提高為 34.37 uSv/h，兩者相較更改前確有上升。

因此該放射免疫分析室試劑更改後產出之廢棄物輻射劑量率，確有增加。

不過試劑活度更改後，作業量增加之 8.62%，與總輻射劑量率之 8.02% 增長幅度頗為類似。因此仍需更進一步之研究以釐清，究竟為作業量或試劑活度之增加導致廢棄物輻射劑量率之升高。

PC-082

RIA 異常警告值出現率與簡訊通報未處置率之相關性

廖建國[1]、張素雲[1]、黃筱崴[1]、莊紫翎[1,2]

[1]佛教慈濟醫療財團法人大林慈濟醫院核子醫學科
[2]慈濟學校財團法人慈濟大學醫學系

目的：訂定簡訊通報回覆處置指標，並例行的監控及檢討，為 RIA 實驗室常見的管理方式。本實驗室多年來亦建置有簡訊通報未處置率之指標，但異常警告值出現率是否與簡訊通報回覆處置情形有關，不得而知。本研究目的即為分析近 2 年異常警告值出現率、簡訊未處置率以及簡訊未處置之項目與臨床科別，並探討異常警告值出現率與簡訊通報未處置率之相關性，以作為持續改進的參考。

材料方法：以本院雙向簡訊訊息查詢管理系統，收集 2022 年 1 月至 2023 年 7 月之臨床醫師回覆明細以及本科品質指標資料，分別計算異常警告值出現率、簡訊未處置的比率。再進一步分析簡訊未處置之項目及臨床科別。異常警告值之項目及通報上限，分別為 AFP (> 100 ng/mL)、CEA (> 10 ng/mL)、CA125 (> 200 U/mL)、CA15-3 (> 50 U/mL)、CA19-9 (> 150 U/mL)、PSA (> 10 ng/mL)、SCC (> 3.5 ng/mL)、TPA (> 130 U/L) 及 Thyroglobulin (> 100 ng/mL)。

結果：分析結果發現近 2 年之平均異常警告值出現率為 2.52%，而平均簡訊通報未處置率為 0.22%。結果顯示異常警告值出現率與簡訊通報未處置率並無明顯的相關，換句話說，簡訊通報未處置率並不會因異常警告值出現率較高而呈現明顯升高。而進一步分析簡訊未處置之項目及臨床科別，發現未處置的項目以 AFP、CEA、thyroglobulin 最多，PSA、SCC 次之。而在臨床科別方面，則以腸胃內科最多，一般外科、血液腫瘤科、耳鼻喉外科次之。另外，針對各別的醫師，我們發現僅有 7 位醫師曾未回覆處置，且其中並未發現有某一位醫師有重覆發生的狀況。

結論：分析結果顯示，異常警告值出現率與簡訊通報未處置率並無明顯的相關，本院以簡訊方式通報 RIA 異常警告值之平均回覆處置率為 99.78%，顯示絕大多數的科別及醫師皆能在收到簡訊後回覆處置情形，未來可針對簡訊未處置之項目及科別，再加強監控與改善，以持續提升醫療品質與病人安全。

PC-083

以電話提醒方式改善檢查取消率之成效分析

廖建國[1]、許幼青[1]、朱湘蓮[1]、莊紫翎[1,2]

[1]佛教慈濟醫療財團法人大林慈濟醫院核子醫學科
[2]慈濟學校財團法人慈濟大學醫學系

目的：病人取消已約定之檢查，為核醫造影作業中經常發生之事件。本科自 2016 年開始每月監控病人取消檢查之比率，並於檢查前 1 日以電話提醒病人，期望可以減少病人取消檢查之件數，執行多年來確有成果。然而，仍有少數病人無故不來。本研究目的即為回溯性分析近 8 年檢查取消之比率及其原因，以了解年度改善情形，並作為持續改進之參考。

材料方法：回溯性收集 2016 年 1 月至 2023 年 7 月，例行造影檢查之門診排程報到資料，分析各年度之檢查取消率，並探討其發生原因。再進一步分析每日電話提醒是否可以達成預期的效果，例如減少無故不來、忘記日期、未禁食等個案。病人的排程預約，均依病人方便的時間，並考量病人回診日期及開單醫師特別之需求，排定適合醫師與病人的日期，進行造影檢查。

結果：總計收集 29,808 件門診個案，其中檢查取消之個案計 736 件。整理結果發現，2016 年至 2023 年 7 月之間，檢查取消率年度平均值為 2.47%。其中以 2016 年之檢查取消率最高 (3.34%)，而 2020 年之檢查取消率最低 (1.89%)，結果顯示歷年之檢查取消率有逐年下降之趨勢，惟 2023 年略有回升。進一步分析檢查取消之原因，發現排序前 3 名分別為無故不來 (19%)、身體不適 (14%) 及未禁食 (11%)，其次為病患有事 (9%)、病人拒作 (9%)、醫療處置 (8%)、病人出院或轉院 (5%)、病人無法配合 (5%)、儀器故障 (5%)、忘記或記錯日期 (4%) 及其他等因素。再比較歷年來因無故不來、忘記日期及未禁食而取消檢查之比率，發現執行前 5 年確有改善，惟後 3 年則略有回升。雖然我們懷疑這可能與 2020 年起新冠肺炎的疫情因素有關，但仍應再持續觀察與檢討改善。

結論：研究結果顯示，本科近 8 年之檢查取消率平均為 2.47%，除 2016 年及 2017 年檢查取消率相對較高外，2018 年以後皆可控制在 2.5% 以內。雖然疫情期間可能影響病人正常前來檢查，但以每日電話提醒病人之方式，仍是必要且有效的機制，有助於持續降低病人取消檢查的比率。

PC-084

碘 -131 病房病人滿意度調查之初步分析

廖建國[1]、許幼青[1]、朱湘蓮[1]、莊紫翎[1,2]

[1]佛教慈濟醫療財團法人大林慈濟醫院核子醫學科
[2]慈濟學校財團法人慈濟大學醫學系

目的：碘 -131 病房為甲狀腺癌症之患者於接受全甲狀腺切除後之完整摘除治療之用。為提供甲狀腺癌相關病患完整治療服務，提供完整連續性照護服務，本院於 2022 年底開始啟用碘 -131 病房。本研究目的即為分析碘 -131 病房啟用後之初步滿意度調查結果，以作為持續改進之參考。

材料方法：回溯性收集 2023 年執行隨機調查之滿意度調查結果，分別依不同季別以及構面計算滿意度，再進行比較及探討。滿意度調查內容，包括醫療照護 (例如醫師仔細診察及詳細說明病情、護理人員技術純熟等)、服務態度、等候時間、環境設施、作業流程、服務結果等各構面。

結果：由於啟用初期接受住院治療的人數較少，且為隨機調查，總計僅收集 20 件問卷調查結果。整理結果發現，碘 -131 病房啟用後之平均整體滿意度為 92.3%，第 1 季與第 2 季的滿意度差別不大。進一步分析不同構面之滿意度，發現各構面滿意度皆在 90% 以上，其中滿意度較高者為服務態度 (95.5%) 及醫療照護 (92.4%) 2 項，其次則分別為作業流程 (91.7%)、等候時間 (91.3%)、環境設施 (90.7%)。結果顯示，本院提供碘 -131 治療服務的所有同仁皆深獲病患的肯定。不過，因執行滿意度調查也讓我們了解少數病人反映的問題（例如住院前等候檢查的時間、等待住進病房的時間等），而進行檢討與改善。

結論：初步分析結果顯示，本科碘 -131 病房啟用後之平均整體滿意度為 92.3%，各構面滿意度皆在 90% 以上。透過滿意度調查，不僅能了解病人對我們的滿意程度，也可針對病人期待改進之處加以改善。因此，我們將持續進行滿意度調查，並持續改進，以提供病人最優質的服務。

PC-085

RIA 實驗室作業量趨勢分析及探討

廖建國[1]、張素雲[1]、黃筱崴[1]、莊紫翎[1,2]

[1]佛教慈濟醫療財團法人大林慈濟醫院 核子醫學科
[2]慈濟學校財團法人慈濟大學 醫學系

目的：放射免疫分析為核醫專科醫師訓練的項目之一，依現行評鑑的規定，RIA 實驗室的檢驗項目必須包括腫瘤標記、荷爾蒙或肝炎等至少 2 項。本科於 2019 年 4 月即停止肝炎的檢驗服務，2020 年起又因新冠肺炎疫情而影響到其餘 2 大項的作業量。本研究目的即為分析近年 RIA 實驗室之作業量變化趨勢以及各項目最新的分佈情形，以作為檢討與改進之參考。

材料方法：回溯性收集 2019 年 1 月至 2023 年 7 月，實驗室每月檢驗人次之資料，分別依不同年度分析近 5 年 RIA 實驗室之作業量（檢驗人次）變化趨勢，再分析 2023 年（1 ~ 7 月）實驗室自行檢驗之各項目的檢驗件數，並依腫瘤標記、荷爾蒙或其他荷爾蒙等不同類別分析其分佈情形，以進行比較。

結果：整理結果發現，2019 年 1 月至 2023 年 7 月之平均每月作業量為 3,671 人次。其中以 2023 年及 2019 年作業量較高，而 2020 至 2022 年則相對較低。顯示 2020 ~ 2022 年疫情期間作業量確實受到不同程度的影響。而在 2023 年的檢驗件數分析方面，發現每月平均件數為 257 件，其中排序居前 3 位的項目為 TSH、Free T4、CEA，而排序後 3 位者則為 Thyroglobulin、prolactin 及 T4 等項。以項目類別的分佈來看，甲狀腺功能檢查 (40%) 占最多，其次分別為腫瘤標記 (38%)、其他荷爾蒙 (22%)。

結論：本科近 5 年之平均每月作業量為 3,671 人次，2020 年起雖受到疫情的影響，但近 2 年已有逐漸回升的趨勢。目前最大宗的檢驗項目為甲狀腺功能檢查以及腫瘤標記，但針對其中檢驗件數較少的項目，實驗室仍應持續檢討及追蹤觀察，以期能適度提升醫師的利用率。

PC-086

放射免疫分析實驗室報告更改率之分析與比較

廖建國[1]、張素雲[1]、黃筱崴[1]、莊紫翎[1,2]

[1]佛教慈濟醫療財團法人大林慈濟醫院核子醫學科
[2]慈濟學校財團法人慈濟大學醫學系

目的：實驗室訂定報告更改率之指標，進行定期監控與檢討改善，為提升報告品質的重要方式之一。本科多年前即建立報告更改率之品質指標，並持續的改善報告品質。本研究目的即為分析近 7 年報告更改之比率，並與同儕比較，以探討目前是否還有改進的空間，以作為持續改進之參考。

材料方法：回溯性收集 2017 年至 2023 年（1 ~ 7 月）每月整理之品質指標監控結果，分析不同年度之平均報告更改率，並參考醫檢學會台灣臨床實驗室品質指標系列年報 (Taiwan Laboratory Indicator Series, TLIS) 所提供之同儕值，進行比較，以了解實驗室報告品質是否已達國內同儕水準，以及目前是否還有改進的空間。

結果：分析結果發現，本實驗室近 7 年的平均報告更改率為 0.017%，其中以 2017 年報告更改率 (0.04%) 最高，而最低的年度則為 2023（1 ~ 7 月）的平均值 (0.009%)，報告更改率已有逐年下降的趨勢。而分析醫檢學會所提供的同儕值，發現實驗室發生錯誤報告比率之同儕平均值，醫學中心為 0.003%，區域醫院為 0.008%，其中醫學中心歷年的變化不大，而區域醫院則也有逐年下降的趨勢。若與本實驗室 2017 年至 2022 年發生錯誤報告比率之平均值 (0.019%) 比較，發現同儕值比本實驗室略低，也就是我們目前的報告更改率仍有改善的空間。不過，國內各實驗室的人力狀況、操作項目及作業量皆不同，以目前本院放射免疫分析實驗室僅 3 位醫檢師的人力狀況，可視實際情況訂定一個合理可達成的目標。

結論：本實驗室 2017 年的平均報告更改率為 0.04%，2023（1 ~ 7 月）的平均值已降至 0.009%，目前雖已有明顯改善，且與區域醫院的同儕平均值 (0.008%) 相近，但若與醫學中心 (0.003%) 比較，本實驗室仍有改善的空間。實驗室透過與同儕比較，將報告錯誤率與國內其他實驗室比較，可為實驗室設定一個合理可達成的目標，有助於持續追求卓越品質。

PC-087

放射免疫分析 Thyroglobulin 新舊試劑檢驗結果之比對

張素雲[1]、黃筱崴[1]、廖建國[1]、莊紫翎[1,2]

[1]佛教慈濟醫療財團法人大林慈濟醫院 核子醫學科
[2]慈濟學校財團法人慈濟大學醫學系

目的：實驗室可根據品質需求更換試劑，認證實驗室為符合認證要求，應依據 ISO15189 對於檢驗結果可比較性的要求，進行新舊試劑的比對，以評估監測中病患更換試劑前後數值的變化。本研究目的即為比對 Thyroglobulin 新舊試劑檢驗結果之相關性，以查證新試劑品質是否符合要求。

材料方法：收集病人檢體，分別使用新試劑 (IZOTOP HTG(I-125)IRMA) 以及舊試劑 (Beckman Coulter/Immunotech Thyroglobulin IRMA) 進行檢測，依原廠試劑說明書進行操作。兩者方法皆為 IRMA 原理，且參考值皆是 < 50 ng/mL ，IZOTOP 試劑靈敏度為 < 0.03 ng/mL; Immunotech 試劑靈敏度為 < 0.3 ng/mL，均使用同一加馬計數器進行計數。獲得兩組檢驗結果後，再使用 Excel 軟體進行線性回歸分析，以計算其相關性及 r^2 值等數據，並判定新試劑品質是否可接受（允收標準為 $r^2 \geq 0.95$）。

結果：總計收集 31 支病人檢體，其中新舊方法檢驗值皆大於 50 ng/mL 之檢體計 5 支，其餘 26 支檢體之檢驗值皆在正常參考範圍內。另外，有 5 支檢體，用新舊方法測試數值皆 < 0.3 ng/mL。兩組不同廠牌試劑之檢驗結果，經線性回歸分析得知其相關性公式為 $y = 0.8404x - 0.388$，r^2 值為 0.9945 ，符合允收標準，顯示新試劑 (IZOTOP) 之品質可接受。

結論：Thyroglobulin 在追蹤甲狀腺癌方面是非常有價值的指標，對於正在追蹤監測或已接受外科手術和大劑量碘 -131 治療的病患，通常成功治療後 Thyroglobulin 的數值會下降到極低的數值，若治療失敗則會再度上升，所以試劑品質非常重要。本研究比對 IZOTOP 新試劑與 Immunotech 舊試劑之相關性，結果顯示兩組試劑 Thyroglobulin 檢驗結果呈現高度相關，表示新試劑品質可符合要求。

PC-088

Utilization of F-18 FDG PEC/CT in Evaluation and Treatment Monitoring of Mixed Cutaneous, Lymph Node, and Soft Tissue T-cell Lymphoma: A Case Report

Yu-Chien Shiau, Po-Wei Li, Chao-Chun Huang, Ya-Huang Chen, Chia-Wen Lai, Che-Wei Chang, Yen-Wen Wu, Shan-Ying Wang

Division of Nuclear Medicine, Far Eastern Memorial Hospital, New Taipei, Taiwan

Introduction: In literature review, T-cell lymphoma involving skin, lymph nodes, and soft tissue is a relatively rare disease condition. We report a case of T-cell malignant lymphoma involving skin, lymph nodes, and soft tissue. F-18 FDG PET/CT studies were used for evaluation and treatment monitoring.

Case Report: The 19-year-old man suffered from fever up to 38–39°C for three months. Lab data showed normocytic anemia, elevated LDH, no leukocytosis, autoimmune marker negative, and HIV negative. CT showed 1. Multifocal areas of cutaneous and subcutaneous lesion all over the body, with increased vascularity and fat stranding. Ddx: autoimmune disease, skin/subcutaneous lymphoma, atypical infection...etc, advise clinical correlation. 2. Clustered lymphadenopathy in the left axilla, bilateral inguinal areas. 3. Increased soft tissue density at the right pelvic side wall attached to the right side of the urinary bladder, nature to be determined. F-18 FDG PET/CT was arranged and showed hypermetabolism noted in right temporal scalp, skin of bilateral neck, bilateral upper extremities, bilateral chest wall, bilateral abdominal wall, both thigh, bilateral axillary lymph nodes, bilateral peritoneum, mesentery, pelvic wall, and inguinal lymph nodes, hepatomegaly and splenomegaly, which could be due to lymphoma involvement. AJCC stage T3N2M0 and NCCN T3bN3M0, stage 4. Skin biopsy at abdomen showed atypical lymphoid infiltration, positive for CD3 and CD8. Stain of CD20, CD56, and CD4, favored cutaneous T cell lymphoma. He was admitted and received chemotherapy with CHOPEx6 and ESHAP. Six months later, F-18 FDG PET/CT was arranged again for treatment monitoring, which showed partial metabolic response of previous multifocal subcutaneous lymphoma involvement, residual malignant involvement at trunk, bilateral arms, bilateral thighs, and right medial lower leg noted, and complete metabolic response of previous bilateral inguinal nodal involvement. Based on the findings of PET/CT, he was arranged for bone marrow transplant.

Conclusions: T-cell lymphoma involving skin, lymph nodes, and soft tissue is a relatively rare disease condition. Using F-18 FDG PET/CT for evaluation and treatment monitoring was considered to be beneficial in clinical situation. In the future, we hope to gather more cases for more detailed statistical analysis.

PC-089

碘 -131 治療與檢查期間低碘飲食衛教——個案報告

邱禹臻[1]、許幼青[1]、廖建國[1]、莊紫翎[1,2]

[1]佛教慈濟醫療財團法人大林慈濟醫院 核子醫學科
[2]慈濟學校財團法人慈濟大學 醫學系

簡介：美國甲狀腺協會建議執行「低碘飲食」者，每天攝取碘含量不要超過 50 微克 (μg)。接受碘 -131 治療或檢查前須降低體內碘含量，主要目的為減少身體上儲存的碘，以提高甲狀腺組織與腫瘤細胞對服用放射性碘的攝取，充分發揮治療效果，因此治療前四星期必須採低碘飲食，以控制碘攝取量。本個案報告為本科教導極度焦慮之病人接受碘 -131 治療與檢查期間飲食注意事項之經驗，提出分享。

個案報告：52 歲男性病人，有高血壓及糖尿病病史已有十多年，每日服用藥物控制中，本身為 B 肝帶原者，每年門診定期追蹤，在 2022 年 7 月份開始摸到右側頸部有硬塊但不以為意，之後開始有聲音沙啞及咳嗽症狀，進食時也常有吞嚥困難的情形，甲狀腺超音波導引下細針穿刺細胞學檢查診斷為甲狀腺癌，於 2022 年 9 月 14 日行雙側甲狀腺切除術及右側頸部根治術，病理報告：pT1aN1bN0，stage I，預於 2022 年 10 月 26 日入住碘 -131 病房，醫師叮囑入住碘 -131 病房前需低碘飲食四週，病人職業為台西客運司機，上班時間平均十小時以上，三餐大多外食，每天至少一杯手搖飲，用餐時間不固定，病人表示對於低碘飲食事項毫無概念，不知道哪些食物可以吃？哪些不能吃？擔心吃得太簡單會不會沒有體力？詢問是否需要再另外補充營養品嗎？覺得需低碘飲食四週這件事情對他而言是很困難的，對於即將入住碘 -131 病房感到很焦慮不安。

討論：碘 -131 治療前後，建議飲食事項如下：（一）使用無加碘食鹽取代加碘鹽，目前市售加碘鹽每五公克約含 75 ~ 100 微克的碘，故建議使用無加碘食鹽，購買時請認明標示成分為不含碘酸鉀、碘化鉀。台鹽有數種市售無碘鹽：如意精鹽、天然超鮮鹽。（二）避免食用高含碘食材食物，特別是海產之動、植物含碘量較高，應避免食用。（三）避免食用含食用色素 7 號食品或藥品，如紅 / 橘色糖果、果凍或含碘藥品（如感冒藥水）、耳鼻喉科醫生塗抹喉嚨的藥水。（四）避免食用含碘維他命或食物補充品，如綜合維他命、鯊魚軟骨素、亞培、安素等營養品。（五）其他宜避免之食物，我們請病人參閱本科提供之碘 -131 治療與檢查期間飲食指引。

結論：利用飲食指引向病人一一衛教說明後，病人表示能了解低碘飲食的內容，其家人表示會協助一起準備低碘飲食。出院後病人回門診時表示在低碘飲食這段時間全家都盡量不外食，家人會協助準備中午的便當，晚上則由病人自己準備晚餐，能了解需盡量避免攝取的有哪些食物，在低碘飲食四週的這段時間並沒有食慾差及體力不足的症狀，也讓病人改變以往的飲食習慣，培養健康的飲食型態。

PC-090

碘 -131 住院治療病人類別及其常見問題之回溯性分析

邱禹臻[1]、許幼青[1]、廖建國[1]、莊紫翎[1,2]

[1]佛教慈濟醫療財團法人大林慈濟醫院核子醫學科
[2]慈濟學校財團法人慈濟大學醫學系

目的：根據國民健康署的最新統計，「甲狀腺癌」已是國人癌症排名第七位。甲狀腺癌病患在手術切除甲狀腺組織後，可接受碘 -131 輔助治療清除殘餘組織及治療轉移病灶。本科碘 -131 病房於 2022 年 9 月啟用，發現甲狀腺癌的病人對於即將入住碘 -131 病房感到很焦慮不安，因此經常詢問各類的問題。本研究目的為回溯性分析近 1 年碘 -131 住院治療病人類別之分佈以及常問的問題，以作為日後衛教改進之參考。

材料方法：回溯性收集 2022 年 9 月至 2023 年 9 月期間，病人的衛教紀錄以及所詢問的問題。依不同性別、年齡、TNM 分期、收案來源、是否服用甲狀腺素、是否施打人工合成甲促素、治療藥物劑量等進行病人類別之分析，再整理病人常問之問題，依治療前、中、後進行分類，並探討其分析結果，以了解目前衛教之表單及內容是否還有改進的空間。

結果：總共收案 49 位病患，其中以女性病人居多，年齡以 51 ~ 60 歲較多，TNM 分期則以第 I 期最多。針對病患提問之問題進行分析後，發現治療前常見的問題以治療後的問題最多（占 43%），其次為治療前 (37%) 及治療中 (20%)。各類問題中，排序居前 3 項者為低碘飲食 (100%)，其次為輻射影響 (97%) 及住院天數 (85%)。另外，也發現所提問的問題，在男女性別上似乎有較多差異之處，例如多數男性病患提問重點在多久能回去上班、輻射對家人及同事的影響、如何準備低碘飲食等，而女性病患提問則著重於如何準備低碘飲食、輻射是否影響生育能力、住院攜帶用物、住院如有不適該如何求助等。

結論：本科碘 -131 病房啟用 1 年來，病人以第 I 期最多，顯示接受治療的病人多屬早期發現的病人。手術切除腫瘤加上碘 -131 治療，是目前公認甲狀腺癌的最佳治療方式，多數病人入住碘 -131 病房前都有諸多疑問，依據本研究分析之結果，未來可針對病人經常提問的問題，製作問與答之衛教資料，於衛教時提供病人參考，讓衛教內容更貼近病患之需求，以提升衛教品質。

PC-091

多種示蹤劑正子影像檢查對攝護腺癌生化性復發之評估——個案報告

張佳琪[1]、莊志堅[1]、曾能泉[1]、黃振義[2]、歐宴泉[3]

[1]童綜合醫療社團法人童綜合醫院 核子醫學科
[2]童綜合醫療社團法人童綜合醫院 影像醫學部
[3]童綜合醫療社團法人童綜合醫院 泌尿腫瘤中心

背景介紹：台灣的攝護腺癌發生率近幾年快速上升，目前是男性國人的第五大癌症，為早期偵測到轉移病灶，以利後續治療，各項正子示蹤劑檢查已被開發出來應用於臨床診斷上，如Ga68-PSMA-11 PET/CT、Axumin PET/CT、NaF PET/CT等三個檢查項目，可用於攝護腺癌之分期、復發、轉移、及療效評估等臨床時機，而這些正子影像檢查各有其優勢，擬藉由此案例影像來展示。

病例報告：此病例為一 74 歲男性，於 2021 年確診攝護腺癌並開刀治療，2023 年病例回診追蹤，發現攝護腺特異抗原檢驗 (PSA) 數值為 5.224，接受 NaF PET/CT 發現有骨轉移，後續 2 個月內陸續完成 Ga68-PSMA-11 PET/CT、Axumin PET/CT、Tc99m MPD BONE Scan 等檢查，檢查時序為先執行 NaF PET/CT 約 1 個月後執行 GA68-PSMA-11 PET/CT，隔天執行 Tc99m MPD BONE Scan，再過 2 週後執行 Axumin PET/CT。結果發現 NaF PET/CT 顯示較多骨骼病灶；Ga68-PSMA-11 PET/CT 顯示較多之遠端淋巴結轉移；Axumin PET/CT 也可以發現淋巴結轉移病灶，且因造影程序不同，原先手術部位影像不易受膀胱內尿液放射活性影響。此外，部分淋巴結轉移皆可於 Ga68-PSMA-11 PET/CT 及 Axumin PET/CT 發現。病患後經荷爾蒙治療及放射治療後 PSA 有明顯下降。

結論：NaF PET/CT & Ga68-PSMA-11 PET/CT 可應用於分期、偵測復發骨轉移、療效評估，NaF PET/CT 可發現較多骨骼病灶，Ga68-PSMA-11 PET/CT 可發現較多軟組織及淋巴結等病灶，而 Axumin PET/CT 對於局部偵測復發有其優勢，因此，這三種正子影像檢查對生化性復發之攝護腺癌病患在臨床應用上是各有意義的，也能較完整評估骨性及軟組織病灶的腫瘤負荷 (tumor burden)，有利臨床決策及治療計畫。

PC-092

Hypermetabolism in the Hemostatic Granuloma of a Patient after Receiving Total Callosotomy

Tse-Hao Lee[1], Yuh-Feng Wang[1,2], Nan-Jing Peng[1,3]

[1] *Department of Nuclear Medicine, Taipei Veterans General Hospital, Taipei, Taiwan*
[2] *Department of Medical Imaging and Radiological Technology, Yuanpei University of Medical Technology, Hsinchu, Taiwan*
[3] *School of Medicine, National Yang Ming Chiao Tung University, Taiwan*

Introduction: Brain ^{18}F-FDG PET can be used for preoperative evaluation in patients with epilepsy. Alterations of glucose metabolism demonstrated by brain ^{18}F-FDG PET might help in defining epileptogenic zone

Case Report: This 13 year-old boy has history of epilepsy and developmental delay. He has first seizure onset since he was 2 years old. He was considered for brain surgery due to his seizure being drug-resistant. He underwent preoperative evaluation including EEG, brain MRI, and Brain ^{18}F-FDG PET. PET showed hypometabolism in bilateral anterior temporal, left lateral temporal, and right parietal-temporal cortices. But brain MRI showed no evident focal lesion. He underwent total callosotomy and follow-up brain PET 16 months postoperatively, and three intense FDG uptake (hypermetabolism) foci in the surgical site were revealed. Corresponding MRI localized these foci as hemostatic granuloma. Using hemostatic agent in the neurosurgery is not rare, and the residual hemostatic agent might induce brain tissue reaction including granulomatous inflammation, in which giant cells are accumulated. The gathering of giant cells in the granuloma might concentrate glucose absorption and metabolism, presenting hypermetabolism in the ^{18}F-FDG PET

Conclusions: Hypermetabolism in the brain ^{18}F-FDG PET of patients with epilepsy usually is due to ictal change of epileptogenic lesion. However, non-epileptogenic etiology such as granulomatous inflammation might also be considered. Carefully combined evaluation of other examination such as brain MRI and EEG might help in differential diagnosis.

PC-093

Distant Metastasis Detected in Multi-modal Imaging of Post-treatment HNSCC

Yi-Hsun Chen, Yu-Ling Hsu

Department of Nuclear Medicine, Ditmanson Medical Foundation Chia-Yi Christian Hospital, Chiayi, Taiwan

Introduction: Multiple medical imagings are likely to be great tools for cancer staging and re-staging. For example, whole-body bone scan is very useful for detecting bone metastases after cancer treatment. And, 18F-FDG PET/CT has already become the main important diagnostic method in the evaluation of head and neck squamous cell carcinoma (HNSCC), from pre-treatment staging to radiation therapy planning, treatment response assessment and post-operative follow-up. Also, MRI can be used clinically to help differentiate between different diseases status especially in soft tissue. The different characteristics of each imaging examination can help clinicians to determine the current state of the disease as malignancy diseases may change very quickly according to the treatment or be affected by different treatment choices.

Case Report: A 57-year-old man with history of squamous cell carcinoma of the head and neck was followed using whole-body bone scan. Increased Tc-99m MDP uptake in the proximal left femur was noted. He was later arranged F-18 FDG PET/CT and MRI for further examination. On PET/CT imaging, no definite FDG uptake abnormalities were found in the original head and neck region indicating regress of disease. However, there was incidentally enhanced FDG uptake over left proximal femur, which was reasonably to be suspected as bone metastasis. Confirming MRI images showed abnormal bone marrow replacement in the proximal part of the left femur; mild cortical infiltration but intact adjacent muscles, no obvious invasion, and bone metastases to the proximal femur were identified.

Conclusions: Since malignancy has its variable forms of development, it is possible to develop distant metastases without local recurrence. In this case, bone metastasis over the left femur was diagnosed through the evaluation of whole-body bone scan, PET/CT, and MRI. Notably, this reveals the important role of FDG PET/CT in detecting distant metastases in patient follow-up and re-staging of diseases.

PC-094

Thyroid Storm Triggered by Radioactive Iodine Therapy due to Functioning Metastatic Thyroid Cancer: A Case Report

Tsu-Kang Chen, Yen-Hsiang Chang

Department of Nuclear Medicine, Kaohsiung Chang Gung Memorial Hospital and Chang Gung University, Kaohsiung, Taiwan

Introduction: Thyroid storm, a life-threatening condition associated with thyrotoxicosis, is seldom attributed to functioning metastatic thyroid cancer. We report an exceptional case of thyroid storm triggered by radioactive iodine therapy in the context of functioning metastatic thyroid cancer, a rarely documented occurrence.

Case Report: A 67-year-old woman presented to the hospital for palpitation and shortness of breath. She had a longstanding goiter with progressive enlargement, and laboratory studies confirmed hyperthyroidism with elevated serum free thyroxine (T4) and suppressed thyroid-stimulating hormone (TSH) levels. Image studies revealed a left thyroid mass, multiple lung nodules, and multiple sites of bone destruction with soft-tissue mass, raising the concern for thyroid cancer with distant metastases. A biopsy of the metastatic bone lesion confirmed the diagnosis of metastatic follicular carcinoma of the thyroid. After her serum free T4 level normalized with antithyroid therapy two months later, she underwent a total thyroidectomy. Subsequently, two months after thyroidectomy, she received a radioactive iodine therapy of 200 mCi after levothyroxine withdrawal, albeit her serum TSH level remained undetectable. However, six days after the administration of the radioactive iodine, she experienced dyspnea with orthopnea, palpitation, a low-grade fever, and diarrhea. Laboratory data indicated overt hyperthyroidism with markedly elevated free T4 and suppressed TSH levels. Post-therapeutic whole-body scan showed widespread lung and bone metastases. An electrocardiogram showed atrial fibrillation, and a chest radiography showed right-side pleural effusion, identified as transudate after drainage. A diagnosis of thyroid storm was established. She was treated accordingly and gradually recovered.

Conclusion: This case underscores the significance of considering thyroid storm as a potential complication in functioning metastatic thyroid cancer despite its rarity. The rapid and severe course of this condition necessitates timely intervention and clinical awareness.

PC-095

[68Ga]Ga DOTATOC PET for Detecting Recurrent Medullary Thyroid Cancer

Hsin-Chang Chen, Yen-Hsiang Chang

Department of Nuclear Medicine, Kaohsiung Chang-Gung Memorial Hospital and Chang-Gung University, Kaohsiung , Taiwan

Introduction: Medullary thyroid carcinoma (MTC) is a malignant tumor derived from the para-follicular thyroid C cells. It may occur in sporadic or hereditary forms and surgery represents the primary cure. EANM Guidelines endorse [18F]F-FDG PET/CT and [68Ga]Ga-DOTATOC PET/CT as useful tools for recurrent MTC detection.

Case Presentation: A 59-year-old female, previously subjected to total thyroidectomy and central neck dissection for MTC, exhibited escalating serum calcitonin (135 to 410 pg/mL) and CEA (8.99 to 50.4 ng/mL) levels. With a decreasing calcitonin doubling time, [18F]F-FDG PET/CT revealed mild uptake in the right paratracheal lymph node (SUVmax 2.23) and background uptake in pre-tracheal and left paratracheal lymph nodes. Given inconclusive [18F]F-FDG PET/CT results, a subsequent [68Ga] Ga-DOTATOC PET/CT study showcased focal uptake in right paratracheal (SUVmax 5.16), left upper paratracheal (SUVmax 2.27), and pre-tracheal (SUVmax 1.68) lymph nodes. Subsequent surgical dissection unveiled metastases in right neck level IV and VI lymph nodes.

Conclusions: This case illustrates the superior lesion detection capabilities of [68Ga]Ga-DOTATOC PET/CT over [18F]F-FDG PET/CT in recurrent medullary thyroid cancer. These findings underscore the potential of [68Ga]Ga-DOTATOC PET/CT as a valuable diagnostic tool in managing MTC recurrence.

PC-096

^{18}F-FDG PET/CT Imaging for Diffuse Large B Cell Lymphoma of Tongue Base: A Case Report

Chi-Jung Tsai[1], Che-Hsuan Lin[2], Wen-Sheng Huang[3]

[1] *Department of Nuclear Medicine, Taipei Medical University Hospital, Taipei, Taiwan*
[2] *Department of Otolaryngology, Taipei Medical University Hospital, Taipei, Taiwan*
[3] *Department of Nuclear Medicine, Cheng Hsin General Hospital, Taipei, Taiwan*

A female patient had history of rheumatoid arthritis (RA). She suffered from gradual hoarseness and lumping sensation in throat for months and endoscopy depicted a large fungating mass over tongue base, extending to larynx, favoring squamous cell carcinoma. The initial MRI showed abnormal space-occupying tumor at larynx and tongue base; laryngeal cancer is considered, as well as amorphous enhancing soft tissue lesion within the right carotid space. The following FDG-PET revealed an intense-FDG-avid mass in tongue base expanding to supraglottis of larynx and a longitudinal FDG-avid mass in right carotid space (both sizes: about 3 cm). The final excisional pathology of tongue base revealed diffuse large B cell lymphoma. Literally, lymphomas primarily located in the tongue base are very rare. It is well-known that patients with RA have a greater risk of developing both Hodgkin lymphoma (HL) and non-HL than the general population. Whole-body^{18}F-FDG PET/CT is mainly applied to determine the clinical stage of lymphoma and to guide treatment. Few studies have discussed the imaging performance of tongue base lymphoma. Thus, we report ^{18}F-FDG PET/CT of this disease to provide reference information for the diagnosis of similar diseases in the future.

PC-97

Pembrolizumab 免疫療法誘發的對稱性多關節炎，骨骼掃描儀顯示「動作捕捉衣」

游舜宇[1]、賴俊良[2]

[1]佛教慈濟醫療財團法人大林慈濟醫院 核子醫學科
[2]佛教慈濟醫療財團法人大林慈濟醫院 胸腔內科

簡介：一例全身骨骼廣泛、對稱的多關節炎，在 Tc-99m 亞甲基二磷酸鹽 (MDP) 骨閃爍掃描儀上看起來像動作捕捉衣。

病例報告：本例為一名 44 歲患有肺腺癌男性，近日進行 Pembrolizumab 免疫治療，並有多處關節疼痛情形。在 Tc-99m 骨骼掃描結果並未顯示有骨轉移證據，然而在雙側胸鎖骨、肩、肘、腕、手、膝和踝等多處關節周圍有活性閃爍。影像結果與患者的多關節疼痛區域相符。最後給予大劑量類固醇來控制症狀。

討論：骨掃描除常規檢測惡性腫瘤骨骼轉移外，在此案例顯示亦可檢測免疫相關不良反應（例如 Pembrolizumab 誘導的發炎性關節炎）。發炎性多關節炎廣泛且對稱的雙側關節攝取表現類似於動作捕捉服上的球感測器。為方便識別，建議將此獨特影像外觀命名為「動作捕捉衣」標誌。

PC-98

運用醫療照護失效模式與效應分析 (HFMEA) 方法降低碘 131 廢水管道及衰減槽異常事件發生風險

林至群、鄭如伶、徐健欽、陳郁豔、邱藍儀、湯淑雯

長庚醫療財團法人高雄長庚紀念醫院 核子醫學科

背景介紹：醫療照護失效模式與效應分析 (HFMEA) 是一種系統性方法針對醫療作業流程做全面性的風險評估，找出流程中潛在失效模式及其原因，以預應方式對高風險指數的流程步驟重新審視改善，能預防重大危害錯誤的發生。碘 131 病房的廢水管道及衰減槽異常事件可能導致輻射廢水滲漏，是輻射防護的重大議題，本研究目的在以跨部門團隊方式運用 HFMEA 方法分析碘 131 病房廢水管道及衰減槽可能發生異常事件的潛在原因並提出改善對策，以減少異常事件發生機率及提升監控管理與緊急應變處理能力。

方法：本院輻射防護委員會、核醫科、新陳代謝科、工務、警衛、環管及安全衛生各相關單位成立跨部門團隊，運用 HFMEA 方法收集流程資料，針對嚴重度及發生機率進行討論並評分危險指數，識別潛在導致異常事件的原因並制定改善對策。

結果：透過 HFMEA 的方法，我們識別出 7 個失效模式和 14 個失效原因，提出相應的改善對策，包括：增設區域輻射偵檢器、增設漏水感知器、增加每日水位紀錄和現場查核表、擬定緊急應變程序、辦理緊急應變演習、調整住院天數、啟用備援衰減槽等，改善方案能將危險指數從 34 顯著降低至 16，降幅 53%

結論：運用 HFMEA 方法能有效提升碘 131 病房廢水管道及衰減槽的監控預警系統及異常事件發生時的緊急應變能力，降低異常事件發生危害的風險。

PC-99

Non FDG-avidity Urine in Urinary Bladder on ^{18}F-FDG PET/CT Images of a Colon Cancer Patient

Chang-Chung Lin[1], Liang Lo Sha[2], Su Shih Chi[1]

[1] *Department of Nuclear Medicine, Kaohsiung Veterans General Hospital, Kaohsiung, Taiwan*
[2] *Department of Radiology, Kaohsiung Veterans General Hospital, Kaohsiung, Taiwan*

A 69-year-old man had sigmoid colon cancer with urinary bladder invasion. He received diverting proximal T-loop colostomy and partial cystectomy with cystoplasty. He was referred for an ^{18}F-FDG PET/CT scan for staging. The FDG PET/CT scan revealed Non FDG-avidity urine in upper urinary bladder. After walking and jumping, the delayed scan demonstrated uniform FDG-avid urine in urinary bladder. Combining the FDG PET/CT scan, clinical findings, and past history, we made the diagnosis of atonic bladder.

PC-100

利用氟化鈉全身骨骼正子斷層造影與奧攝敏正子斷層造影偵測攝護腺癌骨轉移病人之比較——病例報告

蔡沛君[1]、許雅斐[1]、莊志堅[1]、曾能泉[1]、黃振義[2]、歐宴泉[3]

[1]童綜合醫療社團法人童綜合醫院 核子醫學科
[2]童綜合醫療社團法人童綜合醫院 影像醫學部
[3]童綜合醫療社團法人童綜合醫院 泌尿腫瘤中心

簡介：現今用於攝護腺癌的正子造影檢查近年來日漸興盛並受到重視，成為不可或缺的檢查。奧攝敏正子斷層造影（Axumin PET/CT scan，以下簡稱 Axumin），適用於先前接受治療後因 PSA 濃度上升而懷疑攝護腺癌復發之病患，以協助診斷攝護腺癌之復發；而氟化鈉全身骨骼正子斷層造影（^{18}F-NaF PET/CT scan，以下簡稱 NaF）用於癌症骨轉移之診斷、治療效果評估與追蹤。

病例報告：病患為 73 歲第四期攝護腺癌且骨轉移男性，於手術治療後 PSA 數值降至正常值；前述療程後約 2 年該病患 PSA 數值再度上升，懷疑生化復發。故於同一時期接受 Axumin 造影與 NaF 造影。正子造影掃描儀型號為 GE Discovery MI。Axumin 檢查前需空腹 4 小時，示蹤劑注射完 4 分鐘後立即進行造影，造影範圍為骨盆至頭頂。影像發現脊椎與骨盆有不具示蹤劑活性之骨增生性變化，應為治療後之結痂，且無淋巴結及臟器轉移。NaF 造影不需禁食，於靜脈注射 ^{18}F-NaF 示蹤劑後 1 小時後進行造影，並於等待期間多攝取水分（約 400 毫升）。影像結果發現多處骨轉移，之後接受治療後 PSA 數值下降。但約 1 年後又發現生化復發，並再次接受 Axumin 檢查及 NaF 檢查。於 Axumin 檢查發現多處新骨轉移病灶，包括骨盆、股骨及雙側肩胛骨等，但無淋巴結及臟器轉移。於 NaF 檢查中發現新骨轉移病灶較上次較多，故繼續使用進一步荷爾蒙治療及追蹤。在前後兩次 Axumin 加上 NaF 檢查發現無淋巴結及臟器轉移，特別是 NaF 檢查發現骨轉移病灶明顯變多，可能意指疾病進展 (progression)。

結論：攝護癌好發骨轉移並有可能發生淋巴結及其他器官轉移，利用 NaF 正子造影評估骨轉移的情形，並採用 Axumin 正子造影來檢視病患淋巴結及其他軟組織器官有無轉移情形，兩種造影流程雖然有明顯不同，但搭配檢查下能提供臨床更完整的資訊。本案病患於檢查中，發現 NaF 檢查能較 Axumin 檢查得到更多骨性病灶資訊，若在軟組織的部分則是 Axumin 檢查較為優異。

PC-101

不同 SPECT-CT 造影模式在影像重組時對位之分析探討

吳忠順、蔡富任

高雄榮民總醫院核醫科

目的：SPECT-CT 於核醫造影時可用於衰減校正與核醫病灶之解剖定位，SPECT-CT 掃描時通常在同一個 protocal 執行，但是若因為機器或操作人員因素而無法在同一個 protocal 執行時，要如何執行快速且正確的對位常常是影像分析人員感到棘手的問題，本研究在探討使用 GE DR-870 執行 SPECT-CT 時，不同造影模式對 SPECT 與 CT 對位之比較探討。

材料方法：使用 5 個核醫校正小瓶，瓶內同時放入 Tc99m 0.3 ~ 0.5 mCi 與 Iodine 對比劑 1 cc，分別放入核醫校正模板內 5 個位置，使用 GE DR-870 執行 SPECT-CT，SPECT-CT 掃描分別使用 SPECT 與 CT 在同一 protocal 及 SPECT 掃描後再單獨執行 CT 2 種模式。後續再將校正小瓶放在校正模板內不同的 5 個位置，重複執行以上 2 個造影模式 2 次，將 6 組 SPECT 與 CT 分別使用 GE Volmetrix 程式執行對位測試，將 6 組對位測試結果應用在臨床受檢者因故未在同一個 protocal 執行 SPECT-CT。

結果：探討 GE DR-870 在不同造影模式於對位時 6 個定位點 (Roll, Azimuth, Elevation, Pan Head, Pan Post, Pan Left) 發現，在同一個 protocal 執行 SPECT-CT 時，此 6 個定位點都為 0 時可正確將 SPECT 與 CT 對位，而當 SPECT 掃描後若再單獨執行 CT，使用 GE DR-870 各種對位工具來執行時，機器會給予初步的定位，此時反而會增加對位的難度，在 SPECT 與 CT 掃描位置未改變時，使用 by user 模式進行對位校正，先將 Pan Head 以外的 5 個定位點設定為 0，再改變 Pan Head 將 SPECT 的位置與 CT 執行對位，可以得到正確的對位結果，將此方式應用在因故未在同一個 protocal 執行 I-131 head SPECT-CT 時亦能得到正確的對位結果。

結論：使用 GE DR-870 執行 SPECT-CT 掃描，若因為機器或操作人員因素而無法在同一個 protocal 執行 SPECT-CT，可在不改變病人位置（含掃描的床高）的狀態下執行單獨 CT 掃描，影像分析使用 by user 模式進行對位，先將 Pan Head 以外的 5 個定位點設定為 0，再改變 Pan Head 將 SPECT 的位置與 CT 執行對位，可以得到正確的對位結果。

PC-102

正子電腦斷層掃描在青年人造成體外曝露輻射劑量評估之研究

俞長青[1]、丁健益[2,3]、趙菁禾[3]

[1]高雄榮民總醫院 核子醫學科
[2]中山醫學大學附設醫院
[3]中山醫學大學 醫學影像暨放射科學系

背景介紹：正子電腦斷層掃描 (PET/CT) 結合正子斷層掃描 (PET) 和電腦斷層 (CT) 的優點，能更全面的在早期發現腫瘤病灶，但同時也面臨著輻射量提高的問題。目前也用於青少年癌症之篩檢，本篇想要探討在青少年接受 PET/CT 檢查下，由體外曝露造成不同性別之器官劑量分布差異。

方法：本研究使用蒙地卡羅為基礎之軟體 (Virtual DoseCT) 進行體外暴露劑量模擬。使用條件為 120 kV 及 95 mA，曝露時間為 4.25 秒。使用兩種不同 PET/CT 設備，機型為 GE Discovery 590 跟 GE Discovery 750 進行模擬。模擬男性及女性青少年之結果將依據 ICRP103 進行分析。

結果：結果顯示在使用 GE Discovery 590 跟 GE Discovery 750 兩種機型中模擬出的結果大致相似。模擬中得知除了大腦以外之所有器官，女性青少年的器官劑量都是略大於男孩的，造成之有效劑量差約 0.89 mSv，推測與女孩模擬假體結構造成之散射劑量占比有關。其中乳房的劑量差異是最大的，女孩比男孩高了約 16 倍。而在唾液腺、膀胱和皮膚之器官劑量差異都在 0.03 mGy 以內。

結論：本研究顯示，青少年在進行 PET/CT 可能會造成體外曝露的劑量增加，為避免不必要的輻射風險。建議如果照射範圍外之器官可以增加適當的防護，而在女性青少年則可再增加乳房的防護。

PC-103

Prognostic Impact of Maximum Standardized Uptake Value on ^{18}F-FDG PET/CT Imaging in Stage IV Lung Adenocarcinoma: Exploratory Analysis Comparing Primary Tumor with Distantly Metastatic Lesion

Chang Yen-Hsiang

Nuclear Medicine Department, Kaohsiung Chang Gung Memorial Hospital, Kaohsiung, Taiwan

Background: 18F-FDG PET/CT has been proved as valuable noninvasive tool for diagnosing and staging lung cancer. Primary tumor maximum standardized uptake value (SUVmax) on 18F-FDG PET/CT imaging has been studied as a potential prognostic factor for survival. However, the value of SUVmax of metastatic lesions is unclear. This retrospective study aims to compare the prognostic value of SUVmax of primary tumor and distantly metastatic lesion from pretreatment 18F-FDG PET/CT imaging in patients with stage IV lung adenocarcinoma.

Method: This study includes 21 patients of median age 61 years, with biopsy-confirmed lung adenocarcinoma. All patients received staging 18F-FDG PET/CT before therapy and were classified as stage IV. The SUVmax of primary tumor and distant metastatic lesion were recorded. Overall- and progression-free survival were estimated by the Kaplan-Meier method. These values were categorized as low or high according to the median SUVmax measure of the study population.

Results: Among these 21 patients, 7 (33.3%) were diagnosed as stage IVa disease, and 14 (66.7%) were diagnosed as stage IVb disease. The median SUVmax of primary tumor was 13.2, and the median SUVmax of distant metastatic lesion was 5.3. Median follow-up for the cohort was 21 months. Median overall survival (OS) and progression-free survival (PFS) were 21.4 and 11.4 months, respectively. The primary tumor SUVmax with a cutoff of 13.2 predicted for OS ($p=0.0256$) but was marginally significant for PFS ($p=0.1432$). However, the SUVmax of distantly metastatic lesion with a cutoff of 5.3 did not achieve significance for predicting OS nor PFS ($p = 0.1057$ and $p = 0.7228$).

Conclusion: The results of this study involving patients with stage IV lung adenocarcinoma provide evidence that SUVmax of primary tumor is a better prognostic factor than that of metastatic lesion from pretreatment 18F-FDG PET/CT. The high value of primary tumor SUVmax is associated with poorer OS and PFS.

PC-104

探討年齡、體重、性別與靜脈注射 Dipyridamole 造成注射處刺激之關聯性

劉姿君、郭建瑋

屏東榮民總醫院 核子醫學科

背景介紹：施行核醫心肌血流灌注造影過程中，藉由靜脈注射藥物 Dipyridamole（雙嘧達莫）達到壓力測試階段，其 Dipyridamole 副作用除了頭痛、頭暈、胸痛、噁心、腹痛等症狀外，部份受檢者表示注射藥物部位有刺痛或酸之不適感。本研究探討心肌血流灌注造影之受檢者予以靜脈注射 Dipyridamole 造成注射部位不適感與其年齡、性別、體重之關聯性。

方法：採問答收集資料方式連續收集 76 位心肌血流灌注造影受檢者，男性 49 位，女性 27 位。依年齡區分為 59 歲以下：22 位，60 ~ 69 歲：29 位，70 歲以上：25 位。依體重區分為 55 kg 以下：12 位，56 ~ 65 kg：22 位，66 ~ 75 kg：19 位，76 ~ 85 kg：12 位，86 kg 以上：11 位。在受檢者接受靜脈注射 0.568 mg/kg 之 Dipyridamole 過程當下，以主觀感受定性方式表達其注射藥物部位有無刺激之不適感。

結果：年齡、體重與注射處刺激之關聯性分別以二元羅吉斯迴歸分析並檢定，年齡之截距為 1.069，係數 -0.017，Exp(B)=0.983，overall Chi-Square 檢定 p = 0.402，體重之截距為 -1.385，係數 0.019，Exp(B)=1.020，overall Chi-Square 檢定 p = 0.221；性別與注射處刺激之關聯性以 Chi-Square 檢定分析 p = 0.583。

結論：年齡、體重、性別與靜脈注射 Dipyridamole 造成注射處刺激之關聯性在統計上並無顯著意義。

PC-105

評估 F-18 FDG 正子檢查病人禁食時間及生理參數對於肝臟標準攝取值之影響

龔瑞英[1,2]、林友琮[1]、林宜瀞[1,2]、張振榮[2]、蔡世傳[1,2*]

[1]臺中榮民總醫院 核子醫學科
[2]中臺科技大學 醫學影像暨放射科學系
[*]指導作者

背景介紹：F-18 FDG PET/CT 可以提供細胞關於代謝和解剖構造學上的重要信息，目前常被用在癌症病人的常規評估，其定量化標準攝取值 (SUV) 數值可以用來協助評估疾病狀態，一般常使用肝臟 SUV 值當作基準值，本研究評估病人禁食時間及生理參數對於 FDG 肝臟攝取的影響。

方法：本研究為回溯性試驗，收集 2020 ~ 2021 年間，F-18 FDG 正子造影病例 208 例（99 位男性，109 位女性，年齡 59.67 ± 11.99 歲）。收集注射後約 1 小時後的全身正子影像，並回溯檢查時相關生理參數資料，包括身高、體重、檢查時血糖及檢查前禁食時間。利用最大強度投影重建影像，於肝臟部位圈選感興趣區，進行 SUV 定量化分析。進一步統計分析病人禁食時間、身高、體重、身體質量指數、血糖與病人是否患有糖尿病對於肝臟最大標準攝取值 (SUVmax) 之影響。(IRB 編號：CE22147B)

結果：本研究經由單變數分析發現肝臟 SUVmax 與病人的體重、身體質量指數及血糖均有顯著相關（p 值分別為 < 0.001, < 0.001 及 0.02），但與身高、禁食時間、病人是否患有糖尿病則無顯著相關（p 值分別為 0.173, 0.249, 0.773）。進行雙變數分析時，發現僅有身體質量指數對 SUVmax 有顯著影響。

結論：本回溯性研究僅發現身體質量指數對肝臟 SUVmax 有顯著影響，禁食時間及其他生理參數則無顯著差異。但由於本研究分析數量僅 208 例，後續進一步可能須納入更多個案，並嘗試增加不同分析參數之樣本數，以更加了解 F-18 FDG PET/CT 體內 SUV 數值的生理性變化。

PC-106

Case Report: Intra-Abdominal Splenosis Mimicking Liver Malignancy.

Fu-Ren Tsai, Chin Hu, Chang-Ching Yu, Yi-Shun Chen

Department of Nuclear Medicine, Kaohsiung Veterans General Hospital, Kaohsiung, Taiwan

Introduction: Splenosis, a common sequela among patients with a history of splenic trauma or splenectomy, refers to heterotopic autotransplantion of splenic tissue following rupture of splenic capsule. It may present as disseminated nodular lesion in abdomen and in pleural spaces, particularly among patients who also had diaphragmatic trauma and hemopneumothorax, and growth over time, demonstrating preserved blood supply and frequently mistaken for metastatic nodules.

Case Report: A 48 year-old female patient with splenic trauma in her childhood had incidentally noticed liver nodule on sonography during a health exam. The noted liver nodule demonstrated wash-in and washout appearance on following CT images. Also, lobulated small-sized spleen was noticed. For differentiating possible intrahepatic or inreaabdominal splenosis from primary liver neoplasm, she was referred to nuclear medicine department for selective spleen scintigraphy with heat denatured Tc-99m labeled RBC. Tc-99m labeled RBC was prepared via modified in-vivo method. 10 mg stannous pyrophosphate was administered to patient via intravenous injection. About 5–10 mL of blood was collected 20 minutes later and labeled with 10 mCi Tc-99m pertechnetate. The Tc-99m labeled RBC was then heated for 20 minutes in a water bath between 49°C to 50°C, cooled in room temperature and then re-injected to the patient.

Whole body images and spot views revealed hot uptake in spleen and several discrete hot foci in abdomen, which are localized to right subphrenic space, Morrison pouch and pericecal recess via SPECT/CT.

Discussion: Tc-99m heat denatured RBC scan is a reliable technique for detection of heterotopic splenic tissue due to higher specificity than other conventional imaging modality (CT, sonography, or MRI), high lesion-background ratio and good availability.

PC-107

碘 -131 甲狀腺掃描膠囊滯留食道之案例報告

林易、許沛瑩、洪伶玟

輔大醫院 核子醫學科

簡介：碘是甲狀腺合成甲狀腺激素的主要原料，所以碘 -131 能被甲狀腺細胞攝取和吸收。碘 -131 進入人體後，大部分在 24 小時內經消化道排出體外，存留在體內的部分幾乎全部聚集在有功能的甲狀腺組織內，因此口服碘 -131 後獲得的影像可代表具功能的甲狀腺組織。

病例報告：病人為 70 歲女性，口服 0.1 mCi 碘 -131 膠囊進行碘 -131 甲狀腺掃描。檢查前七天起，停止服用抗甲狀腺藥物及進行低碘飲食直到檢查結束。口服碘 -131 膠囊前 3 小時至後 3 小時內禁食，以利碘 -131 的吸收。服用藥物後 2 小時及 24 小時接受掃描，第一次掃描時間約需時 15 分鐘，第二次掃描時間約需時 60 分鐘，第二次掃瞄結束後可恢復正常飲食及繼續服用抗甲狀腺藥物。

病人臨床上懷疑為亞急性甲狀腺炎，一個月內的甲狀腺功能正常 (TSH = 5.122 uIU/mL, free T4 = 0.83 ng/dL)。在 2 小時的影像中，發現在下胸腔有焦點 (Focal) 活性，而沒有甲狀腺的攝取，可能是因為食道至胃的傳輸功能受損所導致，病患沒有抱怨任何不適，後續請她大量喝水後 1 小時掃描即改善。碘 -131 甲狀腺掃描結果為 3 hour uptake = 1.97% (normal 5%–23%)；24 hour uptake = 17.69% (normal 16%–50%)，結果顯示甲狀腺的形狀和位置正常，但甲狀腺右下葉有輕度熱區 (hot area)。臆斷 (impression) 結果為：(1) 放射性碘攝取百分比較低或在下限邊緣 (2) 甲狀腺右下葉懷疑有功能性結節，需要超音波確認 (3) 懷疑食道傳輸功能有受損。

結論：若進行碘 -131 甲狀腺掃描時，發現甲狀腺沒有攝取時，可以儀器確認藥物是否停留在食道處，若有此情形可以大量喝水改善。

PC-108

Discussion on the Abnormal Event Caused by Different Tungsten PET Pigs

Chia-Hao Chang[1], Yu-Sheng Hung[1], Chiang-Hsuan Lee[2]

[1] *Division of Nuclear Medicine, Department of Medical Imaging, Chi Mei Medical Center, Liouying, Tainan, Taiwan*
[2] *Division of Nuclear Medicine, Department of Medical Imaging, Chi Mei Medical Center, Tainan, Taiwan*

Introduction: PET drugs are widely used in cancer examinations. However, the Tungsten PET Pigs are different occasionally from radiopharmaceutical company. One time when injecting with Tungsten PET Pig that we occasionally used, the PET injection slipped out with syringe shield from Pig. This study will explore the differences between different Tungsten PET Pigs, and the change in our SOP for PET injection.

Methods: After exploring the different Tungsten PET Pigs, we found that there is extra movable syringe shield in the main body of Pig that we occasionally used, but the main body of Pigs that we usually used is one-piece-formed without syringe shield. If we move Tungsten PET Pig without head shield close to patient's bedside, the syringe shield may slip out due to inertia.

Results: We revised standard operating procedure for PET drug injections in our department. From moving Tungsten Pig without head and tail shield, changed to without tail shield only. When moving Pig in this way, the weight on the hand of the staff from 5.1 kg increased to 6.95 kg, but the PET drug no longer slipped out so far.

Conclusions: Due to a little difference of hand held way in injection, there is crucial variance in the Tungsten PET Pigs. If the radiopharmaceutical company changed Pigs occasionally, it may cause PET drug consumption or radiation pollution. When radiopharmaceutical company uses Tungsten PET Pig with extra movable syringe shield, it is necessary to add warnings on this matter.

PC-109

Liver and Bones Visualized in Initial Lymphoscintigraphy Image: A Unique Case of Lymphoscintigraphy in Chronic Cellulitis

Hsinning Wang

Department of Nuclear Medicine, Linkou Chang Gung Memorial Hospital, Taoyuan, Taiwan

Introduction: Lymphedema is a common complaint in clinical practice. It occurs due to malfunction in the lymphatic system, leading to the retention of lymphatic fluid. Several factors can induce this dysfunction, with chronic cellulitis being one example. Addressing the underlying cause can potentially cure lymphedema. To differentiate the causation of lymphedema, lymphoscintigraphy has replaced lymphangiography as the gold standard for confirming the diagnosis of lymphedema. Lymphoscintigraphy has a sensitivity of 97% and a specificity of 100%, providing accurate results with relatively low safety concerns.

Case Report: This 56-year-old male has suffered from cellulitis for at least 20 years. His poor hygiene habits, exacerbated by mental retardation, led to copious secretions on his legs, necessitating dressing changes twice daily by family members. The patient had undergone multiple cycles of antibiotics at various medical centers over the past decades, with limited improvement. Consequently, he sought assistance at our hospital. Lymphoscintigraphy revealed that the initial image displayed increased uptake throughout the soft tissue, clearly depicting bilateral lower limbs, and even visualizing the liver and bones. In the delayed view, there was notable increased uptake in the inguinal lymph nodes, with a pattern similar to the initial image. Repeated examinations yielded consistent results.

Discussions: The patient's lymphatic system appeared to be dysfunctional. Chronic cellulitis likely triggered angiogenesis in his bilateral lower limbs. In legs with a rich micro-vessel supply, capillaries might have compensated for the lymphatic system's function. Consequently, excess fluid from soft tissue was efficiently removed and directly drained into the veins. As a result, his liver and bones exhibited radioactivity in the early image. Unlike typical lymphedema patients, the rich capillary network in the patient's legs facilitated fluid drainage, preventing the typical swelling associated with lymphedema. This unique case underscores the complexity of lymphatic system disorders and the need for precise diagnostic tools to guide appropriate treatment.

PC-110

Positron Emission Tomography in Nuclear Protein in Testis (NUT) Midline Carcinoma: A Case Report

Kuo-Wei Ho

Department of Nuclear Medicine, Chiayi Chang Gung Memorial Hospital, Chiayi, Taiwan.

Introduction: Nuclear protein in testis (NUT) midline carcinomas are defined by the presence of a chromosomal rearrangement of the NUT gene. NUT midline carcinomas are rare and aggressive disease encountered in the midline of body, such as head and neck and thorax. A case of tracheal NUT carcinoma who underwent fluorodeoxyglucose positron emission tomography/computed tomography (FDG PET/CT) was presented.

Case Report: A 39-year-old woman suffered from cough and hemoptysis for 6 months. Bronchoscopic excisional biopsy of the tracheal tumor was done and the pathology revealed NUT carcinoma. In addition, a nodular lesion about 1.9 cm and adjacent tree-in-bud opacity in RUL of lung were also noted on chest CT, in suspicious of lung metastasis or synchronous cancer. Therefore, FDG PET/CT was arranged for evaluation of distant metastasis. The FDG PET/CT showed intense FDG uptake at tracheal tumor (SUVmax: 10.77), moderate to mild FDG uptakes at RUL lung nodule (SUVmax: 5.30) and tree-in-bud opacity (SUVmax: 2.43), and no other abnormal FDG uptake to suggest nodal or distant metastasis. Surgical investigations with wide excision of tracheal tumor and bilateral neck dissection were performed. The pathological results revealed tracheal NUT carcinoma, pT2N0. CT-guided biopsy for the RUL lung nodule was also done, while the pathology reported negative for malignancy. She received adjuvant concurrent chemoradiotherapy postoperatively. A subsequent post-treatment FDG PET/CT showed complete metabolic response of tracheal NUT tumor and the RUL lung nodule.

Discussion: NUT midline carcinomas are aggressive, poorly differentiated tumors that include variable degrees of squamous differentiation in approximately one-half of cases. These tumors are defined by the presence of a chromosomal rearrangement of the NUT gene and have a distinct clinical presentation and clinical course. Although the genetic and pathologic features of this disease process have been extensively described in the recent literature, the role of FDG PET/CT has not been adequately illustrated in this disease. We reported a patient with NUT midline carcinoma who received FDG PET/CT initially in assessing for metastatic disease. After concurrent chemoradiotherapy, the subsequent PET/CT also plays a role in evaluation of the treatment response. Meanwhile, FDG PET/CT is also very useful in directing percutaneous biopsy to obtain viable tissue because extensive necrosis is typically seen in this tumor that may cause inconclusive pathologic result. These advances make FDG PET/CT an essential imaging modality for surveillance of NUT midline carcinoma.

PC-111

^{99m}Tc-MDP Bone Scintigraphy in Detecting Osteolytic Skeletal Metastases

Ya-Cing Hsu, Yu-Ling Hsu

Department of Nuclear Medicine, Ditmanson Medical Foundation Chia-Yi Christian Hospital, Chiayi, Taiwan

Introduction: Bone scan is one of the most and oldest examinations among all nuclear medicine procedures. It is used in the evaluation of benign bone disease such as infection/inflammation and is also the standard of care for evaluating metastatic diseases.

Case Report: A 57-year-old man suffered from chronic low back-pain. In consideration of bone related problems, the first MDP bone scan image showed decreased radioactivity at sacrum and right sacroiliac joint compared to left side. Later biopsy results and other imaging modalities revealed highly suspicious gastric cancer with oligo-right sacral metastasis.

Conclusion: Gastric cancer is the third leading cause of cancer-related death worldwide. The most frequent sites of metastases from gastric cancer are liver, lymph nodes, and lung. However, the disease prognosis in gastric cancer with bone metastases is unclear, which may be related to the underestimation of bone lesions for the rarity.

Bone scintigraphy, as long thought to be less sensitive in osteolytic lesions, still has its role in detecting all kinds of bone changes. Combined with other imaging modalities, such as CT and MRI, the modality can definitely increase the accuracy of diagnosis.

PC-112

The Application of Detecting the Heterogeneity of Estrogen Receptor By ^{18}F-fluoroestradiol PET/CT: A Systematic Review

Li-Yu Chen[1], Shiang-ling Lin[1], Ya-Yao Huang[1,3], Ya-Ting Huang[1,2]

[1] *Primo Biotechnology Co., Ltd, Taipei, Taiwan*
[2] *Department of Medical Education and Research, Camillian Saint Mary's Hospital Luodong, Yilan, Taiwan*
[3] *Molecular Imaging Center, National Taiwan University, Taipei, Taiwan*

Background: ^{18}F-fluoroestradiol positron emission tomography/computed tomography (18F-FES PET/CT) is a new convenient way to screen and analyze metastatic breast cancer (MBC) patients with uncertain estrogen receptor (ER), which the heterogeneity expression has long been a problem in figuring out how to treat MBC. This systematic review aimed to integrate the study of ER heterogeneity detection by ^{18}F-FES PET/CT.

Methods: PubMed/MEDLINE and Cochrane Library databases were used to perform a comprehensive and systematic search and were updated till August 15, 2022. Two authors independently reviewed the titles and abstracts of the retrieved articles by using the search algorithm and selected the articles based on the inclusion and exclusion criteria. All statistical analyses were conducted using R statistical software.

Results: This systematic review included six studies with 881 breast cancer patients in the qualitative and quantitative synthesis, which estimated the FES-positive detection rate and the rate of ER heterogeneity. In included 6 studies, the overall pooled detection rate of 18F-FES PET/CT was 0.82 (95% CI 0.70–0.89). In addition, the FES uptake threshold of 1.5–1.82 could not only identify the positive ER but also detect 11.1%–45% ER heterogeneity.

Conclusions: 18F-FES PET/CT could identify patients with ER heterogeneity. Future, the study can explore the correlation between ER heterogeneity and prognosis.

PC-113

The Economic Evaluation of Diagnostic Tool with ^{18}F-Fluorodeoxyglucose from Clinical Practice: A Systematic Review and Network Meta-analysis

Ya-Ting Huang[1,2], Yu-Ming Fan[3,4], Li-Yu Chen[3], Shiang-ling Lin[3], Chih-Yi Wu[3], Guang-Uei Hung[5], Ya-Yao Huang[1,6]

[1] *Primo Biotechnology Co., Ltd, Taipei, Taiwan*
[2] *Department of Medical Education and Research, Camillian Saint Mary's Hospital Luodong, Yilan, Taiwan*
[3] *Department of Nuclear Medicine, Cardinal Tien Hospital, New Taipei City, Taiwan*
[4] *School of Medicine, College of Medicine, Fu-Jen Catholic University, New Taipei City, Taiwan*
[5] *Department of Nuclear Medicine, Chang Bing Show Chwan Memorial Hospital, Changhua, Taiwan*
[6] *Molecular Imaging Center, National Taiwan University, Taipei, Taiwan*

Background: Imaging with ^{18}F-fluorodeoxyglucose (FDG) plays a significant diagnostic role in cancer and non-cancer followed by influencing treatment decision-making. Because of the clinical benefits of FDG imaging, its cost-effectiveness is of interest. We aimed to integrate these varied studies of the economic evaluation of FDG imaging and to better understand the cost-effectiveness of FDG imaging by comparing it with other diagnostic methods and tools.

Method: The PubMed/MEDLINE and Cochrane Library databases were used to perform a comprehensive and systematic search and were updated on October 25, 2022. The cost was standardized, and the incremental net benefit (INB) with its variance was estimated. Then, a Bayesian network meta-analysis was performed by classifying health outcomes, such as quality-adjusted life years, life expectancy, and diagnostic accuracy. The mean differences (MDs) with 95% confidence intervals (CIs) were calculated for continuous outcomes as INB.

Result: The current network meta-analysis included 23 studies conducted between 2000 and 2023. Among the included studies, 13 used CEA, and 10 used CUA to conduct economic evaluations. In the league table, the estimated INBs of FDG imaging compared with other diagnostic methods and tools were positive, indicating that it was cost-effective, except for CT-guided aspiration (CTG) in CUA. Comparing both FDG imaging modalities in CEA for predicting life expectancy, the cost-effectiveness of PET/CT+CT was better than that of PET/CT, and PET+CT was superior to PET alone.

Conclusion: According to the current network meta-analysis for economic evaluation, FDG imaging outperformed other diagnostic methods and tools for CEA and CUA.

PC-114

The Differences of Time Periods between Visual and SUVR Assessments in Highly Suspected Alzheimer's Disease Patients on Amyloid PET

Hung-Pin Chan[1,2], Hsiao-Chi Hou[1], Yow-Ling (Shirley) Shiue[2,3], Chin Hu[1], Daniel Hueng-Yuan Shen[1]

[1] *Department of Nuclear Medicine, Kaohsiung Veterans General Hospital, Kaohsiung City, Taiwan*
[2] *Institute of Biomedical Sciences, College of Medicine, National Sun Yat-sen University, Kaohsiung City, Taiwan*
[3] *Institute of Precision Medicine, College of Medicine, National Sun Yat-sen University, Kaohsiung City, Taiwan*

Introduction: Alzheimer's disease (AD) is a chronic illness in present days with long preclinical and prodromal periods more than 10 years. The accumulation of amyloid-β (Aβ) is found and considered a diagnostic feature of AD. Amyloid positron emission tomography (PET) imaging enables non-invasive detection of brain Aβ deposition, one of the neuropathological hallmarks of AD. However, patients sometimes not only present memory loss, but also can't cooperate with examination due to their agitation status. It caused inadequate imaging and waste the radiopharmaceutical cost. The aim of this study is to determine the differences of time periods between Visual and SUVR managements in AD patients on Amyloid PET to find the latest time but adequate imaging quality for proper diagnosis.

Methods: Ten patients were suspected AD referred by neurologists for Amyloid PET imaging. The time period was divided in 5th, 10th, 15th, and 20th minutes, respectively. The completed scan time with 20 minutes was suggested from instructions. Patients would be excluded due to could not finish complete scan. Visual and SUVR assessments were performed for Amyloid PET reporting by two experienced nuclear medicine physicians.

Results: Ten patients were enrolled for this study. Two patients were excluded due to failed in examination. We found the 5th- minute scan time got negative result in all patients. It may suggest due to inadequate imaging related. In the 10th-minute scan, the results were consistent in both visual and SUVR ratio in all patients. Interesting, the comparison with the 10th- and the 20th- minutes also were consistent in both visual and SUVR ratio in all patients.

Conclusions: The adequate imaging time for diagnosis AD by Amyloid PET is at least > 15 minutes in our study. The latest scan time is 10th- min which is consistent in both visual and SUVR ratio results as compared with 20th min. However, the SUVR ratio was strong suggested for assist to visual assessment reporting system.

PC-115

針頭回套模組之改善與臨床運用

林雯君、蘇詩琪、胡璿、邱宇莉

高雄榮民總醫院 核子醫學科

背景介紹：自 2012 年政府為了減少「針扎」問題，繼而開始推動「安全針具」使用規範。核醫輻射物質藥物為避免因溢漏而造成輻射污染之故，一直無法適用。回溯年度本科接受藥物注射的受檢者平均約 13000 多位，如何避免針扎事故的發生。研發及精進針具安全設計的回套裝置尤其重要。

方法：本次設計延續之前的第二代產品「回套立方」概念，以避免回套動作與針頭的暴露為主，加重筆座的重量防止使用時因受力不均而傾倒。且在考量成本、效能和便利性之下，取用身邊容易取得之物件「螺母和墊片」做成筆筒型之回套模組。

結果：「針頭回套筆座」穩固且方便移動攜帶，經不同醫事同仁使用不同劑型試用月餘後，回饋良好，目前已成為本科安全回套使用的利器。

結論：「針頭回套筆座」物件的來源及製作成本價低約 20 ~ 50 元，「螺母和墊片」坊間五金行即可輕鬆購得，固定筆座部分可請醫院的工務部門協助。因為此針頭回套的安全且便利，可推廣至某些無法適用安全針具的使用單位，避免因為針扎帶來的職業傷害。

PC-116

I131NP59 in Diagnosis of Primary Aldosteronism, APA vs. BAH—KMUH Case Serial Study

Yu Wen Chen[1,2,3], Hsiang Ying Lee[2,3,4], Shang Jyh Huang[2,3,5], Wen Jenn Wu[2,3,4]

[1] *Department of Nuclear Medicine, Kaohsiung Medical University Hospital, Kaohsiung, Taiwan*
[2] *PA Committee, Kaohsiung Medical University Hospital, Kaohsiung, Taiwan*
[3] *School of Medicine, Kaohsiung Medical University, Kaohsiung, Taiwan*
[4] *Department of Urology, Kaohsiung Medical University Hospital, Kaohsiung, Taiwan*
[5] *Department of Internal Medicine Division of Endocrine, Kaohsiung Medical University Hospital, Kaohsiung, Taiwan*

Introduction: Primary aldosteronism is the etiology of the most common secondary hypertension. I131 NP59 functional image represents the regulation of enzyme, CYP 112B in the aldosterone synthesis while certain gene mutation happen, eg KCN J5 etc.

Methods: During past two years, we collected 15 patients (gender ratio, as M: F 9:6; age 41–85 year-old) with hypertension, hypokalemia and metabolic alkalosis in the uni-center (KMUH). The blood pressure of patients is from 110/60 to 210/90 mmHg and potassium level is from 2.2 to 3.1 mg/dL. Initially, XCT was arranged to detect adrenal nodules. Then, 1-2mCi I131NP59 scintigraphy and SPECTCT were prepared with standard protocol to identify the functional nodule for surgical indication. Fewer cases (1–2 patients) had AVS study.

Results: All of them have adrenal nodules on XCT, about 60% with multiple nodules. There are five cases with typical high NP59 avidity nodules and > 1 cm in size. Three of them received surgery by imaging lateralization. The rest six patients have faint NP59 avidity and smaller in size, while suspicious patients with MRA medicine treatment. The other three cases were diagnosed as BAH with multiple tiny faint/ nonNP59 acid adrenal nodules. Another one has a large nodule, 1.9 cm without NP59 avidity. She was still followed in clinic.

Conclusion: I131NP59 SPECTCT provides noninvasive functional and anatomical imaging to identify high NP59 avid nodule (> 1 cm) for surgical lateralization and genomic studies. However, radiopharmaceutic, I131NP59 is not available in routine clinic.

PC-117

To Differentiate Hypopharyngeal Cancer from Cervical Esophageal Cancer Does Matter on FDG PET/CT Scan

Hsin-Hui Tsai, Chi-Wen Huang, Jui-Hung Weng

Department of Nuclear Medicine, Chung Shan Medical University Hospital, Taichung, Taiwan

Introduction: A 64-year-old courtyard farmer presented with dysphagia. Esophageal cancer was impressed by gastroscopy and therefore biopsy was taken. Squamous cell carcinoma was later proven pathologically. A positron emission tomography-computed tomography (PET/CT) scan was performed for pre-treatment staging.

Methods: The FDG PET scan was performed after fasting for 6 hours with a GE Discovery MI PET/CT scanner at 60 minutes after intravenous injection of ^{18}F-FDG. The scan area covers vertex to above knees. Images are reconstructed iteratively with attenuation correction.

Results: An abnormal hypermetabolic elongated lesion involved posterior hypopharyngeal wall, post-cricoid region, prevertebral fascia, and upper cervical esophagus, which showed a transverse extension on image. There were also multiple regional lymph nodes metastases at the same time. The hypopharyngeal part of the tumor seemed significantly larger than the esophageal part. The FDG PET/CT scan suggested hypopharyngeal cancer and a corresponding stage instead of esophageal cancer.

Conclusions: Hypopharyngeal cancer and cervical esophageal cancer belong to different disease entities. Not only staging systems but also prognosis and cancer registry differ. Correct differentiation when interpreting FDG PET/CT scan for such entities is warranted.

MASSIA R4200

RIA 檢測的全自動系統

檢體與試劑的分注、培育、試管清洗、珈瑪計數 四合一

(衛部醫器輸壹字第 022913 號)

大昇生物科技股份有限公司
電話:02-26954758 傳真:02-26956680 新北市汐止區福德三路 363 號 12 樓

NOW AVAILABLE

RAPID PRONOUNCED DURABLE

對於放射性碘 (RAI) 治療無效之分化型甲狀腺癌 (DTC) 患者，顯著延長無惡化存活期 (PFS) 中位數超過 18個月

LENVIMA®
(lenvatinib) capsules

健保給付規定（給付生效日 2018 年 7 月 1 日）
用於放射性碘治療無效之局部晚期或轉移性的進行性 (progressive) 分化型甲狀腺癌 (RAI-R DTC)：

1. 需經事前審查核准後使用，每次申請之療程以 3 個月為限，送審時需檢送影像資料，每 3 個月評估一次。
2. Lenvatinib 與 sorafenib 不得合併使用。

適應症

放射性碘治療無效之進行性，且為局部晚期或轉移性之分化型甲狀腺癌之成人患者。

劑型劑量

LENVIMA® 有 4 mg 和 10 mg 兩種劑量之膠囊劑型。

用法用量

- 建議起始劑量為 24 mg 每日一次 (兩顆 10 mg + 一顆 4 mg 膠囊)
- 重度腎功能不全 (CLcr < 30 mL/min) 及重度肝功能不全 (Child-Pugh C) 患者，建議起始劑量為 14 mg 每日一次 (一顆 10 mg + 一顆 4 mg 膠囊)

Eisai hhc human health care TW-LV-MH-18G-01 衛部藥輸字第 026933、026934 號 北市衛藥廣字第 112020066 號
衛采製藥股份有限公司 www.eisai.com.tw 電話：02-2531-4175

Ref:Schlumberger M, et al. Lenvatinib versus placebo in radioiodine-refractory thyroid cancer. N Engl J Med. 2015 Feb 12;372(7):621-30

LUTATHERA®

鐳住新希望

為神經內分泌腫瘤病患，精準擊殺腫瘤的新希望

處方資訊摘要

[本藥須由醫師處方使用]

北市衛藥廣字第 112090019 號

北市衛食藥字第 1123054149 號

產品名稱：鐳德平®注射液 LUTATHERA® (衛部藥輸字第R00104號)

主成分：Lutetium Lu 177 dotatate 適應症：LUTATHERA用於治療成人無法手術切除或轉移性，分化良好(G1及G2)且經體抑素類似物(somatostatin analogue)治療無效之體抑素受體(somatostatin receptor)陽性的胃腸道胰腺神經內分泌腫瘤 用法/用量：LUTATHERA建議劑量為7.4 GBq (200 mCi)，每8週一次共4劑。LUTATHERA不良反應的建議劑量調整請參考詳細仿單。禁忌:本品為具放射線藥品，確定或疑似懷孕，或尚未排除懷孕的情況下請勿使用。警語：1.放射線暴露風險LUTATHERA會增加病人長期整體放射線暴露量。長期累積放射線暴露量則會增加罹患癌症的風險。LUTATHERA投藥後可於尿液內偵測到放射線最長30天。依醫院良好放射線安全性規範、病人處置程序、行政院原子能委員會輻射防護規範，以及病人居家追蹤放射線保護說明，於LUTATHERA治療期間與治療後使病人、醫療人員以及家庭接觸者能盡量減少放射線暴露量。2.骨髓抑制監測血球細胞計數。依骨髓抑制嚴重程度暫停投藥、降低劑量或永久停用[請參考詳細仿單]。不建議於Lutathera治療之前對基準點血液功能嚴重受損的病人開始進行治療(例如Hb < 4.9 mmol/L或8 g/dL，血小板< 75 x 109/L或75 x 103/mm3或白血球< 2 x 109/L或2000/mm3)。3. 繼發性骨髓增生不良症候群及白血病在NETTER-1中，追蹤時間中位數為24個月，2.7%接受LUTATHERA加上長效octreotide的病人通報發生骨髓增生不良症候群(MDS)，相較之下接受高劑量長效octreotide則無病人發生MDS。4.腎毒性監測血清肌酸酐並計算肌酸酐廓清率。依腎臟毒性嚴重程度暫停投藥、降低劑量或永久停用LUTATHERA。5.肝臟毒性於治療期間監測轉胺酶、膽紅素與血清白蛋白。依肝功能不全嚴重程度暫停投藥、降低劑量或永久停用LUTATHERA 。6.過敏反應接受 Lutathera 治療的病人發生過敏反應，包括血管性水腫。 在具有心肺復甦藥物和設備的環境下，於 LUTATHERA 給藥期間和之後，密切監測病人是否出現過敏反應的徵兆和症狀，至少 2 小時。 在第一次觀察到與嚴重過敏反應有關的任何徵兆或症狀時停止輸注，並給予適當的治療。7.神經內分泌荷爾蒙危象監測病人是否出現潮紅、腹瀉、低血壓、支氣管收縮或其他腫瘤相關荷爾蒙分泌徵兆及症狀。視情況靜脈投予體抑素類似物、液體、皮質類固醇以及電解質。8. 胚胎-胎兒毒性所有放射性藥物(包括LUTATHERA)都可能對胎兒造成傷害。使用LUTATHERA前請先確認具生育能力女性的懷孕狀態。應向具生育能力女性病人告知，在LUTATHERA治療期間與最後一劑後7個月內應使用有效的避孕方式。若男性病人的女性伴侶具生育能力，應向男性病人告知，在接受治療期間以及最後一劑藥物後4個月內應使用有效的避孕方式。9. 不孕風險LUTATHERA可能導致男性和女性不孕。10. 與胺基酸溶液相關的高血鉀症接受精胺酸(arginine)和離胺酸(lysine)的病人可能會出現血清鉀濃度的短暫升高，通常在開始輸注胺基酸後的24小時內恢復正常值。每次接受胺基酸溶液治療之前，必須檢測血清鉀濃度。若發生高血鉀症，應檢查病人的高血鉀症病史和併用藥物治療。開始輸注之前，必須隨之矯正高血鉀症。11.與胺基酸溶液相關的心臟衰竭由於可能出現與容量過度負荷相關的臨床併發症，因此，在NYHA分類(美國紐約心臟協會)定義為第III級或第IV級的嚴重心臟衰竭病人，應謹慎使用精胺酸和離胺酸。12.與胺基酸溶液相關的代謝性酸中毒於酸中毒的形成可能與血漿鉀的迅速增加有關。副作用：最常見的不良反應(發生率30% 以上) 為噁心、嘔吐、疲倦。最常見第3 至第4 級不良反應(發生率2% 以上) 為噁心、嘔吐、腹痛、腹瀉、高血壓、背痛、腎衰竭。最常見實驗室數值異常(發生率50% 以上)為淋巴球減少症、貧血、白血球減少症、血小板減少症、肌酸酐增加、高血糖、GGT增加、鹼性磷酸酶升高、AST增加。最常見第3/4 級的實驗室數值異常(發生率3% 以上) 為淋巴球減少、嗜中性白血球減少症、高血糖、高尿酸血症、低血鉀症、GGT增加、鹼性磷酸酶升高、AST增加、ALT增加。

詳細資訊請參閱完整仿單TW2212149870

NOVARTIS
台灣諾華股份有限公司
10480台北市中山區民生東路三段2號8樓
電話：(02)2322-7777 傳真：(02)2322-7328
免費諮詢專線：0800-880-870
http://www.novartis.com.tw

使用前請詳閱說明書警語以及注意事項

TW2308178384

VERITON-CT ®
D-SPECT ® CARDIO

CHANGING THE SHAPE OF NUCLEAR MEDICINE
CZT BASED SOLID STATE SPECT IMAGING

D-SPECT Series
CARDIOLOGY DIGITAL SPECT IMAGING

VERITON Series
360° TOTAL BODY DIGITAL SPECT/CT IMAGING

D-SPECT CARDIO

VERITON-CT
SPECT/CT 16/64

Digital SPECT Technology for Throughput and Diagnostic Efficency

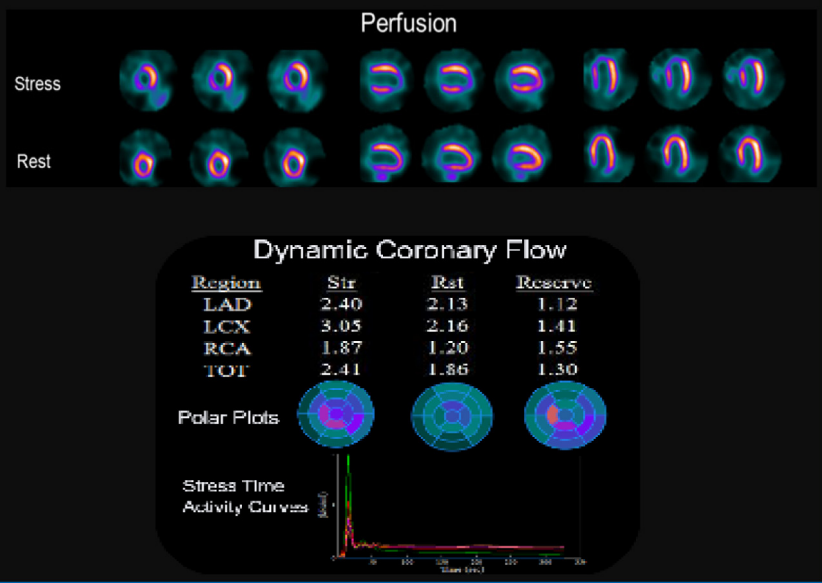

Benefits of Ring-Type TWB Digital SPECT/CT System

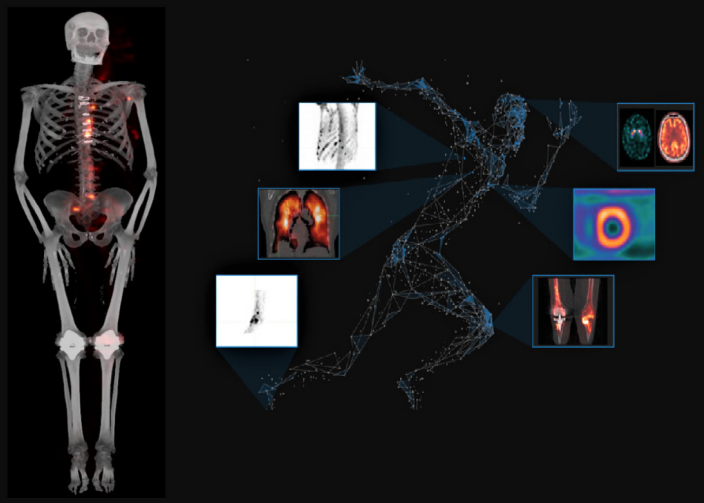

SPECTRUM DYNAMICS MEDICAL
www.spectrum-dynamics.com

總代理
常捷生醫科技股份有限公司 (02)2808-5960
www.grever.com.tw

大會組織

主辦單位 中華民國核醫學學會
臺中榮民總醫院
國家原子能科技研究院
經濟部產業技術司

協辦單位 台灣分子生物影像學會

大會會長 王心怡

指導委員

王安美、王秀珊、王昱豐、何恭之、吳彥雯、汪姍瑩、林立凡、林宜瀞、林昆儒、林明賢、邱南津、洪光威、胡蓮欣、張文議、張晉銓、莊紫翎、許幼青、陳志成、陳惠萍、陳傳霖、彭南靖、曾能泉、程紹智、黃文盛、黃玉儀、黃奕琿、黃莆蓉、楊邦宏、路景竹、樊修秀、樊裕明、蔡世傳、鄭媚方、諶鴻遠、龔瑞英

法律顧問 蔡雅琴

論文評選組

召集人 胡蓮欣
執行秘書 楊依婷
口頭基礎 吳駿一、張文議
口頭臨床 林宜瀞、柯冠吟、許沛瑩、陳世欣、黃玉儀、蔡雅琴
壁報基礎 高志浩、陳志成、楊邦宏、楊宛甄、溫湘萍、陳惠萍
壁報臨床 王安美、汪姍瑩、邱宇莉、莊紫翎、許幼青、陳毓雯、曾能泉、程紹智、黃奕琿、黃潔宜、詹勝傑、鄭乃銘

秘書處

秘書長 李哲皓
副秘書長 李建穎、黃佳文
秘書 石采庭、吳璟莛、廖婷婷

贊助廠商

大昇生物科技股份有限公司

元新儀器股份有限公司

吉晟生技股份有限公司

台灣拜耳股份有限公司

台灣諾華股份有限公司

西門子醫療設備股份有限公司

貝克西弗股份有限公司

奇異亞洲醫療設備股份有限公司

昶洋貿易股份有限公司

恩典科研股份有限公司

泰歷藥品儀器股份有限公司

常捷生醫科技股份有限公司

富特茂股份有限公司

量子輻射科技有限公司

臺灣新吉美碩股份有限公司

衛采製藥股份有限公司

龍霆科技企業有限公司

（依筆畫排序）